5-2012

Novel Use of Dual Anti-Inflammatory Therapy to Overcome Drug Resistance and Improve Functional Recovery Following Spinal Cord Injury

Jennifer Dulin

NOVEL USE OF DUAL ANTI-INFLAMMATORY THERAPY TO OVERCOME DRUG RESISTANCE AND IMPROVE FUNCTIONAL RECOVERY FOLLOWING SPINAL CORD INJURY

by

Jennifer Natalie Dulin, B.S.

APPROVED:

_____

Raymond J. Grill, Ph.D., Supervisory Professor

_____

David S. Loose, Ph.D.

_____

M. Neal Waxham, Ph.D.

_____

Michelle A. Hook, Ph.D.

_____

Olivera Nesic, Ph.D.

APPROVED:

_____

Dean, The University of Texas
Graduate School of Biomedical Sciences at Houston

NOVEL USE OF DUAL ANTI-INFLAMMATORY THERAPY TO OVERCOME DRUG RESISTANCE AND IMPROVE FUNCTIONAL RECOVERY FOLLOWING SPINAL CORD INJURY

A
DISSERTATION

Presented to the Faculty of
The University of Texas
Health Science Center at Houston
and
The University of Texas
M. D. Anderson Cancer Center
Graduate School of Biomedical Sciences

in Partial Fulfillment

of the Requirements

for the Degree of

DOCTOR OF PHILOSOPHY

by

Jennifer Natalie Dulin, B.S.
Houston, Texas

May 2012

This work is dedicated to all of those who are living with a spinal cord injury and to their loved ones.

Acknowledgments

I am incredibly grateful to be immersed in such a rich network of support. I would not have made it this far without all of the people who have guided, taught, and encouraged me during my time in graduate school.

I would like to thank the University of Texas Center for Clinical and Translational Sciences for providing me with the funding for this project. I have enjoyed my time in the program immensely and I have learned a great deal through CCTS program activities. A special thanks is owed to George Stancel and Lisa Wetter for their support through the CCTS T32 program, and to Gerard Francisco for serving as co-mentor on my training grant.

I thank all of my supervisory committee members (Michelle Hook, David Loose, Olivera Nesic-Taylor, and Neal Waxham) for providing the outside perspective and constructive criticism that shaped this project into its current form. Your guidance and patience has been deeply appreciated.

I am grateful to Michael Blackburn for his incredible generosity in training me on, and allowing me to use, his HPLC setup; to Neal Waxham for his continued support in reading manuscript drafts and writing multiple recommendation letters; to David Loose for being such a strong student advocate and for encouraging me to get involved in CRB activities, as well as the writing of recommendation letters.

Alissa Poteete, your friendship has meant so much to me. You have been the best lab-mate that I could ever ask for. Thank you for teaching me to have more patience and for inadvertently guilting me into being more organized. More importantly, thank you for being there by the elevator that day to witness the orange juice thief in action. I am so happy to have made a lifelong friend in you and I am extremely proud of all that we have accomplished!

To the ever-fabulous Meredith Moore, thank you for your guidance and patience in teaching me various experimental and analytical techniques over the years; you are an amazing scientist and I hope to someday be half as vigilant as you are in the lab. Thank you for being there to listen and give great advice on many occasions. I really admire your eternally positive attitude, your ability to laugh things off, and most of all, your impeccable hostess skills.

Andy Dowsey, you have been such a sweet and supportive companion to me throughout the shambolic experience of grad school. I could never, ever thank you enough for the immense amount of love, patience, and understanding his Lordship has shown me over the past four years. I love you very much.

To my amazing and wonderful family, thank you for your infinite understanding and support. Katie and Heather, I'm very proud of you both. I am so glad that I have two such amazing, supportive, and caring sisters. Dad and Leslie, thank you for supporting me in a million ways, helping me to have a sense of humor and keep things in perspective, and teaching me that "success is the intelligent use of failure". Tanner and Jake, I love you boys so much and watching you both grow up has been one of the best things in my life. Mama and Don, thank you for giving me moral support and countless home-cooked meals, for your pride and excitement about my work, and your endless love, encouragement, and praise. To all of my grandparents, Nana, Papa, Honey, Paw Paw, and George, you have all contributed to who I have become. It makes me so happy to know that you are proud of me.

To everyone at Mission Connect: I cannot overstate how much it has influenced me, personally and professionally, to be involved in this excellent collaborative research effort. I have learned so much through Mission Connect scientific meetings, annual symposiums, and fundraising activities. To Cynthia Adkins, Sandra Jochen, Caroline Mark, and Robin Williamson, thank you so much for your graciousness and support during my time in grad school. I am incredibly grateful for you ladies and I really admire your hard work to make Mission Connect such a success.

To Ray Grill: I cannot imagine a more ideal Ph.D. advisor than you. You have been a major driving force in my intellectual and professional growth, and you have pushed me to achieve more than I thought possible. I am so thankful that you have taken me seriously and valued my scientific input on everything I've done in your lab; not once have you been demanding, impatient, unreasonable, or dismissive. You have educated me about every aspect of being an academic researcher, and equipped me well to make the transition to the next step of my career. Ray, you are a brilliant scientist and I genuinely look forward to a long collaborative relationship (I really gotta get you those stem cells). More than a mentor, you are also a good friend. My family and I are supremely grateful for your presence in my life and all you have done to help me not only succeed, but flourish.

NOVEL USE OF DUAL ANTI-INFLAMMATORY THERAPY TO OVERCOME DRUG RESISTANCE AND IMPROVE FUNCTIONAL RECOVERY FOLLOWING SPINAL CORD INJURY

Publication No._____
Jennifer Natalie Dulin, B.S.
Supervisory Professor: Raymond J. Grill, Ph.D.

Abstract

Over 1.2 million Americans are currently living with a traumatic spinal cord injury (SCI). Despite the need for effective therapies, there are currently no proven effective treatments that can improve recovery of function in SCI patients. Many therapeutic compounds have shown promise in preclinical models of SCI, but all of these have fallen short in clinical trials.

P-glycoprotein (Pgp) is an active transporter expressed on capillary endothelial cell membranes at the blood-spinal cord barrier (BSCB). Pgp limits passive diffusion of blood-borne drugs into the CNS, by actively extruding drugs from the endothelial cell membrane. Pgp can become pathologically up-regulated, thus greatly impeding therapeutic drug delivery ('multidrug resistance'). Importantly, many drugs that have been evaluated for the treatment of SCI are Pgp substrates. We hypothesized that Pgp-mediated drug resistance diminishes the delivery and efficacy of neuroprotective drugs following SCI.

We observed a progressive, spatial spread of Pgp overexpression within the injured spinal cord. To assess Pgp function, we examined spinal cord uptake of systemically-delivered riluzole, a drug that is currently being evaluated in clinical trials as an SCI intervention. Blood-to-spinal cord riluzole penetration was reduced following SCI in wild-type but not Pgp-null rats, highlighting a critical role for Pgp in mediating spinal cord drug resistance after injury. Others have shown that pro-inflammatory signaling drives Pgp up-regulation in cancer and epilepsy. We have detected inflammation in both acutely- and chronically-injured spinal cord

tissue. We therefore evaluated the ability of the dual COX-/5-LOX inhibitor licofelone to attenuate Pgp-mediated drug resistance following SCI. Licofelone treatment both reduced spinal cord Pgp levels and enhanced spinal cord riluzole bioavailability following SCI. Thus, we propose that licofelone may offer a new combinatorial treatment strategy to enhance spinal cord drug delivery following SCI.

Additionally, we assessed the ability of licofelone, riluzole, or both to enhance recovery of locomotor function following SCI. We found that licofelone treatment conferred a significant improvement in hindlimb function that was sustained through the end of the study. In contrast, riluzole did not improve functional outcome. We therefore conclude that licofelone holds promise as a potential neuroprotective intervention for SCI.

Table of Contents

List of Illustrations

List of Tables

Abbreviations

5-LOX	5-lipoxygenase
AA	Arachidonic acid
ABC	ATP-binding cassette
ANOVA	Analysis of variance
ALS	Amyotrophic lateral sclerosis
AIS	ASIA Impairment Scale
ASIA	American Spinal Injury Association
BBB	Basso, Beattie, and Bresnahan
BSCB	Blood-spinal cord barrier
b.i.d.	Twice daily
CNS	Central nervous system
COX	Cyclooxygenase
CST	Corticospinal tract
CysLT	Cysteinyl leukotriene
DPI	Days post-injury; post-injury day
EC	Endothelial cell
ELISA	Enzyme-linked immunosorbent assay
EP1	Prostaglandin E receptor 1
GI	Gastrointestinal
HPLC	High-performance liquid chromatography
IgG	Immunoglobulin G
IL-1β	Interleukin-1 beta
i.p.	Intraperitoneal
LPS	Lipopolysaccharide
LTB_4	Leukotriene B4
MDR	Multidrug resistance
MPSS	Methylprednisolone sodium succinate
MRI	Magnetic resonance imaging
NACTN	North American Clinical Trials Network

NASCIS	National Acute Spinal Cord Injury Study
NF-kB	Nuclear factor-kappaB
NSAID	Non-steroidal anti-inflammatory drug
PAS	Photobeam activity system
PGE_2	Prostaglandin E2
Pgp	P-glycoprotein
PLA_2	Phospholipase A_2
ROS	Reactive oxygen species
s.c.	Subcutaneous
SCI	Spinal cord injury
T10	Spinal cord thoracic level 10
TBS	Tris-buffered saline
TBST	Tris-buffered saline + 0.1% Tween-20
TNF-α	Tumor necrosis factor-alpha

CHAPTER 1

Introduction

Spinal Cord Injury: Prevalence, Consequences, and Clinical Management

Spinal cord injury (SCI) can be fundamentally described as an event causing damage to the spinal cord, resulting in partial to complete loss of neurological function below the level of injury. SCI is a particularly devastating form of trauma for which no proven effective treatment is yet available; as a result, the majority of SCI patients suffer from lifelong paralysis and other functional impairments. Recently, the impact of SCI in the United States has been found to be greater than previously thought. In 2009, the Christopher & Dana Reeve Foundation's Paralysis Resource Center published the largest, most comprehensive study of SCI and paralysis statistics in the U.S. in history (1). This report, the result of an exhaustive survey of more than 33,000 American households, revealed that approximately 1,275,000 individuals (0.4% of the U.S. population) are currently living with SCI; a startlingly high figure compared to a previous estimate of 262,000 (2). Most cases of SCI result from accidental trauma; the most commonly reported causes of SCI are work-related accidents (28%), motor vehicle accidents (24%), and sporting or recreation accidents (16%) (1). The majority of injuries (80.8%) are sustained by males, and the average age at injury is 40.2 years (2). Notably, the cost of SCI is substantial, both to the individual—the estimated lifetime cost of SCI to a 25-year old patient is $3,273,270 (2) —and to society. The financial burden incurred by SCI on the American health care system amounted to $40.5 billion in 2009, a figure that continues to grow (1).

SCI most often occurs when a ballistic insult to the spinal column results in a contusion and compression to the spinal cord (3, 4). However, SCI can also result from other forms of trauma such as penetrating injuries from stab or gunshot wounds, or non-traumatic events such as cancer, infection, or ischemia. SCI can be classified as solid cord injury, laceration, contusion/cavity-type injury, or massive compression (5). Furthermore, injury may occur at any level of the spinal cord, from the first cervical level to the conus medullaris and cauda equina. For these reasons, the resulting neurological deficits can vary dramatically from patient to patient. It is also partially because of its pathological diversity that SCI remains such a challenging condition for which to develop effective therapeutic treatments.

The physiological impact of SCI depends upon a number of factors. The location of injury largely determines the degree of function retained by the patient, with injuries to more rostral regions of the spinal cord typically resulting in the greatest degree of functional impairment (**Fig. 1.1**). An individual's level of injury is determined by diagnostic imaging, such as MRI

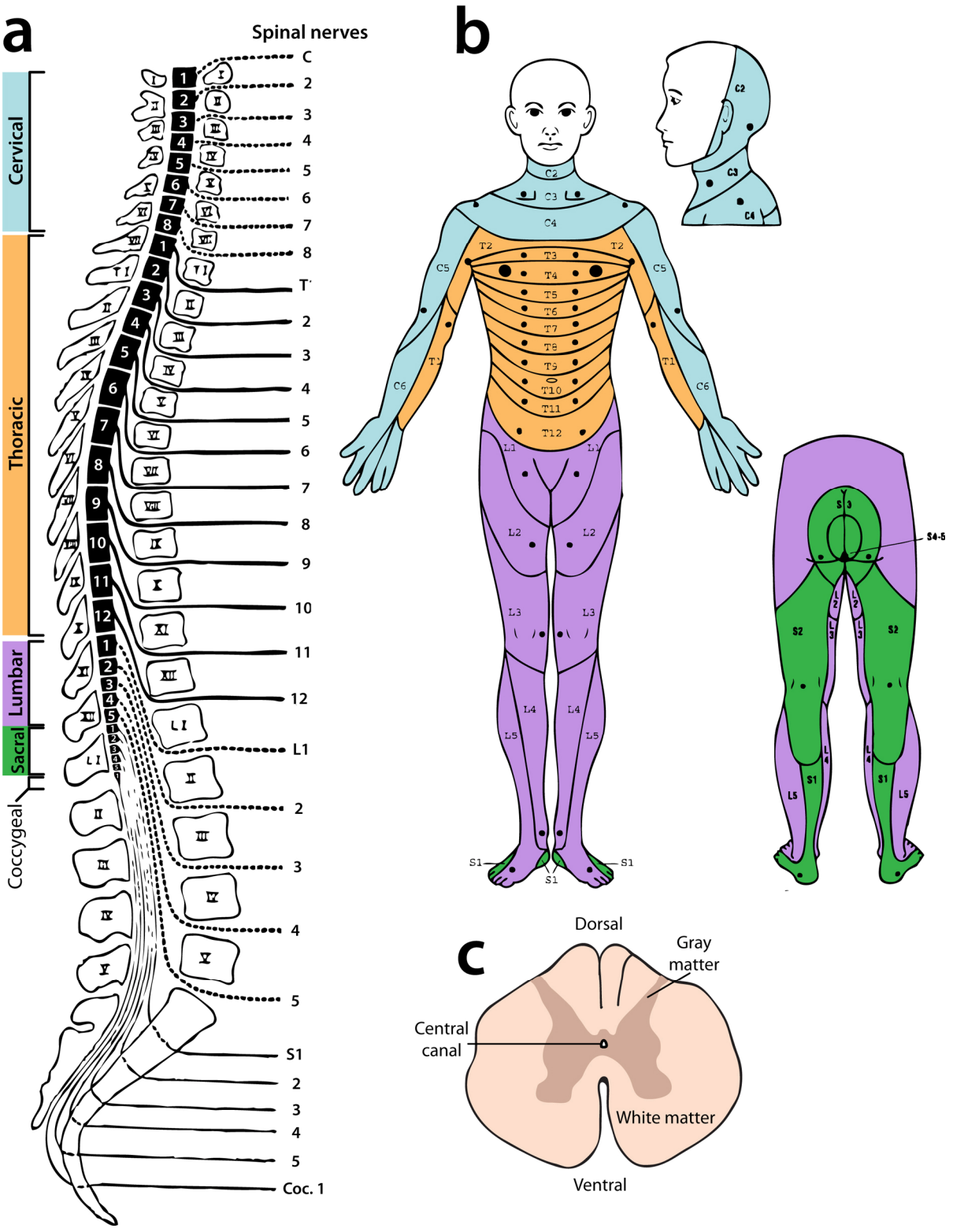
a
Spinal nerves
Cervical
Thoracic
Lumbar
Sacral
Coccygeal
C
2
3
4
5
6
7
8
T1
2
3
4
5
6
7
8
9
10
11
12
L1
2
3
4
5
S1
2
3
4
5
Coc. 1
b
C2
C3
C4
C5
C6
T1
T2
T3
T4
T5
T6
T7
T8
T9
T10
T11
T12
L1
L2
L3
L4
L5
S1
S2
S3
S4-5
c
Dorsal
Gray matter
Central canal
White matter
Ventral

(On previous page)

Figure 1.1. Anatomy and innervation of the human spinal cord. (**a**) The human spinal cord is approximately 42-45 cm in length, and about 1 cm in diameter. The spinal cord is divided into 8 cervical segments (C1-C8), 12 thoracic segments (T1-T12), 4 lumbar segments (L1-L5), 5 sacral segments (S1-S5), and 1 coccygeal segment (Co1). The spinal cord proper ends at approximately between vertebral levels L1 and L2, and is succeeded by the conus medullaris (L2-L5) and cauda equina (S1-S5). Spinal nerve roots at levels C7 and above exit the vertebral column above the corresponding vertebral body, and spinal nerve roots below C7 exit below the corresponding vertebra (6). (**b**) Dermatomes, the areas of skin innervated by each individual spinal nerve [adapted from (7)]. (Note that the face and head are innervated by the twelve cranial nerves, rather than the spinal nerves.) Injury to the spinal cord results in loss of sensation at and below the dermatome innervated by the spinal nerve at that level, as well as loss of motor control of muscles innervated by spinal nerves at and below the level of injury. (**c**) Cross-section of the spinal cord. Neuronal cell bodies are located in the gray matter, and ascending and descending axonal fiber tracts are located in the white matter. The central canal is filled with cerebrospinal fluid and extends the full length of the spinal cord. SCI can lead to a condition called syringomyelia, in which obstruction of the central canal results in the formation of a fluid-filled cyst (syrinx) which can cause adverse neurological effects.

and/or CT, in combination with a comprehensive neurological evaluation (3). SCI patients with high cervical injuries may lose function in all four limbs (tetraplegia). Patients receiving injuries above cervical level 5 (C5) often lose diaphragm function, thus forcing the patient to rely on a mechanical ventilator to breathe. Approximately 55% of injuries to the spinal cord occur at cervical levels, whereas injuries to the thoracic, lumbar, or sacral spinal cord levels are evenly distributed with each representing about 15% of all injuries (3). Injuries to more caudal spinal cord locations are generally associated with an improved prognosis compared to cervical SCI. However, injuries below cervical levels can still result in loss of sensory and motor function in the trunk and legs (paraplegia), bowel and bladder incontinence, and sexual dysfunction.

Severity of injury is the largest predictor of an SCI patient's functional outcome (8). The majority of injuries are termed 'incomplete', with some degree of sensory or motor function retained below the level of injury; in a 'complete' injury, no below-level movement or feeling is retained at all (2). To assess the severity of injury, the patient undergoes neurological testing in which the degree of above- and below-level sensory function and muscle strength are evaluated. Injury severity is diagnosed according to the assessment criteria of the American Spinal Injury Association (ASIA) Impairment Scale (AIS)[1] (7). According to AIS classification, a patient categorized as ASIA A has sustained a complete SCI, whereas a patient receiving an ASIA D or -E rating retains a relatively high level of function below the neurological level of injury (See **APPENDIX A** for ASIA Standards for Neurological Classification of SCI Worksheet). The specific functional deficits resulting from an injury to the spinal cord are determined by the particular motor and sensory pathways that are damaged (**Fig. 1.2**). Anatomically, a complete injury affects all ascending and descending spinal tracts, though not necessarily as a result of a complete spinal cord transection, with no axons traversing the injury site. A complete SCI can also result from chronic spinal cord compression

[1] While the ASIA Spinal Cord Injury Classification system has now been widely adopted as the standard motor and sensory assessment scheme for SCI patients, there also exist other functional ranking systems including the Modified Benzel Classification (9), the Walking Index for Spinal Cord Injury (WISCI) (10), and the Spinal Cord Injury-Functional Ambulation Inventory (SCI-FAI) (11). Additionally, the AIS does not score outcome measures such as bowel, bladder, and sexual function or degree of independence. Functional deficits of this nature may be assessed by rating systems such as the Spinal Cord Independence Measure (SCIM) (12), the Barthel Index (13), or the ASIA Autonomic Standards Assessment Form (**APPENDIX A**).

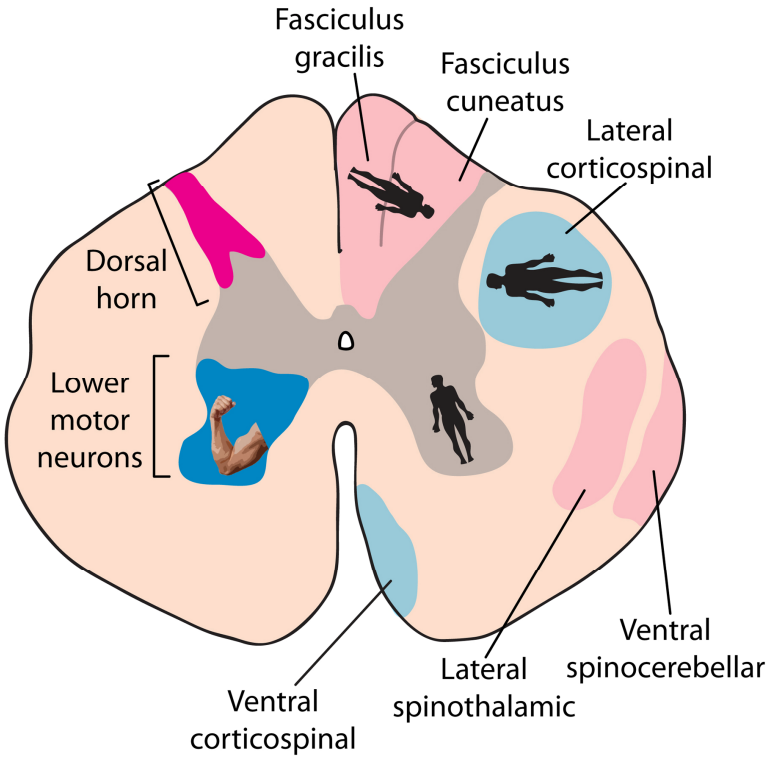

Figure 1.2. Organization of spinal motor and sensory pathways. Cartoon depicting a cross section of the spinal cord, with the locations of select white matter spinal tracts and gray matter neuron pools highlighted and labeled (14). **Left half** illustrates the location of the lower motor neuron pools of the ventral horn (dark blue), and the sensory neurons of the dorsal horn (dark pink). Flexed arm cartoon in ventral horn illustrates the *flexor-extensor rule*: motor neurons innervating flexor muscles (*e.g.*, biceps) are located more dorsal to those innervating extensor muscles (*e.g.*, triceps); as well as the *proximal-distal rule:* motor neurons innervating distal muscles (hands) are located laterally, and motor neurons that innervate proximal muscles (shoulders) are located medially. **Right half** depicts the major descending motor pathways (light blue) and ascending sensory pathways (light pink) of the spinal cord white matter columns. The corticospinal tract (CST) is comprised of fibers originating from cortical motor neurons and synapsing on lower motor neurons of the ventral horn (dark blue). Fibers of the *lateral corticospinal tract* (90% of CST axons) control the distal musculature, including fine control of the hands and fingers, and the *ventral corticospinal tract* (remaining 10% of CST axons) carries fibers that innervate proximal musculature. The *ventral spinocerebellar tract* conveys information about joint position (proprioception) to the cerebellum, and plays an important role in coordination. The *lateral spinothalamic tract* is a major conduit for pain and temperature sensation. The dorsal column of the spinal cord contains the *fasciculus gracilis* and *fasciculus cuneatus*, which transmit fine touch, vibration, and proprioceptive information from spinal levels below and above spinal level T6, respectively. Orientations of human silhouettes indicate *neuronal layering*, in which fibers within a tract (or neurons in a pool) are organized in layers corresponding to the order in which fibers are added to or exit the tract along the rostral-caudal axis.

or ischemia due to loss of blood supply, and in these cases function can be recovered by removing decompression or reperfusion, respectively (15). In contrast, an incomplete SCI only partially damages the spinal cord at the level of injury, damaging some spinal tracts and sparing others. Incomplete injuries may be described as one of five 'classical' clinical syndromes (**Fig. 1.3**), collections of common functional deficits attributed to generally similar patterns of damage to spinal cord tracts (7). For example, unilateral damage to the spinal cord generally leads to loss of ipsilateral motor function and contralateral sensory function, similar to that observed following lateral hemisection in Brown-Séquard syndrome (See **Fig. 1.3** for a description of this syndrome). However, spinal injuries are highly heterogeneous, and an individual's degree of functional impairment is always assessed on a case-by-case basis. The ASIA grading system is at best a rough classification of injury severity, and a patient's ASIA score upon initial evaluation is not a reliable predictor of his or her recovery trajectory[2]. In general, in SCI patients with incomplete injuries, the extent of function that is eventually recovered is inversely proportional to the severity of injury; in other words, the greater the initial neurological deficit, the less function the patient can expect to regain (17).

Physiological Consequences of Spinal Cord Injury

Perhaps the most recognizable functional deficit resulting from SCI is paralysis, which results from damage to the descending spinal motor tracts and/or lower motor neurons of the spinal cord. Paralysis is one of the principal factors affecting quality of life for the majority of SCI patients. According to the 2009 Christopher & Dana Reeve Foundation's Paralysis Resource Center report, 48% of individuals with paralysis resulting from SCI report "a lot of difficulty" or "complete inability" moving (1). The degree of motor function lost due to SCI depends on the spinal motor pathways affected by injury. For example, damage to the lateral corticospinal tract (CST), the major motor pathway allowing fine motor control of the extremities, will impact an individual's ability to perform tasks requiring manual dexterity,

[2] This is particularly true due to the effects of spinal shock, a transient phenomenon occurring in the first days to weeks following injury to the spinal cord. Spinal shock may be defined as a reduction or absence of spinal reflexes below the injury level that are gradually recovered (16). The precise etiology and physiological significance of spinal shock are not yet clear.

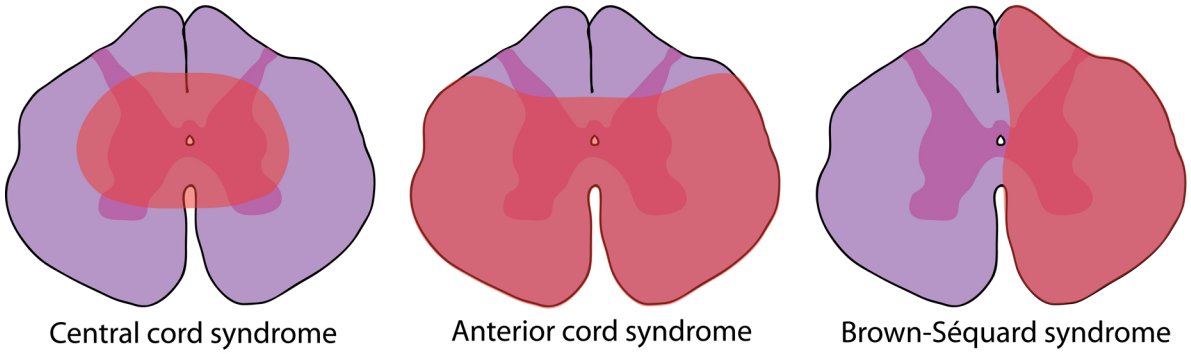

Figure 1.3. Clinical syndromes associated with incomplete spinal cord injury. The American Spinal Injury Association (ASIA) has described five clinical syndromes commonly exhibited by patients with an incomplete SCI (7). Each of these conditions can be identified by its set of common functional deficits; in each syndrome, a conserved pattern of tissue damage results in a unique array of neurological symptoms due to the organization of fiber tracts in the spinal cord. The most common of these, *central cord syndrome* (left), is often a result of hyperextension injury. This condition is characterized by significant muscle weakness in the arms and hands (upper limbs) with a smaller degree of impairment in the legs and feet (lower limbs). The functional deficits in central cord syndrome are due to neuronal layering in the spinal cord gray matter. *Anterior cord syndrome* (middle) results most often from a loss of blood supply from the anterior spinal arteries, which supply the anterior two-thirds of the spinal cord. This type of injury spares the dorsal spinal columns, thus preserving below-level sense of light touch and proprioception; however, below-level motor function and at- and below-level pain and temperature sensation is lost. *Brown-Séquard syndrome* (right) results from a lateral hemisection of the spinal cord, resulting in 1) loss of below-level motor control, proprioception, and sense of vibration on the ipsilateral side, 2) contralateral loss of below-level pain and temperature sensation, and 3) total at-level sensory loss on both sides (resulting from at-level sensory fiber decussation). Not pictured: *Cauda equina syndrome*, which results from damage to the lower motor neurons of the lumbosacral nerve roots, causing flaccid paralysis of lower limb muscles and loss of bowel and bladder reflexes; *conus medullaris syndrome*, damage to the conus medullaris (L1-L2), which results in similar functional deficits to cauda equina syndrome.

such as writing, picking up a fork, or carrying out personal hygienic routines. This type of functional impairment can be devastating, as it dramatically decreases a person's degree of independence and quality of life. In a 2004 survey in which tetraplegic SCI patients ranked the abilities that would most dramatically improve their quality of life if regained, 48.7% rated regaining arm and hand function as most important, in comparison, only 7.8% of respondents ranked regaining walking ability as most important (18).

Following damage to spinal motor tracts, spared parallel descending pathways can recover a modest degree of lost motor function, generally for coarse, voluntary movements. Approximately 41% of SCI patients experience some degree of spontaneous neurological recovery within the first year following injury (19). However, fine motor control cannot be recovered unless spared CST axons undergo compensatory sprouting (20), or severed CST axons regenerate across the lesion (21), to a sufficient enough extent to have a significant functional impact. Despite limited functional recovery, the lack of extensive regenerative CST growth following injury generally results in permanent loss of fine control of the extremities (6). Restoring even partial function to tetraplegic patients is therefore a highly desirable goal, and the development of novel therapies to promote CST regeneration remains a major objective in SCI research (22).

SCI can also affect the autonomic nervous system; depending on the type of injury, a patient may experience bowel, bladder, and sexual dysfunction. In fact, regaining sexual function was ranked as the highest priority by the greatest percentage of surveyed SCI paraplegics (26.7%), followed closely by improved bowel and bladder function and eliminating autonomic dysreflexia (18%) (18). Neurogenic bladder resulting from SCI can perhaps be best understood as "failure to store" and/or "failure to empty" urine due to dysfunction of the urinary sphincters (23). Complications resulting from neurogenic bladder are injury-specific but very frequently lead to upper and lower urinary tract infections, which usually plague the SCI patient throughout his or her lifetime. Bowel dysfunction resulting from SCI is also complex and depends on the type of injury. Patients may suffer from debilitating constipation as well as the humiliation of accidental bowel incontinence (24). Individuals with impaired bowel function must follow personalized bowel management regimens, which can be incredibly time-consuming and difficult to manage (23). Moreover, approximately 36% of those living with SCI require assistance with bowel care, a socially agonizing experience that

can severely detract from quality of life (25). Men with SCI commonly experience erectile and ejaculatory dysfunction as well as infertility (26), whereas female SCI patients may suffer from impaired sexual arousal and anorgasmia (27). The most potentially life-threatening complication of SCI is autonomic dysreflexia, a condition that can occur in patients with injuries above spinal cord level T6, the location of the splanchnic outflow (a major sympathetic output) (28). In autonomic dysreflexia, strong, below-level afferent sensory input, such as tight clothing, an overfilled bladder, or an ingrown toenail, is unable to travel past the spinal lesion site, and as a result it stimulates neurons in the sympathetic ganglia. The major reflex sympathetic response that results causes a sudden, significant vasoconstriction below the level of SCI; this response runs unopposed by the parasympathetic system which lies above the level of injury. The exaggerated, hyperreflexive sympathetic response is characterized by extreme hypertension, bradycardia, sweating, headaches, and anxiety (29). If the sensory stimulus is not removed, the sympathetic reflex response will continue to increase in the presence of persistent input; this can lead to seizures, hemorrhage, and death (28).

In addition to these serious consequences of SCI, patients also frequently suffer from uncontrolled muscle spasticity (29), chronic neuropathic pain (30), and a systemic inflammatory response that impacts peripheral organs including the lungs and kidneys (31), liver (32), bladder (33), and testes (34). A recent clinical study reported that the majority of acute traumatic SCI patients experience multiple organ failure (35). Life expectancy of SCI patients varies with severity of injury, age at injury, and time since sustaining the injury; however, life expectancy for those with SCI is universally lower than that for uninjured persons (2). Currently, the causes of death that most greatly impact life expectancy for SCI patients are pneumonia, septicemia and pulmonary embolism (2). Clearly, the field of translational SCI research is an area with multiple unmet needs for therapeutic intervention.

The culmination of the myriad of complications experienced by SCI patients is a dramatically reduced quality of life. SCI is a complex condition that profoundly impacts not only multiple aspects of physical health, but psychological and social well-being as well. Researcher Kim D. Anderson of the University of California Reeve-Irvine Research Center summarizes the difficulties faced by those living with SCI:

> What constitutes quality of life? That is a very subjective question because people value different things. After a spinal cord injury, many things are lost …. *Being paralyzed is so much more than not being able to walk*. Physiologically, there are severe impairments in bladder, bowel, cardiac, respiratory, sensory, and sexual function. Socially, relationships are difficult to maintain, and reintegration into society is quite challenging. Financially, initial and long-term medical costs are extremely burdening and, unfortunately, large proportions of people living with paralysis are not able to return to full-time work and, thus, are dependent upon state and federal assistance. Psychologically, the loss of a "normal" life can be devastating for months or years depending upon the person, and this can result in further physiological, social, and financial problems. All of these issues factor in definitions of the quality of life. [emphasis added] (18)

Clinical Management of Spinal Cord Injury

SCI is a form of acute trauma that must be managed in a careful, timely, and judicious manner in order to optimize patient outcome. Surgical intervention is needed to remove fractured bone or disc fragments compressing the spinal cord tissue (decompression) and to realign and stabilize the vertebral column (36). Though the optimal timing for surgical decompression has been debated, it is currently believed that surgery should ideally be performed between 8 and 24 hours after SCI (37). Once in the clinic, most acute SCI patients are first subjected to a comprehensive preoperative evaluation, unless decompressive surgery is deemed emergent (38). This evaluation includes a medical history, complete neurological sensory and motor evaluation, assessment of autonomic and cardiovascular dysfunction, laboratory blood tests, electrocardiogram, and diagnostic imaging (39). In addition, there is a considerable possibility that the trauma producing SCI has also resulted in injury to other vital organs, *e.g.*, the brain or liver; thus, a full physical evaluation must be performed. Such thorough medical evaluations are critical in determining outcome due to the potential importance of systemic factors, for example, hemodynamic stability, on spinal cord perfusion (39). Following preoperative evaluation, the patient may be administered medications such as antibiotics, anxiolytics, or agents to promote gastrointestinal (GI) motility, depending on the circumstances. After spinal surgery, the median length of acute-care hospitalization for an SCI patient is about twelve days (2).

There are currently no proven effective, FDA-approved interventions that can improve functional outcome if administered to an acute SCI patient. However, if patients meet the

inclusion criteria for a currently enrolling clinical trial, they may be presented with the option of receiving an experimental treatment. Due to some clinical studies demonstrating modest functional improvement if administered within eight hours of injury, many hospitals have historically administered high-dose methylprednisolone sodium succinate (MPSS), a synthetic anti-inflammatory corticosteroid, for acute SCI patients (19). However, the use of MPSS has now dramatically declined due to the considerable negative side effects associated with high-dose steroids, as well as mounting criticism surrounding the clinical trials reporting its therapeutic benefits (40, 41). A 2006 survey revealed that only 24% of spinal surgeons believed MPSS improved patient outcome and that in fact, most surgeons continued to administer the drug primarily out of a fear of litigation (42).

For SCI patients with incomplete, sub-acute (weeks) or chronic (months) injuries, physical rehabilitation may be a useful tool to improve functional recovery. Studies of body weight-supported treadmill training indicate that gait rehabilitation produces a modest improvement in patients with chronic SCI (43). The average patient with a motor incomplete SCI generally spends between five and six weeks in a clinical rehabilitation unit subsequent to leaving an acute care facility (2). After completing rehab, however, SCI patients are far from finished with medical care. During the chronic phase of injury, a plethora of medical complications may arise; each year, 30-50% of all individuals with SCI will be readmitted to the hospital (2). These patients are at particularly high risk for complications such as urinary tract infections, respiratory disease, pressure sores, and circulatory problems, all of which can be life-threatening if untreated (2). In addition, SCI patients will likely require regular follow-up medical care; for example, to assess efficacy of pain and spasticity medications, to evaluate whether adjustments need to be made to bladder or bowel programs, and to receive routine neurological and psychological evaluations. As a result, the lifetime cost of SCI-associated medical care can be as high as $4 million (2).

Experimental Models of Spinal Cord Injury

The inherent complexity of the molecular and cellular pathophysiology of SCI requires the use of experimental animal models in SCI research. These *in vivo* models are critical tools for evaluating the effects of experimental treatments on complex physiological processes like axonal regeneration, and examining clinically relevant outcome measures such as locomotor or

neurosensory function. Since human SCI is a highly heterologous condition with many variables affecting outcome, selection of the appropriate experimental model can be challenging for SCI researchers. Furthermore, the myriad of anatomical, behavioral, and pathophysiological differences between humans and laboratory animals can limit experimental studies in a variety of ways. Regardless, experimental animal models are invaluable in the ongoing search for effective new therapies for SCI (6).

The most common cause of SCI in human patients is contusion and/or compression injury (4), and a variety of animal models have been developed to approximate human contusion injury pathology (44). One of the most frequently used models is the weight-drop model of SCI, such as the NYU Spinal Cord Injury Device (45), which entails dropping a calibrated weight from a defined height onto the exposed spinal cord, resulting in a rapid and controlled displacement of spinal cord tissue (45, 46). Another common contusion injury model utilizes a mechanical impactor, such as the Ohio State University Electromechanical Spinal Cord Injury Device (47) or the Infinite Horizon Spinal Impactor Device (48), to deliver a rapid force-controlled contusion to the exposed spinal cord. A review of the various experimental contusion/compression injury models emphasizes the importance of consistency in force and displacement parameters in producing reproducible histological and behavioral outcomes (49). Though spinal contusion injury models are frequently used due to their approximation of human spinal contusion pathology, models of spinal cord transection and hemisection are also frequently utilized in SCI research. In an experimental transection model, the spinal cord is completely severed via a scissor or blade; in a hemisection model, either the dorsal or lateral half of the spinal cord is incised at one or more spinal levels (47). Though complete transection of the spinal cord is a relatively rare occurrence in humans, these models have a particular utility for investigating the mechanisms of SCI pain (50), regeneration of CST axons (51, 52), or to kindle a more hospitable environment for the introduction of therapeutic stem cells, which can be sensitive to the high levels of inflammation associated with contusion/compression injuries (47, 52-54). Dorsal hemisection models are useful for the study of discrete lesions of motor or sensory pathways; this type of injury usually leaves gray matter intact, allowing the researcher to assess the suitability of gray versus white matter for regenerative or plastic growth (47). Lateral hemisection models are suitable for assessing the ability of spared pathways on the contralateral uninjured half of the spinal cord to sprout and/or contribute to recovery of function (47).

Experimental animals are also useful for modeling injuries that produce different types of neurological deficits. Contusion/compression models can be tailored to produce mild, moderate, or severe injuries, which are associated with increasing degrees of impairment in neurological and motor recovery (55). Additionally, selecting the location of injury in animal models allows the experimenter to examine specific behavioral outcome measures. Cervical SCI models result in loss of fine motor control and ability to perform tasks requiring forelimb dexterity, while preserving normal hindlimb function (6). Models of cervical injury are frequently utilized to investigate the efficacy of treatment on CST regeneration by examining performance in fine motor tasks. In contrast, thoracic injury models produce hindlimb functional deficits, and as such are best suited for evaluating parameters such as locomotor recovery and the development of neuropathic pain (56). Whereas animals with cervical injuries of sufficient severity can lose their ability to ambulate and feed, animals with thoracic injuries retain full use of the forelimbs and can still perform these functions. Because of the significantly greater amount of post-operative animal care needed with cervical injury models, thoracic injury models are generally more practical to the researcher.

The vast majority of experimental SCI studies utilize rats and mice. The advantages of rodent models, aside from the relatively low cost and ease of experimentation, include the abundance of reproducible rodent SCI models, the relative homogeneity of genetic background and the ease of genetic manipulation, and the wealth of sensitive behavioral assessments developed for mice and rats. Rodent models are useful in optimizing the parameters of delivery for, or assessing the potential harmful side effects of, a novel or exploratory therapy (57). Rodents have been used extensively to assess the potential neuroprotective benefits of novel treatments for SCI, and rodent studies have also led to great gains in knowledge of the pathophysiology of SCI. However, there are key disadvantages to relying upon rodent models. First, there are key differences in the pathophysiology of SCI between mice, rats, and humans (6, 58-60). For example, the cellular inflammatory process exhibited by rats is different than that of humans, and is better modeled using nonhuman primates (61). Perhaps the most obvious disadvantage is the discrepancy between the nervous systems of rodents and humans, both in size and in the anatomy of neural networks (6). Large animals offer an advantage in that axonal regeneration must occur over a larger distance within the spinal cord, similar to humans (57). Additionally, because neuroanatomical tract distribution is different in bipeds and quadrupeds,

the regenerative growth and locomotor recovery of bipedal nonhuman primates following SCI are more clinically relevant than those of quadrupedal rodents (6, 61).

It is clear that rodent models alone are inadequate for assessing the safety and efficacy of novel therapies. Treatments exhibiting efficacy in rodents must subsequently be validated in large animal models, such as pigs or nonhuman primates, before translation to clinical trials. Recently, Levine and colleagues have pointed to the naturally occurring canine disorder of thoracolumbar intervertebral disk herniation as a useful model of large animal SCI, providing an alternative to nonhuman primates for the validation of therapies (62). Other models of large animal SCI, such as pigs (63) and felines (64), have also historically been used in experimental research studies. Ultimately, the choice of experimental animal utilized must be based on a careful consideration of many factors, including the nature of the research question being investigated or the intervention being tested, and the suitability of the animal model in addressing those questions.

§

Molecular and Cellular Pathophysiology of Spinal Cord Injury

Contusion injury, such as that occurring when a fractured disc impinges into the spinal cord tissue secondary to fracture-dislocation or burst fracture of the spinal column, represents the most common type of SCI (3). This type of traumatic SCI is characterized by a biphasic pattern of injury (**Fig. 1.4**). The immediate mechanical insult (primary injury) is a direct result of acute contusion and/or compression of the spinal cord tissue by displaced disc or bone fragments. Immediately, there is disruption of the vasculature causing hemorrhage, substantial cell death within the gray matter due to both the actual mechanical force of impact as well as ischemic insult, generation of a necrotic epicenter of injury, and mechanical shearing of axons in the white matter (3, 6, 65). The primary insult to the spinal cord sets into motion a prolonged, expanding wave of secondary injury, which can best be described as a cascade of pathological cellular and molecular processes that contribute to further tissue death and degeneration during sub-acute and chronic injury (6). A central goal of current SCI research is

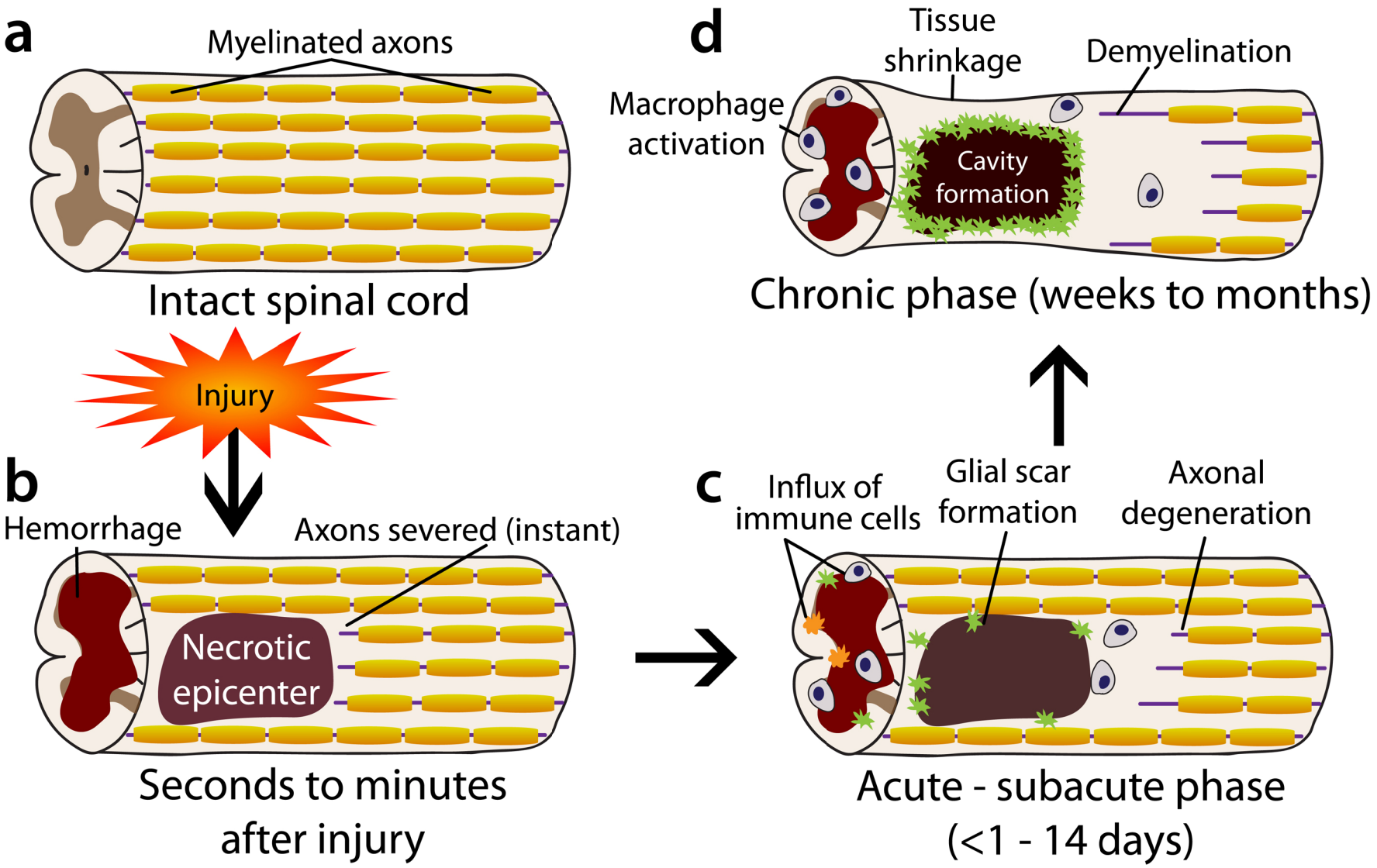
a
Myelinated axons
Intact spinal cord
Injury
b
Hemorrhage
Axons severed (instant)
Necrotic epicenter
Seconds to minutes after injury
c
Influx of immune cells
Glial scar formation
Axonal degeneration
Acute - subacute phase (<1 - 14 days)
d
Tissue shrinkage
Demyelination
Macrophage activation
Cavity formation
Chronic phase (weeks to months)

(On previous page)

Figure 1.4. Timeline of pathological secondary injury processes following spinal cord injury. (**a**) Cartoon depiction of an uninjured spinal cord, illustrating the presence of normal, healthy myelinated axons and gray matter. (**b**) Traumatic injury to the spinal cord results in an immediate death of neurons in the gray matter, thereby generating a necrotic epicenter of injury. This cell death is caused by both force of impact to the cell bodies, and hemorrhagic and ischemic insult due to mechanical disruption of the microvasculature. The large blood vessels on the spinal cord surface are more resistant to physical damage as a result of contusion injury. However, disruption of the spinal cord blood supply via occlusion of the spinal arteries leads to gray matter infarction, and subsequent reperfusion of the ischemic tissue results in the generation of cytotoxic free radicals, exacerbating injury (65). The mechanical force of the primary injury also instantly severs axonal fibers within the white matter of the cord; however, the primary injury causes considerably more damage to the gray matter with relative sparing of the peripheral white matter. Within minutes, activated microglia accumulate at the site of injury and begin to secrete cytotoxic factors including pro-inflammatory cytokines (66). (**c**) In the days to weeks following SCI, secondary injury processes continue to shape pathological changes to the injured spinal cord. Within hours, there is a massive invasion of neutrophils from the bloodstream, producing free radicals and pro-inflammatory cytokines. The first few days to weeks after injury are characterized by: accumulation of activated microglial cells and invasion of peripheral macrophages/monocytes that also secrete pro-oxidative and pro-inflammatory factors; healing of the damaged BSCB; axonal degeneration; and proliferation of glial cells that begin to form the glial scar (67). (**d**) Several weeks to months post-SCI, there is deposition of components of the extracellular matrix that cause inhibition of axonal regeneration. During this time, the glial scar also stabilizes around the cystic cavity that forms at the epicenter, presenting an additional barrier to regrowth of axons. Demyelination and degeneration of axons in and surrounding the injury site cause the spinal cord to atrophy due to loss of white matter volume (68). Furthermore, there is T cell invasion and chronic macrophage activation in the injured cord that may last months to years (69, 70).

to develop a better understanding of the complex pathophysiology of secondary injury, in order to identify and target the molecular mechanisms contributing to cell death (71).

The earliest aspects of the secondary injury cascade can be largely attributed to a massive influx of cytotoxic substances into the spinal cord tissue in the minutes to hours following injury, a direct result of the cellular damage and vascular disruption caused by the primary insult (65). Early events in the initial pathological cascade include extracellular accumulation of excitotoxic neurotransmitters, oxidative stress resulting from free radical formation and lipid peroxidation, ionic imbalance, edema formation, and an infiltration of immune cells that secrete cytotoxic factors such as cytokines and chemokines, free radicals, pro-inflammatory lipid mediators, and proteases (65, 71). Each of these in turn activates downstream intracellular signaling pathways, resulting in further cell death and demyelination in the acutely injured spinal cord (68). Diffusible factors such as cytokines also serve to recruit additional immune cells into the injured cord for days to weeks following injury, thus perpetuating the secondary injury pathology further. Furthermore, inflammation mediates a progressive opening of the blood-spinal cord barrier (BSCB), allowing inflammatory immune cells and cytotoxic factors to permeate into the cord (72). These pathological events are not simply confined to the acute phase; apoptosis, demyelination, BSCB breakdown, and axonal degeneration have been shown to continue into the chronic phase, weeks to months following SCI (73-76). Clearly, the process of secondary injury is extraordinarily complex, and as such is not fully understood.

Many drug compounds that have been evaluated as potential therapeutics for preclinical and clinical SCI are intended to target the early components of secondary injury, with the goal of attenuating the destructive cascade as early as possible and protecting the spinal cord from further secondary injury-induced damage (77). One such drug, riluzole, is a neuroprotective compound that has to date been evaluated in nine experimental studies as a potential SCI intervention (78-86), and is currently being evaluated in a Phase I clinical trial as an acute intervention for human SCI patients (87). Riluzole exerts an anti-glutamatergic effect by both blocking voltage-sensitive Na^+ channels and attenuating Ca^{2+}-dependent presynaptic glutamate release, thus protecting neurons against excitotoxic cell death (88, 89). Interest in riluzole as a treatment for SCI originated because of the central role of excitotoxicity in early secondary injury, as well as the fact that riluzole is already FDA-approved for treatment of the neurodegenerative disease amyotrophic lateral sclerosis (ALS), thus making it a highly

translatable drug for clinical SCI studies (89). Other neuroprotective compounds that have been evaluated in SCI clinical trials include MPSS (90), the neuronal membrane component monosialoganglioside GM-1 (91), and the tetracycline antibiotic minocycline (77). Unfortunately, clinical trials in SCI patients have thus far failed to produce any statistically significant functional improvements, with the dubious exception of MPSS[3] (96). Despite the failure to translate neurological benefits in preclinical studies to human SCI patients, preclinical evaluation of neuroprotective compounds continues to push forward in the hope of finding a novel effective therapy.

Role of Inflammation in Spinal Cord Injury Pathophysiology

Inflammation is the endogenous, multifaceted physiological response to injury or disease, and it encompasses a host of molecular and cellular processes with complex, diverse effects on the different tissues and organ systems in the body (97). Inflammation is one of the major forces in the secondary injury cascade, and as such, plays a central role in the pathophysiological processes that occur in the acutely injured spinal cord (98). Components of the molecular and cellular inflammatory response drive a host of adverse pathological events following SCI, such as cell death (98), disruption of the BSCB (72), generation of the glial scar (99, 100), and sensitization of neural pathways leading to neuropathic pain (30). For this reason, attenuating inflammation following SCI has been viewed as a promising therapeutic strategy for decades, and to date researchers continue to investigate the efficacy of anti-

[3] The clinical studies leading to the widespread of the steroid MPSS as an acute SCI intervention are controversial (40, 92). This is chiefly due to the fact that those studies reporting its neurological benefits exhibited statistical significance only when subjected to extensive post-hoc analysis. NASCIS I, a large, randomized multicenter clinical trial (1979-1984), showed no benefit of acutely (<12 hours post-SCI) administered MPSS over the opioid antagonist drug naloxone or placebo in improving neurological outcome up to one year post-injury (93). A subsequent study, NASCIS II (19, 94), was conducted to evaluate the efficacy of a much higher dose of MPSS for acute SCI. NASCIS II, like NASCIS I, failed to show any overall neurological improvement in patients receiving MPSS. However, a post hoc analysis detected a small gain in functional outcome of a small subgroup of patients who received the drug 3-8 hours post-injury. As a direct result of this finding, the high-dose MPSS infusion tested in NASCIS II quickly became a standard of care for acute SCI in many clinical settings throughout the world, despite the failure of subsequent clinical studies to replicate these findings (92). Today, MPSS is widely considered to be ineffective for improving function in acute SCI patients; moreover, the harmful side effects of high-dose steroid treatment actually make MPSS a dangerous clinical approach for acute SCI (40, 41, 95).

inflammatory treatment as a neuroprotective intervention for SCI. However, the cellular inflammatory response is also extraordinarily complex, and paradoxically, it alters the local environment in ways that both foster and discourage regenerative regrowth (101).

Injury to the spinal cord invokes a complex cellular response involving several different immune cell types. There is an invasion of peripheral circulating immune cells (*i.e.*, neutrophils, dendritic cells, and macrophages) into the injured spinal cord, as well as widespread activation of resident microglial cells (102). The major activities of these immune cells include phagocytosis of cellular debris, presentation of degraded peptides to helper T-lymphocytes, secretion of pro-inflammatory cytokines, chemokines, and growth factors, and free radical production (102). The dual nature of the effect of inflammation in the injured spinal cord microenvironment becomes apparent upon examining the multifaceted role of activated microglia (103). Following injury, activated microglial cells release factors, such as glial cell line-derived neurotrophic factor and transforming growth factor-beta1 (TGF-beta1), that promote neurite growth and survival (104). In contrast, these cells also produce pro-inflammatory cytokines and reactive oxygen species (ROS) that promote neuronal cell death and secrete proteoglycans that are inhibitory to neurite growth (66). These diverse functions of microglia and other immune cell types underlie the complexity of the inflammatory response and its duality in promoting both tissue damage and repair after SCI.

Historically, much attention has been focused on the potential of immunosuppressive therapies to improve functional recovery after SCI, an initiative that has been largely motivated by the desire to combat immune cell-mediated tissue damage in the injured spinal cord (102). However, as more information has been gained about the intricate forces contributing to tissue damage and tissue repair following SCI, it has become increasingly apparent that more targeted therapies must be developed. These therapies must be able to attenuate the destructive effects of the cellular immune response, such as secretion of cytotoxic factors, while preserving the processes that enhance repair and regrowth, such as clearance of cellular debris and secretion of growth factors. This type of therapeutic goal will be achieved by specifically inhibiting the intracellular signaling cascades that mediate tissue-destructive effects within the injured spinal cord; one particularly important target is pro-inflammatory signaling. One of the hallmarks of the acute inflammatory response after SCI is the oxidative metabolism of arachidonic acid

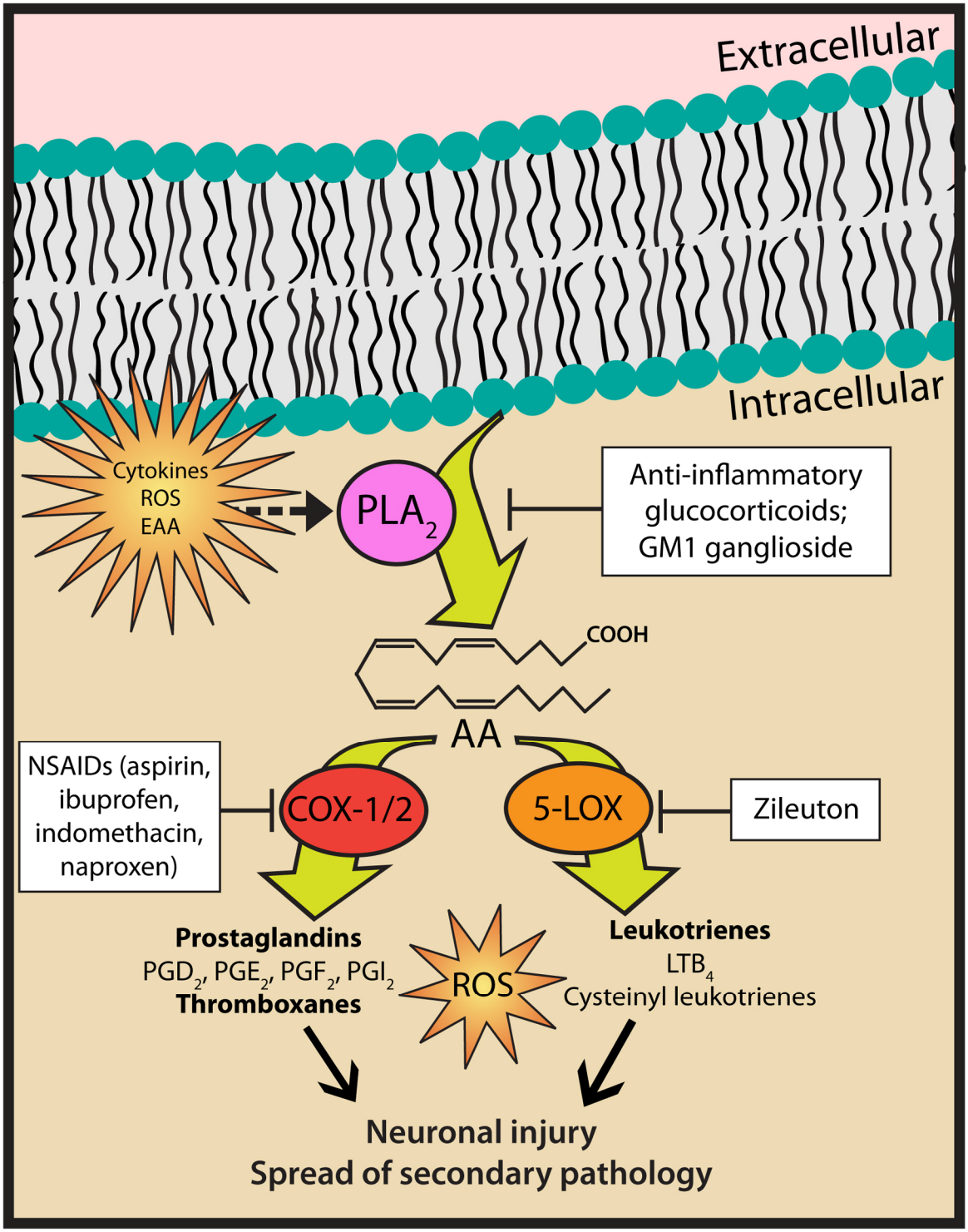
Extracellular
Intracellular
Cytokines
ROS
EAA
PLA2
Anti-inflammatory
glucocorticoids;
GM1 ganglioside
COOH
AA
NSAIDs (aspirin,
ibuprofen,
indomethacin,
naproxen)
COX-1/2
5-LOX
Zileuton
Prostaglandins
PGD2, PGE2, PGF2, PGI2
Thromboxanes
ROS
Leukotrienes
LTB4
Cysteinyl leukotrienes
Neuronal injury
Spread of secondary pathology

(On previous page)

Figure 1.5. Phospholipase A_2 activation and oxidative arachidonic acid metabolism mediate secondary neuronal injury in the injured spinal cord. Injured spinal cord tissue is an environment rich in neuroinflammation and excitotoxicity. Under these conditions, high levels of pro-inflammatory cytokines, reactive oxygen species (ROS), and excitatory amino acids lead to activation of the lipolytic enzyme phospholipase A_2 (PLA_2). When PLA_2 becomes activated, it hydrolyzes membrane-bound phospholipids into the free polyunsaturated fatty acid, arachidonic acid (AA), which in turn is metabolized by cyclooxygenase (COX-1/2) and 5-lipoxygenase (5-LOX) enzymes into the potent pro-inflammatory mediators, the prostaglandins and the leukotrienes, respectively. These bioactive eicosanoids, along with ROS produced via oxidative AA metabolism, contribute to further neuronal injury and tissue damage within the injured spinal cord. This pro-inflammatory cascade is a major and destructive component of the secondary injury process following SCI. Pharmacotherapies targeting multiple elements of this signaling network have been evaluated extensively in preclinical and clinical SCI studies. These include the PLA_2 inhibitor GM1 ganglioside, COX inhibitors such as ibuprofen and naproxen, the 5-LOX inhibitor zileuton, as well as the cysteinyl leukotriene (CysLT) receptor antagonist montelukast.

(AA). This cascade is triggered by the activation of the phospholipase A_2 (PLA_2) family of lipolytic enzymes (**Fig. 1.5**). The PLA_2 family contains the isoforms cytosolic PLA_2 ($cPLA_2$), Ca^{2+}-independent PLA_2 ($iPLA_2$) and secretory PLA_2 ($sPLA_2$), and each are activated differentially by Ca^{2+} and/or phosphorylation (105). All classes of PLA_2 isoforms are known to be expressed in the spinal cord, though their individual roles following injury have yet to be fully understood (106). It is known that PLA_2 activation begins within a few minutes after SCI and sets into motion a variety of downstream events promoting inflammation and oxidative stress, thus exacerbating neuronal injury and spread of secondary pathology (107). Thus, PLA_2 and its downstream effectors are critical elements driving the acute SCI pathological cascade, making them a major target for neuroprotective therapies.

PLA_2 activation, one of the earliest events in the neuroinflammatory process following SCI, is induced largely by activated microglia that accumulate at the site of injury within minutes (108). These activated microglia secrete free radicals and pro-inflammatory cytokines such as tumor necrosis factor-alpha (TNF-α) and interleukin-1 beta (IL-1β), resulting in increased neuronal PLA_2 expression and activation (105, 107). Excitatory amino acids, released by cellular membrane damage upon injury, further induce PLA_2 activation (105). Activated PLA_2 exerts a hydrolytic activity on membrane phospholipids within the injured tissue, releasing the polyunsaturated omega-6 fatty acid, AA. The enzymes cyclooxygenase (COX)-1 and COX-2, and 5-lipoxygenase (5-LOX), which are also stimulated by SCI (108, 109), catalyze rate-limiting steps in the conversion of AA into the bioactive eicosanoids, 20-carbon lipids that are potent mediators of inflammation and secondary injury. High levels of ROS are also produced during this process of oxidative AA metabolism. These free radicals contribute to further neuronal damage, exacerbate the cellular inflammatory response, and promote upstream PLA_2 activation, thus perpetuating the secondary injury cascade (107).

Because the PLA_2 pro-inflammatory signaling network plays such an early and central role in SCI secondary pathology, various groups have evaluated the therapeutic potential of inhibiting PLA_2 family members. Michael-Titus and colleagues demonstrated that inhibiting both $cPLA_2$ and $iPLA_2$ enzyme activity shortly following SCI in rats conferred some neuroprotection (110). In addition, there is much preclinical evidence indicating the neuroprotective benefits of the gangliosides, inhibitors of intracellular PLA_2 (111), though clinical studies examining the efficacy of gangliosides for acute SCI have not seen therapeutic

benefits in human patients (91). Until recently the specific contributions of the different PLA_2 isoforms to SCI pathology have been unclear. López-Vales *et al.* demonstrated that in mice, blocking all three PLA_2 isoforms actually inhibits recovery; interestingly, the $cPLA_2$ GIVA isoform was shown to exert a tissue-protective effect (106). These findings demonstrate that a deeper understanding of the divergent roles of PLA_2 isoforms within the injured spinal cord is needed in order to develop more effective, targeted therapies. In fact, the majority of investigations have not focused on PLA_2, but rather on the therapeutic potential of targeting downstream components of this network, such as COX signaling.

Cyclooxygenase and Lipoxygenase in Spinal Cord Injury

COX-1 and COX-2 are the rate-limiting enzymes in the biological pathway converting AA into the prostanoids—the prostaglandins, thromboxanes, and prostacyclin (**Fig. 1.6**). Activity of COX-1 and -2 is inhibited by classical non-steroidal anti-inflammatory drugs (NSAIDs), a class of nonselective COX inhibitors that includes such commonly used drugs as aspirin and ibuprofen (112). Structurally and functionally, COX-1 and -2 are very similar, both catalyzing the stepwise conversion of AA into the prostaglandins PGG_2/PGH_2 (112). The crucial distinction between these two enzymes lies in their tissue-specific expression. COX-1 is expressed constitutively in most tissues, whereas the inducible isoform COX-2 is not usually detectable in most normal tissue (though it is constitutively expressed in some tissues under normal conditions (113)) but rather is expressed predominantly by immune cells, such as activated macrophages, under inflammatory conditions. Thus, COX-1 activity plays a variety of normal homeostatic roles in various tissues of the body, but the induction of COX-2 activity is usually a strong indicator of the pathophysiological inflammatory response (112, 114).

The prostanoids are synthesized directly from the COX product PGH_2 via the activity of different enzymes, and are ubiquitously expressed throughout the body. The prostanoids have diverse physiological functions, *e.g.*, protection of the gastric mucosa, controlling menstruation and parturition, and maintaining normal kidney function; during disease pathophysiology, they also play central roles in the inflammatory process (115, 116). In the central nervous system (CNS), COX-derived prostanoids have been shown to be strong contributors to the pathological processes of a host of neurodegenerative diseases and neurological insults (117). COX

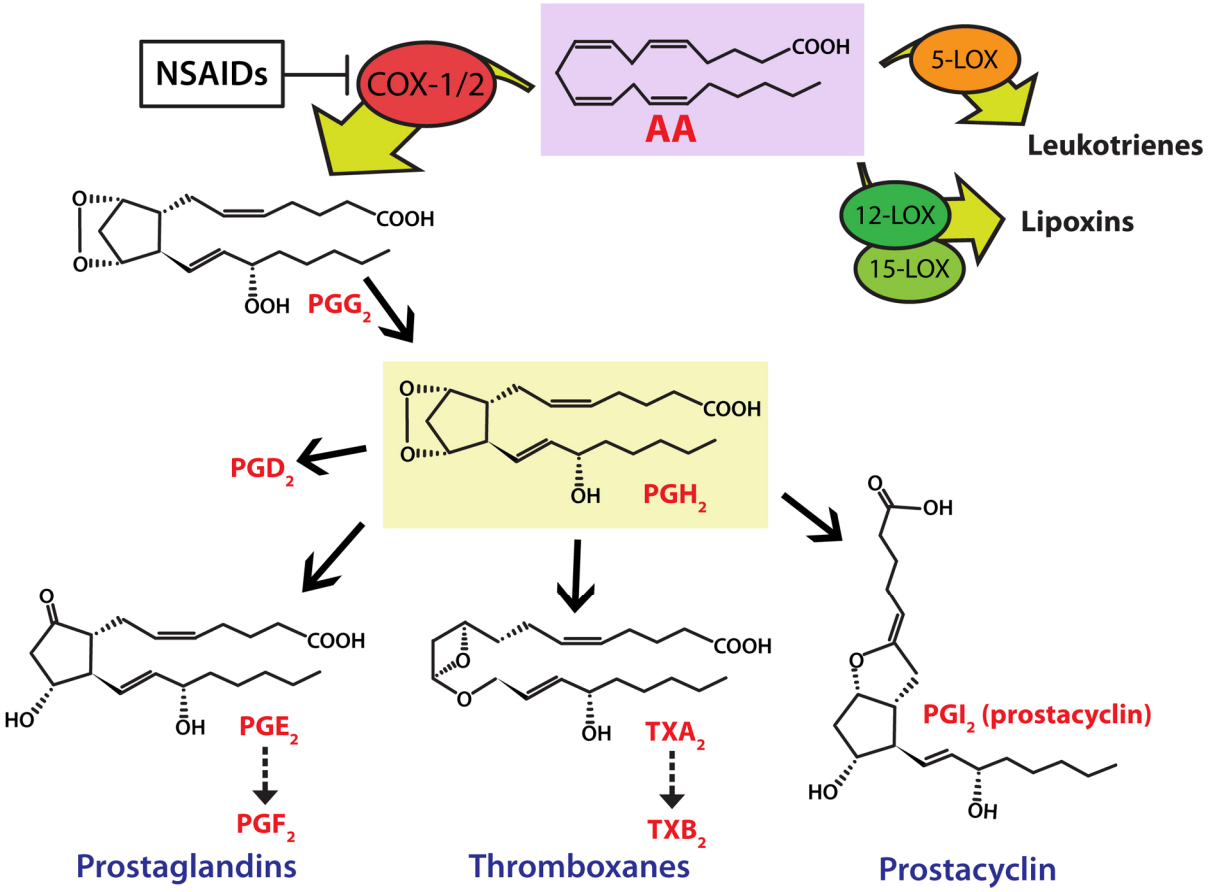

Figure 1.6. Cyclooxygenase enzymes generate prostanoids from arachidonic acid. Cyclooxygenase (COX) enzymes, COX-1 and COX-2, both catalyze the conversion of arachidonic acid (AA) into prostaglandin G_2 (PGG_2), then PGH_2. Prostaglandin synthases convert PGH_2 into the prostaglandins PGD_2, PGE_2, and PGF_2. PGH_2 can be shunted into the thromboxane (TXA_2) pathway via thromboxane synthase activity, or it be converted into prostacyclin (PGI_2) by prostacyclin synthase. Non-steroidal anti-inflammatory drugs (NSAIDs) block COX-1/2 activity, thus inhibiting production of the pro-inflammatory prostaglandins, mediators of inflammatory pain and arthritis (112).

signaling is central in pain transmission in the spinal cord, both under normal physiological conditions as well as during pathophysiological pain states following SCI (118-120). The specific contribution of COX signaling to secondary SCI pathology has long been a subject of investigation. It has been demonstrated that increased spinal cord COX-2 expression (121) and prostanoid synthesis (122) occur from very early after injury. Studies utilizing treatment with NSAIDs or COX-2-specific inhibitors prior to injury (119, 123-128) or shortly following injury (121, 129-137) have largely detected improvement in neurological and histological outcome in animal models of SCI. Of these preclinical studies, the drug that has been most frequently evaluated is indomethacin, a nonselective COX inhibitor (77). However, the clinical relevance of the findings is dubious; relatively few studies of indomethacin's efficacy have reported behavioral outcome, and most utilized pre-treatment or very early treatment during an unrealistic window of efficacy. According to Kwon and colleagues (77), greater potential may lie in ibuprofen, which has demonstrated neurological benefits even when administered up to a week following SCI (136).

The lipoxygenase (LOX) family of enzymes is parallel to the COX pathway in the oxidative AA metabolism signaling network. The LOX family is comprised of 5-LOX, 12-LOX, and 15-LOX, all of which catalyze the conversion of AA into bioactive eicosanoids (**Fig. 1.7**). The 12-LOX and 15-LOX pathways produce the lipoxins, which are unique among the lipid mediators in that they exert anti-inflammatory action (138) and, interestingly, appear to play a role in attenuating inflammatory pain within the spinal cord (139). 5-LOX, however, catalyzes the rate-limiting step in the conversion of AA into the pro-inflammatory leukotrienes: leukotriene B4 (LTB_4) and the cysteinyl leukotrienes (CysLTs). The leukotrienes have long been recognized for their fundamental role in promoting and sustaining inflammation, especially in asthma and the allergic response (140). As such, drugs such as the 5-LOX inhibitor zileuton and the CysLT receptor antagonist montelukast are commonly used in the clinical treatment of asthma and bronchial constriction.

Though the potential role of lipoxins in SCI has not yet been explored, it is now known that the leukotrienes are important mediators in the secondary pathogenesis of SCI. Experimental studies have revealed that LTB_4 levels are increased within the injured spinal cord in the hours to days following SCI (141, 142). Genovese and colleagues have shown that

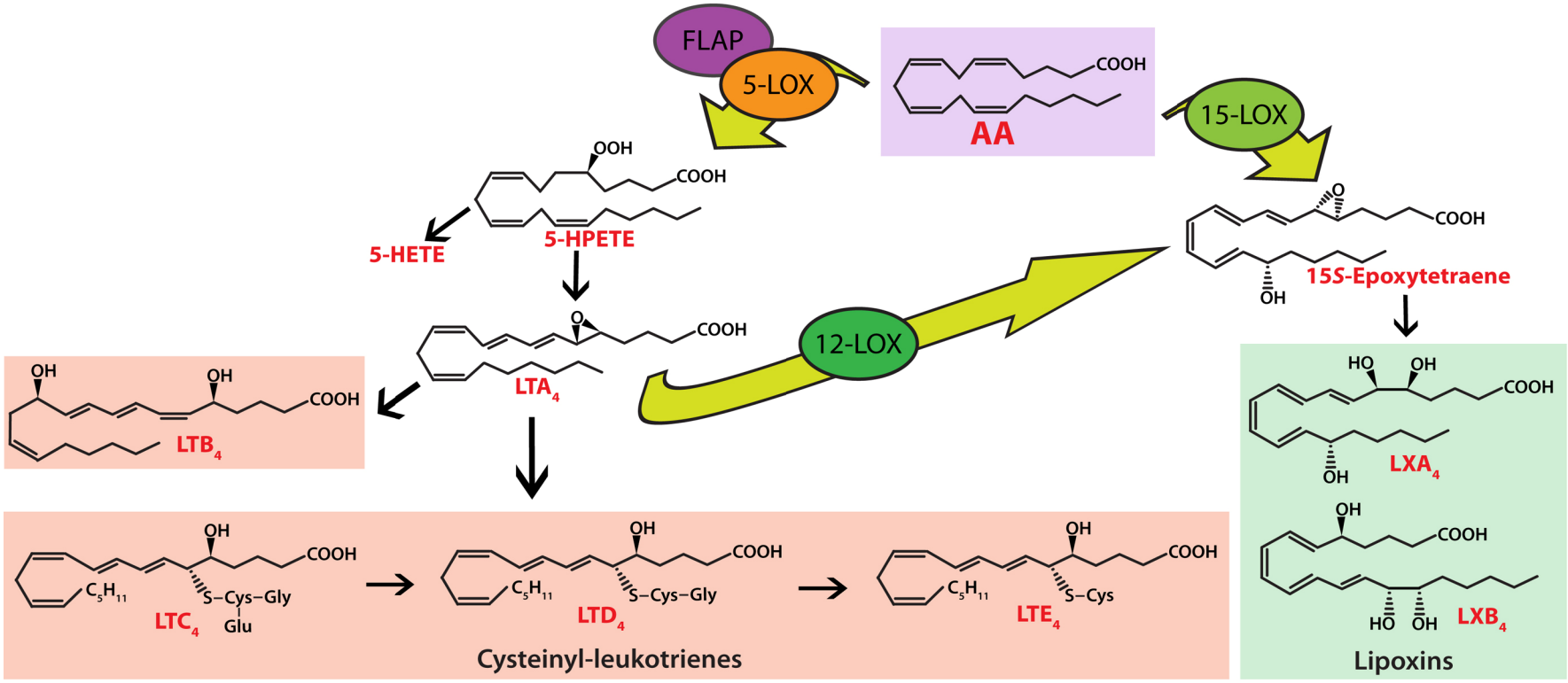
FLAP
5-LOX
AA
COOH
15-LOX
OOH
COOH
5-HETE
5-HPETE
O
COOH
OH
15S-Epoxytetraene
12-LOX
OH
OH
COOH
LTB4
LTA4
HO
OH
COOH
LXA4
OH
C5H11
S–Cys–Gly
Glu
LTC4
LTD4
LTE4
S–Cys
Cysteinyl-leukotrienes
OH
COOH
HO
OH
LXB4
Lipoxins

(On previous page)

Figure 1.7. Lipoxygenase enzymes catalyze conversion of arachidonic acid into the pro-inflammatory leukotrienes and the anti-inflammatory lipoxins. Arachidonic acid (AA), freed by PLA_2 hydrolysis of membrane phospholipids, is metabolized by 5-lipoxygenase (5-LOX) and the 5-lipoxygenase-activating protein (FLAP) into 5-hydroperoxyeicosatetraenoic acid (5-HPETE). 5-HPETE is reduced to 5-hydroxyeicosatetraenoic acid (5-HETE), and then converted by 5-LOX to leukotriene A4 (LTA_4). Via the activity of LTA_4 hydrolase, LTA_4 is converted into the pro-inflammatory lipid mediator, leukotriene B4 (LTB_4). LTB_4 is a potent chemoattractant mediating leukocyte infiltration into the spinal cord and aggravating the secondary injury process. Via glutathione-*S*-transferase II activity in cells such as mast cells, LTA_4 can also be converted into leukotriene C_4 (LTC_4), a member of the cysteinyl leukotriene (CysLT) family. LTC_4 can then be converted to the other two CysLTs, leukotrienes D4 (LTD_4) and -E4 (LTE_4), by the enzymes gamma-glutamyl transpeptidase and dipeptidase, respectively (143). 15-lipoxygenase (15-LOX), expressed in leukocytes, produces the anti-inflammatory lipoxins, which promote processes such as vasorelaxation and inhibition of polymorphonuclear cell infiltration through the vascular endothelium (138).

5-LOX knockout mice exhibit reduced neutrophil infiltration, neuronal death, and axonal degeneration after SCI compared to wild-types; additionally, they found that these mice have improved motor function following SCI (144). In a subsequent study, the same group showed similar histological and functional improvements with zileuton and montelukast treatment, specifically revealing the importance of the CysLTs in driving SCI pathology (142). Recently, Saiwai *et al.* demonstrated that interaction between LTB_4 and its receptor, the leukocyte-specific LTB_4 receptor 1 (BLT1), promotes the infiltration of neutrophils, macrophages, and microglia into the injured spinal cord within the first week following SCI (145). Importantly, blocking the LTB_4-BLT1 axis reduced secondary pathophysiologies including neuronal death and white matter loss, and enhanced motor recovery. Together, these studies reveal that both LTB_4 and CysLT signaling mediate secondary SCI pathology early after injury.

Pharmacological Inhibition of COX and 5-LOX Activity

COX inhibition has been extensively evaluated as a potential neuroprotective therapy for acute SCI, but there are multiple complications with the clinical use of COX inhibitors. The first-generation COX inhibitors, the classical NSAIDs, nonselectively inhibit COX-1 and COX-2; common over-the-counter drugs such as aspirin and ibuprofen belong to this class of drugs, and each inhibits COX-1 and -2 at approximately equal potency. Though these drugs are very widely used to treat inflammatory pain, long-term or high-dose NSAID use is associated with adverse side effects. About 1% of chronic NSAID users experience GI complications such as ulcers and GI bleeding (112) and acute renal failure (113). Because of the potential severity of these side effects, NSAIDs are implicated in almost half of all drug-related medical emergencies (146). These side effects have been largely attributed to the inhibitory action of NSAID treatment on normal physiological COX-1 activity, which is necessary for protection of gastric and renal tissues (113). In 1988, it was discovered that the inducible COX-2 isoform is the primary COX enzyme responsible for inflammatory pain, thus opening the door for a new approach to anti-inflammatory treatment (112). The COX-2-specific inhibitors, the coxibs, were developed in the 1990s as a novel solution to sidestep GI irritation while still maintaining therapeutic efficacy comparable to classical NSAIDs (147). The coxibs have indeed demonstrated improved GI tolerability over NSAIDs in clinical trials (148). However,

subsequent studies have found that COX inhibitors—most notably, rofecoxib (Vioxx)—can cause a dramatic increase in potentially fatal cardiovascular side effects including heart attack, stroke, and thrombosis (149). As a result, rofecoxib was pulled off the market in 2004, and to date there has been relatively little progress in the development of safer COX inhibitors with enhanced tolerability (149).

Based on the findings that both COX and 5-LOX signaling contribute to the secondary pathology of SCI (121, 142), one may speculate that inhibiting the COX arm of AA metabolism alone may be an insufficient strategy by which to attenuate inflammation in the acutely injured spinal cord. Rather, dual blockade of both COX and 5-LOX pathways may be crucial in order to overcome the potent inflammation that drives vascular disruption, cell death, and a host of other destructive processes early after SCI. Lending support to this idea is the finding that AA can be "shunted" into one arm of AA metabolism when the other is blocked, effectively compensating for pharmacological inhibition of one pathway by increasing AA flux through the other pathway. An example of the AA shunt can be found in the phenomenon of aspirin-induced asthma. In this condition, treatment of asthmatic patients with NSAIDs acutely exacerbates the symptoms of asthma (150), primarily due to COX inhibition promoting formation of leukotrienes in the lungs (151). Further evidence for the concept of an AA shunt can be found in studies of lung cancer, a disease for which it is known that the prostanoids and leukotrienes both exert pro-tumorigenic effects (152). Ye and colleagues showed that pharmacological COX-2 inhibition decreased levels of the COX product PGE_2, but actually increased LTB_4 levels, in cigarette smoke-induced colonic adenomas (153). Notably, they found that dual inhibition of COX-2 and 5-LOX inhibited tumor growth more effectively than either COX-2 inhibition or 5-LOX inhibition alone, illustrating a synergistic effect of simultaneously blocking both pathways (153). Furthermore, clinical studies of heavy cigarette smokers found that one month of treatment with the COX-2 inhibitor celecoxib suppressed PGE_2 but markedly increased LTB_4 levels in the alveolar macrophages of smokers' lungs (154, 155). As a result of these findings, dual COX/5-LOX inhibition has been suggested as an effective prophylactic for lung cancer prevention with efficacy superseding that of COX or 5-LOX inhibition alone (152). Together, this data demonstrates that COX inhibition can lead to a shunt of AA metabolism toward the 5-LOX pathway, increasing production of the pro-inflammatory leukotrienes, which paradoxically enhances the inflammatory response (156).

It is because of both of these undesirable effects of COX inhibition—the marked increase in GI, renal, and cardiovascular side effects, as well as the shunting of AA through the pro-inflammatory 5-LOX pathway—that a new strategy in anti-inflammatory therapy has received increasing attention in the last decade. The approach of dual COX and 5-LOX inhibition has gained popularity because of the benefits of increased anti-inflammatory potential (compared to classical anti-inflammatory drugs), as well as its demonstrated utility in blocking the development and progression of cancer, in which both COX and 5-LOX products promote cancer cell growth and survival (157). The dual-acting COX/5-LOX inhibitor that has been most extensively studied in human clinical trials is licofelone, which has now successfully passed Phase III clinical trials for osteoarthritis (158). Licofelone is a competitive inhibitor of COX-1, COX-2, and 5-LOX enzymes and blocks formation of the pro-inflammatory prostanoids and leukotrienes, while exhibiting improved GI tolerability compared to classical NSAIDs such as naproxen (158, 159). Importantly, licofelone does not inhibit the 12-LOX or 15-LOX pathways, which synthesize the anti-inflammatory lipoxins (160) (**Fig 1.7**), as previous generations of COX/LOX inhibitors have done (161). In addition, studies have shown that treatment with licofelone is neuroprotective and improves behavioral outcome in experimental models of Huntington's disease (162, 163) and Parkinson's disease (164). These findings strongly suggest a potential neuroprotective role of licofelone treatment for other neurological disorders.

In summary, experimental studies have found that COX and 5-LOX activity are both detrimental to neurological outcome following SCI, and as a result it is thought that early inhibition of these pathways should produce neuroprotective, beneficial effects in SCI. However, to date no one has performed an extensive evaluation of the neuroprotective properties of combined COX/5-LOX inhibition in an acute SCI model. Due to the recent clinical advancement of dual COX/5-LOX inhibitors such as licofelone, which confer neuroprotective benefits while exhibiting reduced side effects versus classical anti-inflammatory drugs, a combined anti-inflammatory therapeutic approach for acute SCI may therefore be a promising, novel therapeutic strategy.

§

The BSCB is the specialized system of capillary endothelial cells (ECs) and associated structures that serves the important function of limiting the diffusion of substances between the bloodstream and the spinal cord tissue (**Fig. 1.8**) (165, 166). The BSCB is similar to the blood-brain barrier in its composition and functionality; however, there are key differences between the two barrier systems, and as such the BSCB should be considered as distinct and separate from the blood-brain barrier (166). One major distinction is that BSCB permeability is moderately higher than that of its counterpart in the brain (166), probably because of relatively lower expression of some tight junction and adherens junction proteins (167). Compared to the blood-brain barrier, which has been a topic of frequent investigation, much remains to be understood about BSCB properties under normal physiological or pathological conditions.

BSCB dysfunction following traumatic SCI has been extensively studied by assessing its permeability to tracer molecules of various sizes. Intravascular delivery of low molecular weight, fluorescently-labeled tracers, albumin-binding dyes, and contrast agents such as gadolinium allows BSCB function to be assessed both histologically (168-170) and via functional imaging techniques such as dynamic contrast-enhanced MRI (DCE-MRI) (171, 172). Using these techniques, it has become evident that an extended time course of BSCB disruption takes place following trauma to the spinal cord. The mechanical force of injury instantly compromises the integrity of the BSCB, and the secondary injury cascades appear to contribute to a biphasic pattern of barrier breakdown over the days to weeks following SCI (72). Roughly, peak disruption occurs early after injury, barrier properties are re-established by 2-4 weeks post-SCI (173-176), and a secondary disruption appears to occur in the weeks to months following injury, with gradual restoration of barrier integrity (177). In addition, loss of BSCB integrity is not limited to the initial site of injury, but spreads along the axis of the spinal cord, likely due to factors such as oxidative stress that are associated with the spread of secondary injury pathology (72, 173). Unfortunately, a cohesive understanding of the BSCB response to SCI still remains elusive, in large part because of the literature's considerable variability in SCI models used, time windows analyzed, and size of vascular tracers utilized.

The changes in the BSCB underlying increased permeability after SCI include compromised tight junctional integrity and increased vesicular transcellular transport (166, 178). These morphological changes are thought to be largely driven by the sustained release of

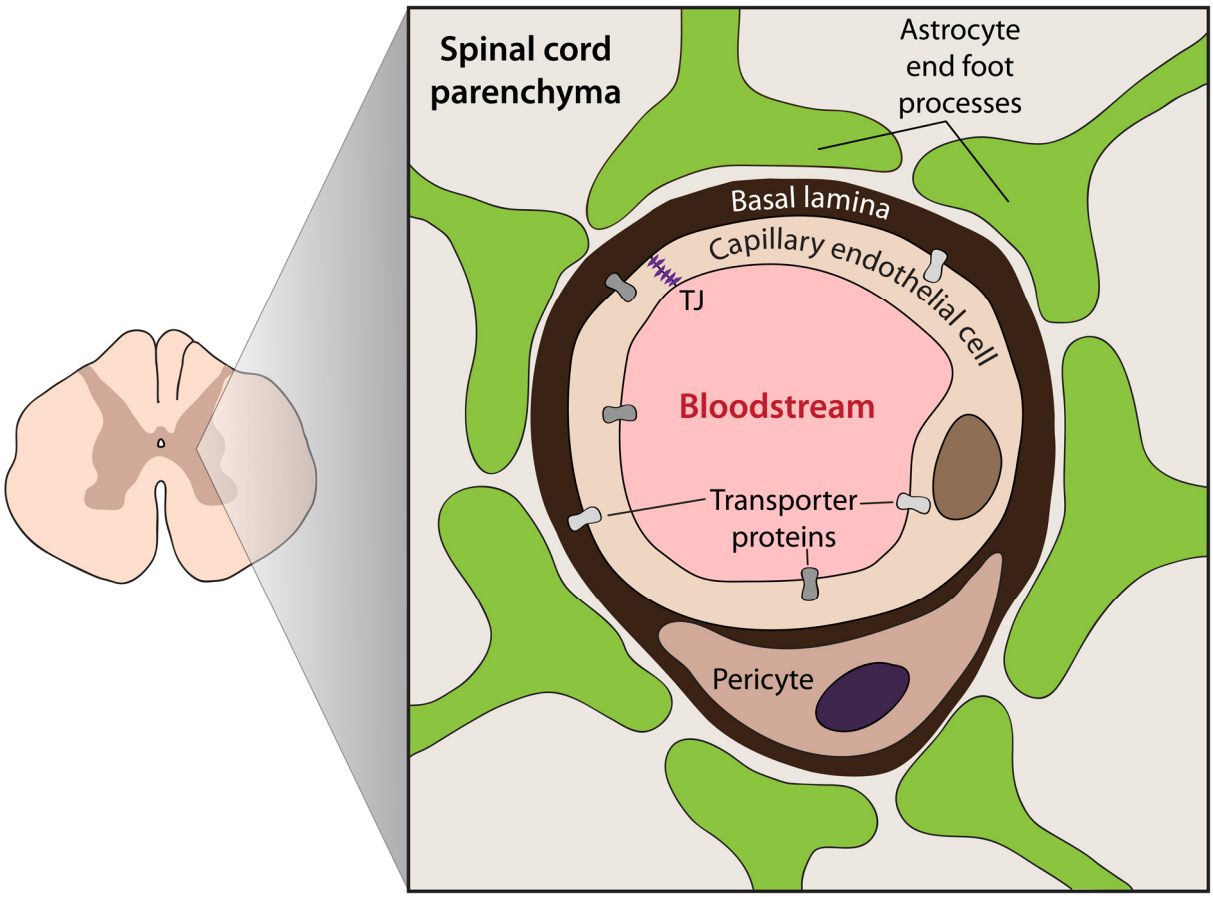

Figure 1.8. The blood-spinal cord barrier. Illustration depicting the components of the blood-spinal cord barrier (BSCB), the system of microvascular structures that tightly regulates the flow of substances between the bloodstream and spinal cord. Capillaries within the spinal cord are composed of endothelial cells (ECs) that lack cell membrane fenestrations and pinocytic vacuoles, thus preventing transcellular diffusion of molecules (179). Instead, a variety of active transporters are expressed on the luminal and adluminal EC membranes, allowing selective transport of substances in and out of the cell. Tight junctions (TJ) between ECs restrict the paracellular passage of substances. The basal lamina is composed of a layer of extracellular matrix which is maintained by the other cells of the BSCB; it engulfs capillary ECs as well as pericytes, which are cells that associate with the outer wall of the capillary. Pericytes function as regulators of EC proliferation, migration, and differentiation (166). The outermost component of the BSCB is comprised of the endfoot processes of astrocytes. These processes secrete factors that maintain the barrier properties of the BSCB, but are not actually involved in directly limiting molecular diffusion (166).

pro-oxidative and pro-inflammatory factors by infiltrating immune cells (166, 180, 181). Active transport at the BSCB is a sophisticated system allowing for the selective uptake and efflux by ECs of a very large variety of endogenous and exogenous compounds, thus greatly influencing BSCB permeability to specific substrates. Despite the central role that transporter systems play in a large number of neurological diseases (182-188), SCI-associated changes in BSCB selective transport has not been extensively studied. It has been shown that differential EC expression of glucose-1 transporter (Glut-1) following injury is closely linked to blood vessel permeability (189). Additionally, several studies have demonstrated acute and chronic changes in expression of glutamate transporters (190-192) and the water transport channels, aquaporins (193, 194) after SCI. However, there is one particular class of BSCB transporters that is known to play a significant role in several CNS pathologies, but which has not yet been characterized in SCI—the ATP-binding cassette (ABC) transporters.

P-glycoprotein: Multidrug Efflux Transporter

The ABC transporter superfamily is among the largest and oldest classes of proteins known. Members of this family of transmembrane proteins share a conserved domain structure, each possessing two nucleotide-binding domains (the active sites for ATP hydrolysis), and two substrate-binding domains (195, 196). All ABC transporters share a common function of translocation of substrates from one side of the lipid bilayer to the other, though the incredible variability in substrate recognition and the diverse expression patterns of these proteins give them an extraordinary range of biological functions (182). ABC transporters are evolutionarily ancient; expressed in bacteria and archaebacteria, they serve a vital function in the active import of nutrients, peptides, ions, and vitamins (195). In mammals, this family of transporters functions in the transport of both endogenous and xenobiotic substrates between different biological compartments, and are particularly important for the function of blood-tissue barriers (197). Many ABC transporter family members are expressed at the blood-CNS barriers where they have important roles in maintaining homeostasis in the brain and spinal cord, and are also implicated in various disease pathologies (182, 198).

P-glycoprotein (Pgp, ABCB1/MDR1) is one of the most extensively characterized ABC transporters. Pgp is a 170-kDa, 12-transmembrane glycoprotein expressed on cell membranes

of a variety of cell and tissue types. Its fundamental mechanism of action is to extrude substrates against their concentration gradients from within the cell membrane to the extracellular space, using the energy from ATP hydrolysis. The crystal structure of Pgp was recently solved (199), revealing the structural basis for the transporter's substrate binding and efflux activity (**Fig. 1.9**). Pgp can exist in two fundamental conformations: 1) an "inward facing conformation", in which a large, open cytoplasmic pocket allows the binding of two ATP molecules from the cytosol and one molecule of substrate from the inner leaflet of the cell membrane; 2) an "outward facing conformation", assumed via an ATP hydrolysis-powered conformational shift, which exposes the substrate-binding domain to the extracellular space, thus releasing the substrate (199).

Pgp is expressed in several tissues of the body, where its efflux transport activity allows it to serve a variety of functions. In the intestinal epithelium, Pgp regulates drug absorption (200); in hepatocytes, it regulates excretion of bile salts (201); it regulates renal clearance of drugs in the kidney (202). Pgp is expressed on the luminal membrane of capillary ECs of the blood-brain- and blood-spinal cord barriers, where it limits the blood-to-CNS penetration of various substances (203). Pgp is also expressed in the blood-testis barrier (204), blood-placental barrier (205), and the retinal pigment epithelium (206). The ability of one single transporter protein to perform such a wide range of biological actions is due to a remarkably broad substrate specificity (203). Pgp possesses a promiscuous binding pocket, with an upper half rich in hydrophobic and aromatic residues, and a lower half with charged and polar residues; it is this domain that enables Pgp to bind such hundreds of compounds with dramatically different structures and sizes (199). Pgp is able to bind several types of endogenous substrates, *e.g.*, bile salts (201), endogenous opioid peptides (207), oxidized lipids (208), somatostatin and substance P (209), endogenous steroid hormones (210), beta amyloid peptide (211), and platelet-activating factor (212). Furthermore, Pgp also recognizes a staggering variety of xenobiotic substrates, including the therapeutic drugs colchicine, taxol, paclitaxel, phenytoin, rapamycin, ivermectin, glucocorticoids, cyclosporin A, dexamethasone, digoxin, and HIV protease inhibitors, to name a few (203). This substrate promiscuity equips Pgp with the ability to serve a highly protective "gatekeeper" function at the blood-CNS barriers, limiting the CNS entry of a multitude of potentially cytotoxic compounds (213). This protective function, however, is a double-edged sword—it is precisely because of Pgp's strict "gatekeeping" activity that it is now recognized as a major obstacle to therapeutic drug delivery (214).

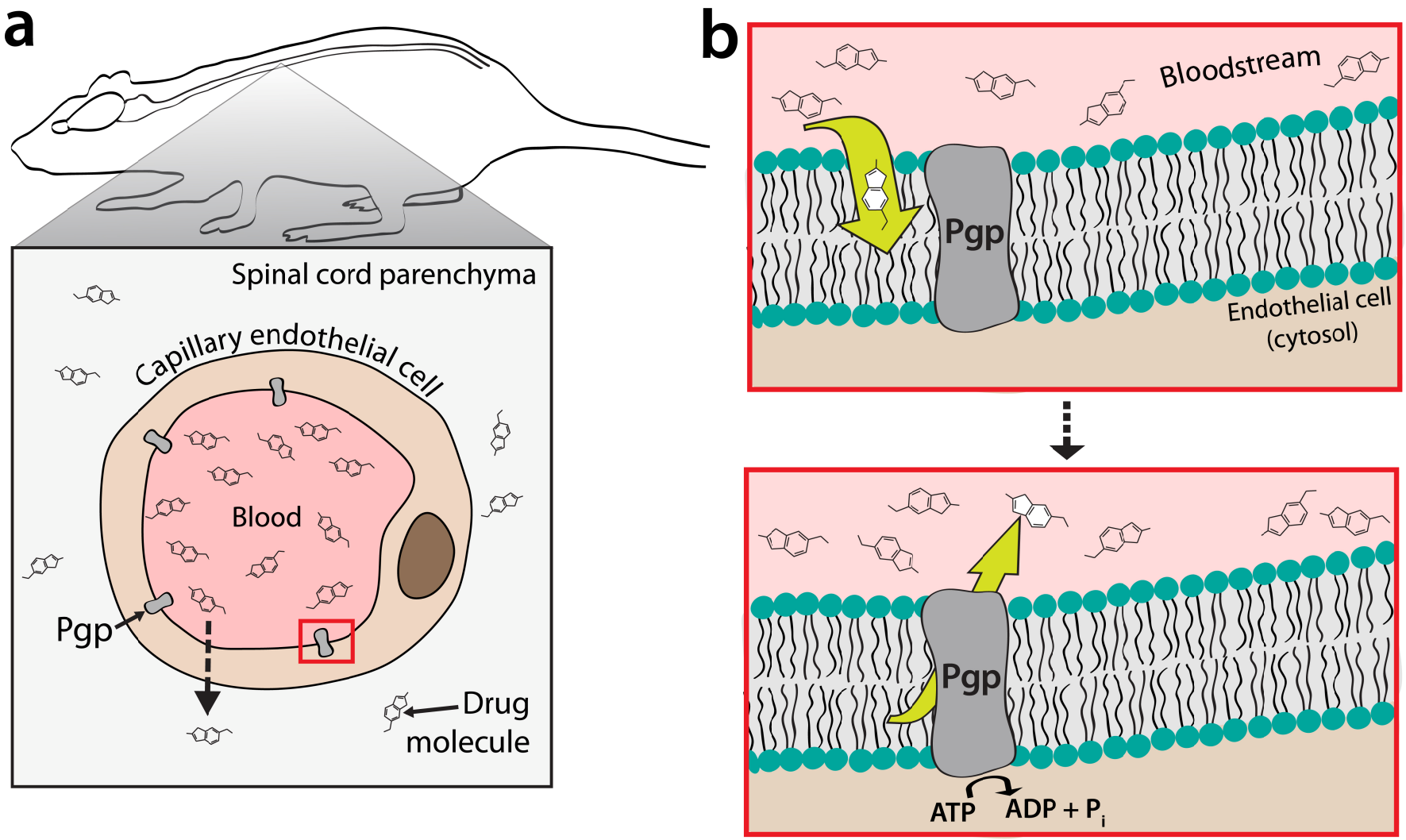
a
Spinal cord parenchyma
Capillary endothelial cell
Blood
Pgp
Drug
molecule
b
Bloodstream
Pgp
Endothelial cell
(cytosol)
Pgp
ATP
ADP + P$_i$

(On previous page)

Figure 1.9. Mechanism of P-glycoprotein-mediated active transport. Cartoon depicting the conformational change of P-glycoprotein (Pgp) which occurs during efflux transport of substrates. (**a**) Pgp is a 12-transmembrane glycoprotein with two large intracellular domains. In the inward-facing conformation of Pgp, its two structurally similar halves form a large internal pocket which allows access to the cytoplasm and the inner leaflet of the membrane. Substrate (blue) originating from the extracellular space diffuses into the lipid membrane and enters directly from the inner leaflet into Pgp's substrate binding pocket (green). Substrate binding stimulates binding of one ATP molecule to each of Pgp's two nucleotide-binding domains. (**b**) (View rotated 90°) ATPase activity is thought to cause a dimerization of the nucleotide-binding domains, thus shifting Pgp to the outward facing conformation, and releasing bound substrate into the extracellular space. It is through this drug efflux transport activity that Pgp expressed at the BSCB limits drug penetration from bloodstream to spinal cord tissue. Illustration is based on crystal structure of Pgp from Aller *et al*. (199).

Pgp is notorious for the phenomenon of multidrug resistance (MDR), for which it received its original genetic nomenclature, MDR1 (215). Pgp was first described in colchicine-resistant tumor cells (216), and it has since become well established that overexpression of Pgp causes simultaneous cross-resistance to chemotherapeutics in multiple types of cancer (217, 218). As a result, a major goal of current oncology research is overcoming Pgp-mediated MDR in order to improve the efficacy of cancer therapy (219, 220). More recently, it has become recognized that pathological Pgp overexpression also presents a significant impediment to the therapeutic treatment of CNS diseases[4]. Several preclinical studies have detected altered brain Pgp expression in models of epilepsy (221, 222), cerebral ischemia (223), ALS (224, 225), and Alzheimer's disease (226). In addition, clinical studies have shown altered brain Pgp expression and activity in patients with Parkinson's disease (227-229), Alzheimer's disease (230), seizure (231), schizophrenia (232), and HIV encephalitis (233). In neurological diseases where Pgp is overexpressed at the blood-brain barrier, delivery of therapeutic drugs to the brain can be dramatically impaired. It is therefore evident that Pgp-mediated pharmacoresistance is a barrier to the effective treatment of not only cancer, but multiple neurological diseases, and it must be overcome in order to improve treatment of these disorders.

There are a variety of pharmacological Pgp inhibitors available; however, the use of these inhibitors to combat Pgp-mediated pharmacoresistance has been historically difficult due to low tolerability, pharmacokinetic interactions with chemotherapeutics, and cross-interactions with other ABC transporters (220). Recently, some have suggested that rather than directly inhibiting Pgp activity, modulating Pgp expression by targeting the intracellular mechanisms that drive its up-regulation may be a more effective strategy to overcome drug resistance (187, 214, 234). Whether it is disease-associated pathophysiological mechanisms, or the pharmacological compounds used to treat the disease itself, which drives Pgp overexpression in neurological diseases largely remains unclear. According to *in vitro* studies in brain capillaries, ABCB1 gene expression in the CNS can be up-regulated by pro-inflammatory mediators (*e.g.*, TNF-α, endothelin-1, and PGE_2), oxidative stress, or nuclear receptors (198, 214). However, to date relatively few studies have examined the mechanisms of Pgp regulation in clinically relevant animal models. Some important insight can be gained from the work of Potschka and

[4] In this dissertation, the term "pathological Pgp overexpression" will be used to indicate Pgp up-regulation and/or overexpression driven by pathological, disease-associated mechanisms.

colleagues, who have characterized the molecular mechanisms responsible for Pgp overexpression in drug-resistant epilepsy (221). Through their studies, they have formulated a model describing how seizure activity induces Pgp overexpression via a glutamate-signaling cascade involving COX-2 and the prostaglandin E receptor 1 (EP1) (**Fig. 1.10**) (222, 235). Notably, Potschka *et al.* have demonstrated that treatment with the COX-2 inhibitor celecoxib counteracted seizure-induced Pgp overexpression and enhanced therapeutic brain delivery of the anti-epileptic drug phenytoin in rats (236). These promising findings may lead the way toward a simple strategy to overcome resistance to therapeutic drug delivery for epileptic patients. Such a strategy could also have potential for the attenuation of drug resistance in CNS pathologies with shared pathological characteristics such as glutamate toxicity or neuroinflammation.

Interestingly, Milane *et al.* have recently demonstrated that mice expressing mutant SOD1—a commonly used model of the neurodegenerative disease ALS—overexpress Pgp in the brain and exhibit decreased brain concentrations of systemically administered riluzole (224). Though this group has not yet isolated the pathway(s) underlying this phenomenon, it is tempting to speculate that signaling through the glutamate/COX-2/PGE_2 axis is a likely candidate, since glutamate excitotoxicity is a major component of ALS pathology (237). In addition, several groups have shown that COX inhibition is also effective in attenuating Pgp-mediated MDR in various cancer cell lines (238-241), suggesting that COX-mediated pro-inflammatory signaling may even be a universal pathway by which Pgp becomes pathologically overexpressed.

A Potential Role for P-glycoprotein in Spinal Cord Injury

In 2000, Bernards and colleagues (242) were the first to acknowledge the potential role of Pgp in limiting therapeutic delivery of methylprednisolone to the spinal cord. Systemic, high-dose MPSS is fraught with side effects (*e.g.,* pneumonia and sepsis) that can seriously threaten the health of an already critical acute SCI patient, which is one of the major reasons why MPSS use for acute SCI has dramatically declined (40, 95). Koszdin *et al.* demonstrated that in the pig, spinal cord bioavailability of MPSS is dramatically lower following *i.v.* administration compared to intrathecal injection, an observation that they speculated was due to Pgp efflux

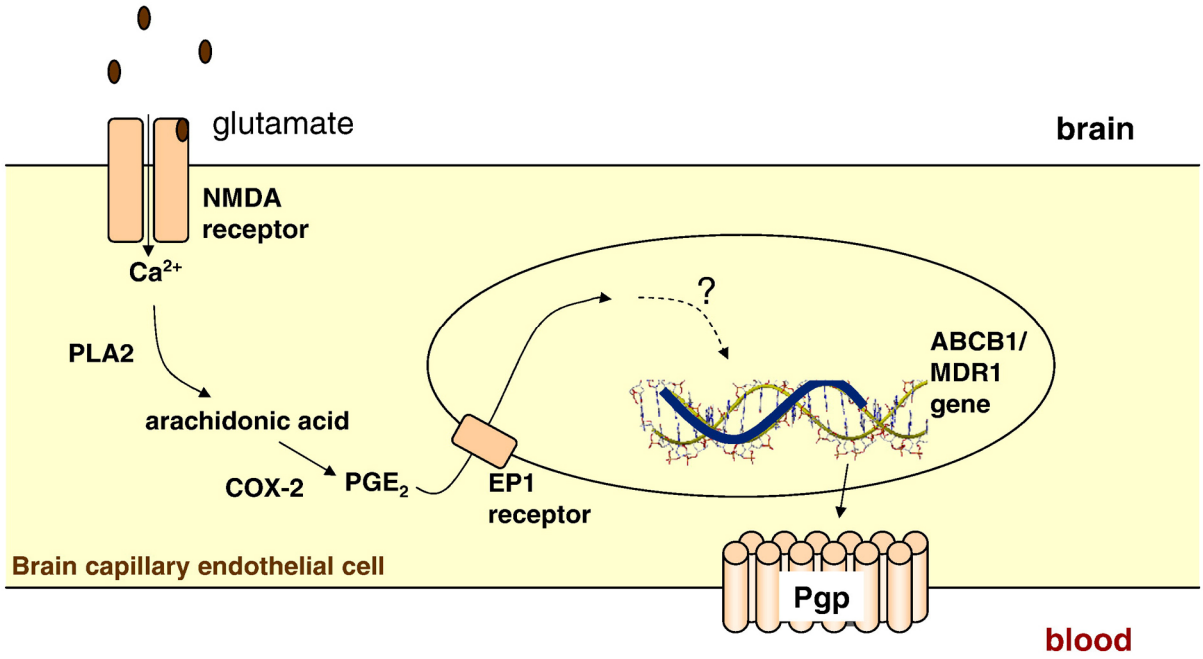

Figure 1.10. Model of P-glycoprotein transcriptional activation by seizure activity in the brain. Seizure activity in the brain releases glutamate into the extracellular space, activating NMDA receptors on endothelial cells (222). NMDA receptor activation allows Ca^{2+} influx into the cell, triggering PLA_2 activation and AA release (105). COX-2 oxidative metabolism of AA yields production of the pro-inflammatory prostaglandin PGE_2, which in turn activates the downstream endothelial EP1 receptor (222, 235, 244). Potschka (2010) suggests that the transcription factor nuclear factor-kappaB (NF-kB) is a likely transcriptional activator of ABCB1 in this scenario, based on evidence that COX-2 signaling in the brain can induce NF-kB activation (245, 246). Figure from: Heidrun Potschka, Targeting regulation of ABC efflux transporters in brain diseases: A novel therapeutic approach, *Pharmacology & Therapeutics*, Volume 125, Issue 1, January 2010, Pages 118-127. Reprinted with permission (234).

activity (242). Subsequently, Bernards (243) found that MPSS bioavailability in the pig spinal cord could be increased by treating with the Pgp inhibitor cyclosporin-A. The authors proposed that inhibiting Pgp activity could reduce the therapeutic dose of MPSS for SCI patients and consequently the harmful peripheral side effects of high-dose glucocorticoid treatment (242, 243). These are significant findings, as they are the first (and only) studies to propose that Pgp might decrease the efficacy of therapeutic intervention for SCI. Nevertheless, whether Pgp becomes pathologically overexpressed in the injured spinal cord, and whether SCI patients become resistant to treatment, are topics that have not yet been investigated. Braughler and Hall performed a series of studies in the early 1980s in which they analyzed MPSS levels in injured cat spinal cord (247-250). However, most of these studies only reported measurements taken within hours of a single large bolus; the authors did not perform longitudinal assessments of spinal cord MPSS levels in a 24-hour continuous, high-dose treatment paradigm such as that utilized in the National Acute Spinal Cord Injury Study (NASCIS) II (94). To date, no group has yet performed an experimental study examining spinal cord resistance to systemic drug treatment following SCI.

Development of drug resistance in the injured spinal cord could have potential to impact the therapeutic efficacy of drugs other than MPSS as well. Significantly, several drugs that have been evaluated as potential SCI interventions, in addition to drugs that are used clinically for the treatment of pain in SCI patients, are known Pgp substrates, and thus susceptible to Pgp-mediated drug resistance (**TABLE 1.1**). This list includes riluzole, a drug that is currently being evaluated in a clinical trial as an acute SCI intervention (87). Because Milane and colleagues have recently shown that Pgp-mediated drug resistance hampers riluzole treatment in ALS (224), it is reasonable to speculate that shared pathological mechanisms (*i.e.*, glutamate excitotoxicity, inflammation, and oxidative stress) could underlie a similar phenomenon in SCI. Pgp-mediated drug resistance in SCI patients would have dramatic implications, with the capacity to impact not only the current riluzole clinical trial, but the efficacy of other neuroprotective drugs for SCI, as well as the treatment of patients with chronic SCI pain and spasticity. Despite decades of intensive research, there are no effective therapies that can improve functional recovery in SCI patients. Thus, the prospect of multidrug resistance following injury to the spinal cord is a potentially major obstacle to treatment that must be investigated.

Drug	Preclinical Evidence of Therapeutic Benefits for SCI	Clinical Trials and/or Clinical Use	Evidence that P-glycoprotein Activity Affects Therapeutic Efficacy and/or CNS Disposition
Methylprednisolone sodium succinate (MPSS)	MPSS exhibits neuroprotective effects in preclinical models of acute SCI (Young and Bracken, 1992; Tator, 1996, 1998; Zeidman *et al*., 1996; Amar and Levy, 1999)	**NASCIS I:** No benefit of MPSS over naloxone or placebo (Bracken *et al*., 1985) **NASCIS II:** Post-hoc analysis detected modest neurological improvement in a subset of patients receiving MPSS 3-8 h post-injury (Bracken *et al*., 1990, 1992); subsequently criticized due to questionable statistical analysis and lack of clinically significant functional outcome measures (Tator, 2006; Hurlbert and Hamilton, 2008) **NASCIS III:** No significant difference in motor recovery or FIM with 24-h or 48-h MPSS treatment (Bracken *et al*., 1998) The clinical use of MPSS for acute SCI has greatly declined, as the evidence suggesting harmful medical side effects of high-dose MPSS is more consistent than evidence suggesting its therapeutic benefit (Hawryluk *et al*., 2008)	Methylprednisolone is a Pgp substrate (Saitoh *et al*., 1998) Intravascular delivery of MPSS results in lower spinal cord bioavailability than intrathecal delivery in pigs; Pgp knockout mice have increased spinal cord penetration of *i.p.* MPSS (Koszdin *et al*., 2000) Pgp inhibition with cyclosporin-A increased CSF levels of *i.v.*-delivered MPSS in the pig (Bernards, 2006)
Minocycline	Neuroprotective effects for acute SCI (Lee et al., 2003; Stirling *et al*., 2004; Festoff *et al*., 2006; Yune *et al*., 2007) Attenuated neuropathic pain in SCI rats (Marchand *et al*., 2009)	Phase I/II trial, **Minocycline and Perfusion Pressure Augmentation in Acute Spinal Cord Injury** (NCT00559494) (University of Calgary, 2007- [cited 2012 Mar 13]) Current status: Currently recruiting	Minocycline is a substrate and inhibitor of Pgp (Milane *et al*., 2007)

Riluzole	Neuroprotective effects for preclinical models of acute SCI (Fehlings and Agrawal, 1995; Schwartz and Fehlings, 2001, 2002; Wang *et al*., 2004) Reversed neuropathic pain behavior in SCI rats (Hama and Sagen, 2010) Attenuated spastic muscle activity in rats (Kitzman, 2009)	Phase I trial, **Safety of Riluzole in Patients with Acute Spinal Cord Injury** (NCT00876889) (The Methodist Hospital System, 2009- [cited 2012 Feb 29]) Current status: Ongoing, but not recruiting participants	Riluzole is a Pgp substrate (Milane *et al*., 2007) Pgp overexpression in the mSOD1 mouse brain decreases brain concentrations of *i.p.*-delivered riluzole (Milane *et al*., 2010)
Nimodipine	Improved spinal cord axonal function and blood flow in preclinical SCI models (Fehlings *et al*., 1989)	Phase III RCT (France) (Petitjean *et al*., 1998): Compared to MPSS and placebo, no difference detected between groups (study likely underpowered) Blind RCT (France) (Pointillart *et al*., 2000): Compared to MPSS, no neurological differences detected between groups	Nimodipine is a Pgp substrate (Zhang *et al*., 2003)
Lamotrigine	-	Lamotrigine is used clinically as a pain treatment in SCI patients (Baastrup and Finnerup, 2008; Wiffen *et al*., 2011)	Lamotrigine is a Pgp substrate (Potschka *et al*., 2002; Luna-Tortos *et al.,* 2008)
Amitriptyline	-	Amytriptyline is used clinically as a pain treatment in SCI patients (Baastrup and Finnerup, 2008)	Amitriptyline is a Pgp substrate (Uhr *et al*., 2000)

(Continued from previous page)

(On previous pages)

TABLE 1.1. Several drugs that have been evaluated for the treatment of spinal cord injury are substrates of P-glycoprotein. Abbreviations: FIM, functional independence measure; NASCIS, North American Spinal Cord Injury Study; RCT, randomized controlled trial. References are listed in bibliography (19, 40, 82, 85, 87, 93, 94, 224, 225, 242, 243, 251-279).

CHAPTER 2

Materials & Methods

Animals and Surgeries

All applicable institutional and governmental regulations concerning the ethical use of animals were followed during the course of this research. This study was carried out in strict accordance with the recommendations in the Guide for the Care and Use of Laboratory Animals of the National Institutes of Health. The animal protocol used in this study was approved by The University of Texas Health Science Center Institute for Animal Care and Use Committee. All efforts were made to minimize suffering and distress.

Animals

Adult female Sprague-Dawley rats weighing 250-300 g were used for Pgp immunoblot studies (See *Chapter 3*). Adult male Sprague-Dawley rats weighing 250-300 g were used for all remaining studies. All wild-type Sprague-Dawley rats were purchased from Harlan Laboratories (Houston, Texas).

Transgenic mice: Adult female *mdr1a/b* constitutive double knockout mice (FVB.129P2-*Abcb1a*^{tm1Bor}*Abcb1b*^{tm1Bor} N12) and wild-type mice (FVB.129P2) were purchased from Taconic (Germantown, New York).

Transgenic rats: Four-week-old male *mdr1a* knockout rats (SD-*Abcb1a*^{tm1sage}) were purchased from SAGE Labs (St. Louis, Missouri).

Spinal Cord Injury Surgery

All surgical procedures were performed on animals that were deeply anesthetized with a ketamine cocktail [ketamine (80 mg/kg), xylazine (10 mg/kg), acepromazine (0.75 mg/kg)] at a dose of 0.01 ml/kg body weight. Spinal cord injury surgeries were performed as previously described (48). Incisions were made on the animals' dorsal skin and overlying muscles and the vertebral column was exposed. A laminectomy was performed at thoracic level 10 (T10) and the vertebral column was stabilized using forceps that grasp the ventral surface of the lateral spinous processes at vertebral levels T9 and T11. Using an Infinite Horizon Spinal Impactor Device (Precision Systems and Instrumentation, LLC, Fairfax Station, VA), moderate

contusion/compression injuries were delivered to the T10 spinal cord using 150 kdynes of force with a 1 s dwell. Immediately following injury, the overlying muscles were sutured and the skin was securely closed using stainless steel wound clips.

Post-Operative Animal Care

Beginning on the day of surgery, animals received Baytril injections (2.5 mg/kg *s.c.*, *b.i.d.*) for 10 days to prevent post-operative infections. Beginning on post-operative day one (DPI 1), animals' bladders were manually expressed 2-3 times daily until control of bladder function was completely regained. To minimize pain, animals received buprenorphine injections (0.02 mg/kg *s.c.*, *b.i.d.*) for one week following surgery. To prevent dehydration, animals received 0.9% saline (3-5 ml *s.c.*) daily for five days following surgery.

Exclusion Criteria

To maximize reproducibility of results, spinal cord-injured animals were excluded from this study if the force of impact to the spinal cord fell outside a range between 150 and 175 kdynes, a criterion that is consistent with previous studies (48). Additionally, injured animals exhibiting an open field locomotor score greater than two on DPI 1 were also excluded.

Drug Treatment

Licofelone (Santa Cruz Biotechnology) was suspended in 0.5% carboxymethylcellulose in 0.9% saline (vehicle) to a final concentration of 50 mg/ml, and administered to animals via oral gavage (100 mg/kg). Riluzole (Sigma-Aldrich) was dissolved in ethanol to a concentration of 50 mg/ml, and this stock solution was stored at -20°C for up to 3 months. Riluzole stock solution was diluted with vehicle to a final working concentration of 2.5 mg/ml, and administered to animals (8 mg/kg *i.p.*). All working drug solutions were prepared fresh daily.

Behavioral Assessments

Open Field Locomotor Testing

Animals' locomotor function was examined using the Basso, Beattie and Bresnahan (BBB) open field locomotor scale (280). This test is a sensitive measure of multiple aspects of hindlimb function that is commonly used to assess locomotor recovery following SCI. Animals were allowed to acclimate to the open field testing environment (a 40"-diameter plastic wading pool) in groups of four for 10 minutes daily until they ceased to exhibit fear-associated behavior (*e.g.*, crouching, cowering away from the examiner, vocalizing) and displayed signs of comfort (*e.g.*, grooming, accepting treats from the examiner's hand, exhibiting continuous locomotion and exploration). No further acclimation to the testing environment was performed. Baseline testing began once the examiner felt confident that all animals were comfortable in the testing environment. Animals were placed into the open field and allowed to freely explore for a period of 4 minutes. Two independent observers scored each hindlimb using a scoring sheet (**Fig. 2.1**). Hindlimb BBB scores were rated using the 21-point BBB open field rating scale (**APPENDIX B**), and inter-rater reliability was confirmed. For each animal, the locomotor scores for both hindpaws were averaged to produce one score per test session. Animals were tested once prior to receiving SCI surgery (baseline measurement) and again on post-operative days 1, 2, 3, 5, 7, 10, 14, 21, 28, 35, and 42. BBB data did not pass the Shapiro-Wilk normality test ($p < 0.05$) and therefore nonparametric statistical analysis was chosen to analyze the effects of treatment on BBB scores. For each individual time point, BBB scores were analyzed using a nonparametric Kruskal-Wallis test followed by a Dunn's post-test.

Photobeam Activity System

A photobeam activity system (PAS) (San Diego Instruments, San Diego, California) was employed to study multiple measures of locomotion and overall activity. PAS chambers were made up of 16" x 16" x 16" Plexiglas enclosures, equipped with interlocking infrared photobeam emitters and receptors spaced at regular intervals. Animal movement ("activity data") in the PAS chamber is monitored by infrared light beam breaks. The PAS stores a sequential list of data, recording when each beam was broken, including X-Y location, serial number, and timestamp, on the computer analyzer. The analyzer allows the viewer to develop a dynamic view of several aspects of spontaneous activity, including: total activity, total ambulatory activity, total fine movement, time at rest, number of rearing events and the amount of time spent rearing.

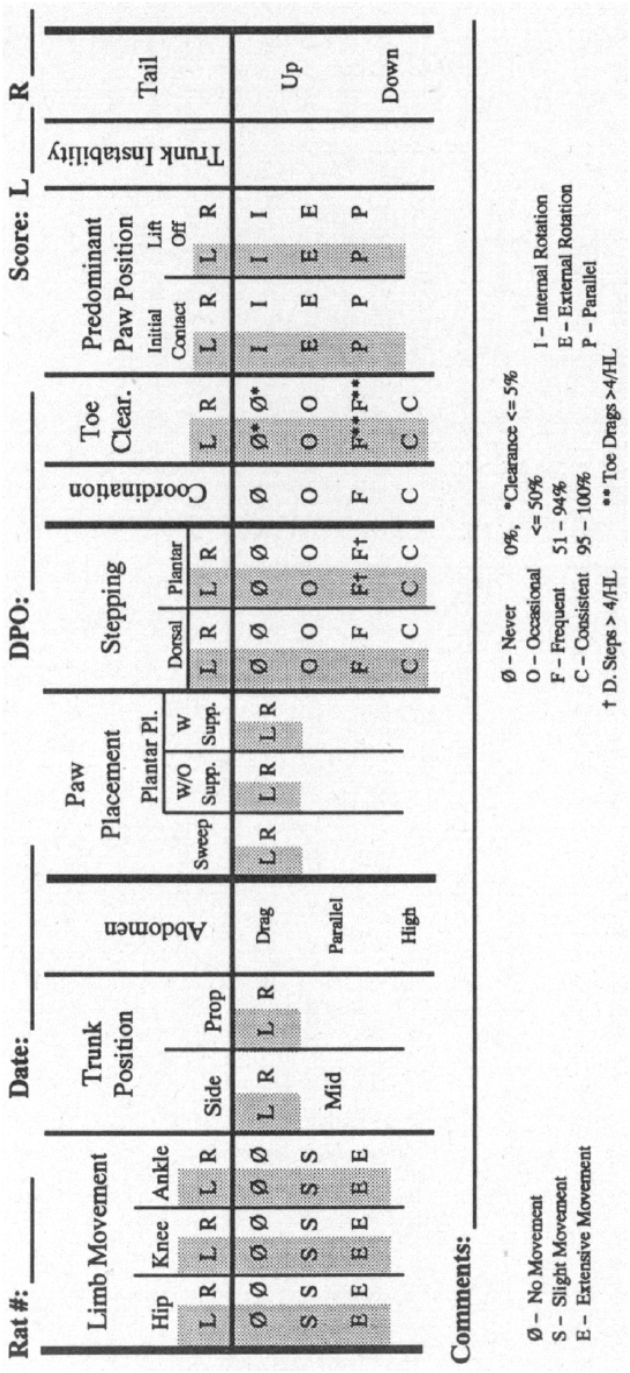

Figure 2.1. BBB scoring sheet. Hindlimb locomotor function was rated systematically using this scoring sheet. Both hindlimbs were rated and assigned an individual BBB score using the BBB locomotor rating scale (See **APPENDIX B**). Abbreviations: *DPO*, days post-operation; *plantar Pl.*, plantar placement of the paw; *toe clear.*, toe clearance during swing of the hindlimb; *W/O supp.*, without weight support; *W supp.,* with weight support. Scoring sheet obtained with permission from the authors of: A Sensitive and Reliable Locomotor Rating Scale for Open Field Testing in Rats, D. Michele Basso, Michael S. Beattie, Jacqueline C. Bresnahan, Journal of Neurotrauma. February 1995: 1-21. (280)

To avoid behavior specific to a novel environment, animals were allowed to acclimate to the PAS chambers for a 15-minute period on the day before baseline testing. During testing, animals were individually placed in PAS chambers, and the tester immediately left the room. PAS testing was performed in a dark environment during the dark cycle (in the evening), to encourage maximum animal activity. Each PAS chamber was cleaned with Cavicide medical disinfectant (Kerr) between tests in order to eliminate olfactory cues. PAS testing was performed once prior to receiving SCI surgery ("Baseline") and again on post-operative days 7, 14, 21, 28, 35, and 42. All session activity was recorded over a 20-minute period and exported in tabular format. All PAS data was analyzed using two-way repeated measures ANOVA, followed by a Bonferroni post-test. The following parameters were assessed:

Distance, speed, and rest time: Distance of movement (cm), average movement speed (cm/s), and time spent at rest (s) over the testing period were calculated. A "rest" period was defined as a period of 2.0 seconds or more with no beam breaks.

Fine movement and ambulatory movement: The PAS software differentiated between ambulatory movement (continual locomotion over several beam breaks) and fine movement (movement without displacement, which indicates grooming, head movements, and other stereotypical behaviors). Ambulatory movement was defined as the distance (cm) of movement over the testing period. Fine movement was defined as the total distance (cm) of beam breaks attributed to small movements confined to an area of $\leq$2 x 2 beams following a minimum resting delay of 0.5 s (281).

Rearing events and rearing time: Number of rearing events was determined automatically by the PAS by calculating the number of events breaking upper-level photobeams. We also extrapolated the cumulative time spent by animals in the rearing position, which has been suggested to be more indicative of a rat's rearing ability/endurance (281).

Tissue Processing

All animals were deeply anesthetized with Beuthanasia (390 mg/ml pentobarbital sodium, 50 mg/ml phenytoin sodium) (75 mg/kg *i.p.*). For all of the following experiments (except microarray and qRT-PCR studies, for which perfusion was not performed), animals were

transcardially perfused with ice-cold saline. Tissue was then harvested, immediately snap-frozen on either dry ice or liquid nitrogen, and stored at -80°C.

Microarray Analysis

Spinal cord tissue from T10 was harvested immediately following sacrifice and snap-frozen in liquid nitrogen. Total RNA from spinal cord tissue was isolated using the mirVana miRNA Isolation Kit (Ambion). RNA was applied to RatRef 12 whole genome arrays (Illumina). Arrays were hybridized, washed and scanned by The University of Texas Medical School Microarray Core Laboratory. Data was analyzed with Illumina BeadStudio software. Group data was compared by Student's *t* test. All microarray experiments were performed in collaboration with Dr. Meredith Moore in The University of Texas Medical School, Department of Neurosurgery.

Quantitative Real-Time PCR

DNase-treated total RNA, isolated as above, was reverse transcribed using the High Capacity Reverse transcriptase kit (Ambion). The cDNA was amplified in the presence of gene specific primers and fluorescent probes with TaqMan Fast Universal reagents (Applied Biosystems, Inc.). *abcb1b* (Rn01529260_m1) expression was examined and the housekeeping gene glyceraldehyde 3-phosphate dehydrogenase (*gapdh*, Rn01775763_g1) was used as an internal control. Expression levels of *abcb1b* were normalized to *gapdh* expression levels. Data collection and C_t analysis was performed with a StepOne Plus real-time thermocycler and associated software (Applied Biosystems, Inc.). Data was analyzed by one-way ANOVA, followed by the Student-Newman-Keuls post test. All qRT-PCR experiments were performed in collaboration with Dr. Meredith Moore in The University of Texas Medical School, Department of Neurosurgery.

Immunohistochemistry

For all immunohistochemical procedures, frozen spinal cord tissue was cryosectioned in the coronal plane to a thickness of 10 µm. Sections were directly mounted to gelatinized slides,

air dried, and post-fixed in 4% paraformaldehyde at 4°C for 15 minutes, then in 1:2 acetic acid: methanol solution at -20°C for 10 minutes.

DAB Staining

Following post-fixation, sections were washed 3X for 10 minutes in tris-buffered saline (TBS, 10 mM Tris, pH 8.0; 150 mM NaCl), then incubated for 30 minutes in H_2O_2 buffer (0.6% H_2O_2 in TBS) at room temperature. Sections were washed 2X for 10 minutes in TBS, then blocked with blocking-permeabilization buffer (BPB) (5% normal horse serum in TBS, 0.1% Triton-X-100) for 1 hour. Sections were then incubated in BPB containing primary antibody (1:250 mouse monoclonal anti-P-glycoprotein C219, Calbiochem) for 2 hours at room temperature, then washed 3X for 10 minutes in TBS. Samples were incubated in BPB containing 1:200 biotinylated anti-mouse IgG antibody (Vector Labs) for 3 hours at room temperature, then washed 3X for 10 minutes in TBS. Samples were processed with the Vectastain ABC Kit (Vector Labs), and immunoreactivity was then visualized by incubation in diaminobenzidine (DAB) solution. Samples were counter-stained with hematoxylin to visualize nuclei. Sections were dehydrated, mounted, and coverslipped with Fluoromount-G (Fisher).

Immunofluorescence

Following post-fixation, sections were washed 3X for 10 minutes in TBS, then non-specific IgG was blocked with 5% normal serum for 1 hour. Sections were then incubated in TBS containing primary antibodies against P-glycoprotein (1:250 mouse monoclonal anti-P-glycoprotein C219, Calbiochem), GFAP (1:1000 rabbit polyclonal, Dako), von Willebrand factor (1:1500 rabbit polyclonal, Sigma-Aldrich), ED2/CD163 (1:750 mouse monoclonal, Serotec), or 5-lipoxygenase (1:1000 goat polyclonal, Novus Biologicals) overnight at 4ºC on a rotating shaker. Sections were washed 3X for 10 minutes in TBS, and incubated with Alexa Fluor conjugated secondary antibodies (1:500, Invitrogen) for 3 hours. Sections were washed, dried, and coverslipped with Fluoromount-G.

For all immunohistochemical experiments, labeled sections were imaged using an Olympus BX61 wide-field upright microscope with fluorescence optics with a SPOT Flex microscope digital camera. Every sixth section in series was chosen for histological analysis.

Immunoblotting

Tissue samples were homogenized in Tissue Protein Extraction Reagent (T-PER, Thermo Scientific) containing protease inhibitor cocktail tablets (Complete Mini, Roche) using an electric tissue homogenizer. Lysate was centrifuged at 14,000 x g for 30 minutes at 4°C, and the supernatant was removed and stored at -80°C. Protein concentration of samples was determined using a Pierce BCA Protein Assay (Thermo Scientific), using bovine serum albumin as the standard. Approximately 50-100 µg of tissue lysate was resolved onto polyacrylamide Tris-HEPES-SDS gels (Thermo Scientific) under reducing conditions. HeLa cell lysate (Santa Cruz Biotechnology) was used as a positive control for immunodetection of Pgp. Equality of loading was confirmed by Coomassie Brilliant Blue staining of gels. Proteins were transferred to Immobilon-FL PVDF membranes (Millipore) using a semi-dry transfer apparatus. For Pgp detection, transfer buffer was prepared without methanol to optimize large protein transfer efficiency. Following transfer, non-specific antigens were blocked by incubation in Odyssey Blocking Buffer (LI-COR Biosciences) for 1 hour at 4°C. Blots were then incubated in blocking buffer containing primary antibodies at the following concentrations:

P-glycoprotein (C219): 1:250 mouse monoclonal, Calbiochem (#513710)
Mdr-1 (D-11): 1:100 goat polyclonal, Santa Cruz Biotechnology (#sc-55510)
Beta-actin: 1:20,000 mouse monoclonal, Abcam (#ab6276)
1:20,000 rabbit polyclonal, Abcam (#ab8227)
Cyclooxygenase-1: 1:200 mouse monoclonal, Cayman Chemical (#160110)
Cyclooxygenase-2: 1:200 rabbit polyclonal, Cayman Chemical (#160126)
5-Lipoxygenase: 1:250 mouse monoclonal, BD Biosciences (#610694)

Membranes were incubated in primary antibodies at room temperature for 1 hour, or at 4°C overnight. Blots were then washed in TBS containing 0.1% Tween-20 (TBST), 5X for 5 minutes, then incubated in blocking buffer containing species-specific IRDye-conjugated infrared secondary antibodies (1:500, LI-COR Biosciences). Blots were imaged using the Odyssey Infrared Imaging System (LI-COR Biosciences). This detection method has the advantages of high sensitivity of detection and increased signal-to-noise ratio over chemiluminescence, as well as capability to detect two different antigens on the same blot simultaneously. Band intensity was quantified using Odyssey software (LI-COR), and data was

analyzed using one-way ANOVA followed by the Student-Newman-Keuls post test (when more than two groups were compared), or by Student's *t* test (when two groups were compared).

Enzyme-Linked Immunosorbent Assay

A 1.5-cm piece of spinal cord tissue spanning the epicenter of injury was harvested, snap-frozen in liquid nitrogen, and stored at -80°C. Homogenization buffer (0.1 M phosphate, pH 7.4, 1 mM EDTA, 10 μM indomethacin; 1 ml per 100 mg tissue) was added and tissue was homogenized on ice using a Polytron homogenizer. For detection of PGE_2 only, a purification step was performed using a PGE_2 Affinity Sorbent Kit (Cayman Chemical Co., Ann Arbor, MI). PGE_2, LTB_4, and CysLT levels were quantified using the appropriate EIA kits (Cayman Chemical). All samples were prepared and analyzed in triplicate, and absorbance at 405 nm was read in a Model 680 Microplate Reader (Bio-Rad). Standard curves were generated and sample concentrations were determined using Cayman EIA data analysis worksheets (www.caymanchem.com/analysis/eia). Data was analyzed by one-way ANOVA followed by the Student-Newman-Keuls post test. ELISA experiments for chronic spinal cord samples were performed in collaboration with Dr. Henry Strobel in The University of Texas Medical School, Department of Biochemistry and Molecular Biology.

Metabolomic Profiling

Six hours following the final drug treatment, animals were sacrificed and tissue was immediately harvested and snap-frozen in liquid nitrogen. A 10-mm segment of spinal cord tissue encompassing the lesion site was utilized for metabolomic analysis. Unbiased metabolomic profiling of spinal cord samples from uninjured and chronic SCI rats was performed using liquid-/gas chromatography coupled to mass spectrometry (LC/GC-MS) as previously described (282). At the time of publication, the metabolomics platform is capable of detecting approximately 2,400 named metabolites, of which 257 metabolites were detected within this study. A data normalization step was performed to correct variation resulting from instrument inter-day tuning differences. Each compound was corrected in run-day blocks by registering the medians to equal one (1.00) and normalizing each data point proportionately

(termed the "block correction"). Following log2 transformation and imputation with minimum observed values for each compound, Welch's two-sample *t* test was used to identify biochemicals that differed significantly between two groups. Lists of biochemicals that achieved statistical significance ($p \leq 0.05$), as well as those approaching significance ($0.05 < p < 0.10$), are given in **TABLES 4.1** & **4.2**. An estimate of the false discovery rate (*Q* value) was calculated to take into account the multiple comparisons that normally occur in metabolomic-based studies; as *Q* values were reasonable for $p \leq 0.05$, no *Q* value cutoff was established for this study. Outliers were defined as 1.5*(inter-quartile range) and removed from analyses. Heat maps of metabolomics data (**Figs. 4.7, 4.8,** & **4.10a**) were generated using the open-source software package MultiExperiment Viewer version 4.7.3, part of the TM4 Microarray Software Suite (Dana-Farber Cancer Institute, Boston) (283). Scaled, imputed, log2-transformed data was used to generate heat maps and to perform clustering analysis. Pearson distances (1-*r*, where *r* is the Pearson correlation coefficient) were used as the pairwise distance between individual replicates for hierarchical clustering by biochemical.

High-Performance Liquid Chromatography

All reagents used for HPLC experiments were HPLC-grade (ChromaSolv, Sigma-Aldrich). Riluzole stock solutions (1 mM) were prepared by dissolving riluzole in 1:1 H_2O:CH_3OH. Stock solutions were stored for up to 3 months at -20°C. Serial dilutions of riluzole stock solutions were prepared and known amounts of riluzole were injected onto the HPLC system in the following quantities: 0.05, 0.1, 0.5, 1, and 2 nmoles. A calibration curve was generated using Empower 3 Chromatography Data Software program (Waters) (**Fig. 2.2**). The R^2 value obtained for the riluzole calibration curve was 0.998.

Tissue Extraction of Riluzole

Animals were dosed with riluzole, and sacrificed 2 hours later. Animals were transcardially perfused with ice-cold saline, and spinal cords were immediately harvested, rinsed, and snap-frozen on dry ice.

Spinal cord riluzole extraction: A 1.5-cm segment of spinal cord tissue centered around the lesion site was homogenized, and riluzole was extracted with ethyl acetate as previously described (284). Samples were re-suspended in 100 µl mobile phase buffer.

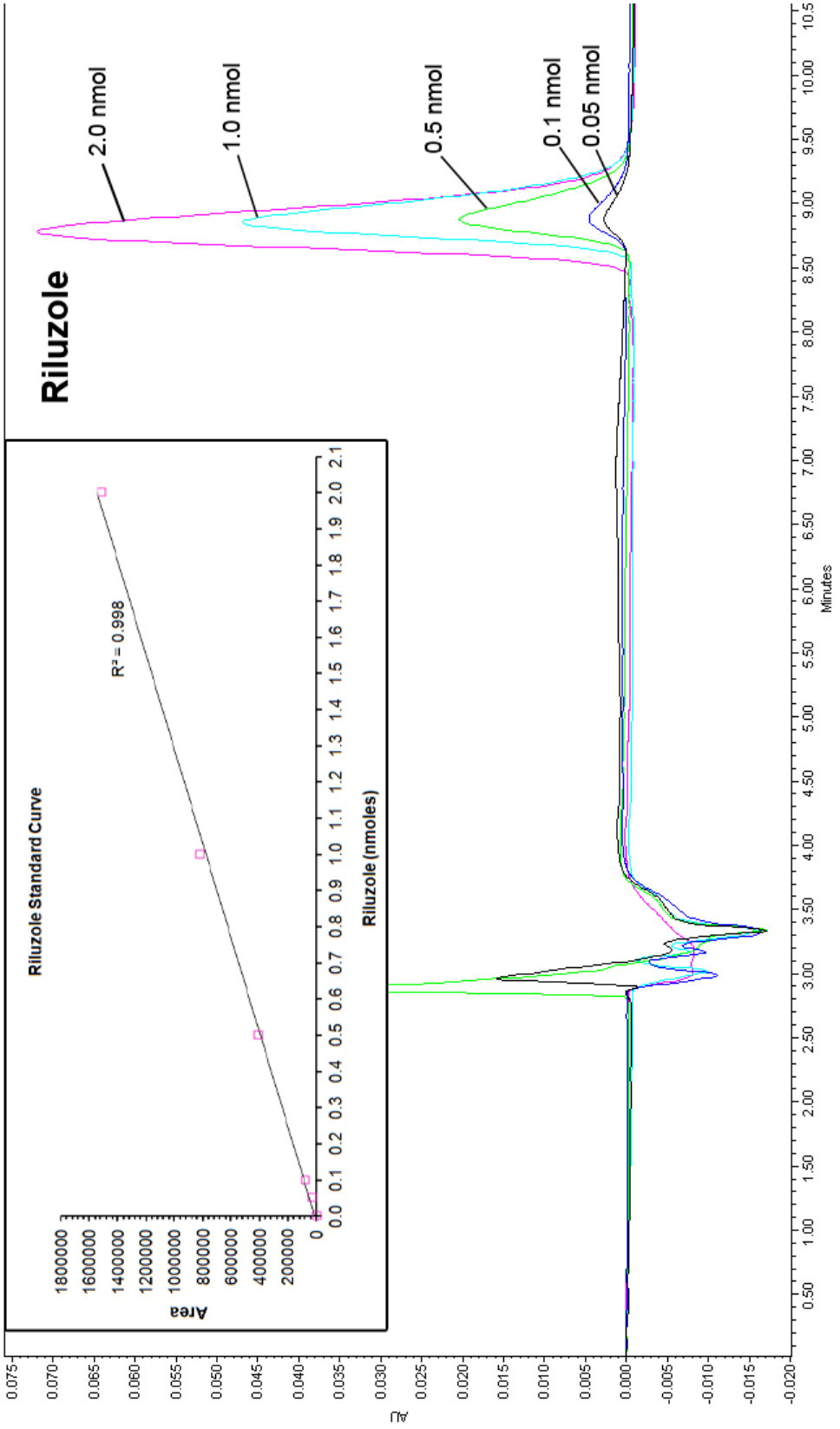

Figure 2.2. HPLC chromatograph and calibration curve for riluzole. Known amounts of riluzole were injected onto the HPLC system, generating a series of chromatographic peaks that were integrated to produce a calibration curve (inset). AU, absorbance units.

Plasma riluzole extraction: Whole blood was obtained by cardiac puncture immediately following sacrifice, and plasma was recovered by centrifugation at 1,300 x *g* for 10 min at 4°C. Plasma samples were diluted 1:2 in 0.01 M phosphate buffer, pH 7.4 and riluzole was recovered via solid-phase extraction as previously described (285). Samples were re-suspended in 75 µl mobile phase buffer and filtered through Millex-GV4 0.22 µM membranes (Millipore) before injection onto the HPLC system.

High-Performance Liquid Chromatography Separation and Analysis

The HPLC system consisted of a Waters 515 HPLC pump, a Waters 996 Photodiode Array Detector, and a CI-10B integrator (LDC Analytical). Separation was achieved through a ZORBAX Extend-C18 column (4.6 x 150 mm) (Agilent Technologies) with a 20-mm ODS pre-column (Custom LC, Inc.). The mobile phase consisted of 68% CH_3OH and 32% of [1% TEA in H_2O, adjusted to pH 3.2 with H_3PO_4]. The flow was isocratic with a constant flow rate of 0.5 ml/min. The sample injection volume was 100 µl (spinal cord samples) or 75 µl (plasma samples). Absorbance was continuously monitored at a wavelength of 254 nm. Riluzole peaks (retention time = ~9 minutes) were identified and integrated at 264 nm, and quantified using previously run calibration curves. Naïve spinal cord and plasma samples were spiked with 0.5 nmoles riluzole and extracted, then analyzed by HPLC to determine percent recovery of riluzole (63.2% in spinal cord; 76.4% in plasma). Riluzole concentrations in spinal cord samples were normalized to plasma concentrations to obtain a spinal cord/plasma ratio for each animal. Riluzole concentrations were analyzed by one-way ANOVA followed by the Student-Newman-Keuls post test.

Statistical Analysis

All statistical analysis was performed using SigmaPlot 11 (Systat Software, Inc., Chicago, Illinois) or GraphPad Prism 5. Student's *t* test was used for comparisons between two groups. For comparisons among more than two groups for parametric data, one-way ANOVA followed by the Student-Newman-Keuls post test was used. Multiple-group, repeated-measures comparisons of parametric data were performed using a two-way repeated measures ANOVA, followed by appropriate multiple comparisons tests. Nonparametric data (BBB scores) were

compared across groups using a Kruskal-Wallis test followed by a Dunn's post-test. p values < 0.05 were considered statistically significant.

CHAPTER 3

Assessment of P-glycoprotein Expression and Function Following Spinal Cord Injury in the Rat

Background

It has long been known that treatment with chemotherapeutic drugs can induce overexpression of Pgp in multiple types of cancer, conferring tumor cells with simultaneous cross-resistance to multiple cytotoxic chemotherapeutic compounds (286-288). This phenomenon, known as multidrug resistance, is a major obstacle to the efficacy of cancer therapy, and identifying new avenues to circumvent this obstacle remains a chief priority in the field of oncology research (289, 290). More recently, several preclinical and clinical studies have shown that in neurological diseases characterized by high levels of excitotoxicity, oxidative stress, and inflammation in the brain, Pgp can become pathologically overexpressed at the blood-brain barrier (223, 224, 235, 244). As a consequence, it is now acknowledged that Pgp overexpression presents a formidable obstacle to effective CNS drug delivery in patients suffering from neurological diseases (214).

Pgp expression and function in the healthy and diseased brain has been a subject of much investigation over the last few decades. Despite this, relatively few groups have focused on the role of Pgp drug efflux activity in the BSCB. Bernards and colleagues have drawn attention to Pgp efflux activity as a barrier to penetration of systemically-delivered methylprednisolone into spinal cord tissue in SCI patients (242, 243). They emphasized that the high dose of MPSS needed to approach therapeutic spinal cord levels is associated with harmful peripheral side effects that might be avoided by circumventing Pgp efflux activity. However, whether Pgp undergoes pathological up-regulation following SCI, as has been observed in other neuroinflammatory conditions, has not yet been addressed. If multidrug resistance does develop in the spinal cord following traumatic injury, then Pgp may present an even more insurmountable barrier to effective delivery of neuroprotective drugs than previously speculated (243).

Specific Aims

1. A central feature of multidrug resistance in neurological diseases is overexpression of Pgp at the blood-brain barrier (234). Previous work has shown that the BSCB undergoes multiple structural and functional alterations after traumatic SCI (72, 168, 173, 291); however, Pgp expression at the BSCB in response to SCI has not yet been investigated.

We therefore sought to assess the temporal and spatial expression profiles of Pgp within the spinal cord following SCI.

2. The functional consequence of pathological Pgp overexpression at the blood-brain barrier is reduced brain penetration of blood-borne drugs such as riluzole (224). Therefore, we anticipated that Pgp overexpression within the injured spinal cord would also correspond with reduced spinal cord drug bioavailability. We investigated this possibility by evaluating spinal cord concentrations of systemically-delivered riluzole during acute and sub-acute phases of SCI, and using transgenic *mdr1a*$^{-/-}$ rats to delineate the role of Pgp in conferring spinal cord drug resistance[5].

Results

Expression of ABC Transporter Genes Following Spinal Cord Injury

In humans, there is only one Pgp gene product that confers multidrug resistance—MDR1 (292). Rodents express two 90% homologous isoforms, Mdr1a (Abcb1a) and Mdr1b (Abcb1b), and both confer multidrug resistance (293). The distinction between the expression patterns of these two isoforms is somewhat unclear. It has been reported that only the Mdr1a gene product is expressed in rodent brain capillary endothelial cells under normal conditions (294, 295) and loss of *mdr1a* gene expression results in heightened CNS sensitivity to drugs (296). Schinkel and colleagues demonstrated that the accumulation of digoxin (a Pgp substrate) in the brains of *mdr1a/1b*$^{-/-}$ mice was only slightly greater than that of *mdr1a*$^{-/-}$ mice (295). However, other studies have reported an increased expression of both *mdr1a* and *mdr1b* genes in mouse brain capillary endothelial cells in response to inflammatory lipopolysaccharide (LPS) treatment (245), which is accompanied by an increase in Pgp protein expression and activity (297). The differential regulation of both Mdr1a and Mdr1b gene products under pathological conditions is unclear, but their considerable functional redundancy suggests that both may play a role in multidrug resistance under neuroinflammatory conditions.

Microarray analysis was performed to detect changes in expression of ABC transporter genes within the T10 spinal cord at one week after SCI (n = 6) compared to uninjured controls

[5] The term *drug resistance* is used in this dissertation to indicate a reduction in the spinal cord penetration of drug from the plasma following systemic (*i.v.* or *i.p.* delivery) of that drug.

(n = 6) (**TABLE 3.1**). Microarray data revealed differential expression of several ABC transporter genes within the lesion site of animals one week after injury. Of these family members, *abcb1b*, encoding the Mdr1b isoform of Pgp, exhibited the most dramatic up-regulation with ten-fold higher expression levels compared with controls (+10.05-fold, $p < 0.001$)[6]. Among other family members exhibiting up-regulation was *abcb4* (*mdr2*), a selective transporter of phosphatidylcholine, expression of which was increased substantially in injured tissue (+6.07-fold, $p < 0.001$).

	Synonym	Fold Change vs. Uninjured
7 days post-SCI		
abca3 (predicted)		1.97
abca5		-2.59
abcb1	***mdr1; pgy1; abcb1b***	**10.05**
abcb4	*mdr2; pgy3*	6.07
abcb6		-1.71
abcb7		2.06
abcb9	*tap1*	-3.91
abcc2		-13.92
abcc3	*mlp2; mrp3*	2.14
abcc6	*mrp6*	-3.44
abcc8	*sur*	-3.00
abcd2	*ALDR*	-5.54
abcd3	*PMP70; pxmp1*	-1.55
abcd4 (predicted)		2.27
abcf2 (predicted)		-1.59
abcf3 (predicted)		-1.38
abcg1	*abc8*	3.36
abcg2		-1.62
abcg4 (predicted)		-1.51

TABLE 3.1. Differential expression of ABC transporter genes 7 days following spinal cord injury. DNA microarray gene expression data for ABC transporter family members at 7 days following SCI in the rat T10 spinal cord. Gene expression is represented as fold change versus uninjured control levels (0 indicates no change in expression versus controls). Up-regulated genes are highlighted in green and down-regulated genes are highlighted in red. *abcb1b* (bold) encodes rat P-glycoprotein. All gene expression data included in this table are $p < 0.01$ versus uninjured controls.

[6] The Illumina microarray chip used in this study did not contain a probe against *abcb1a*.

We also detected significantly decreased expression of several ABC transporter family members during acute SCI. Genes exhibiting the most prominent down-regulation included *abcc2*, encoding the multidrug resistance-associated protein 2 (MRP2), (-13.92-fold, $p < 0.001$), and *abcd2*, encoding the adrenoleukodystrophy-related protein (ALDRP), (-5.54-fold, $p < 0.001$). Like Pgp, MRP2 is expressed on the luminal membrane of brain capillary endothelial cells and possesses broad substrate specificity, contributing to efflux of drugs and other compounds (298). ALDRP does not contribute to multidrug resistance, but its dysfunction is implicated in the neuroinflammatory disease adrenoleukodystrophy (299). It is possible that more than one member of the ABC transporter family, for which we have observed differential expression after SCI, may play a role in the pathophysiology and/or treatment of SCI. For this study, we chose to focus specifically on investigating Pgp, largely due to its extensively described role in a variety of diseases including cancer and several neurodegenerative diseases (224, 227, 230, 300).

To corroborate our microarray data and assess whether Pgp undergoes SCI-induced up-regulation at the transcriptional level, we next performed quantitative real time PCR (qRT-PCR) analysis of *abcb1b* gene expression (**Fig. 3.1**). Our results revealed a twelve-fold increase in the lesion site of rats 7 days post-SCI (RQ = 9.10 ± 0.67, $n = 3$) compared with expression in uninjured controls (0.76 ± 0.12, $n = 4$). Moreover, we observed that *abcb1b* gene expression was also increased three-fold in the T10 cord of rats 8 months post-SCI (2.60 ± 0.24, $n = 5$) compared to age-matched, uninjured controls (0.87 ± 0.077, $n = 5$). These findings suggest that Pgp transcription is increased not only in the acutely-injured spinal cord, but in the chronic phase of injury as well.

Expression of P-glycoprotein Within the Injured Spinal Cord

Pgp expression in the brain is restricted to the luminal membrane of capillary endothelial cells; although one group has reported Pgp expression in the membranes of astrocyte foot processes (301-304), their observations have not been replicated and thus remain dubious (203). We therefore examined the localization of Pgp expression in rat spinal cord tissue. In the wild-type, uninjured rat, Pgp immunoreactivity was restricted to spinal cord blood vessel endothelial cells, and was not observed on astrocytes (**Fig. 3.2**). Immunohistochemical staining

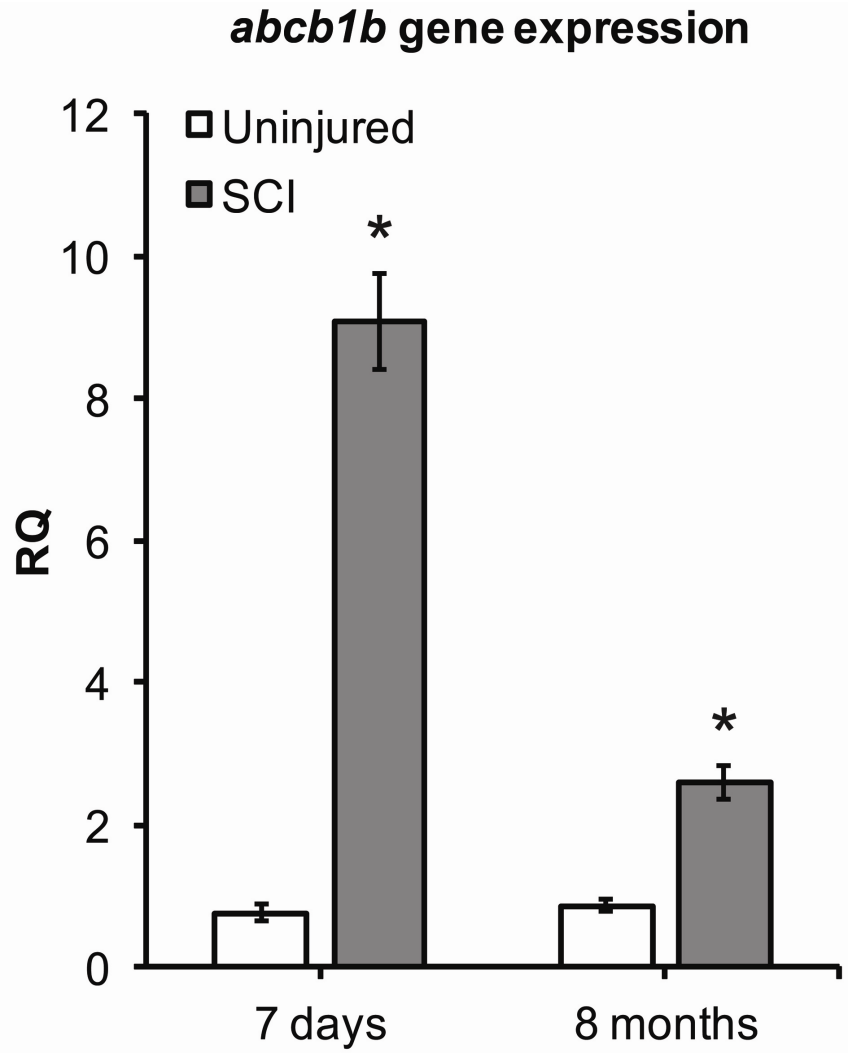

Figure 3.1. Expression of *abcb1b* is increased during acute and chronic spinal cord injury. qRT-PCR gene expression data for T10 spinal cord tissue from rats 7 days and 8 months post-SCI, versus age-matched, uninjured control expression levels. RQ, relative quantity of *abcb1b* expression (fold change). All data are mean ± s.e.m. *, $p < 0.001$ versus uninjured, age-matched controls.

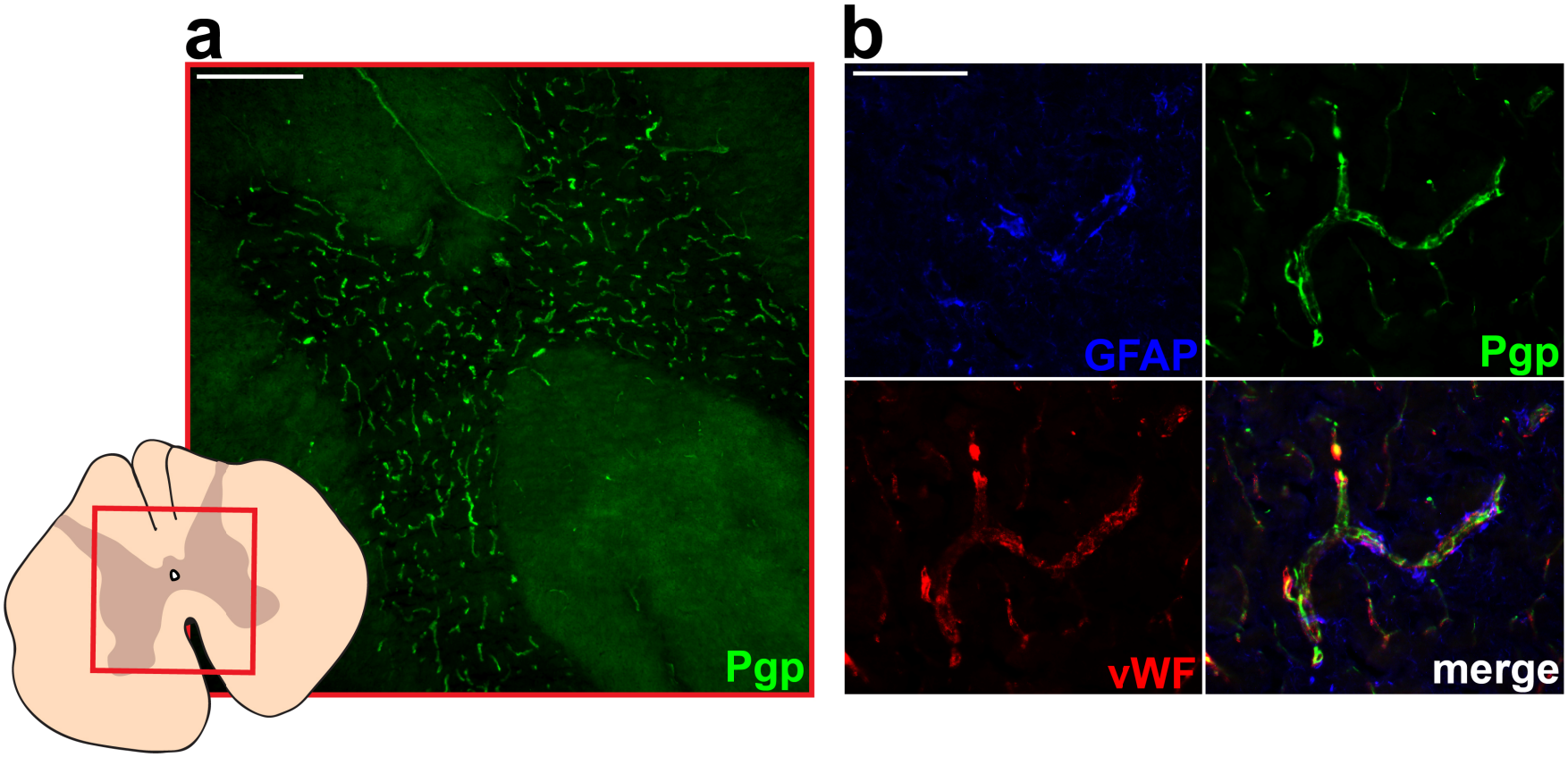
a
Pgp
b
GFAP
Pgp
vWF
merge

(On previous page)

Figure 3.2. P-glycoprotein expression is localized to blood vessels in the intact spinal cord. (**a**) Coronal spinal cord section with Pgp immunoreactivity in green. Cartoon indicates field of view (red-bounded box). Scale bar = 250 µm. (**b**) Pgp immunoreactivity co-localizes with the endothelial marker von Willebrand factor (vWF), but not with the astrocytic marker glial fibrillary acidic protein (GFAP). Scale bar = 100 µm.

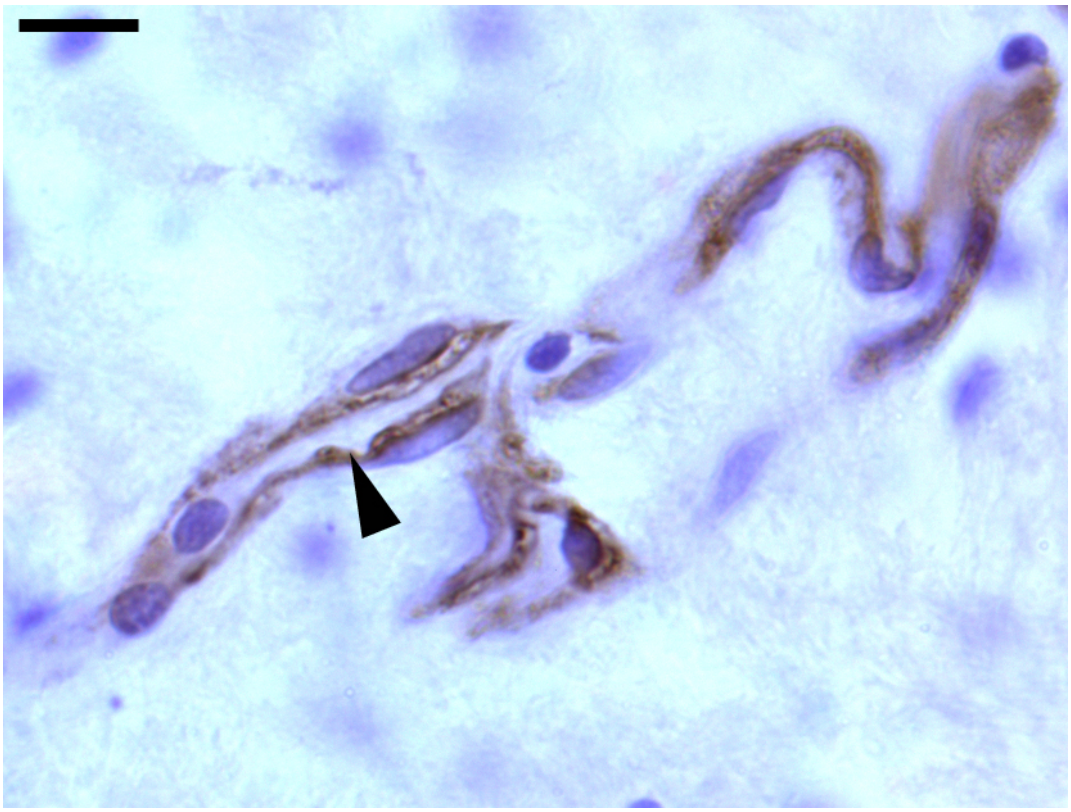

Figure 3.3. P-glycoprotein is expressed on the luminal surface of spinal cord blood vessels. Pgp immunoreactivity (brown) is localized to the luminal surface of capillary endothelial cells in the intact spinal cord (arrowhead). Nuclei are stained blue. Scale bar = 10 µm.

also revealed strong Pgp localization on the luminal surface of capillary endothelial cells in the spinal cord (**Fig. 3.3**), consistent with previous reports (305). We did not observe localization of Pgp immunoreactivity in any other cell types. To evaluate whether different cell types might also express Pgp following SCI, we also examined Pgp immunoreactivity in the spinal cord lesion site 7 days after injury (**Fig. 3.4**). We did not observe co-localization with macrophages (**Fig. 3.4a**) or astrocytes (**Fig. 3.4b**) at this time point; rather, Pgp expression still appeared to be restricted to capillary endothelial cells.

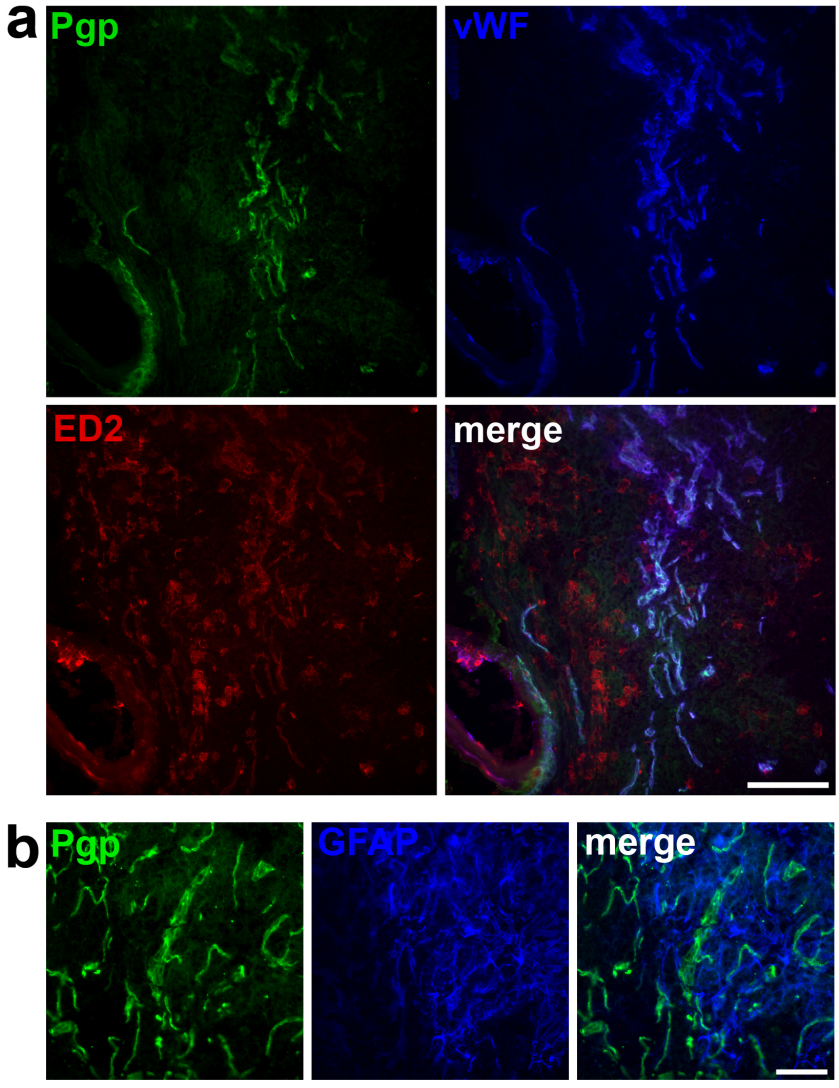

Figure 3.4. P-glycoprotein expression is localized to blood vessels 7 days following spinal cord injury. Pgp immunoreactivity (green) co-localizes with blood vessel endothelial cell markers within the spinal cord lesion site one week post-SCI. (**a**) Pgp co-localizes with spinal cord vasculature and not with macrophages. von Willebrand factor (vWF), blue; ED2, rat mature macrophage antigen, red. (**b**) Pgp does not co-localize with astrocytes. Glial fibrillary acidic protein (GFAP), blue. Scale bars = 100 µm.

For subsequent studies, we elected to examine spinal cord Pgp expression via immunoblot analysis. Mice and rats express two distinct Pgp gene products, Mdr1a and Mdr1b, both of which are expressed in the CNS, though the Mdr1a isoform more predominantly so (198). To verify the efficacy of the anti-Pgp antibody for immunodetection in western blots, we performed SDS-PAGE on total protein samples from uninjured spinal cord tissue harvested from *mdr1a/b*$^{-/-}$ mice (**Fig. 3.5**) as well as *mdr1a*$^{-/-}$ rats (**Fig. 3.6**) (double *mdr1a/b* knockout rats were not available at the time of this study). *mdr1* knockout animals exhibited normal phenotypes, and were indistinguishable from wild-types. We observed multiple non-specific bands on immunoblots for both mouse and rat samples (**Fig. 3.7**, arrowheads), most likely as a result of the high concentration of the primary antibody (1:100) used for immunodetection. Pgp was identified as the prominent band migrating to ~170 kDa, which was conspicuously absent in spinal cord tissue lysates from *mdr1* knockout animals (**Figs. 3.5, 3.6**). Pgp immunoreactivity often appeared as a diffuse band, an observation which is likely attributed to variable states of glycosylation, as Pgp is normally heavily glycosylated (10-15 kDa of glycosylation) on its N-terminal domain (203).

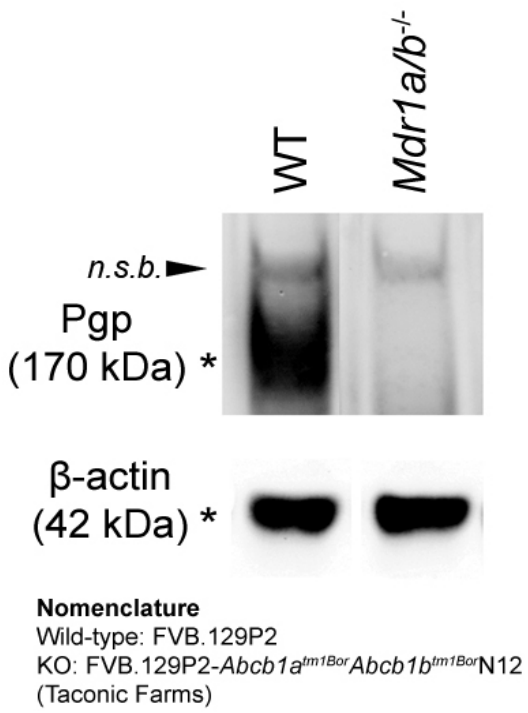

Figure 3.5. P-glycoprotein is absent in spinal cords of *mdr1a/b*$^{-/-}$ mice. Representative immunoblot of total protein extract from spinal cord tissue of uninjured wild-type and *mdr1a/b* knockout mice. Immunoreactivity against Pgp is conspicuously absent in samples from knockout mice. Immunoreactivity in upper band (indicated by arrowhead) is due to non-specific binding.

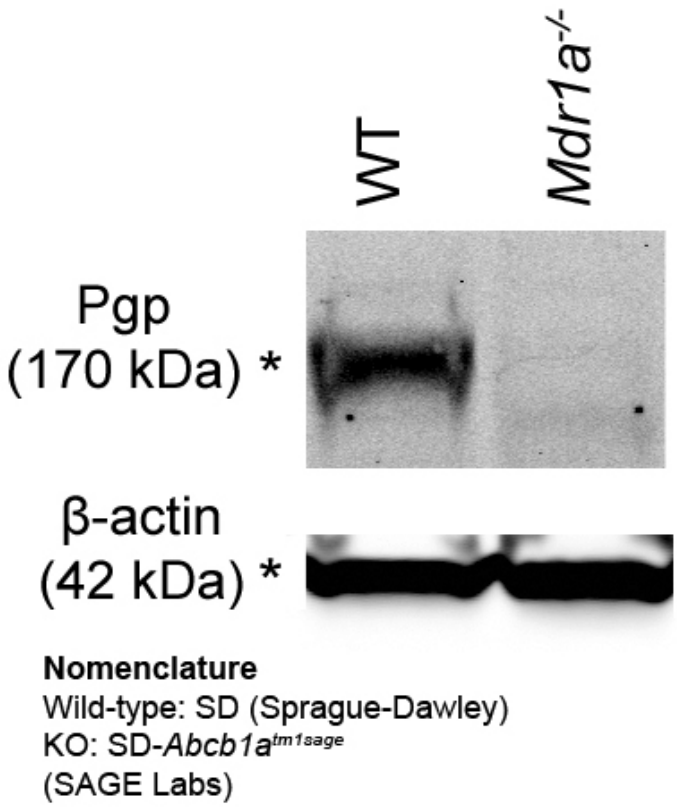

Figure 3.6. P-glycoprotein is absent in spinal cords of *mdr1a*$^{-/-}$ rats. Representative immunoblot of total protein extract from spinal cord tissue of uninjured wild-type and *mdr1a* knockout rats. Pgp immunoreactivity is absent in samples from knockout rats.

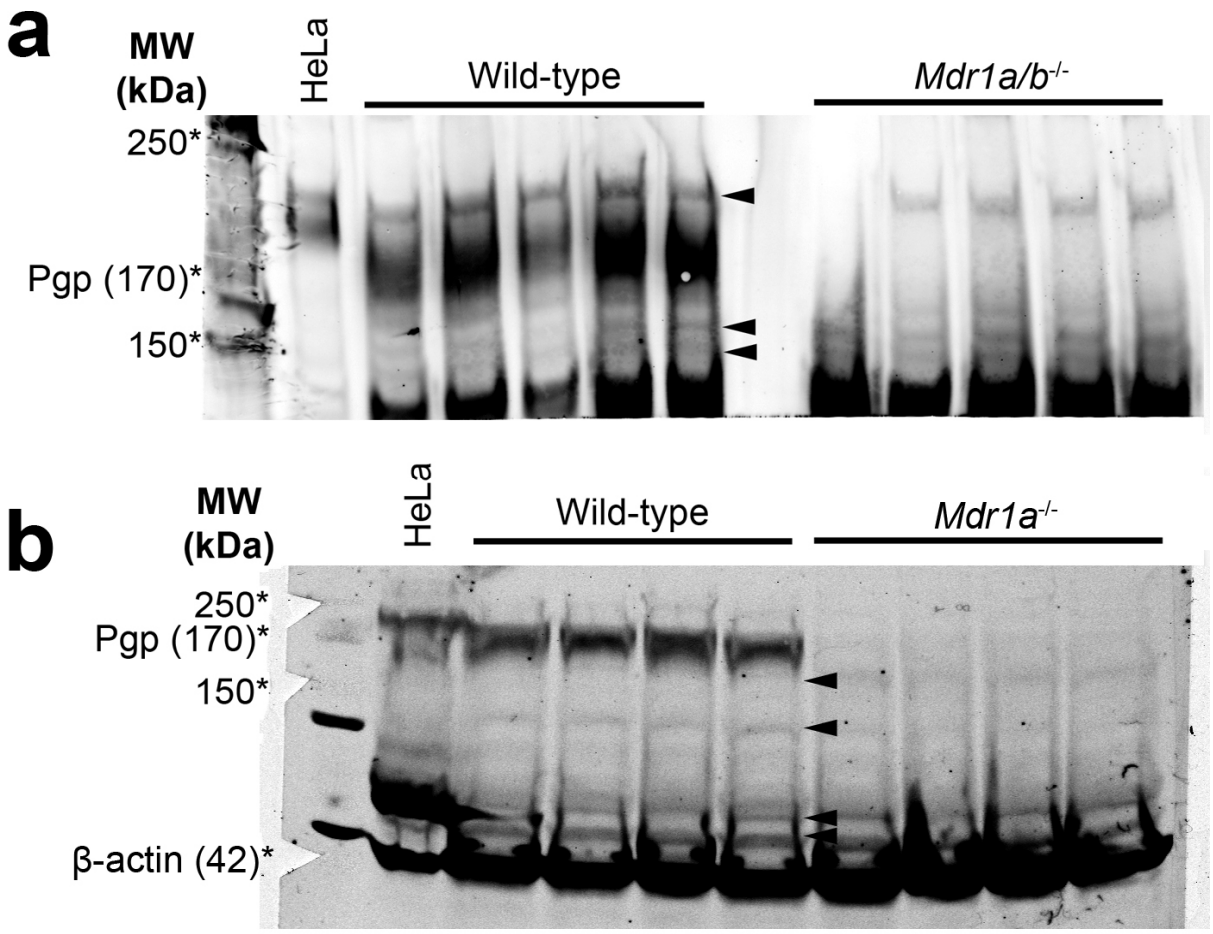

Figure 3.7. P-glycoprotein immunoblots exhibit multiple non-specific bands. Pgp immunoreactivity in protein samples from spinal cord tissue of (**a**) uninjured wild-type and *mdr1a/b* knockout mice, and (**b**) uninjured wild-type and *mdr1a* knockout rats. HeLa cell lysate is a positive control for human MDR immunoreactivity. Arrowheads indicate non-specific bands. Band of Pgp immunoreactivity (170 kDa) is labeled at left.

We next investigated the temporal and spatial expression profile of Pgp within the injured spinal cord. Pgp expression levels at 72 hours, 7 days, 4 months, and 10 months post-SCI were quantified and compared to uninjured, age-matched controls via immunoblot analysis. We observed that Pgp expression was significantly higher within the lesion site of injured animals, compared with thoracic cord tissue of uninjured controls, at all time points from 72 hours to 10 months post-SCI (**Fig. 3.8**). At 3 days post-injury, expression of the transporter protein was nearly three-fold greater than that of uninjured controls, and at 10 months post-SCI, levels were more than four-fold greater. These findings corroborate our gene expression data (**Fig. 3.1**), providing further evidence that Pgp expression is increased in the spinal cord injury site in both the acute and chronic phases of injury.

Previous studies in our lab have revealed that BSCB dysfunction following SCI is sustained into the chronic phase of injury; moreover, this barrier dysfunction spreads to spinal cord regions centimeters away from the T10 lesion site in the rat. This progressive spread of BSCB failure is characterized by reduced expression of adherens junction proteins and increased vascular permeability to large molecules, such as immunoglobulin G (IgG) and albumin (unpublished studies performed by Dr. Raymond Grill). One major goal of our laboratory is to develop a more comprehensive understanding of vascular pathology following injury to the spinal cord. The previously reported deficits in BSCB function have described components of passive BSCB failure—leakiness or increased permeability to small and large molecules due to increased passive paracellular and transcellular diffusion (177). However, it has not previously been investigated whether SCI also induces changes in active transport at the BSCB. The pathological changes in the properties of the BSCB are widely thought to solely encompass passive changes that enhance barrier permeability. An overarching goal of the current study is to investigate whether deficits in the BSCB following SCI extend to alterations in active transport as well.

We evaluated whether there were progressive, spatial changes in Pgp expression patterns following SCI by examining protein levels in spinal cord regions several segments removed from the initial site of injury. We found that Pgp expression was significantly increased within the cervical enlargement (C6-C7) of the spinal cord at 7 days, 4 months, and 10 months post-SCI (**Fig. 3.9**). Furthermore, Pgp expression was increased in the lumbar enlargement (L3-L4) of the spinal cord at 4 months and 10 months following injury (**Fig. 3.10**). Thus, the

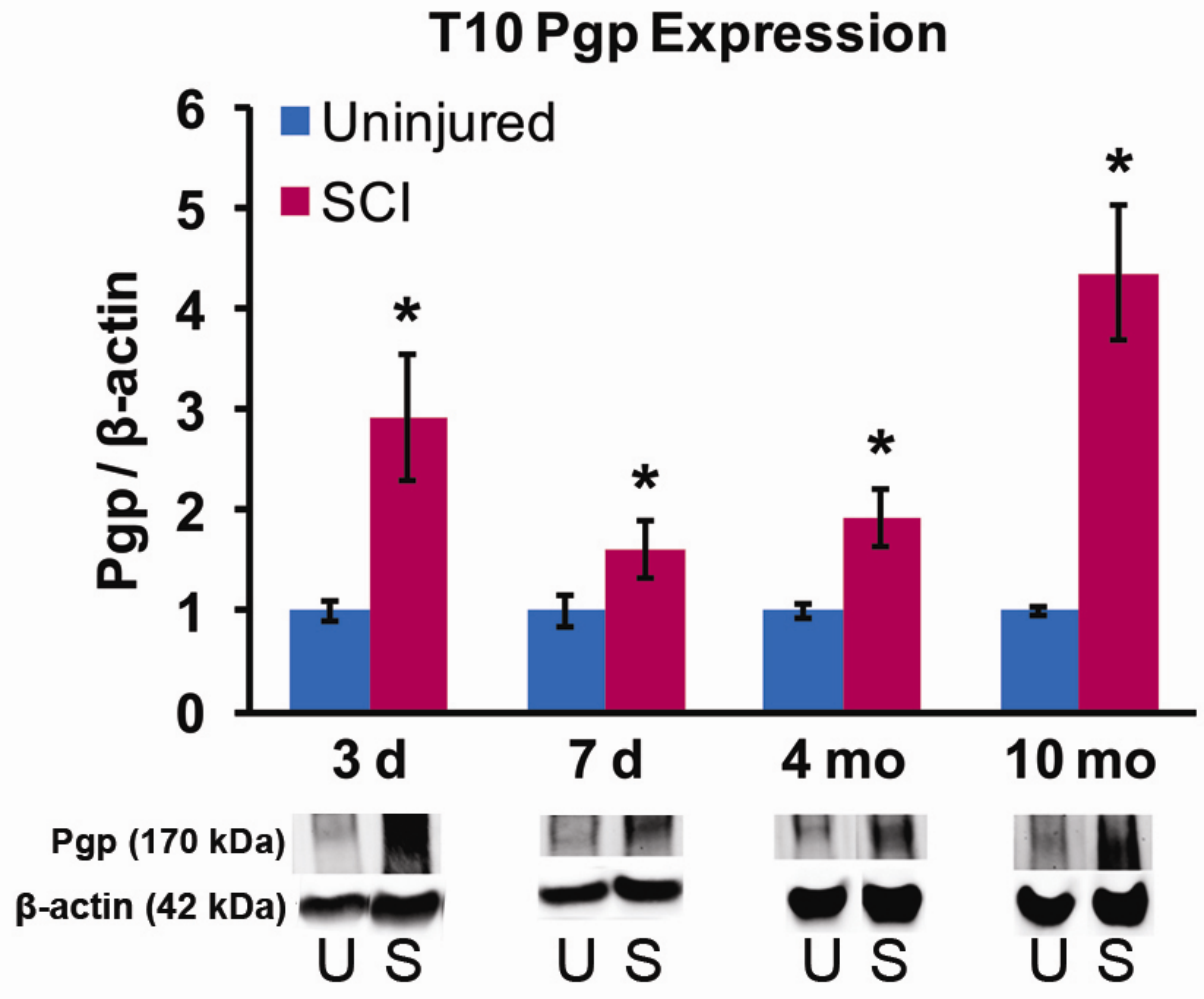

Figure 3.8. P-glycoprotein expression is increased in the spinal cord lesion site during acute and chronic spinal cord injury. Pgp expression levels in T10 spinal cord tissue were quantified by immunoblot analysis and normalized to β-actin. Representative immunoblots are shown below the graph (U, Uninjured; S, SCI). Pgp expression is significantly increased at 3 days [Uninjured = 1.00 ± 0.09 (n = 7); SCI = 2.92 ± 0.63 (n = 6), p = 0.0073], 7 days, [Uninjured = 1.00 ± 0.15 (n = 6); SCI = 1.61 ± 0.29 (n = 7), $p < 0.001$], 4 months [Uninjured = 1.00 ± 0.07 (n = 5); SCI = 1.93 ± 0.27 (n = 6), p = 0.011], and 10 months [Uninjured = 1.00 ± 0.05 (n = 8); SCI = 4.36 ± 0.67 (n = 4), $p < 0.001$] following SCI. All data are mean ± s.e.m. *, $p < 0.05$ versus uninjured, age-matched controls.

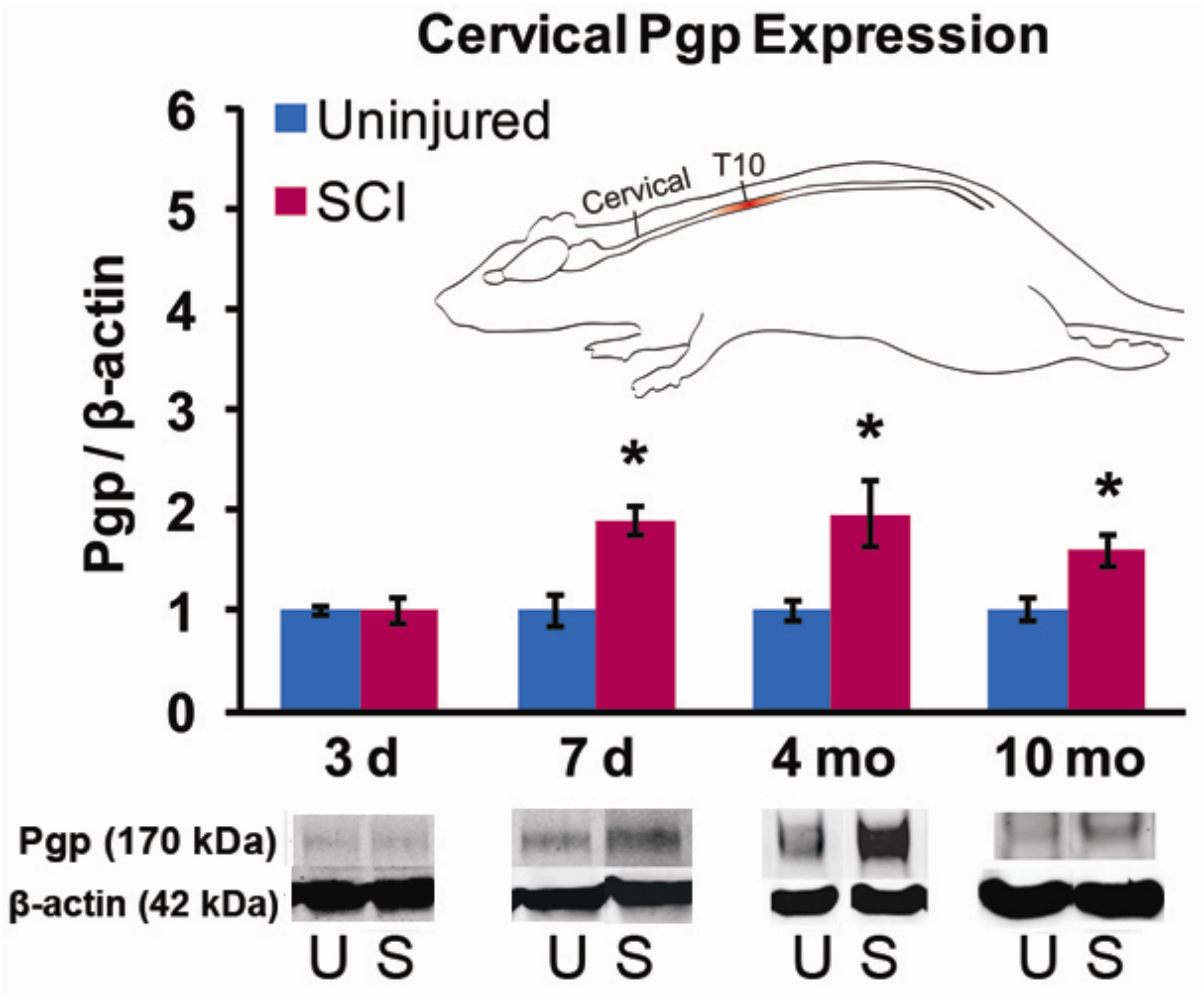

Figure 3.9. P-glycoprotein expression is increased in the cervical spinal cord following spinal cord injury. Pgp expression levels in cervical spinal cord tissue were quantified by immunoblot analysis and normalized to β-actin. Cartoon indicates region of spinal cord tissue analyzed. Representative immunoblots are shown below the graph (U, Uninjured; S, SCI). Pgp expression is significantly increased at 7 days, [Uninjured = 1.00 ± 0.16 (n = 6); SCI = 1.89 ± 0.15 (n = 8), p = 0.002], 4 months [Uninjured = 1.00 ± 0.11 (n = 6); SCI = 1.97 ± 0.33 (n = 6), p = 0.021], and 10 months [Uninjured = 1.00 ± 0.11 (n = 8); SCI = 1.61 ± 0.16 (n = 5), p = 0.009] following SCI. All data are mean ± s.e.m. *, $p < 0.05$ versus uninjured, age-matched controls.

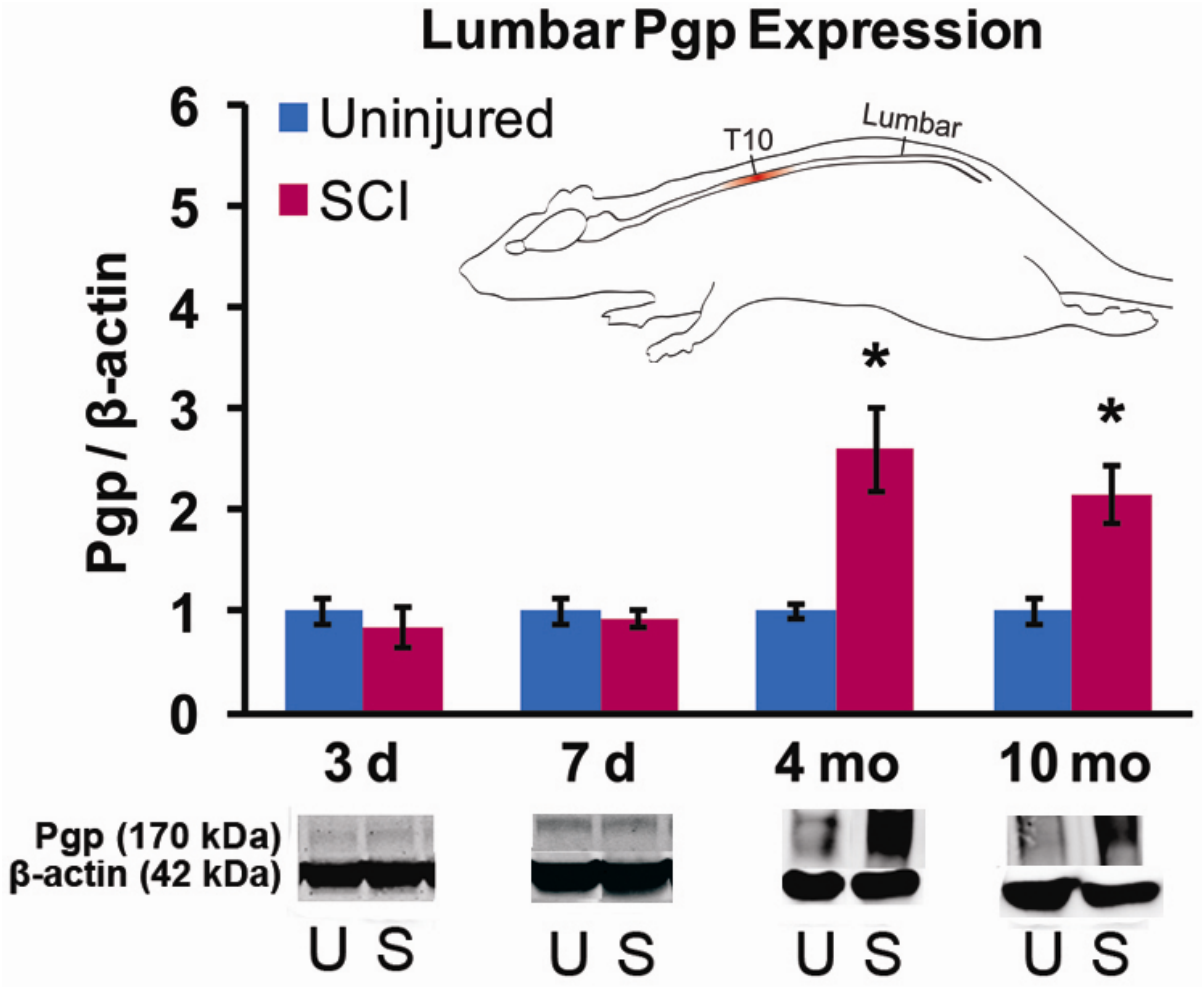

Figure 3.10. P-glycoprotein expression is increased in the lumbar spinal cord during chronic spinal cord injury. Pgp expression levels in lumbar spinal cord tissue were quantified by immunoblot analysis and normalized to β-actin. Cartoon indicates region of spinal cord tissue analyzed. Representative immunoblots are shown below the graph (U, Uninjured; S, SCI). Pgp expression is significantly increased at 4 months [Uninjured = 1.00 ± 0.07 (n = 6); SCI = 2.60 ± 0.42 (n = 6), p = 0.004] and 10 months [Uninjured = 1.00 ± 0.07 (n = 6); SCI = 1.93 ± 0.27 (n = 5), p = 0.011] following SCI. All data are mean ± s.e.m. *, $p < 0.05$ versus uninjured, age-matched controls.

pathological increase in Pgp expression after SCI is not merely restricted to the lesion site. Rather, our data suggests that increased Pgp expression is a progressive and spatially expanding phenomenon, which may reflect a larger, ongoing BSCB pathology secondary to SCI.

Role of P-glycoprotein in Spinal Cord Riluzole Bioavailability Following Spinal Cord Injury

Riluzole is an FDA-approved drug for the treatment of ALS that has neuroprotective and anti-glutamatergic properties (88). Milane and colleagues have demonstrated that riluzole is a substrate of Pgp efflux (225), and that Pgp overexpression in the brain of mice expressing mutant human SOD1 results in reduced brain bioavailability of riluzole subsequent to systemic delivery (224). Riluzole is currently being investigated as an acute neuroprotective SCI intervention in an ongoing national clinical trial (87). The impetus to translate riluzole to the clinic is fueled by several preclinical studies demonstrating its ability to improve histological and functional outcome in animal models of SCI (78-86). If our observations of increased Pgp expression following SCI have the functional consequence of reduced spinal cord riluzole levels, similar to that observed by Milane and colleagues (224), these findings would be highly clinically relevant. We therefore sought to examine whether spinal cord riluzole bioavailability is altered following SCI, and if so, whether Pgp mediates this phenomenon.

In a pharmacokinetics study, Milane *et al*. (306) showed that following *i.p.* delivery, the extent of brain penetration of riluzole is directly proportional to plasma riluzole levels in wild-type mice at a dosing concentration of 10 mg/kg (306), establishing the brain/plasma riluzole concentration ratio as an effective indicator of plasma-to-brain riluzole penetration. The same group has also demonstrated increased brain/plasma ratios of riluzole in *mdr1a* knockout mice (225), and reduced brain/plasma ratios in mSOD1 mice with increased brain Pgp expression (224). These experiments highlight the vital role of Pgp activity at the blood-brain barrier in determining plasma-to-brain penetration of riluzole. We therefore designed an experiment modeled on those previous studies, in order to examine whether the plasma-to-spinal cord penetration of riluzole is altered following SCI. Three weeks following SCI, rats were treated with a single systemic (*i.p.)* bolus of riluzole, and drug concentrations in spinal cord and plasma samples were quantified. We found that the spinal cord/plasma ratio of riluzole was significantly decreased in rats 3 weeks after SCI versus uninjured controls (**Fig. 3.11**).

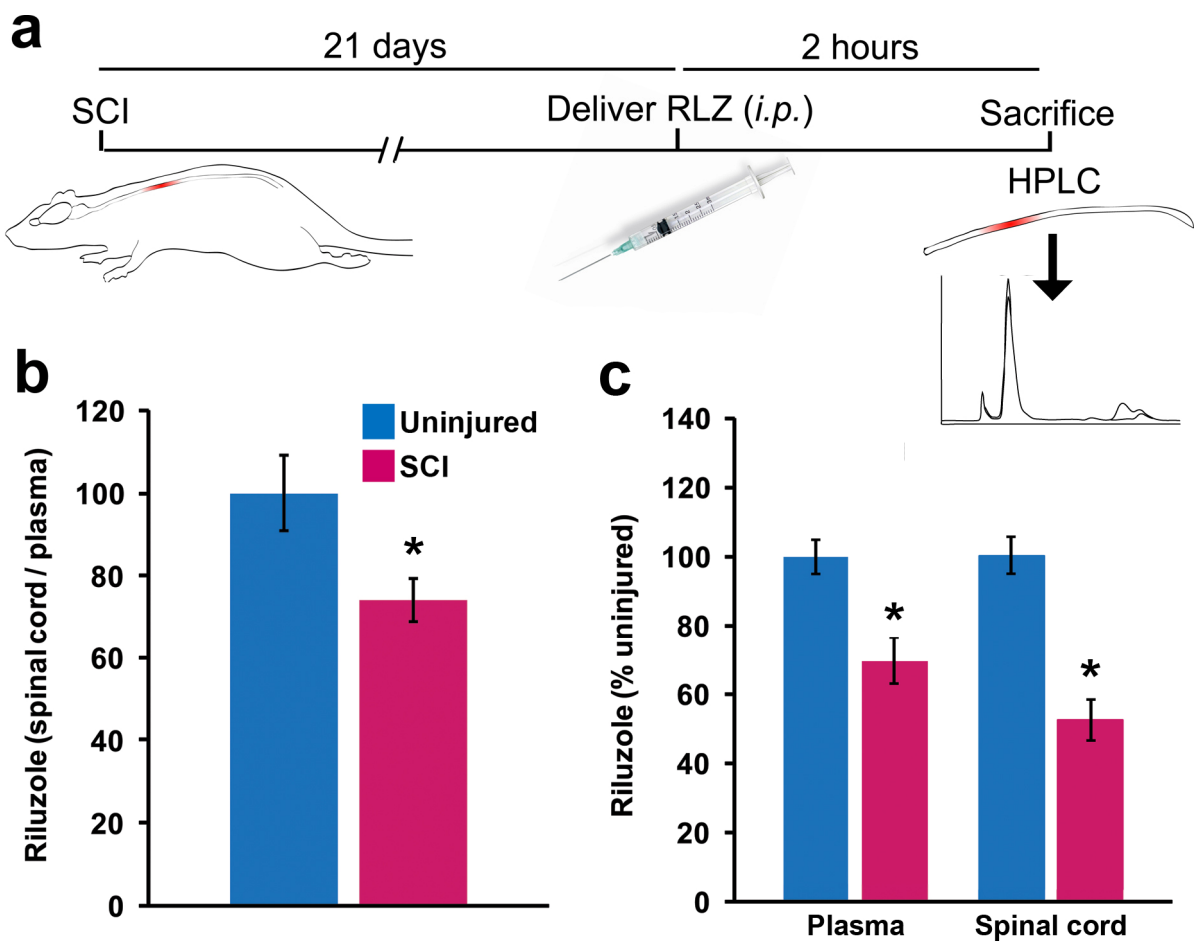

Figure 3.11. Spinal cord riluzole bioavailability is decreased 21 days after SCI. (**a**) Schematic illustrating experimental timeline. Three weeks following SCI, animals received a single *i.p.* bolus of riluzole (RLZ). Two hours later, riluzole concentrations in whole spinal cord tissue and in plasma were measured by HPLC. Spinal cord riluzole concentrations were normalized to plasma concentrations to determine the spinal cord/plasma ratio. (**b**) Spinal cord riluzole levels were significantly reduced in animals three weeks post-SCI (74.1 ± 5.20%, n = 7) versus uninjured controls (100 ± 9.21%, n = 7, p = 0.031). (**c**) Raw riluzole concentrations in plasma and spinal cord tissue were significantly decreased in injured rats compared to uninjured controls. Plasma: Uninjured = 100 ± 4.95%; SCI = 69.7 ± 6.66; p = 0.003. Spinal cord: Uninjured = 100 ± 5.19; SCI = 52.3 ± 6.00; p < 0.001. All data are mean ± s.e.m., expressed as percent of control values. *, p < 0.05 versus uninjured, age-matched controls.

We also examined raw plasma concentrations of riluzole, in order to determine whether the pharmacokinetics of riluzole were altered following SCI. Plasma riluzole levels were also significantly reduced in injured rats (**Fig. 3.11c**). We speculate that this observation might be due to pathological alterations in drug metabolism or excretion during this time point of sub-acute SCI. Milane and colleagues showed that *mdr1a*$^{-/-}$ mice exhibited higher plasma riluzole levels (following *i.p.* injection), presumably due to a reduced biliary excretion rate (306); in contrast, our observed reduction in plasma levels may be explained by increased excretion of riluzole from the plasma compartment because of injury-induced up-regulation of Pgp in the liver. Because the degree of spinal cord riluzole penetration is determined solely by plasma bioavailability (and alterations in blood-spinal cord barrier transport), the spinal cord/plasma concentration ratio is a more accurate representation of plasma-to-spinal cord riluzole penetration than raw spinal cord riluzole levels alone (306). Thus, the reduction that we have observed in drug plasma bioavailability of injured rats is not sufficient to explain the more pronounced reduction in raw spinal cord riluzole levels (**Fig. 3.11c**). Based on the significant reduction in spinal cord/plasma riluzole ratios following injury, we conclude that there is a reduced degree of plasma-to-spinal cord riluzole penetration into the spinal cord, compared to uninjured controls, by three weeks after SCI.

To assess whether this phenomenon might be mediated by Pgp, we utilized *mdr1a* knockout rats for a subsequent assessment of spinal cord riluzole bioavailability after SCI. Because *mdr1a*$^{-/-}$ rats do not express Pgp at the blood-brain barrier (307) or the BSCB (**Fig. 3.6**), they are an ideal tool with which to study spinal cord Pgp function in a rat SCI model[7].

[7] There is a wealth of evidence in the literature that *mdr1a* is the predominant isoform of Pgp expressed at the blood-brain barrier under normal conditions (203). Moreover, a comparison of Pgp transport activity between *mdr1a* and *mdr1a/1b* knockout mice reveals that the loss of both gene products does not substantially affect the brain disposition of systemically-delivered drugs compared to the loss of Mdr1a alone (295); thus, the majority of Pgp function at the blood-brain barrier is most likely normally mediated through the Mdr1a isoform. Despite this, we have observed up-regulation of *mdr1b* gene expression during acute and chronic SCI (**TABLE 3.1** & **Fig. 3.1**). Expression of *mdr1b* has been shown to be up-regulated by neuroinflammatory conditions (245, 297); thus, it is conceivable that the development of resistance to riluzole in the injured spinal cord may be at least partially mediated by the Mdr1b gene product. We chose to utilize the *mdr1a*$^{-/-}$ rat for these studies—despite the availability of single- and double *mdr1* knockout mouse lines—largely because of the distinct behavioral and pathophysiological differences between mouse and rat models of SCI (6, 60). Only *mdr1a* knockout rats were available for purchase from Sage Labs at the time these experiments were performed.

Ten days after SCI was performed on wild-type and *mdr1a*$^{-/-}$ rats, we administered a single *i.p.* bolus of riluzole then examined spinal cord and plasma riluzole concentrations via HPLC (**Fig. 3.12**). We found that normalized spinal cord/plasma riluzole levels were significantly decreased in wild-type rats following injury (p = 0.002), but that there was no detectable difference in drug levels between KO injured and uninjured groups (p = 0.375). Notably, normalized spinal cord/plasma riluzole levels were significantly higher in KO rats, than in WT rats, 10 days post-SCI (p = 0.006). These findings illustrate a critical role for Pgp function in the development of spinal cord drug resistance to riluzole following SCI.

We also evaluated plasma riluzole concentrations (**Fig. 3.13**). There was no significant difference in plasma riluzole levels between uninjured wild-type rats (100 ± 5.83%) and injured wild-type rats (104 ± 4.74%, p = 0.479). There was also no significant difference in plasma riluzole levels between uninjured wild-type rats and *mdr1a*$^{-/-}$ rats (89.3 ± 2.13%, p = 0.577). This was an unexpected finding, in light of the observations of Milane *et al.* that *mdr1a*$^{-/-}$ mice exhibited higher plasma riluzole levels compared to wild-type mice after *i.p.* injection (306). However, our observation is likely explained by the fact that the Mdr1b isoform is expressed at normal levels in the liver of *mdr1a*$^{-/-}$ rats (**Fig. 3.14**); thus, Mdr1b function probably plays a compensatory role in the excretion of riluzole from the plasma in the absence of Mdr1a.

There appeared to be a slight decrease, but no significant difference, in plasma riluzole levels of *mdr1a*$^{-/-}$ rats following injury (KO SCI = 75.2 ± 5.04 %, p = 0.258). Compared with our observations of decreased plasma riluzole levels at 3 weeks after injury, the lack of effect of SCI on plasma drug levels at 10 days after injury suggests that there may be a time-dependent effect on riluzole pharmacokinetics in wild-type rats. Interestingly, we observed a significant effect of genotype on plasma riluzole levels between injured groups (but not between uninjured groups); riluzole plasma levels were significantly lower in *mdr1a*$^{-/-}$ rats compared to wild-type rats. This finding suggests that *mdr1a* knockout rats probably have enhanced metabolism or clearance of riluzole compared to wild-types at 10 days post-SCI, although investigation as to the possible mechanism(s) underlying this requires further study.

In conclusion, we have found that spinal cord/plasma ratios of systemically-delivered riluzole were significantly higher in *mdr1a*$^{-/-}$ rats compared to wild-type rats after SCI (**Fig. 3.12**). Curiously, we did not observe an increase in raw riluzole spinal cord concentrations in

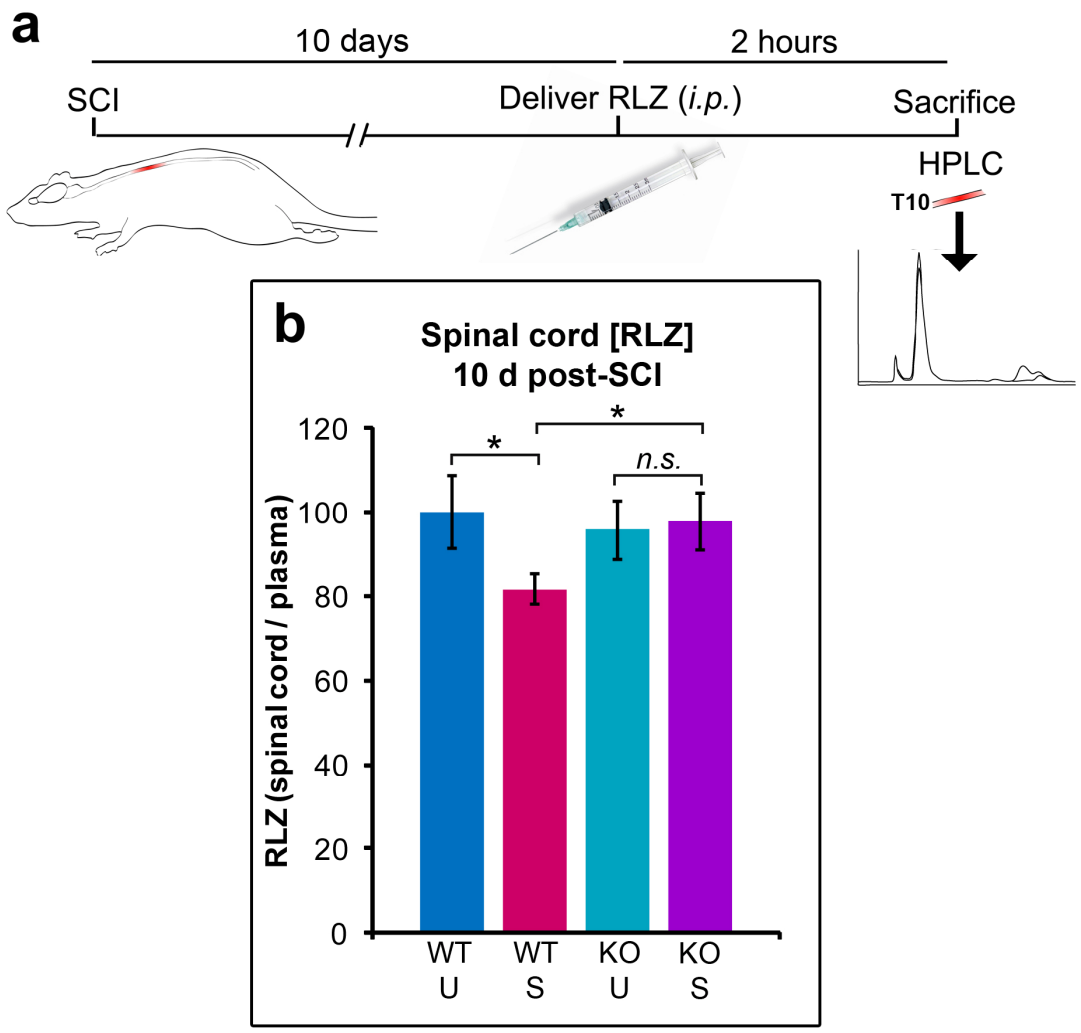

Figure 3.12. Spinal cord riluzole bioavailability is decreased 10 days after spinal cord injury in wild-type but not *mdr1a*$^{-/-}$ rats. Abbreviations: WT, wild-type; KO, *mdr1a* knockout; U, uninjured; S, 10 days post-SCI. (**a**) Schematic illustrating experimental timeline. Ten days following SCI, animals received a single *i.p.* bolus of riluzole (RLZ). Two hours later, riluzole concentrations in T10 spinal cord tissue and in plasma were measured by HPLC. Spinal cord riluzole concentrations were normalized to plasma concentrations to determine the spinal cord/plasma ratio. (**b**) Normalized spinal cord riluzole levels were significantly reduced in WT rats with SCI (81.6 ± 3.54%, $n = 9$) versus WT uninjured controls (100 ± 8.73%, $n = 10$, $p = 0.002$). There was no significant effect of injury on spinal cord/plasma riluzole ratios in KO rats (KO uninjured = 95.8 ± 6.94%, $n = 6$; KO SCI = 97.8 ± 6.91%, $n = 7$, $p = 0.375$). Normalized riluzole levels were significantly higher in injured KO rats compared to injured WT rats ($p = 0.006$). All data are mean ± s.e.m., expressed as percentage of wild-type, uninjured controls. *, $p < 0.05$.

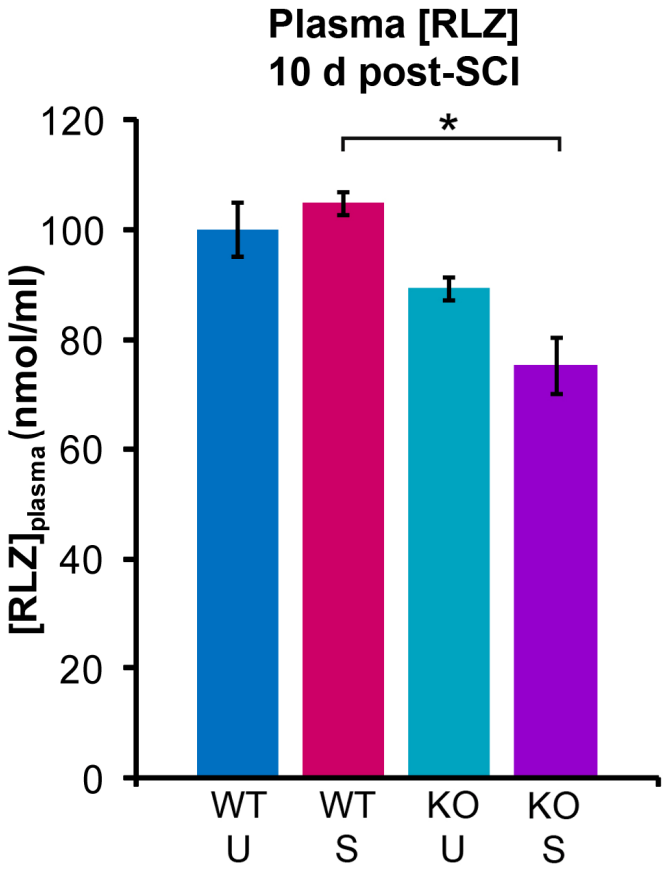

Figure 3.13. Plasma riluzole concentrations are decreased in injured *mdr1a*$^{-/-}$ rats compared to injured wild-type rats. Abbreviations: WT, wild-type; KO, *mdr1a* knockout; U, uninjured; S, 10 days post-SCI. Plasma riluzole levels were significantly reduced in KO rats with SCI (75.2 ± 5.04%) versus WT rats with SCI (104 ± 4.74%, $p = 0.002$). WT uninjured = 100 ± 5.83%; KO uninjured = 89.3 ± 2.13%). All data are mean ± s.e.m., expressed as percentage of wild-type, uninjured controls. *, $p < 0.05$.

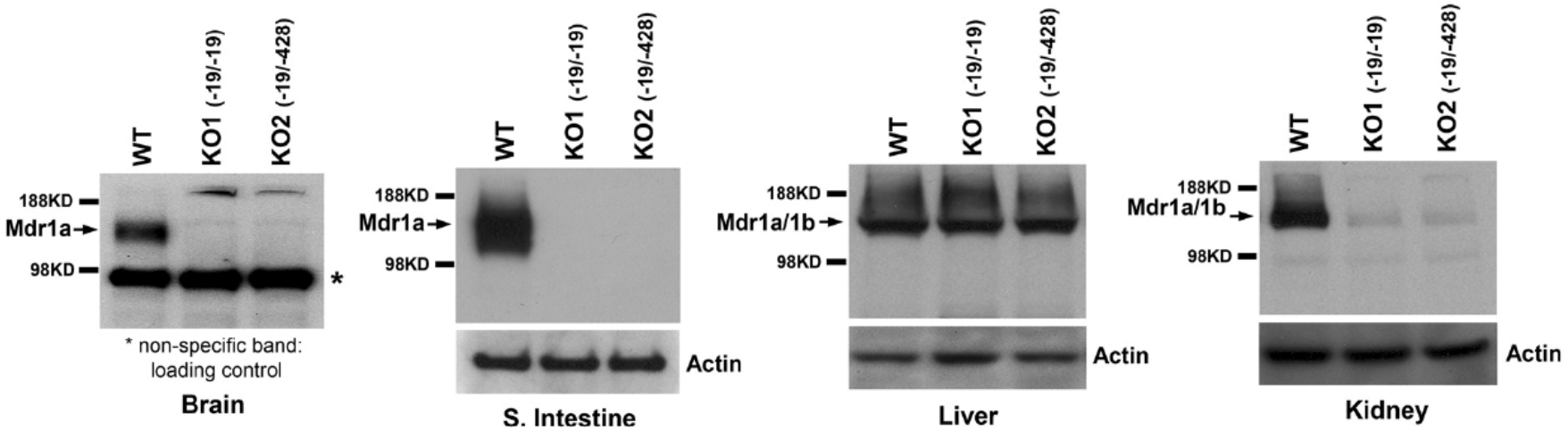
WT
KO1 (-19/-19)
KO2 (-19/-428)
188KD
Mdr1a
98KD
*
* non-specific band:
loading control
Brain
Actin
S. Intestine
Mdr1a/1b
Liver
Kidney

(On previous page)

Figure 3.14. *mdr1a*$^{-/-}$ rats express Mdr1b in the liver. "Western blots showing undetectable levels of Mdr1a protein in the brain and small intestine (S. Intestine) of knockout (KO) rats. In the liver sample, the band with a size that was apparently similar to that of the Mdr1a protein in KO rats may represent the up-regulated Mdr1b protein because of the cross-reactivity of the antibody. The weak potential Mdr1b protein was detected in the kidney of KO rats as well but not as strongly as in liver." Quoted from Xiaoyan Chu, Zuo Zhang, Jocelyn Yabut, Sarah Horwitz, John Levorse, Xiang-qing Li, Lei Zhu, Harmony Lederman, Rachel Ortiga, John Strauss, Xiaofang Li, Karen A. Owens, Jasminka Dragovic, Thomas Vogt, Raymond Evers, and Myung K. Shin, Characterization of Multidrug Resistance 1a/P-Glycoprotein Knockout Rats Generated by Zinc Finger Nucleases, *Mol Pharmacol* February 2012 81:220-227. Reprinted with permission (307).

uninjured *mdr1a*$^{-/-}$ rats compared to wild-type rats (**Fig. 3.15**), which may be attributable to compensatory activity of another drug efflux transporter. Despite this, our finding that spinal cord riluzole delivery is significantly diminished following SCI in wild-type but not *mdr1a*$^{-/-}$ rats provides compelling support for the central role of Pgp in mediating post-SCI spinal cord drug resistance.

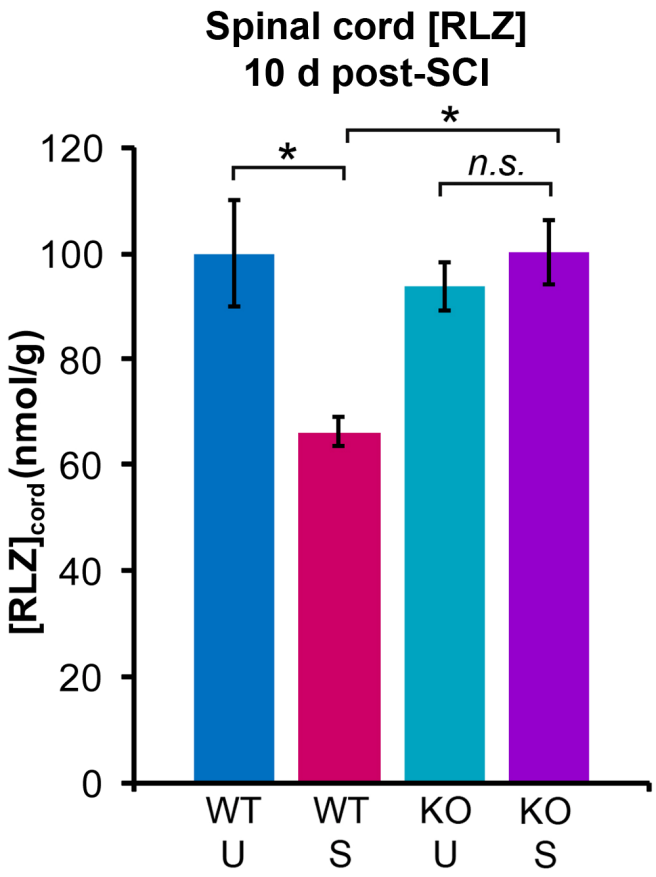

Figure 3.15. Raw spinal cord riluzole concentrations are decreased 10 days after spinal cord injury in wild-type but not *mdr1a*$^{-/-}$ rats. Abbreviations: WT, wild-type; KO, *mdr1a* knockout; U, uninjured; S, 10 days post-SCI. Spinal cord riluzole levels were significantly reduced in WT rats with SCI (66.2 ± 2.84%) versus WT uninjured controls (100 ± 10.18%, $p < 0.001$). There was no significant effect of injury on spinal cord/plasma riluzole ratios in KO rats (KO uninjured = 93.8 ± 4.49%; KO SCI = 100.2 ± 5.94%, $p = 0.767$). Raw spinal cord riluzole levels were significantly higher in injured KO rats compared to injured WT rats ($p = 0.004$). All data are mean ± s.e.m., expressed as percentage of wild-type, uninjured controls. *, $p < 0.05$.

CHAPTER 4

Characterization of Inflammation in the Injured Spinal Cord

&

The Effects of Licofelone Treatment on P-glycoprotein Expression and Riluzole Bioavailability

Increased P-glycoprotein expression is a hallmark of diseases such as cancer, and it has recently been shown to occur in a number of neurological diseases as well. Multidrug resistance caused by heightened Pgp-mediated drug efflux attenuates the efficacy of therapeutic drugs indicated to treat these diseases, and overcoming this phenomenon is a highly desirable goal. Because pharmacological Pgp inhibition is not a viable therapeutic solution to overcome drug resistance (300), a more desirable strategy is to prevent Pgp overexpression by pharmacologically targeting the molecular mechanisms that up-regulate it (234). There is a wealth of evidence that inflammation drives pathological increases in Pgp expression. For example, prolonged (hours) exposure to TNF-α and endothelin-1 increase Pgp expression and activity in brain capillary endothelial cells (308). Other inflammatory mediators, such as IL-1β, as well as substances such as LPS, have been shown to have differential effects on Pgp expression in various *in vitro* and *in vivo* models of central- and peripheral nervous system inflammation (198). Because of the complex nature of inflammatory response, and the diversity of results observed in various dose-dependent and context-dependent models, the exact nature of inflammatory regulation of Pgp expression is still relatively unclear.

Potschka and colleagues have gained much insight into the pathological up-regulation of Pgp via COX signaling in rodent models of seizure (See **Fig. 1.10**) (187). In addition to their work, a variety of recent studies have substantiated the role of COX signaling in driving Pgp up-regulation in experimental models of cancer (238-241, 309). Thus, there appears to be a growing body of evidence showing that pro-inflammatory COX signaling is important for driving pathological Pgp overexpression in various diseases, and that inhibiting this pathway can enhance therapeutic drug delivery. In Potschka's model, it is not indicated exactly how the COX-dependent up-regulation of *Abcb1* gene expression occurs at the transcriptional level, though the author speculates that the transcription factor NF-kB is a likely candidate based on evidence that brain COX-2 activity can induce NF-kB activation (245, 246). More recently, other groups have published findings that NF-kB does indeed promote increased Pgp expression in a kainic acid-induced seizure model (310), and that NF-kB mediates increased transcription of *Mdr1b* in cerebral LPS-induced inflammation (245, 297). Thus, it appears likely that pro-inflammatory COX signaling acts via NF-kB activation to promote up-regulation of Pgp in neuroinflammatory diseases. Interestingly, the parallel pro-inflammatory

5-LOX branch of oxidative AA metabolism is an upstream activator of NF-kB activation as well (311-313). Furthermore, it has been shown that inhibiting 5-LOX activity blocks NF-kB activation during cerebral ischemia (314). Given the intimate relationship between COX and 5-LOX signaling (155, 315), one might speculate that these two pro-inflammatory signaling pathways may act via a common mechanism to promote Pgp up-regulation in the diseased CNS.

We have observed increased Pgp expression within the spinal cord at acute (72 hours, 7 days) and chronic (4 months, 9 months) time points after injury (See *Chapter 3*). Given the large amount of evidence supporting a role for inflammation in driving Pgp up-regulation, we became interested in whether inflammation could also be detected within the injured spinal cord at each of these time points. Because there has historically been much interest in the role of inflammation in acute SCI, a number of studies have investigated the presence of COX- and 5-LOX pathway components within the injured spinal cord at early time points (121, 141). In contrast, relatively little is known about whether inflammatory signaling persists beyond a period of several weeks post-SCI. This unexplored question is largely attributed to the fact that the chronically-injured spinal cord has historically been a subject of relatively little study. Because COX and 5-LOX are both known to contribute to destructive SCI secondary pathology, and because of evidence that COX signaling drives Pgp overexpression in neuroinflammatory conditions (as well as indirect evidence that 5-LOX signaling may do the same), we evaluated whether components of these two pathways are expressed at acute and chronic time points following SCI, mirroring the time points at which we have previously detected increased Pgp expression. We also sought to develop a deeper understanding of the metabolic processes at work in the far chronically-injured spinal cord, as there is very little known about the molecular processes shaping SCI pathology during this time frame.

We have shown that Pgp confers resistance to riluzole uptake in the spinal cord during the sub-acute phase of SCI (See *Chapter 3*). Previous studies have shown that pharmacological COX inhibition down-regulates Pgp-mediated drug resistance in clinically relevant models of seizure and cancer (236, 238, 241). Therefore, our next goal in this study was to assess the efficacy of anti-inflammatory drug treatment to 1) abrogate Pgp overexpression and 2) enhance delivery of systemically-administered riluzole to the injured spinal cord tissue. There are undesirable side effects associated with the clinical use of COX inhibitors; namely, high incidence of gastrointestinal side effects, as well as the shunting of AA into the parallel, pro-

inflammatory 5-LOX pathway, resulting in an antagonized inflammatory response. In order to circumvent these undesirable side effects of selective COX inhibition, for this study we elected to instead utilize the dual COX/5-LOX inhibitor, licofelone, for its superior anti-inflammatory properties and improved GI tolerance in humans.

Specific Aims

1. Several studies have shown that pro-inflammatory signaling drives pathological Pgp overexpression (238-240, 244, 309, 310). Here, we have demonstrated that spinal cord expression of Pgp is increased during the acute and chronic phases of SCI. Therefore, we aimed to assess the presence of components of pro-inflammatory COX and 5-LOX pathways at time points at which we have observed increased Pgp expression—72 hours, 7 days, 4 months, and 10 months following SCI.

2. Furthermore, the biochemical environment of the chronically-injured spinal cord has not previously been well characterized. In order to supplement our understanding of the pathological changes occurring in chronic SCI, we sought to characterize the long-term metabolic alterations in the chronically-injured cord via a metabolomic analysis of spinal cord tissue 9 months following SCI.

3. We have demonstrated that Pgp mediates a SCI-induced decrease in riluzole bioavailability in the weeks following injury. Other groups have shown that treatment with anti-inflammatory COX inhibitors is an effective strategy to attenuate up-regulation of Pgp and enhance CNS delivery of therapeutic drugs that are Pgp substrates (236, 238, 241). Licofelone is a dual COX/5-LOX inhibitor with improved GI tolerability in humans, as well as enhanced anti-inflammatory properties compared to COX inhibitors. Therefore, we aimed to evaluate the efficacy of licofelone to attenuate Pgp overexpression and enhance spinal cord riluzole bioavailability following SCI.

Assessment of COX/5-LOX Enzymes and Pro-Inflammatory Mediators in the Acutely-Injured Spinal Cord

Previous studies in our laboratory have revealed substantial increases in expression of 5-LOX and production of the CysLTs in the spinal cord lesion site at 24 hours post-SCI (**Fig. 4.1**). In order to evaluate whether the COX and 5-LOX pro-inflammatory signaling pathways are up-regulated at additional acute time points following injury, particularly those during which we have observed Pgp up-regulation (**Figs. 3.8-3.10**), we performed immunoblot analysis of T10 spinal cord tissue at 72 hours and 7 days post-SCI. At 72 hours, we observed significantly increased expression of all three enzymes (**Fig. 4.2**), the most dramatic of which being a nearly five-fold increase in COX-2 expression. At 7 days post-injury, we only detected a significant (three-fold) increase in COX-2 expression, and no change in COX-1 or 5-LOX versus uninjured controls (**Fig. 4.3**).

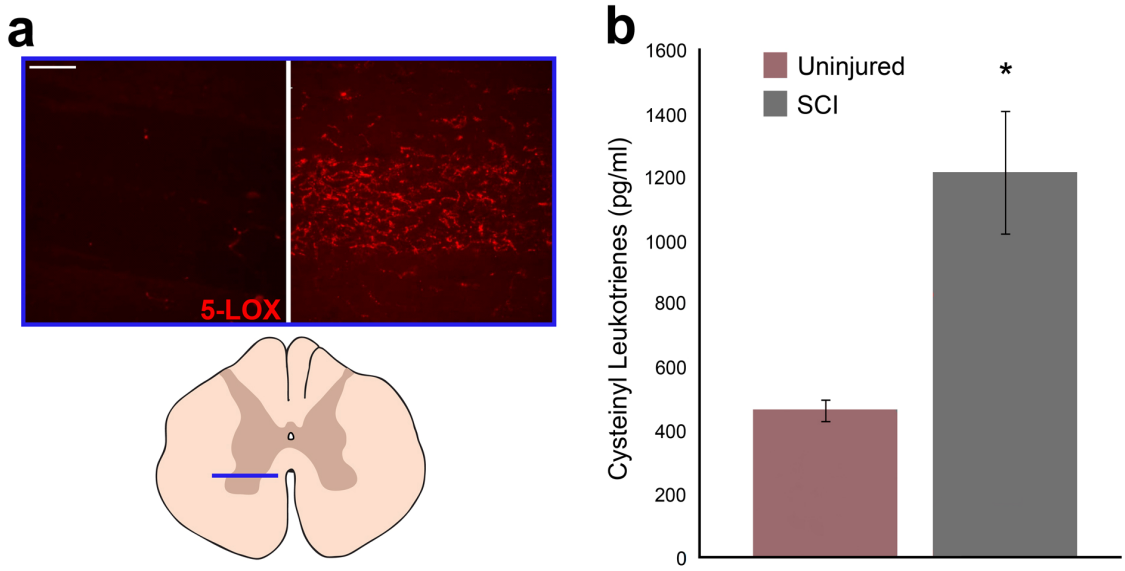

Figure 4.1. 5-lipoxygenase expression and cysteinyl leukotriene production are increased 24 hours following spinal cord injury. (**a**) Top: 5-LOX immunoreactivity (red) is virtually undetectable in the thoracic spinal cord tissue of uninjured controls (left panel), but is markedly increased in the T10 lesion site of rats 24 hours post-SCI (right panel), especially in the gray matter. Bottom: Plane of view for fluorescent images is indicated by the blue line (horizontal plane) in the cartoon. Image provided courtesy of Dr. Raymond Grill. Scale bar = 200 µm. (**b**) Cysteinyl leukotrienes are increased more than two-fold in the spinal cord lesion site compared to uninjured controls 24 hours post-SCI. *, $p < 0.05$. ELISA data provided courtesy of Dr. Meredith Moore.

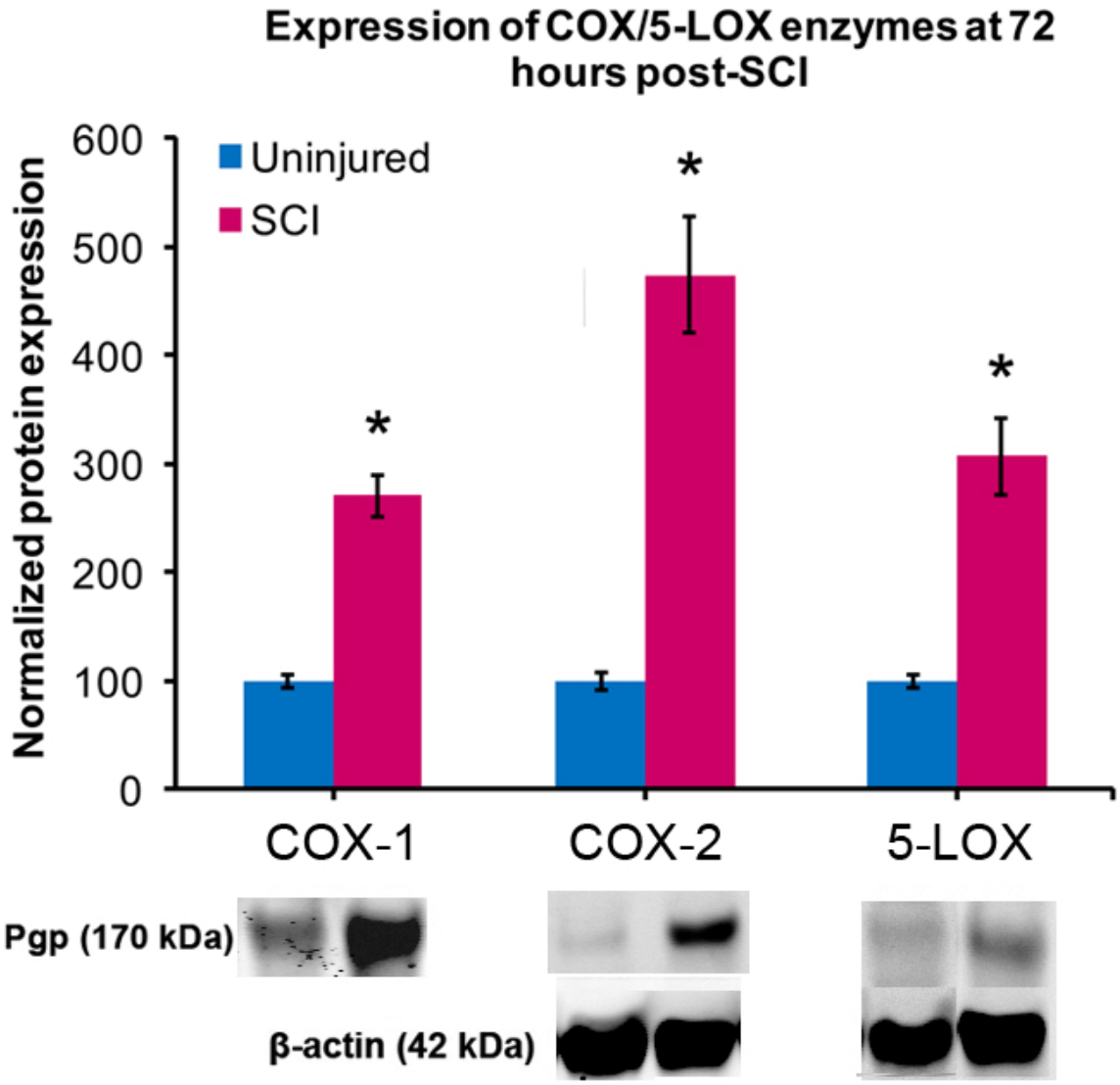

Figure 4.2. Expression of cyclooxygenase-1/-2 and 5-lipoxygenase is increased in the spinal cord lesion site 72 hours after spinal cord injury. Protein expression levels are normalized to β-actin and expressed as a percentage of uninjured control expression levels. 72 hr post-SCI, there is significantly increased expression of COX-1 (Uninjured = 100 ± 5.79%, n = 6; SCI = 271 ± 19.0%, n = 8, $p < 0.001$), COX-2 (Uninjured = 100 ± 8.06%, n = 6; SCI = 474 ± 53.9%, n = 8, $p < 0.001$), and 5-LOX (Uninjured = 100 ± 5.49% n = 6; SCI = 308 ± 35.4%, n = 8, $p < 0.001$) in the T10 lesion site. Representative immunoblots pictured for COX-1 and COX-2 are from the same sample. All data are mean ± s.e.m. *, $p < 0.05$ versus uninjured controls.

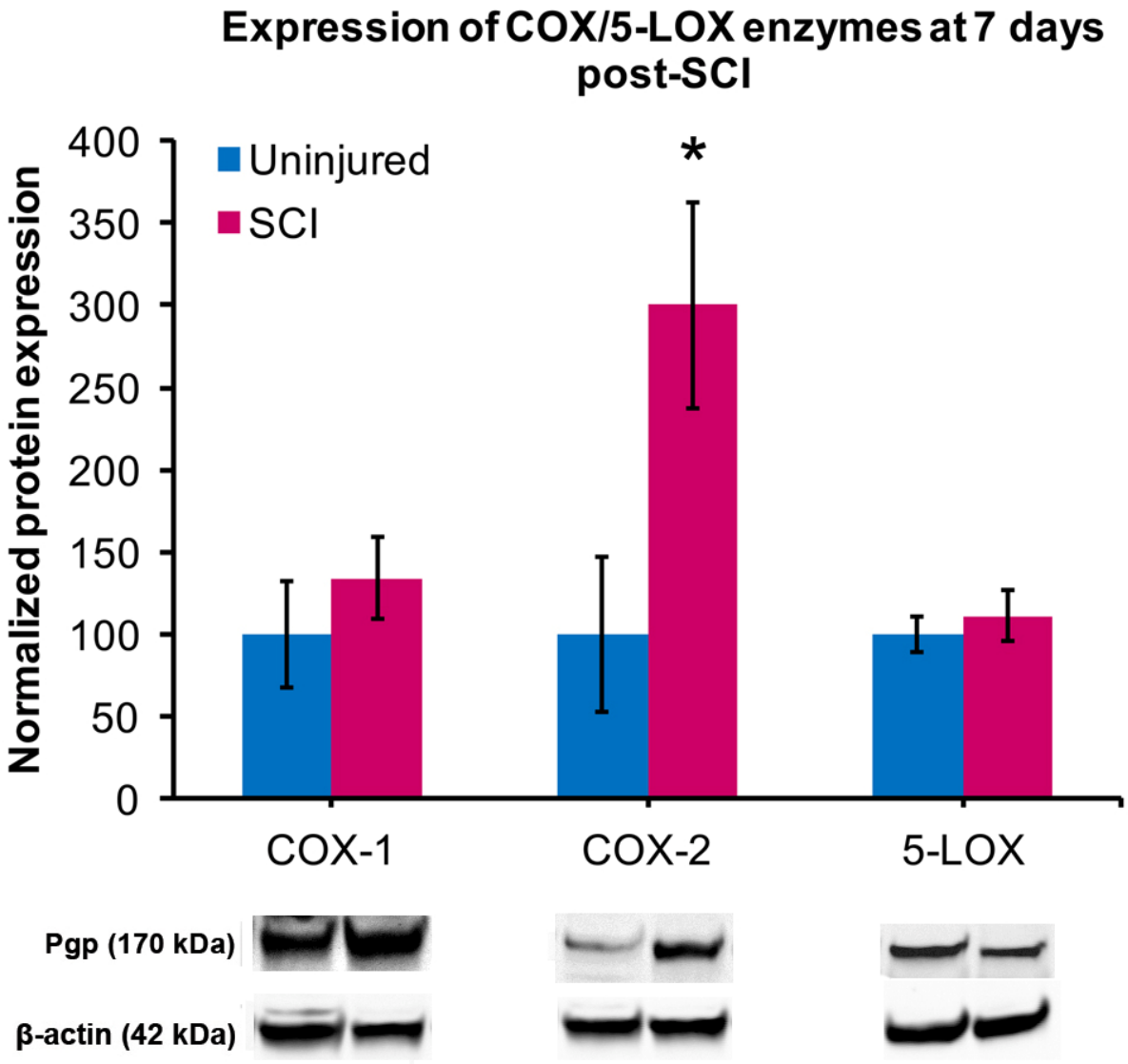

Figure 4.3. Expression of cyclooxygenase-2 is increased in the spinal cord lesion site 7 days after spinal cord injury. Protein expression levels are normalized to β-actin and expressed as percentage of uninjured control expression levels. 7 days post-SCI, there is significantly increased expression of COX-2 (Uninjured = 100 ± 46.8%, n = 6; SCI = 300 ± 63.0%, n = 6, p = 0.029), but not COX-1 (Uninjured = 100 ± 32.6%, n = 6; SCI = 134 ± 24.7%, n = 7, p = 0.418) or 5-LOX (Uninjured = 100 ± 10.8%, n = 6; SCI = 111 ± 15.4%, n = 8, p = 0.561) in the T10 lesion site. Representative immunoblots pictured for COX-1 and COX-2 are from the same sample. All data are mean ± s.e.m. *, $p < 0.05$ versus uninjured controls.

Assessment of Inflammation in the Chronically-Injured Spinal Cord

Because the spinal cord biochemical environment after a period of 1-2 months post-SCI has received relatively little attention compared to the acutely-injured spinal cord, it is unknown whether inflammation is present during the chronic phase of injury. Two goals of the current study were to 1) examine whether COX/5-LOX activity is detectable in the injured spinal cord at several months post-injury, and 2) develop a more comprehensive understanding of the cytotoxic biochemical processes at work in the chronically-injured spinal cord environment. A previous study in our laboratory (performed by Dr. Raymond Grill) has provided novel evidence of pro-inflammatory AA metabolism within the spinal cord during the chronic period of injury. Specifically, this study has revealed increased expression of the cysteinyl leukotriene receptor 1 within the dorsal horn of the lumbar spinal cord 4 months following spinal contusion injury at T10 (**Fig. 4.4**). This is an intriguing finding when compared to our observations of increased Pgp expression in the lumbar spinal cord at 4 months post-SCI (**Fig. 3.10**), and raises the question of whether pro-inflammatory 5-LOX signaling in the lumbar spinal cord may contribute to this component of BSCB pathology.

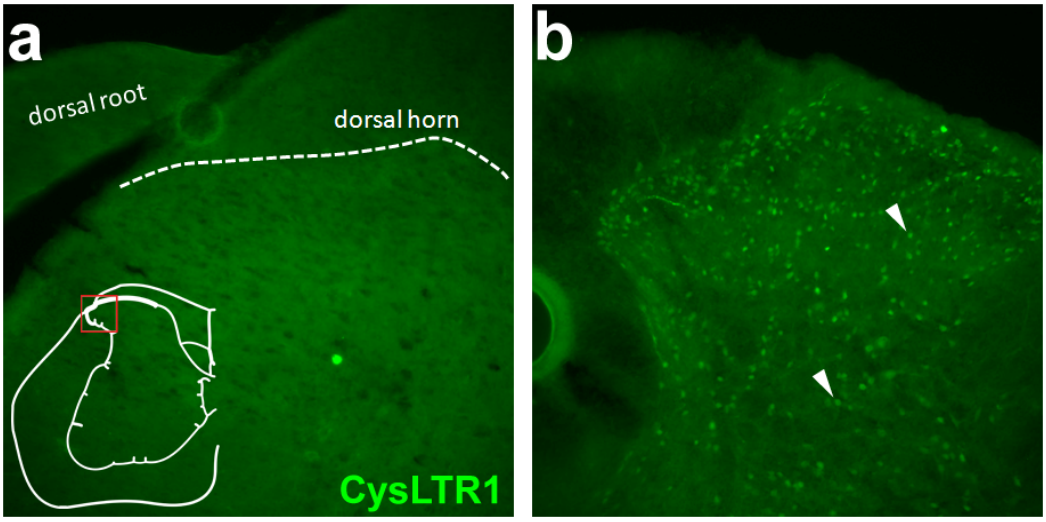

Figure 4.4. Increased expression of the cysteinyl leukotriene receptor 1 four months after spinal cord injury. Immunofluorescent labeling for the cysteinyl leukotriene receptor 1 (CysLTR1, green) in the dorsal horn of the lumbar spinal cord. Inset in (**a**) indicates field of view (red-bounded square). Dashed line in (**a**) indicates boundary of gray and white matter in dorsal horn. (**a**) Spinal cord section from naïve, uninjured, age-matched control animal. (**b**) Spinal cord section from animal 4 months post-SCI. Arrowheads indicate cells exhibiting increased CysLTR1 expression. Image provided courtesy of Dr. Raymond Grill.

Additional investigations in our lab (performed by Dr. Raymond Grill) have shown that at 4 months post-SCI, 5-LOX expression within the spinal cord near the lesion site appears to be closely associated with the vasculature (**Fig. 4.5**). This observation may hold interesting implications for BSCB pathology at far chronic time points.

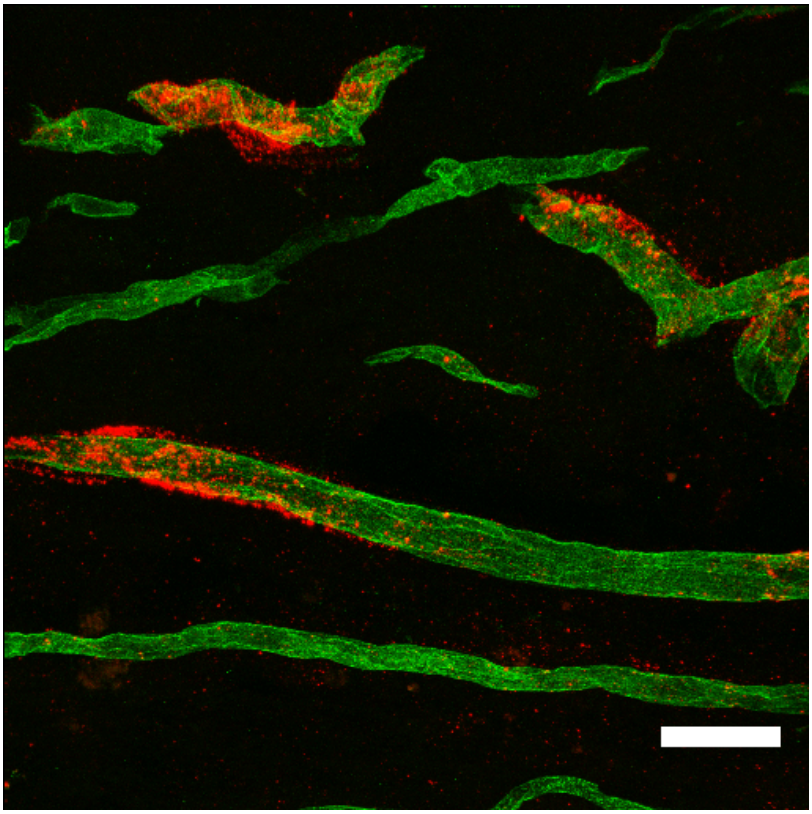

Figure 4.5. 5-lipoxygenase expression is localized to the spinal cord vasculature 4 months after spinal cord injury. Immunofluorescent labeling of 5-LOX (red) and the endothelial cell marker, rat endothelial cell antigen-1 (RECA-1, green) in thoracic spinal cord tissue of rats 4 months after SCI. 5-LOX immunoreactivity appears to be ensheathing the capillary endothelial cells. 5-LOX was undetectable in age-matched, uninjured controls (data not shown). Scale bar = 60 µm. Image provided courtesy of Dr. Raymond Grill.

We used ELISA to measure levels of the major AA-derived mediators, PGE_2 and LTB_4, within spinal cord tissue of rats at the far chronic time point of nine months post-SCI. PGE_2 levels were undetectable in the spinal cord of uninjured, age-matched controls (n = 3) but increased to 87.1 ± 4.91 pg/ml in the lesion site of chronic SCI animals (n = 3) ($p < 0.001$, **Fig. 4.6a**). LTB_4 levels were similarly undetectable in uninjured controls (n = 6) but were significantly increased in T10 spinal cords of chronic SCI rats (n = 6) (10.6 ± 1.67) ($p < 0.001$, **Fig. 4.6b**).

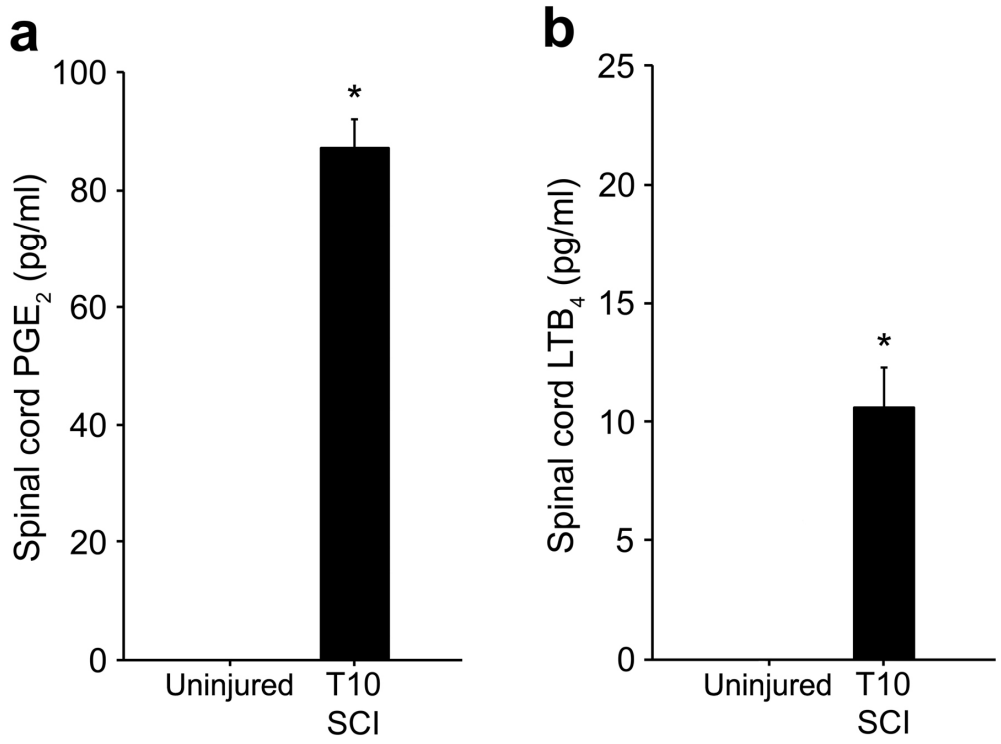

Figure 4.6. Increased levels of prostaglandin E2 and leukotriene B4 in the spinal cord 9 months after spinal cord injury. Prostaglandins and leukotrienes are present in the lesion site of spinal cords nine months following SCI. PGE_2 levels (**a**) and LTB_4 levels (**b**) in T10 spinal cord segments of age-matched, uninjured controls (undetectable) and animals 9 mo post-SCI (black bars). PGE_2 (87.1 ± 4.91 pg/ml, $n = 3$) and LTB_4 (10.6 ± 1.67 pg/ml, $n = 6$). *, $p < 0.001$ versus uninjured controls. All data are mean ± s.e.m.

Metabolomic Profiling of the Chronically-Injured Spinal Cord

To gain a more complete understanding of the biochemical environment within the chronically-injured spinal cord, metabolomic profiling was performed for T10 spinal cord tissue from far chronic (9 months) post-SCI animals ($n = 8$) and uninjured, age-matched controls ($n = 9$). A total of 257 metabolites were identified in spinal cord samples, from the Metabolon library comprising 2,400 named molecules. Tissue expression levels of 126 of these compounds were altered in chronic SCI samples (**TABLE 4.1**). Metabolites belonged to diverse molecular classes (*e.g.*, amino acids, nucleotides, and lipids), and hierarchical clustering revealed multiple clusters of biochemicals similarly altered in SCI tissue (**Fig. 4.7-4.8**). For

Class	Sub-class	Biochemical Name	Fold Change (SCI + VEH / Uninjured)	*p* Value
Amino acid	Glycine, serine and threonine metabolism	glycine	–1.35	**< 0.001**
		homoserine	–1.18	0.0780
		betaine	2.22	**< 0.001**
	Alanine and aspartate metabolism	alanine	1.19	**0.0236**
		aspartate	–1.22	**0.0091**
		N-acetylaspartate (NAA)	–2.38	**< 0.001**
		asparagine	–1.47	0.0557
	Glutamate metabolism	glutamate	–1.45	**< 0.001**
		glutamine	1.06	0.0982
		gamma-aminobutyrate (GABA)	–1.33	0.0650
		N-acetylglutamate	–1.33	**0.0220**
		N-acetyl-aspartyl-glutamate (NAAG)	–1.79	**< 0.001**
	Lysine metabolism	2-aminoadipate	1.38	**0.0040**
		N6-acetyllysine	1.47	**0.0014**
	Phenylalanine & tyrosine metabolism	tyrosine	1.15	0.0581
	Valine, leucine and isoleucine metabolism	isoleucine	1.40	**< 0.001**
		leucine	1.45	**< 0.001**
		valine	1.40	**0.0036**
	Cysteine, methionine, SAM, taurine metabolism	taurine	1.52	**0.0012**
		S-adenosylhomocysteine (SAH)	–1.43	**0.0012**
		methionine	1.18	**0.0260**
		N-acetylmethionine	2.53	**< 0.001**
		2-hydroxybutyrate (AHB)	1.65	**< 0.001**

	Urea cycle; arginine-, proline-, metabolism	citrulline	1.55	**0.0158**
		trans-4-hydroxyproline	2.05	**< 0.001**
	Creatine metabolism	creatine	–1.16	**0.0314**
	Butanoate metabolism	2-aminobutyrate	1.72	**0.0035**
	Glutathione metabolism	glutathione, oxidized (GSSG)	3.19	**< 0.001**
		cysteine-glutathione disulfide	3.19	**< 0.001**
Carbohydrate	Fructose, mannose, galactose, starch, and sucrose metabolism	maltose	1.61	**0.0062**
		mannose	2.77	**< 0.001**
		mannose-6-phosphate	2.57	**< 0.001**
	Glycolysis, gluconeogenesis, pyruvate metabolism	glycerate	1.37	**0.0313**
		glucose-6-phosphate (G6P)	2.53	**< 0.001**
		glucose	2.73	**< 0.001**
		fructose-6-phosphate	2.29	**< 0.001**
		3-phosphoglycerate	–1.35	**0.0195**
		1,3-dihydroxyacetone	2.22	**< 0.001**
		lactate	1.23	**< 0.001**
	Nucleotide sugars, pentose metabolism	arabitol	–1.64	**0.0033**
		ribulose	1.40	**0.0433**
		arabinose	–5.26	**< 0.001**
Cofactors and vitamins	Ascorbate and aldarate metabolism	dehydroascorbate	1.86	**0.0388**
	Nicotinate and nicotinamide metabolism	nicotinamide	1.32	**0.0292**
		nicotinamide adenine dinucleotide (NAD+)	1.45	**< 0.001**
	Pantothenate and CoA metabolism	pantothenate	1.69	**< 0.001**
		phosphopantetheine	1.12	**0.0459**
		coenzyme A	–2.56	**< 0.001**
		3'-dephosphocoenzyme A	–2.78	**< 0.001**
	Pyridoxal metabolism	pyridoxal	2.17	**< 0.001**

	Riboflavin metabolism	flavin adenine dinucleotide (FAD)	1.42	**0.0036**
		riboflavin (Vitamin B2)	1.78	**< 0.001**
	Tocopherol metabolism	alpha-tocopherol	–1.43	**< 0.001**
Energy	Krebs cycle	malate	1.28	**< 0.001**
	Oxidative phosphorylation	acetylphosphate	–1.28	0.0788
		phosphate	–1.25	**< 0.001**
Lipid	Medium chain fatty acid	caproate (6:0)	1.81	0.0526
		pelargonate (9:0)	–1.11	**< 0.001**
	Long chain fatty acid	oleate (18:1n9)	–1.23	**0.0204**
		cis-vaccenate (18:1n7)	–1.43	**< 0.001**
		arachidate (20:0)	–1.18	0.0658
		eicosenoate (20:1n9 or 11)	–1.89	**0.0016**
		dihomo-linoleate (20:2n6)	–1.49	0.0755
		arachidonate (20:4n6)	–1.32	0.0776
	Fatty acid, monohydroxy	13-HODE + 9-HODE	1.93	**0.0051**
	Fatty acid, dicarboxylate	2-hydroxyglutarate	–1.69	**< 0.001**
	Eicosanoid	15-HETE	1.89	**0.0013**
	Endocannabinoid	oleic ethanolamide	–1.96	**< 0.001**
		palmitoyl ethanolamide	–2.22	**< 0.001**
	Fatty acid metabolism (also BCAA metabolism)	propionylcarnitine	1.42	0.0682
	Carnitine metabolism	acetylcarnitine	1.24	0.0648
		myristoylcarnitine	–1.56	0.0791
		palmitoylcarnitine	–1.75	**0.0236**
		stearoylcarnitine	–1.47	0.0812
		oleoylcarnitine	–2.08	**0.0078**
	Glycerolipid metabolism	choline phosphate	–1.14	**0.0076**
		glycerophosphoethanolamine	1.18	0.0558

	glycerol	–1.20	**0.0164**
	glycerol 3-phosphate (G3P)	1.41	0.0514
	glycerophosphorylcholine (GPC)	2.09	**< 0.001**
Ketone bodies	3-hydroxybutyrate (BHBA)	1.50	**< 0.001**
Lysolipid	2-docosahexaenoyl GPE	–1.27	0.0929
	2-palmitoyl GPC	–1.52	**0.0442**
	1-stearoyl GPC	–1.37	0.0754
	2-stearoyl GPC	–1.45	**0.0306**
	1-oleoyl GPC	–1.52	**0.0168**
	2-oleoyl GPC	–1.35	**0.0032**
	1-docosahexaenoyl GPC	–1.69	**0.0263**
	2-docosahexaenoyl GPC	–1.61	**0.0286**
	1-palmitoylglycerophosphoinositol	–2.63	**0.0015**
	1-stearoylglycerophosphoinositol	–2.33	**0.0314**
	1-arachidonoylglycerophosphoinositol	–2.13	**0.0011**
Monoacylglycerol	1-oleoylglycerol (1-monoolein)	–2.04	**< 0.001**
	2-oleoylglycerol (2-monoolein)	–1.79	**0.0049**
Sphingolipid	palmitoyl sphingomyelin	1.60	**< 0.001**
	stearoyl sphingomyelin	–1.39	**0.0342**
Mevalonate metabolism	3-hydroxy-3-methylglutarate	–2.56	**< 0.001**
Sterol/Steroid	cholesterol	–1.15	**0.0011**
	7-alpha-hydroxycholesterol	1.77	**0.0011**
	7-beta-hydroxycholesterol	1.46	**0.0034**
	24(S)-hydroxycholesterol	–1.85	**< 0.001**

Nucleotide	Purine metabolism, (hypo)xanthine/inosine containing	xanthosine	1.25	**0.0451**
		inosine	–1.06	**0.0368**
	Purine metabolism, adenine containing	adenosine	–1.96	**0.0033**
		adenosine 2'-monophosphate (2'-AMP)	1.74	**< 0.001**
		adenosine 3'-monophosphate (3'-AMP)	1.62	**0.0035**
		adenosine 5'-monophosphate (AMP)	–1.23	**0.0198**
	Purine metabolism, guanine containing	guanosine	–1.89	**< 0.001**
	Purine metabolism, urate metabolism	urate	1.64	**< 0.001**
	Pyrimidine metabolism, cytidine containing	cytidine	1.27	**< 0.001**
		2'-deoxycytidine	2.49	**< 0.001**
		uracil	1.54	**0.0017**
		5,6-dihydrouracil	–1.20	0.0852
Peptide	Dipeptide derivative	homocarnosine	–1.37	**< 0.001**
		anserine	1.83	**0.0369**
	gamma-glutamyl	gamma-glutamylglycine	–1.33	**0.0197**
		gamma-glutamylmethionine	1.33	**0.0481**
		gamma-glutamylglutamate	–1.43	**< 0.001**
		gamma-glutamylglutamine	1.28	**0.0275**
		gamma-glutamylphenylalanine	–1.16	0.0969
		gamma-glutamylalanine	1.42	**0.0012**
Xenobiotics	Benzoate metabolism	hippurate	1.32	0.0514
	Chemical	glycolate (hydroxyacetate)	1.35	0.0708
	Food component/Plant	stachydrine	1.51	**0.0109**
		homostachydrine	1.64	**0.0052**
	Sugar, sugar substitute, starch	erythritol	–1.30	**0.0434**

(On previous pages)

TABLE 4.1. Spinal cord metabolites with altered concentrations in chronic spinal cord-injured rats versus uninjured, age-matched controls. Abbreviations: 13-HODE + 9-HODE, 13- and 9-hydroxyoctadecadienoic acid; 15-HETE, 15-hydroxyeicosatetraenoic acid; GPE, glycerophosphoethanolamine; GPC, glycerophosphocholine; SCI + VEH, chronically-injured, vehicle-treated[8]. *p* values are versus uninjured, age-matched controls. Bolded *p* values < 0.05 (104 metabolites); non-bolded *p* values < 0.10 (22 metabolites).

[8] Chronic SCI animals were treated either with licofelone or vehicle; there were no untreated animals in this chronic study.

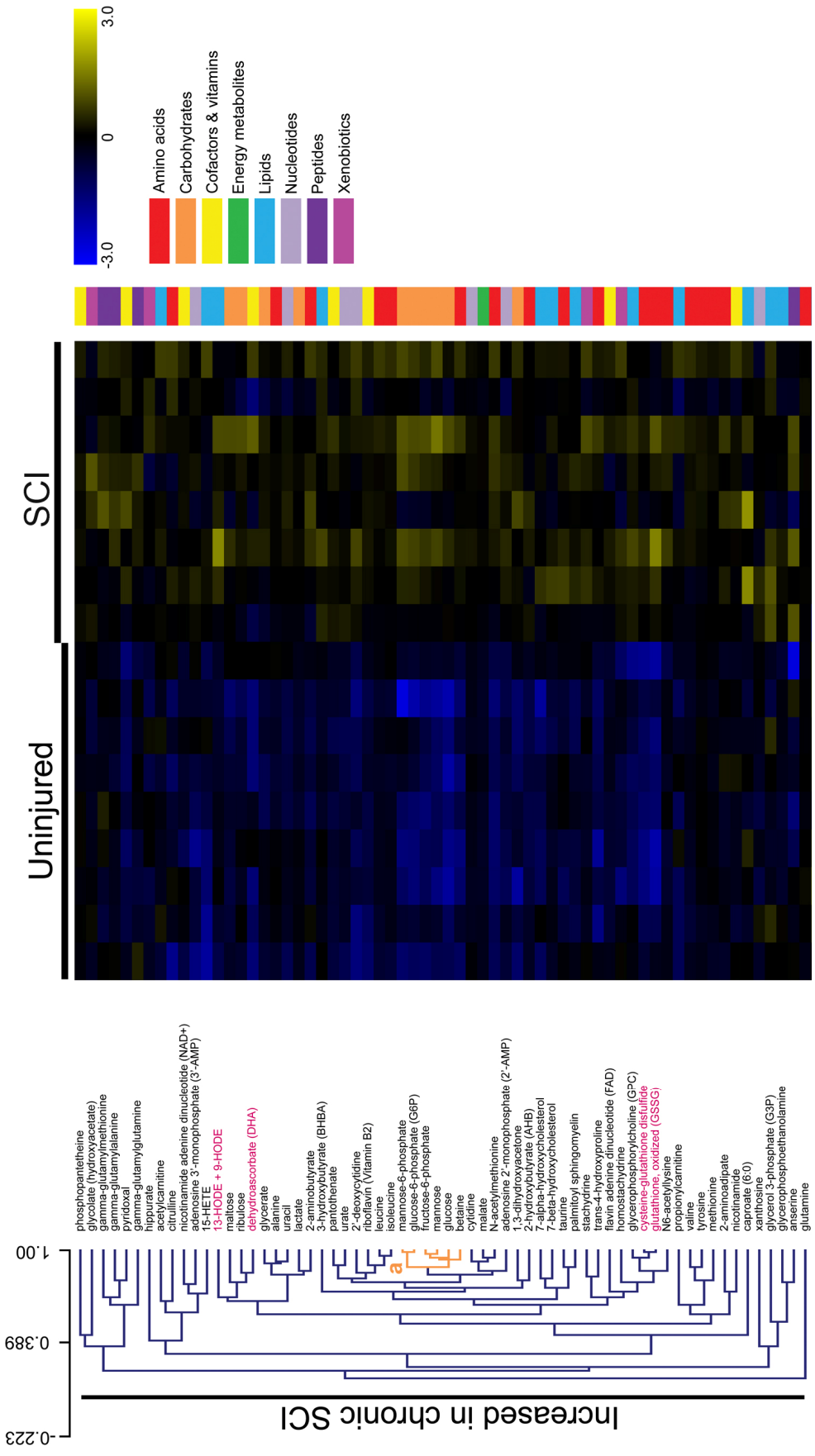
Increased in chronic SCI
1.00
0.389
-0.223
a
phosphopantetheine
glycolate (hydroxyacetate)
gamma-glutamylmethionine
gamma-glutamylalanine
pyridoxal
gamma-glutamylglutamine
hippurate
acetylcarnitine
citrulline
nicotinamide adenine dinucleotide (NAD+)
adenosine 3'-monophosphate (3'-AMP)
15-HETE
13-HODE + 9-HODE
maltose
ribulose
dehydroascorbate (DHA)
glycerate
alanine
uracil
lactate
2-aminobutyrate
3-hydroxybutyrate (BHBA)
pantothenate
urate
2'-deoxycytidine
riboflavin (Vitamin B2)
leucine
isoleucine
mannose-6-phosphate
glucose-6-phosphate (G6P)
fructose-6-phosphate
mannose
glucose
betaine
cytidine
malate
N-acetylmethionine
adenosine 2'-monophosphate (2'-AMP)
1,3-dihydroxyacetone
2-hydroxybutyrate (AHB)
7-alpha-hydroxycholesterol
7-beta-hydroxycholesterol
taurine
palmitoyl sphingomyelin
stachydrine
trans-4-hydroxyproline
flavin adenine dinucleotide (FAD)
homostachydrine
glycerophosphorylcholine (GPC)
cysteine-glutathione disulfide
glutathione, oxidized (GSSG)
N6-acetyllysine
propionylcarnitine
valine
tyrosine
methionine
2-aminoadipate
nicotinamide
caproate (6:0)
xanthosine
glycerol 3-phosphate (G3P)
glycerophosphoethanolamine
arginine
glutamine
Uninjured
SCI
3.0
0
-3.0
Amino acids
Carbohydrates
Cofactors & vitamins
Energy metabolites
Lipids
Nucleotides
Peptides
Xenobiotics

(On previous page)

Figure 4.7. Metabolites increased in the chronically-injured spinal cord. Heat map illustrates the change in levels of 64 metabolites with increased expression in chronic SCI animals versus uninjured, age-matched controls. Increases (yellow) and decreases (blue) in concentration, relative to the median metabolite level, are represented by various shades of intensity (see color scale). Metabolites are arranged by hierarchical clustering, with representative cluster highlighted (**a**). Scale bar (upper left) indicates Pearson correlation coefficient (r). Colored bars indicate super class of each metabolite (amino acids, carbohydrates, cofactors and vitamins, energy metabolites, lipids, nucleotides, peptides, and xenobiotics). The names of representative pro-inflammatory and pro-oxidative metabolites are shown in pink lettering.

Decreased in chronic SCI
1.00
0.389
-0.223
b
c
2-oleoylglycerophosphocholine
1-docosahexaenoylglycerophosphocholine
2-docosahexaenoylglycerophosphoethanolamine
2-palmitoylglycerophosphocholine
2-docosahexaenoylglycerophosphocholine
2-stearoylglycerophosphocholine
1-oleoylglycerophosphocholine
1-stearoylglycerophosphocholine
oleoylcarnitine
palmitoylcarnitine
myristoylcarnitine
stearoylcarnitine
homoserine
gamma-aminobutyrate (GABA)
asparagine
aspartate
adenosine 5'-monophosphate (AMP)
adenosine
gamma-glutamylglycine
gamma-glutamylphenylalanine
3-phosphoglycerate
oleic ethanolamide
palmitoyl ethanolamide
1-arachidonoylglycerophosphoinositol
choline phosphate
1-palmitoylglycerophosphoinositol
1-stearoylglycerophosphoinositol
eicosenoate (20:1n9 or 11)
arachidonate (20:4n6)
dihomo-linoleate (20:2n6)
1-oleoylglycerol (1-monoolein)
cis-vaccenate (18:1n7)
glycerol
oleate (18:1n9)
2-oleoylglycerol (2-monoolein)
acetylphosphate
cholesterol
pelargonate (9:0)
erythritol
arabitol
creatine
N-acetylglutamate
gamma-glutamylglutamate
S-adenosylhomocysteine (SAH)
guanosine
3'-dephosphocoenzyme A
coenzyme A
N-acetylaspartate (NAA)
24(S)-Hydroxycholesterol
3-hydroxy-3-methylglutarate
N-acetyl-aspartyl-glutamate (NAAG)
glutamate
glycine
phosphate
2-hydroxyglutarate
alpha-tocopherol
homocarnosine
arabinose
inosine
arachidate (20:0)
stearoyl sphingomyelin
5,6-dihydrouracil
Uninjured
SCI
-3.0
0
3.0
Amino acids
Carbohydrates
Cofactors & vitamins
Energy metabolites
Lipids
Nucleotides
Peptides
Xenobiotics

(On previous page)

Figure 4.8. Metabolites decreased in the chronically-injured spinal cord. Heat map illustrates the change in levels of 62 metabolites with decreased expression in chronic SCI animals versus uninjured, age-matched controls. Increases (yellow) and decreases (blue) in concentration, relative to the median metabolite level, are represented by various shades of intensity (see color scale). Metabolites are arranged by hierarchical clustering, with representative clusters highlighted (**b-c**). Scale bar (upper left) indicates Pearson correlation coefficient (r). Colored bars indicate super class of each metabolite (amino acids, carbohydrates, cofactors and vitamins, energy metabolites, lipids, nucleotides, peptides, and xenobiotics). The names of representative anti-inflammatory metabolites are shown in green lettering.

example, one cluster of glycolytic intermediates were similarly increased in SCI samples (**Fig. 4.7a**, $r = 0.88$, $p < 0.05$), and two large clusters of lipid metabolites were similarly decreased in SCI samples (**Fig. 4.8b**, r = 0.72, $p < 0.05$; **Fig. 4.8c**, r = 0.53, $p < 0.05$). These analyses reveal alterations in multiple metabolic pathways within the chronically-injured spinal cord.

Evaluation of metabolites increased in chronic SCI revealed that several were strong indicators of oxidative stress conditions (pink lettering, **Fig. 4.7**). These included oxidized glutathione (+3.19 fold), cysteine-glutathione disulfide (+3.19 fold), dehydroascorbate (+1.86 fold), and 13- and 9-hydroxyoctadecadienoic acid (+1.93 fold) ($p < 0.05$, **Fig. 4.9a**). Additionally, chronic SCI tissue contained significantly depleted levels of anti-oxidant and anti-inflammatory metabolites (green lettering, **Fig. 4.8**), such as alpha-tocopherol (-1.43 fold) and 24(S)-hydroxycholesterol (24-OH-Chol) (-1.85 fold) ($p < 0.05$, **Fig. 4.9b**).

Effect of Licofelone on Inflammation and Oxidative Stress Following Spinal Cord Injury

In conjunction with our metabolomic characterization of chronically-injured spinal cords, we also examined the effects of 28-day licofelone treatment on the spinal cord metabolic profile of animals with chronic (8 months) SCI. We detected changes in 26 named metabolites in spinal cord tissue of chronic SCI animals treated with licofelone ($n = 9$), compared to vehicle-treated SCI animals (**TABLE 4.2**). Hierarchical clustering revealed clusters, primarily composed of lipids and carbohydrates, that increased with licofelone treatment (**Fig. 4.10**). Among these were anti-inflammatory and anti-oxidative compounds, including 15-hydroxyeicosatetraenoic acid (15-HETE) (+1.42 fold), 24-OH-Chol (+1.25 fold), chiro-inositol (+1.51 fold), inositol 1-phosphate (+1.22 fold), and homocarnosine (+1.14 fold) ($p < 0.05$, **Fig. 4.10b**). Interestingly, the only metabolite that decreased with licofelone treatment (–2.44 fold) was the bile acid taurocholate (**TABLE 4.2** & **Fig. 4.10a**), a pro-inflammatory bile acid that enhances NF-kB activation (316).

In order to evaluate the ability of licofelone to inhibit production of PGE_2 within the injured spinal cord, we used ELISA to quantify PGE_2 levels in injured rats treated with either vehicle or licofelone (**Fig. 4.11**). At 24 hours after injury, PGE_2 levels within the lesion site were significantly higher than levels in the thoracic spinal cord of uninjured animals ($p < 0.001$). Furthermore, this spike in PGE_2 was completely abolished in rats that were treated with

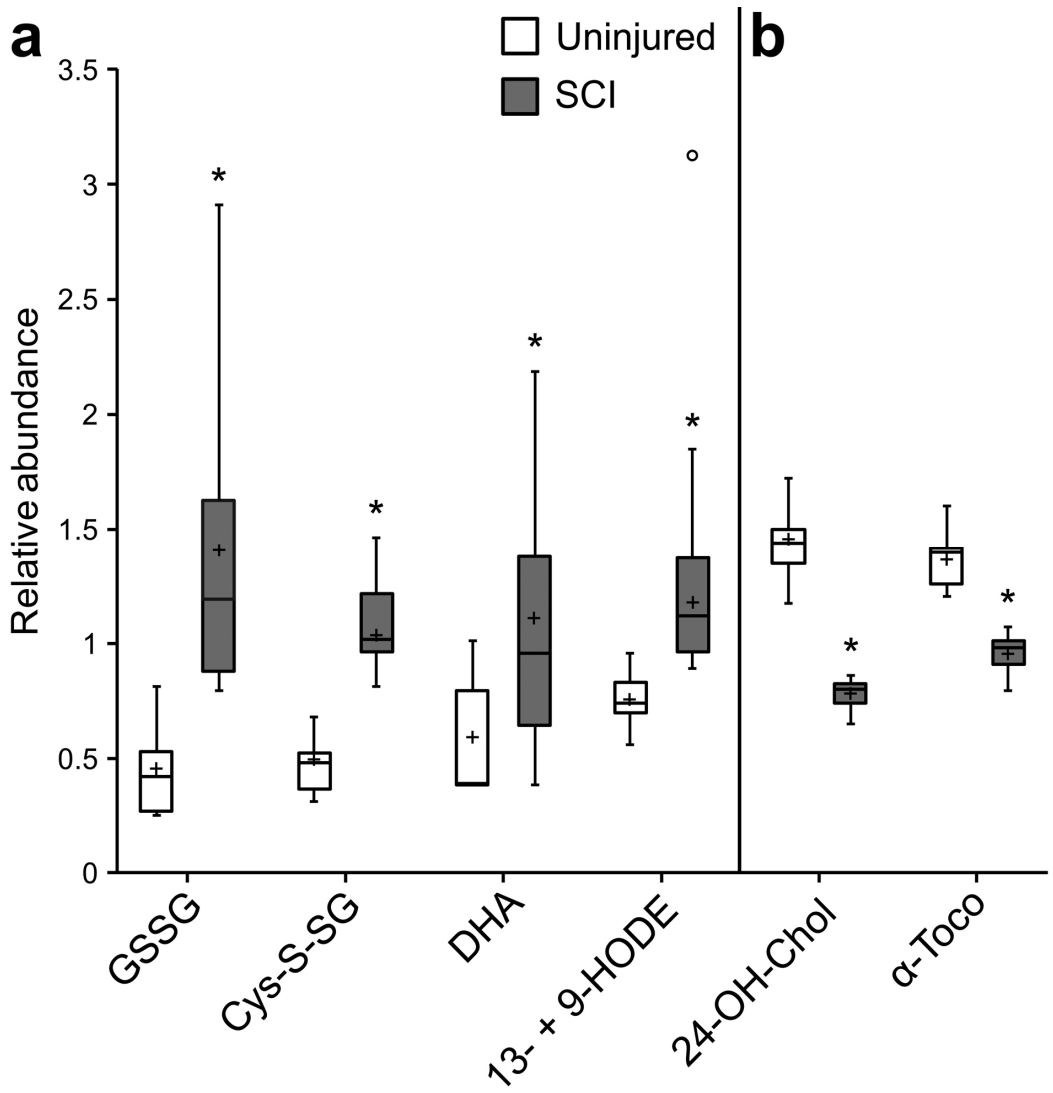

Figure 4.9. Metabolomic analysis reveals oxidative stress and inflammation in the chronically-injured spinal cord. Box plots illustrate changes in abundance of select metabolites within spinal cord tissue of uninjured controls (white) and rats 9 mo post-SCI (gray). For each metabolite, all concentration values have been re-scaled to have a median value equal to 1 for all groups. Box legend: + inside box represents mean value, bar inside box represents median value, upper and lower box boundaries represent 75th percentile and 25th percentile, respectively, upper and lower whiskers represent maximum and minimum of distribution, circles represents extreme data points. (**a**) Several metabolites significantly increased in chronic SCI spinal cords are associated with oxidative stress. (**b**) Levels of anti-inflammatory and anti-oxidative metabolites are decreased in chronic SCI cords. Abbreviations: 24-OH-Chol, 24(S)-hydroxycholesterol; α-Toco, alpha-tocopherol, GSSG, oxidized glutathione; Cys-S-SG, cysteine-glutathione disulfide; DHA, dehydroascorbate; 13- + 9-HODE, 13-hydroxyoctadecadienoic acid and 9-hydroxyoctadecadienoic acid. *, $p < 0.05$ versus uninjured controls.

Class	Sub-class	Biochemical Name	Fold Change (SCI + LIC / SCI + VEH)	*p* Value
Amino acid	Alanine and aspartate metabolism	aspartate	1.10	**0.0471**
Carbohydrate	Aminosugars metabolism	erythronate	1.18	**0.0287**
		N-acetylneuraminate	1.22	**0.0421**
	Fructose, mannose, galactose, starch, and sucrose metabolism	maltose	1.28	**0.0417**
	Glycolysis, gluconeogenesis, pyruvate metabolism	glucose	1.27	0.0633
		lactate	1.11	**0.0223**
	Nucleotide sugars, pentose metabolism	arabitol	1.59	**0.0030**
		ribose	1.47	0.0836
Energy	Krebs cycle	citrate	1.16	0.0877
Lipid	Long chain fatty acid	margarate (17:0)	1.22	**0.0077**
		cis-vaccenate (18:1n7)	1.26	**0.0183**
		behenate (22:0)	1.20	0.0615
	Eicosanoid	15-HETE	1.42	**0.0328**
	Bile acid metabolism	taurocholate	–2.44	0.0625
	Glycerolipid metabolism	glycerol	1.13	**0.0090**
	Inositol metabolism	myo-inositol	1.20	0.0704
		chiro-inositol	1.51	**0.0224**
		inositol 1-phosphate (I1P)	1.22	**0.0163**
	Sterol/Steroid	cholesterol	1.06	**0.0081**
		7-alpha-hydroxycholesterol	1.26	**0.0209**
		7-beta-hydroxycholesterol	1.19	0.0930
		24(S)-hydroxycholesterol	1.25	**0.0013**
Nucleotide	Purine metabolism, urate metabolism	allantoin	1.20	0.0709
Peptide	Dipeptide	glycylglycine	1.24	0.0625
	Dipeptide derivative	homocarnosine	1.14	**0.0071**
Xenobiotics	Sugar, sugar substitute, starch	erythritol	1.30	0.0755

(On previous page)

TABLE 4.2. Changes in levels of spinal cord metabolites of chronically-injured rats treated with licofelone. Abbreviations: 15-HETE, 15-hydroxyeicosatetraenoic acid; SCI + LIC, injured, licofelone-treated; SCI + VEH, injured, vehicle-treated. *p* values are versus chronic SCI, vehicle-treated group. Bolded *p* values < 0.05 (16 metabolites); non-bolded *p* values < 0.10 (22 metabolites).

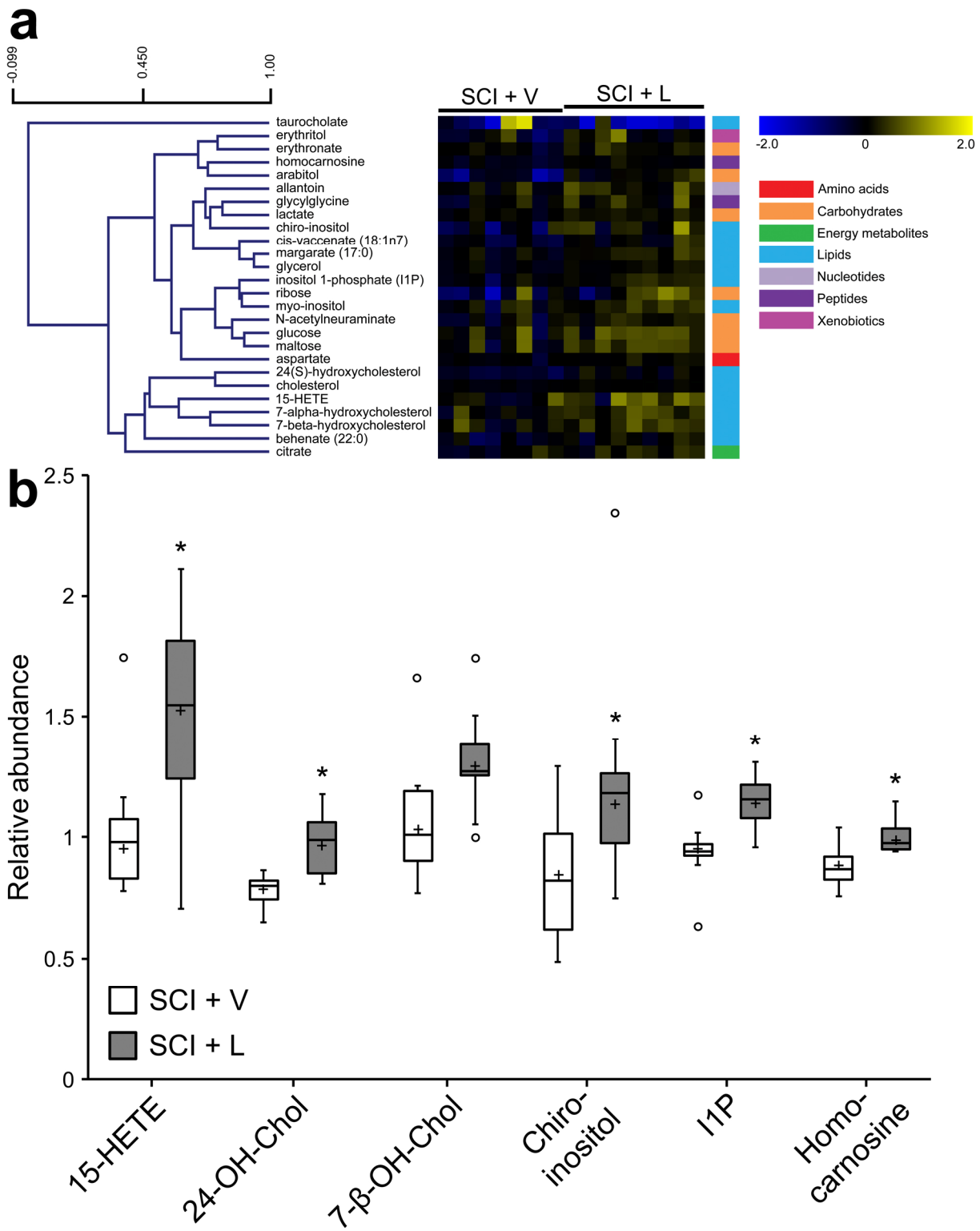
a
-0.099
0.450
1.00
SCI + V
SCI + L
taurocholate
erythritol
erythronate
homocarnosine
arabitol
allantoin
glycylglycine
lactate
chiro-inositol
cis-vaccenate (18:1n7)
margarate (17:0)
glycerol
inositol 1-phosphate (I1P)
ribose
myo-inositol
N-acetylneuraminate
glucose
maltose
aspartate
24(S)-hydroxycholesterol
cholesterol
15-HETE
7-alpha-hydroxycholesterol
7-beta-hydroxycholesterol
behenate (22:0)
citrate
-2.0
0
2.0
Amino acids
Carbohydrates
Energy metabolites
Lipids
Nucleotides
Peptides
Xenobiotics
b
Relative abundance
2.5
2
1.5
1
0.5
0
SCI + V
SCI + L
15-HETE
24-OH-Chol
7-β-OH-Chol
Chiro-inositol
I1P
Homo-carnosine

(On previous page)

Figure 4.10. Changes in the spinal cord metabolic profile of chronically-injured rats following 28-day licofelone treatment. (**a**) Heat map showing 26 metabolites that exhibit changes in chronic SCI, licofelone-treated animals (SCI + L), compared to chronic SCI, vehicle-treated animals (SCI + V). Metabolites are arranged by hierarchical clustering. Scale bar (upper left) indicates Pearson correlation coefficient (*r*). Colored bars indicate super class of each metabolite (*e.g.*, amino acids, carbohydrates). Increases (yellow) and decreases (blue) in concentration, relative to the median metabolite level, are represented by various shades of intensity (see color scale). (**b**) Box plots illustrating changes in levels of select compounds within the chronic SCI, vehicle-treated (white) or licofelone-treated (gray) groups. For box plot legend, see **Figure 4.9**. Abbreviations: 15-HETE, 15-hydroxyeicosatetraenoic acid; 24-OH-Chol, 24(S)-hydroxycholesterol; 7-β-OH-Chol, 7-beta-hydroxycholesterol; I1P, inositol 1-phosphate. *, $p < 0.05$ versus chronic SCI, vehicle-treated group.

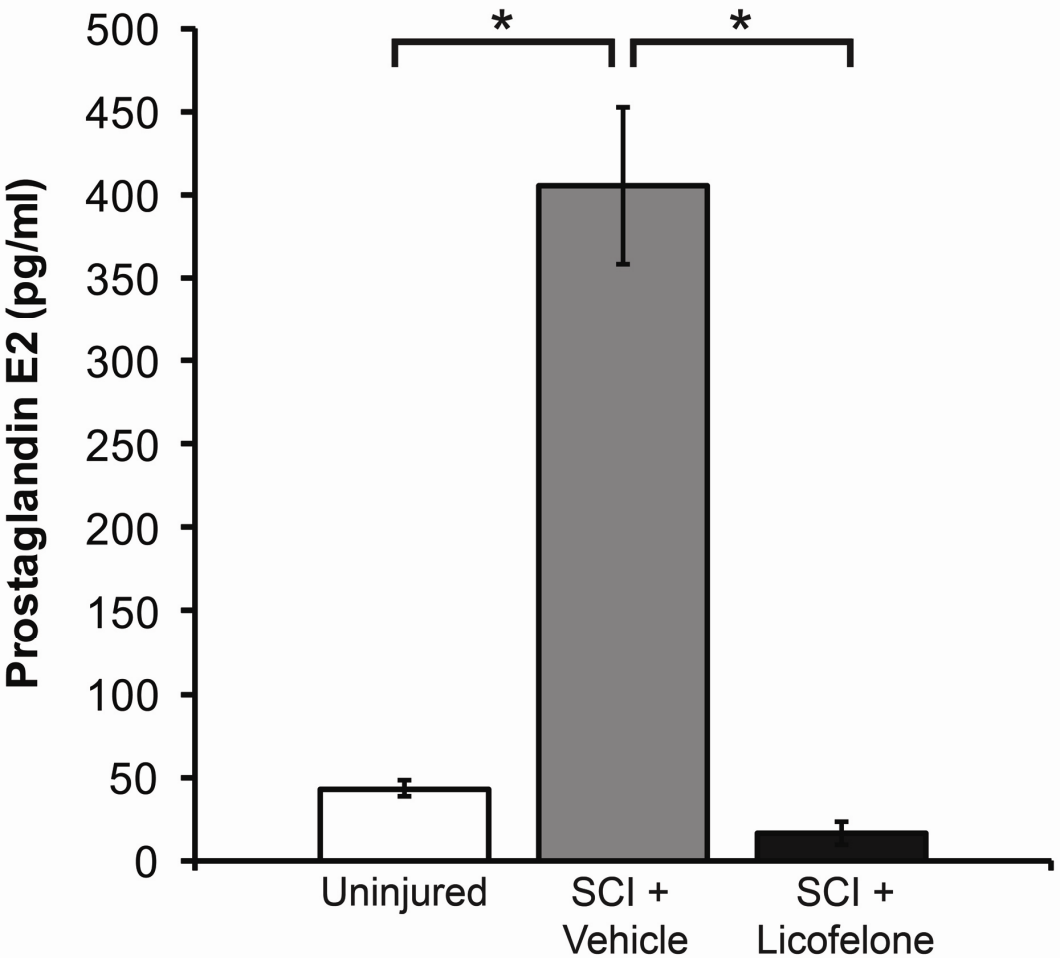

Figure 4.11. Elevated prostaglandin E2 production within the acutely-injured spinal cord is eliminated by licofelone treatment. ELISA quantification of prostaglandin E2 levels within the spinal cord lesion site of animals treated with either vehicle or licofelone at 3 hours after injury, then again at 18 hours after injury. Uninjured (43.2 ± 4.67 pg/ml; $n = 6$); SCI + vehicle (405 ± 47.4 pg/ml; $n = 6$); SCI + licofelone (16.9 ± 6.87 pg/ml; $n = 6$). All data are mean ± s.e.m. *, $p < 0.05$.

licofelone starting at 3 hours post-injury ($p < 0.001$). This data illustrates the efficacy of licofelone to prevent injury-induced production of prostaglandin E2, which has previously been shown to drive brain Pgp overexpression in rodent seizure models (235). Because licofelone inhibits both COX and 5-LOX, we also used ELISA to quantify leukotriene B4 levels in rat spinal cord tissue using the same treatment paradigm. However, the calculated LTB_4 levels in spinal cord tissue for all three groups fell below the sensitivity limit of the assay [Uninjured (6.93 ± 1.13 pg/ml; $n = 6$); SCI + vehicle (7.90 ± 2.56 pg/ml; $n = 6$); SCI + licofelone (5.02 ± 1.66 pg/ml; $n = 6$)]. Thus, we cannot draw any conclusions about the effects of licofelone treatment on LTB_4 levels following SCI from this data.

Effect of Licofelone on P-glycoprotein Expression and Spinal Cord Riluzole Bioavailability Following Spinal Cord Injury

Pekcec *et al.* showed that brain Pgp overexpression following seizure is mediated by PGE_2, and that antagonizing the EP1 receptor was sufficient to increase therapeutic efficacy of the anti-convulsant drug phenobarbital in rodents following seizure (235). Because we have shown that licofelone is effective at decreasing PGE_2 levels in the acutely-injured spinal cord (**Fig. 4.11**), we next wanted to evaluate whether treatment with licofelone could abrogate the effects of SCI on spinal cord Pgp expression and thereby increase riluzole bioavailability. In order to increase the clinical relevance of our experimental paradigm, we chose to focus our subsequent studies on the effects of licofelone treatment during the acute phase of SCI. 72 hours post-SCI was selected as an optimal time point for evaluating these outcome measures because of two main contributing factors. First, our overall goal is to enhance the spinal cord bioavailability and therapeutic efficacy of riluzole, a neuroprotective compound that likely exerts the greatest therapeutic benefit early after SCI. Therefore, we reasoned that positive results with licofelone treatment would hold more clinical relevance if observed as early as possible after injury. Secondly, previous studies in our laboratory have demonstrated that peak BSCB permeability to the protein albumin occurs between 48 and 72 hours post-SCI (**Fig. 4.12**). Accordingly, we hypothesized that 72 hours post-SCI would be a more ideal time point for the assessment of Pgp expression and function, as it is past the peak of BSCB leakiness and might eschew some of the complications arising from increased passive diffusivity at the BSCB during earlier time points.

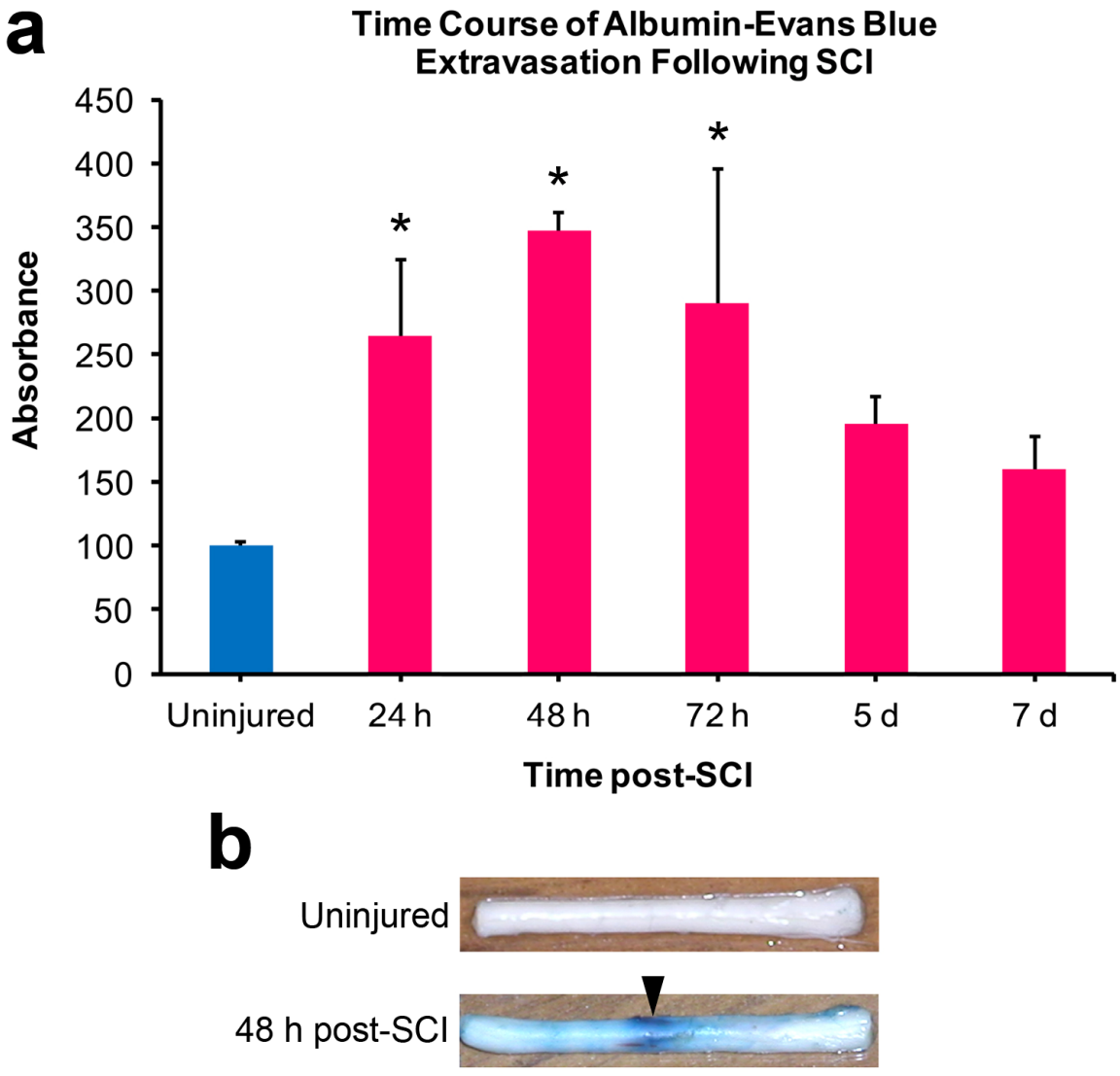
a
Time Course of Albumin-Evans Blue Extravasation Following SCI
Absorbance
450
400
350
300
250
200
150
100
50
0
*
*
*
Uninjured
24 h
48 h
72 h
5 d
7 d
Time post-SCI
b
Uninjured
48 h post-SCI

(On previous page)

Figure 4.12. Time course of blood-spinal cord barrier permeability to albumin during acute spinal cord injury. Albumin (~68 kDa) is a large blood-borne molecule that is normally restricted from passing through the BSCB into the spinal cord tissue. The albumin-binding dye Evans Blue (EB) is therefore a useful tool for the assessment of BSCB permeability to large molecules following injury to the spinal cord. (**a**) EB was delivered *i.v.* to rats at various time points following spinal contusion injury. 30 minutes later, rats were transcardially perfused with saline, and spinal cords were harvested. Extravasation of EB from T10 spinal cord tissue was quantified by fluorometric measurement at 620 nm. Compared to uninjured controls (100 ± 2.38%), EB extravasation was significantly higher in rats 1-3 days following SCI (24 h post-SCI = 264 ± 59.5%; 48 h post-SCI = 348 ± 14.3%; 72 h post-SCI = 290 ± 105%). Furthermore, EB extravasation remained increased for up to one week after injury, though not statistically significant (5 d post-SCI = 195 ± 21.4%; 7 d post-SCI = 160 ± 26.1%). Based on this data, the peak BSCB permeability to albumin following traumatic SCI appears to occur at about 48 hours post-injury. All data are mean ± s.e.m. and presented as percentage of uninjured controls. *, $p < 0.05$ versus uninjured controls. (**b**) Photo illustrating gross anatomy of spinal cord tissue of uninjured rat (top) and rat 48 hours post-SCI (bottom), following systemic delivery of EB dye, and subsequent transcardial perfusion. Spinal cords of uninjured rats appear white because intact BSCB function prevents the entry of the albumin-EB complex into the spinal cord parenchyma. In contrast, vascular leakage of albumin-EB at 48 hours post-SCI is apparent in the spinal cord parenchyma, both within the epicenter of injury (arrowhead), as well as several millimeters rostral and caudal to the lesion site. Data provided courtesy of Dr. Raymond Grill.

Animals were treated with either licofelone (100 mg/kg) or vehicle via the clinically-relevant oral route beginning at 3 hours post-SCI, then once daily for 3 days. At 72 hours, immunoblotting revealed that T10 Pgp expression was significantly increased in the injured, vehicle-treated group compared to uninjured controls (**Fig. 4.13**). This increase is reflective of that observed previously (**Fig. 3.8**). Importantly, we observed that T10 Pgp expression was significantly lower in the injured, licofelone-treated group versus that of the injured, vehicle-treated group. This finding demonstrates that pathological Pgp overexpression within the injured spinal cord can indeed be attenuated by oral treatment with licofelone. Our results also corroborate those of previous studies, which have demonstrated that antagonism of the COX/PGE_2 signaling axis is effective in reducing Pgp overexpression in other neurological disease models.

We next examined whether licofelone treatment exhibited an effect on spinal cord riluzole bioavailability at this same time point. Animals were treated with licofelone or vehicle beginning at 3 hours after injury, then once daily for 3 days. All three groups (both SCI groups as well as uninjured controls) also received riluzole (*i.p.*) during the same dosing schedule. At 72 hours post-injury, spinal cord/plasma ratios of riluzole were assessed (**Fig. 4.14**). We found that normalized spinal cord riluzole levels were slightly decreased in SCI compared to uninjured controls, though this difference is not statistically significant ($p = 0.201$). We have previously demonstrated that normalized spinal cord riluzole levels are significantly decreased in T10 spinal tissue at 10 days post-SCI (**Fig. 3.12**), as well as in whole spinal cords at 21 days post-SCI (**Fig. 3.11**). In light of these observations, the lack of a statistically significant decrease in normalized riluzole levels at 72 hours after SCI might be attributed to increased BSCB permeability observed at 3-7 days post-SCI, an observation supported both in our laboratory (**Fig. 4.12**) and by other groups (189). Notably, we observed that normalized spinal cord riluzole levels of licofelone-treated animals at 72 hours post-SCI were significantly higher versus vehicle-treated animals (**Fig. 4.14**). Together with the observation that licofelone treatment attenuates Pgp overexpression at 72 hours post-SCI (**Fig. 4.13**), the finding that licofelone can also enhance the spinal cord uptake of riluzole supports our hypothesis that pro-inflammatory signaling drives Pgp-mediated spinal cord drug resistance following SCI. These results suggest a new therapeutic avenue for enhancing the therapeutic efficacy of riluzole, a drug that is currently being evaluated in an ongoing clinical trial as a neuroprotective intervention for acute SCI.

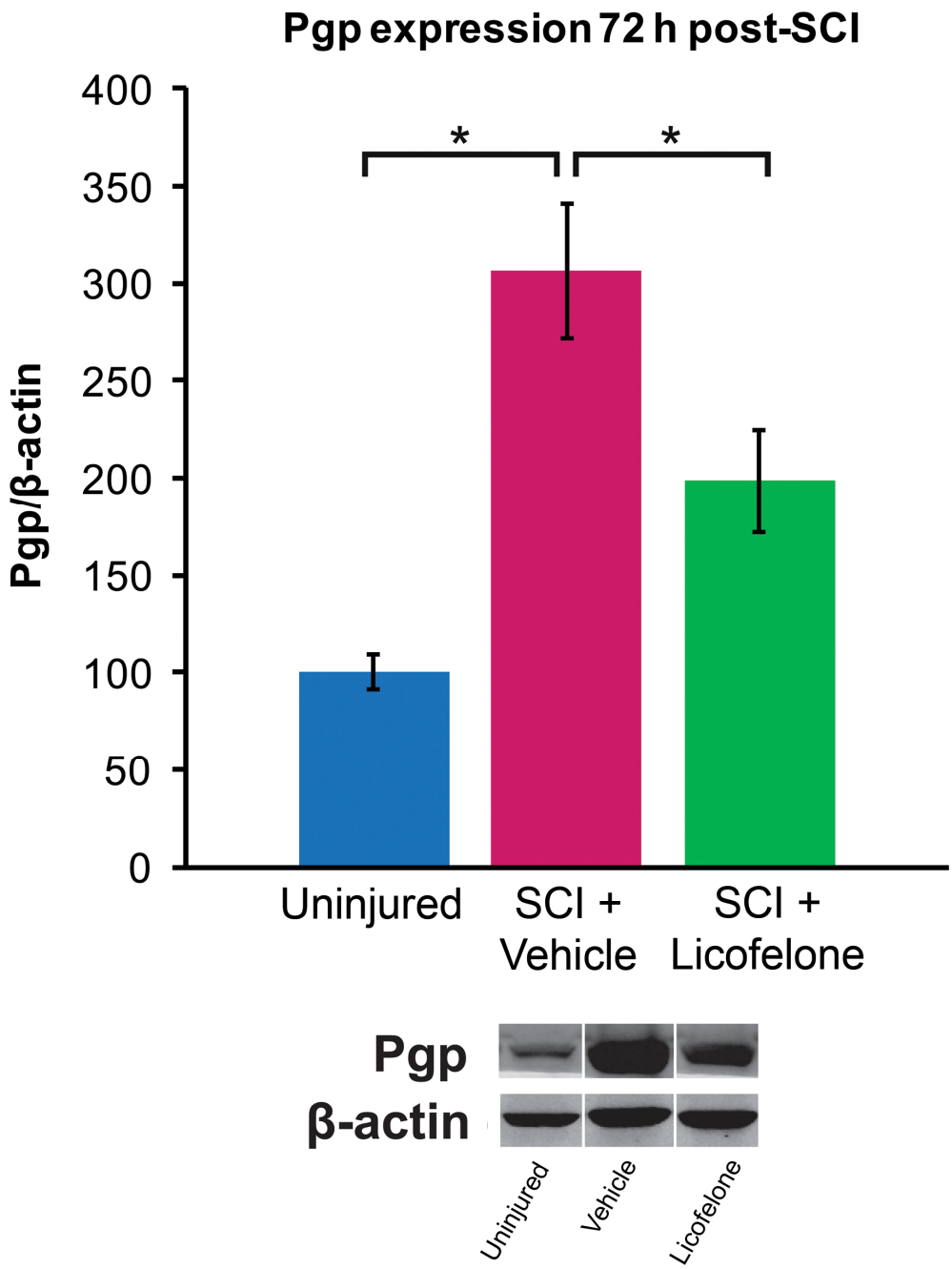

Figure 4.13. Licofelone treatment attenuates P-glycoprotein overexpression 72 hours following spinal cord injury. Immunoblots of T10 spinal cord samples from rats 72 hours post-SCI. Pgp expression levels are normalized to β-actin and expressed as a percentage of uninjured controls (100 ± 9.01%, $n = 8$). Pgp levels in the lesion site of injured, vehicle-treated rats are significantly higher than uninjured controls (SCI + vehicle = 306 ± 34.4%, $n = 10$, $p < 0.001$). Pgp levels of injured, licofelone-treated rats are significantly reduced versus injured, vehicle-treated rats (SCI + licofelone = 198 ± 26.4%, $n = 15$, $p = 0.008$), but are still significantly higher than uninjured levels ($p = 0.022$). Representative immunoblots are pictured below graph. All data are mean ± s.e.m. *, $p < 0.05$.

Figure 4.14. Licofelone treatment enhances spinal cord riluzole bioavailability 72 hours after spinal cord injury. Animals were treated with riluzole alone, or riluzole and licofelone, beginning 3 hours after SCI and again once daily for three days. Normalized spinal cord riluzole levels were reduced (although not significantly so) in the riluzole-treated group 72 hours after injury (81.1 ± 4.53%, n = 6) versus uninjured controls (100 ± 4.24%, n = 7, p = 0.201). Normalized spinal cord riluzole levels were significantly enhanced in injured animals treated with riluzole + licofelone (124 ± 13.8%, n = 8) versus the injured, riluzole-treated group (p = 0.017). Additionally, the increase in spinal cord/plasma riluzole ratio in animals treated with riluzole + licofelone approached statistical significance compared to uninjured controls (p = 0.092). All data are mean ± s.e.m., expressed as percentage of uninjured controls. *, $p < 0.05$.

We also evaluated whether there was differential plasma riluzole bioavailability in these groups (**Fig. 4.15**). Interestingly, we observed that although the raw spinal cord riluzole concentrations in both SCI groups were almost identically lower than uninjured controls (**Fig. 4.15a**), the plasma bioavailability of riluzole in the licofelone-treated group was substantially lower than both uninjured controls and injured, riluzole-treated animals (**Fig. 4.15b**). From this data, we have drawn two conclusions: 1) Because there is no injury-associated effect on plasma riluzole bioavailability at 72 hours (See pink bar in **Fig. 4.15b**), the observed decrease in plasma riluzole bioavailability in the licofelone-treated group must be attributed to licofelone treatment; 2) Though there is no difference in raw spinal cord riluzole concentrations between SCI groups (**Fig. 4.15a**), the reduction in plasma levels in the licofelone-treated group indicates that licofelone enhances plasma-to-spinal cord delivery of riluzole, and suggests that a higher systemic dose of riluzole may increase spinal cord drug delivery further. Because of these observations, we speculate that at this acute time point following SCI, licofelone acts to enhance clearance of riluzole from the plasma and to promote increased delivery of riluzole from the plasma to the spinal cord tissue.

Up-regulation of *Abcb1* transcription at the blood-brain barrier can also occur as a result of drug treatment via activation of the pregnane X receptor, a ligand-activated nuclear receptor (317). Therefore, it is possible that, independent from the effects of SCI-associated inflammation on Pgp expression, treatment with riluzole during the acute phase of injury might also alter spinal cord Pgp expression levels, and consequently the spinal cord uptake of riluzole. We therefore performed a subsequent experiment to rule out this possibility. Beginning 3 hours after injury, rats were treated with vehicle alone, riluzole alone, or riluzole and licofelone, once daily for three days. Immunoblot analysis of Pgp expression revealed no significant effect of riluzole treatment on Pgp expression within the lesion site at 72 hours post-SCI (**Fig. 4.16**). In contrast, spinal cord Pgp expression in rats treated with both riluzole and licofelone was significantly lower than those of vehicle-treated and riluzole-treated groups. Because repeated treatment with riluzole does not significantly affect Pgp expression levels during this acute

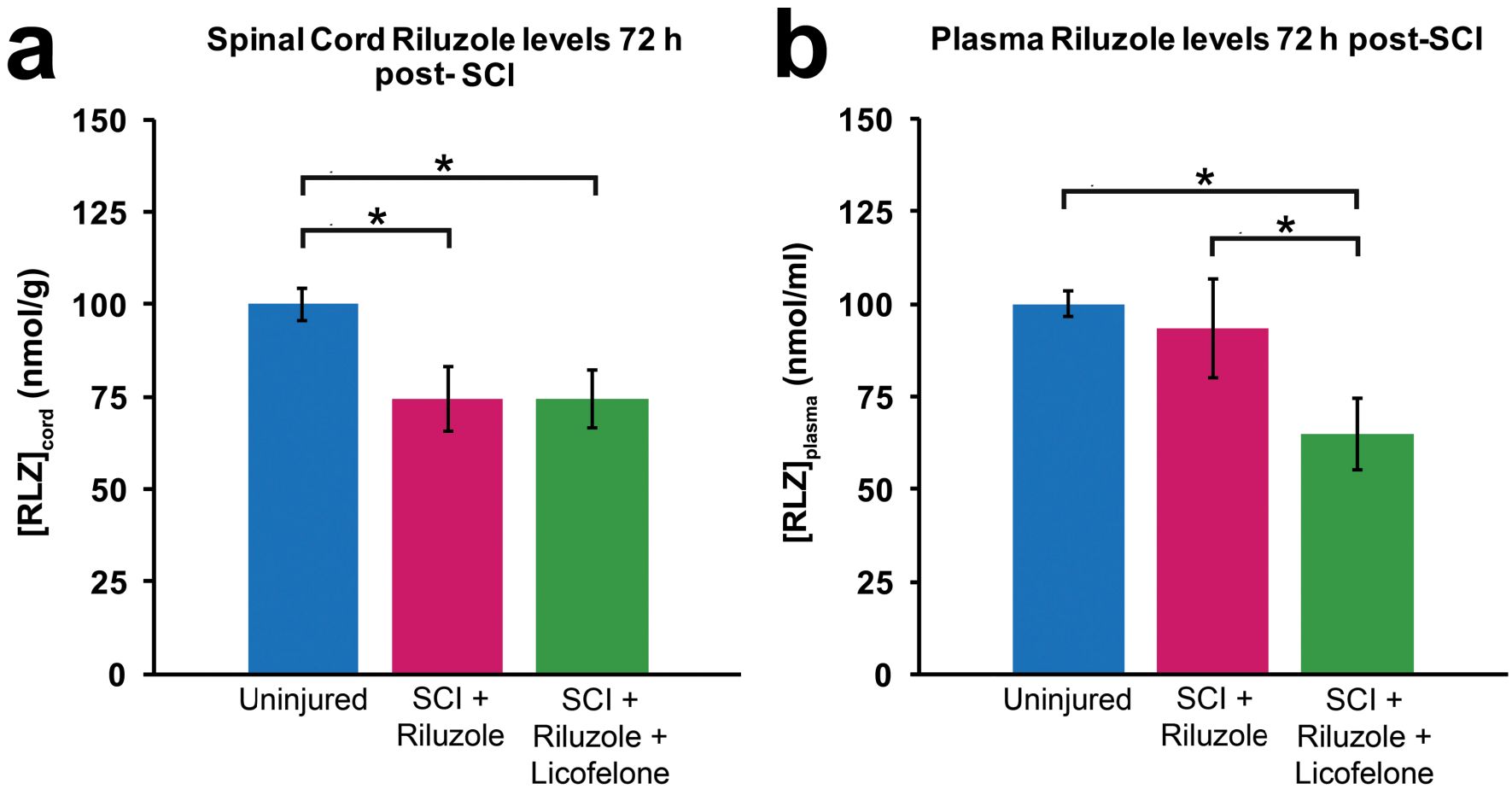
a
Spinal Cord Riluzole levels 72 h post- SCI
[RLZ]cord (nmol/g)
150
125
100
75
50
25
0
*
*
Uninjured
SCI + Riluzole
SCI + Riluzole + Licofelone
b
Plasma Riluzole levels 72 h post-SCI
[RLZ]plasma (nmol/ml)
150
125
100
75
50
25
0
*
*
Uninjured
SCI + Riluzole
SCI + Riluzole + Licofelone

(On previous page)

Figure 4.15. Effects of injury and licofelone treatment on raw spinal cord and plasma riluzole concentrations. Abbreviations: RLZ, riluzole; RLZ + LIC, riluzole + licofelone. (**a**) Compared to raw spinal cord riluzole concentrations of uninjured control rats (100 ± 4.25%), both SCI groups displayed statistically significant decreases (SCI + RLZ = 74.4 ± 8.70%, p = 0.022; SCI + RLZ + LIC = 74.5 ± 7.86%, p = 0.016) that were almost identical (p = 0.988). (**b**) In contrast, there was no significant reduction in plasma riluzole concentrations in the injured, riluzole-treated group (93 ± 13.2%) compared to uninjured controls (100 ± 3.39%, p = 0.640). However, injured rats treated with riluzole and licofelone displayed significantly reduced plasma riluzole levels (64.9 ± 9.81%) compared to uninjured controls (p = 0.036) as well as injured, riluzole-treated animals (p = 0.049). All data are mean ± s.e.m., expressed as percentage of uninjured controls. *, $p < 0.05$.

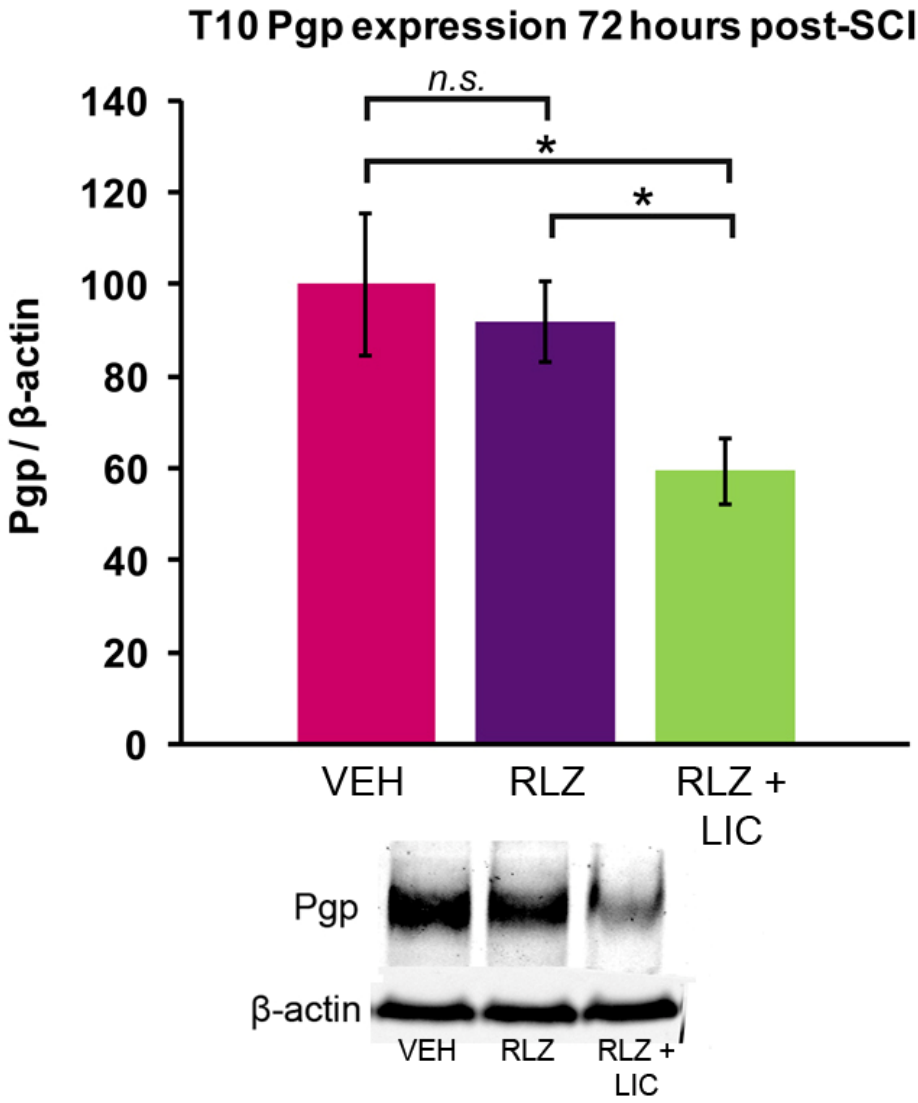

Figure 4.16. Repeated riluzole treatment does not affect spinal cord P-glycoprotein expression. Immunoblots of T10 spinal cord samples from rats 72 hours following SCI. Protein expression levels are normalized to β-actin and expressed as percentage of injured, vehicle-treated (VEH) levels (100 ± 15.4%, n = 8). Pgp levels in the lesion site of riluzole (RLZ)-treated rats are not significantly different than vehicle-treated (RLZ = 91.8 ± 8.83%, n = 9, p = 0.598). Injured rats treated with both RLZ and licofelone (LIC) have significantly reduced Pgp expression (RLZ + LIC = 59.5 ± 7.19%, n = 9) compared to the vehicle-treated group (p = 0.036) and also compared to the riluzole-treated group (p = 0.039). Representative immunoblots are pictured below graph. All data are mean ± s.e.m. *, $p < 0.05$ versus SCI + VEH.

period of SCI, we conclude that the reduced riluzole bioavailability observed in injured, riluzole-treated rats (**Fig. 4.14**) is not attributed to the effects of riluzole treatment itself, but rather can only be due to pathological mechanisms induced by injury.

CHAPTER 5

Effect of Licofelone Treatment on Functional Recovery Following Spinal Cord Injury in the Rat

Background

At present, there are no proven effective therapeutic interventions that can significantly improve functional recovery in SCI patients. To date, a large number of preclinical studies have identified neuroprotective compounds that, if administered to experimental animals in the minutes to hours following injury, can improve functional recovery. Several of these promising neuroprotective compounds have been translated to clinical trials over the last few decades; unfortunately, all have failed to show a robust, statistically significant improvement in functional outcome of human patients. Therefore, a major goal of current SCI research is to identify robust interventions that retain this neurological efficacy when translated to the clinic.

The central principle underlying therapeutic neuroprotection for acute SCI is the desire to attenuate the destructive biochemical cascades that are set into motion immediately upon injury to the spinal cord. Thus, an ideal neuroprotective intervention must be delivered as soon as possible after SCI, in order to quickly attenuate the toxic biochemical processes of secondary injury, minimize the expansion of cell death and tissue degeneration, and therefore maximize preservation of neurological function (318). To minimize delay of treatment, the drug should be administered systemically (intravenously or orally), rather than via invasive and time-intensive surgical delivery (77). An ideal therapy should also exhibit high "translational potential", meaning that it should fall under one of the following categories: 1) an already FDA-approved drug, or 2) a drug that has either undergone extensive evaluation for safety and efficacy in human clinical use or 3) exhibits high potential to be translated to human trials, based on preclinical studies (77). In this way, the time to translation "from bench to bedside" would be minimal, and years of delay before FDA approval could be avoided.

Riluzole is an anti-glutamatergic compound that is FDA-approved as an oral therapy for ALS. Currently, riluzole is under evaluation as an acute SCI intervention in a Phase I clinical trial through the North American Clinical Trials Network (NACTN) (87). The translation of riluzole to clinical trials was largely a result of preclinical evidence suggesting that it provides neuroprotection when delivered 15-30 minutes following injury (77, 78, 82), and was greatly facilitated by its status as an FDA-approved drug. However, subsequent experimental studies in clinically relevant animal models, in which the initial delivery of the drug was delayed to a more clinically realistic time point of 2 hours post-injury, reported that riluzole treatment did not provide any neurological or histological benefits (81). It is reasonable to conclude from

these findings that riluzole may exert therapeutic efficacy for SCI only if administered during a crucial window of efficacy very early after injury. Despite the lack of experimental data supporting any neuroprotective effect of riluzole when delivered at a more clinically relevant time frame following SCI, the current clinical trial seeks to evaluate the efficacy of riluzole in human SCI patients, with an initial therapeutic window extending up to 12 hours following injury (87). It is, then, plausible that this trial may fail to observe any significant neurological improvement in patients receiving riluzole several hours after SCI.

Based on our evidence that increased Pgp expression and activity during acute SCI results in reduced spinal cord bioavailability of systemically-delivered riluzole (See *Chapters 3* & *4*), we speculate that there is a time-dependent loss of efficacy of treatment due to Pgp up-regulation within the injured spinal cord. This injury-induced mechanism could potentially explain the observation that riluzole's efficacy diminishes as the therapeutic window is delayed (81). Moreover, this mechanism might also underlie the failure of neuroprotective drugs previously seen in SCI clinical trials. If this is the case, then identifying a route to overcoming Pgp-mediated drug resistance in the acutely-injured spinal cord is a therapeutic goal of high priority.

Specific Aims

1. Our results thus far have shown that: 1) Spinal cord riluzole bioavailability is decreased during the acute and sub-acute phases of SCI [See *Chapter 3*], and 2) Licofelone treatment enhances riluzole delivery to the injured spinal cord [See *Chapter 4*]. Because of the ability of licofelone treatment to enhance spinal cord riluzole delivery, we sought to examine whether, following SCI in rats, combined treatment of licofelone and riluzole would result in enhanced neurobehavioral outcome compared to riluzole treatment alone.

2. Licofelone is a new generation anti-inflammatory drug that inhibits COX-1 and -2 as well as 5-LOX (159). Previous research studies have indicated that COX and 5-LOX pro-inflammatory signaling pathways both contribute to the pathophysiology of SCI, and that pharmacologically inhibiting either of these branches improves functional recovery in rodent models of SCI (121, 136, 142, 144). For these reasons, the potential

efficacy of NSAIDs for SCI treatment has been recently discussed (77). We speculated that licofelone may hold promise as a neuroprotective treatment for acute SCI based on two reasons. First, there is evidence that dual inhibition of both pathways has a synergistic anti-inflammatory effect, as COX inhibition can shunt AA to 5-LOX metabolism, thus increasing inflammation (153, 319). Second, licofelone use is associated with a lower incidence of GI complications in patients compared to classical COX inhibitors such as naproxen (320), thus making it a more attractive candidate for clinical use than classical NSAIDs. We therefore evaluated whether licofelone treatment following SCI in rats could improve functional recovery.

Results

Basso, Beattie, and Bresnahan Open Field Locomotor Scale

We assessed whether licofelone, alone or in combination with riluzole, could improve locomotor outcome in rats over a six-week period following SCI. In order to evaluate rodents' neurological recovery following a clinically-relevant drug dosing schedule, we reproduced the time course of treatment utilized in the current NACTN riluzole SCI trial (87), in which riluzole treatment is initiated in patients ≤12 hours post-SCI, then continued for 14 days. Following SCI, rats were treated with: 1) vehicle (VEH), 2) riluzole (RLZ), 3) licofelone (LIC), or 4) licofelone and riluzole (LIC + RLZ), beginning at 3 hours following injury, then again once daily until post-injury day 14 (DPI 14). Beginning on DPI 1, motor recovery was assessed using the BBB Open Field Locomotor Scale, a sensitive assessments allowing quantification of multiple aspects of hindlimb motor function in rats (280). BBB scores were assessed on post-operative days 1, 2, 3, 5, 7, 10, 14, 21, 28, 35, and 42. Average BBB scores for all treatment groups at each time point are displayed in tabular format in **TABLE 5.1** and graphically in **Figure 5.1**.

Beginning on DPI 14, BBB scores of the SCI + LIC group and the SCI + LIC + RLZ group were significantly greater than those of the SCI + vehicle group. This effect was observed consistently at each time point from DPI 14 until the last measured time point, DPI 42. In contrast, the SCI + RLZ group scores were not significantly greater than the SCI + vehicle group scores at any point during this study. We also failed to detect any significant difference

	Baseline	Day 1	Day 2	Day 3	Day 5	Day 7
Uninjured	21.0 ± 0.0	21.0 ± 0.0	21.0 ± 0.0	21.0 ± 0.0	21.0 ± 0.0	21.0 ± 0.0
VEH	21.0 ± 0.0	0.3 ± 0.1	1.3 ± 0.3	1.9 ± 0.3	4.5 ± 0.7	5.6 ± 0.9
RLZ	21.0 ± 0.0	0.6 ± 0.1	1.8 ± 0.6	1.9 ± 0.7	4.6 ± 1.1	5.9 ± 1.1
LIC	21.0 ± 0.0	0.9 ± 0.2	2.1 ± 0.7	4.8 ± 1.0	6.9 ± 0.6	7.8 ± 0.7
RLZ + LIC	21.0 ± 0.0	0.7 ± 0.2	2.9 ± 0.7	3.6 ± 0.7	6.5 ± 0.6	7.9 ± 0.4

	Day 10	Day 14	Day 21	Day 28	Day 35	Day 42
Uninjured	21.0 ± 0.0	21.0 ± 0.0	21.0 ± 0.0	21.0 ± 0.0	21.0 ± 0.0	21.0 ± 0.0
VEH	6.6 ± 0.8	7.8 ± 0.4	8.5 ± 0.3	8.8 ± 0.4	9.0 ± 0.3	9.1 ± 0.5
RLZ	8.2 ± 0.7	9.3 ± 0.6	10.0 ± 0.7	10.2 ± 0.6	10.4 ± 0.6	10.4 ± 0.7
LIC	9.3 ± 0.9	9.9 ± 0.9	10.7 ± 0.6	11.3 ± 0.6	11.6 ± 0.7	12.1 ± 0.7
RLZ + LIC	9.0 ± 0.2	9.8 ± 0.2	10.2 ± 0.2	10.8 ± 0.3	11.4 ± 0.3	12.1 ± 0.4

TABLE 5.1. BBB open field locomotor scores. Average hindlimb BBB scores at time points before (baseline) and after injury. Uninjured, n = 17; SCI + Vehicle (VEH), n = 9; SCI + Riluzole (RLZ), n = 7; SCI + Licofelone (LIC), n = 9; SCI + Riluzole + Licofelone (RLZ + LIC), n = 10. All data are mean ± s.e.m.

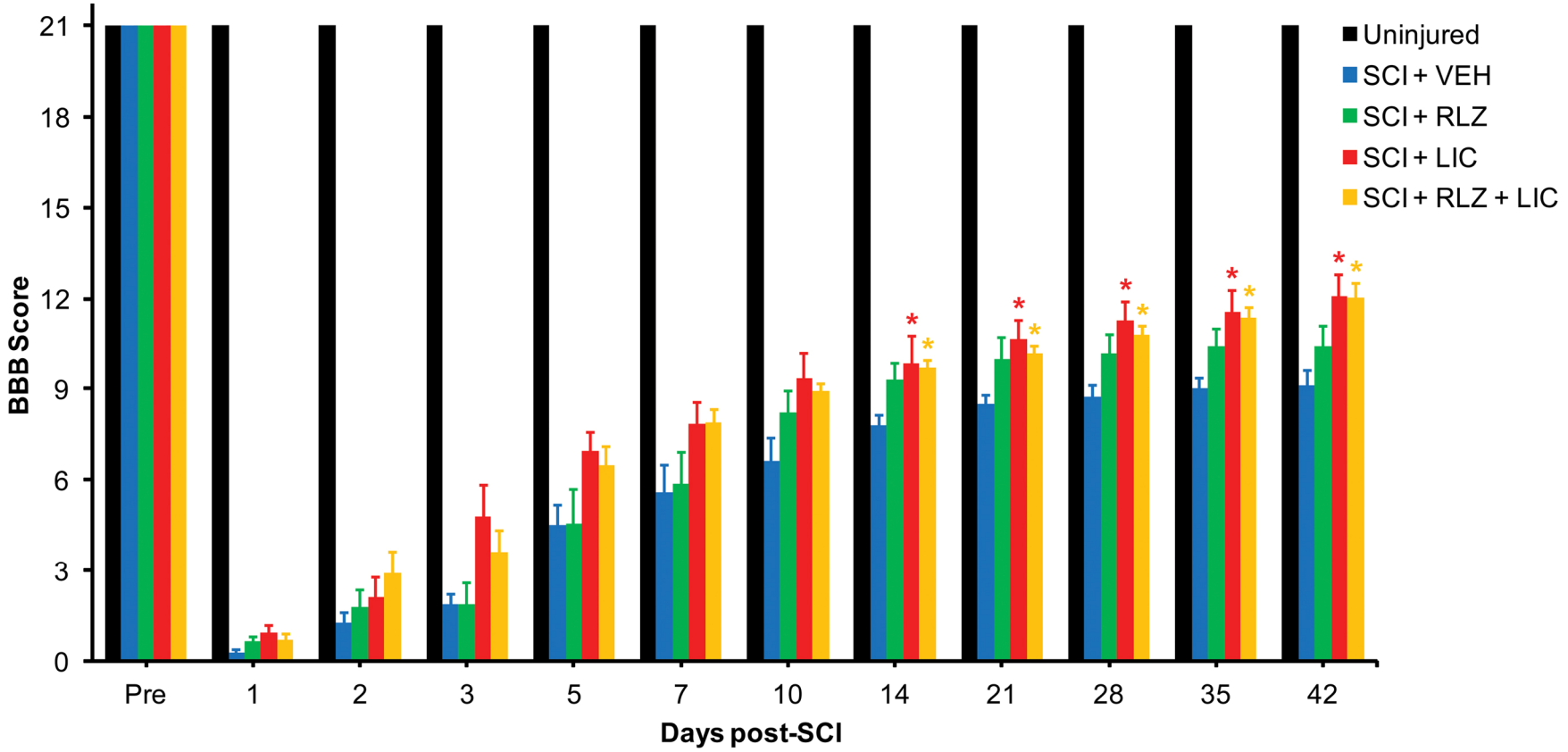

Figure 5.1. BBB scores. Average hindlimb BBB scores at time points before (Pre) and after injury. All data are mean ± s.e.m. *, $p < 0.05$ versus injured, vehicle-treated animals.

between BBB scores of the licofelone-treated group and the licofelone-and-riluzole-treated group at any time point during this study.

Photobeam Activity System

The PAS is a sensitive assessment of multiple measures of gross and fine locomotor activity. During the 20-minute testing period, animals' movements were recorded by the PAS computer, and the following parameters were tabulated: distance traveled, speed of movement, time at rest, fine movement, ambulatory movement, number of rears, and time spent rearing. Each of these activity parameters reflects different aspects of locomotor function and/or ability. For example, an increased speed of movement and/or distance traveled by an animal indicates a heightened overall level of activity; conversely, increased time spent at rest might indicate a state of increased pain or a relative difficulty moving (321). Rearing, in which an animal stands up on its hindlimbs, utilizes not only hindlimb muscles but also trunk muscles for maintenance of posture. It has therefore been suggested that the extent of rearing by animals with SCI is a useful parameter for studying the effects of treatments on postural maintenance that may be relevant to human patients (322).

Distance, Speed, and Rest Time: Total distance traveled by all animals over the 20-minute testing period is displayed graphically in **Figure 5.2**. All SCI groups covered a significantly lower distance versus uninjured controls ($p < 0.05$) at all time points following injury. Similarly, the speed of movement of all SCI groups was significantly reduced versus uninjured controls at all time points point-injury (**Fig. 5.3**), but there was no significant difference in speed between injured groups. Lastly, we examined the time spent resting during the 20-minute testing period (**Fig. 5.4**). We detected statistically significant increases in resting time compared to uninjured controls for the following comparisons: SCI + VEH at DPI 14, -35, and -42; SCI + RLZ + LIC at DPI 14; and RLZ at DPI 21. At DPI 42, time spent at rest by the SCI + LIC group was significantly lower than that of the SCI + VEH group.

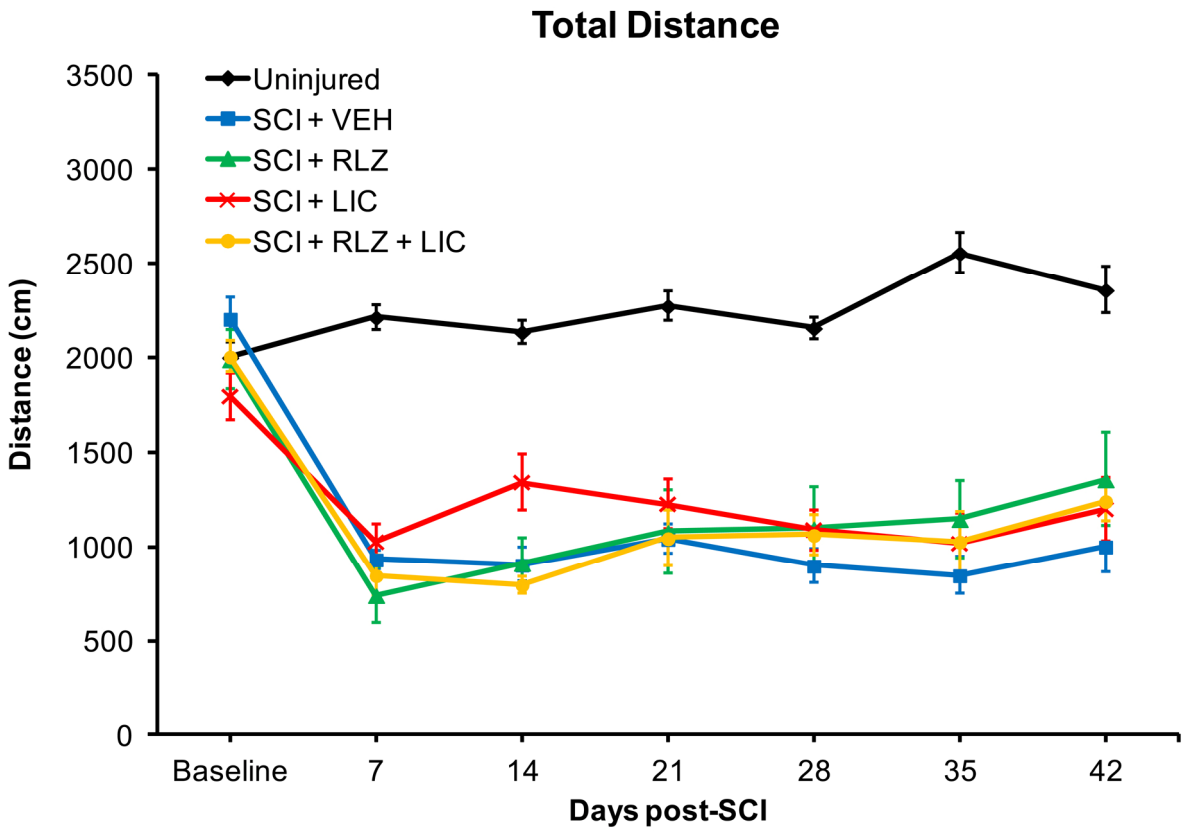

Figure 5.2. Total distance of movement. Total distance (cm) traveled by rats during the 20-minute testing period. All data are mean ± s.e.m.

]

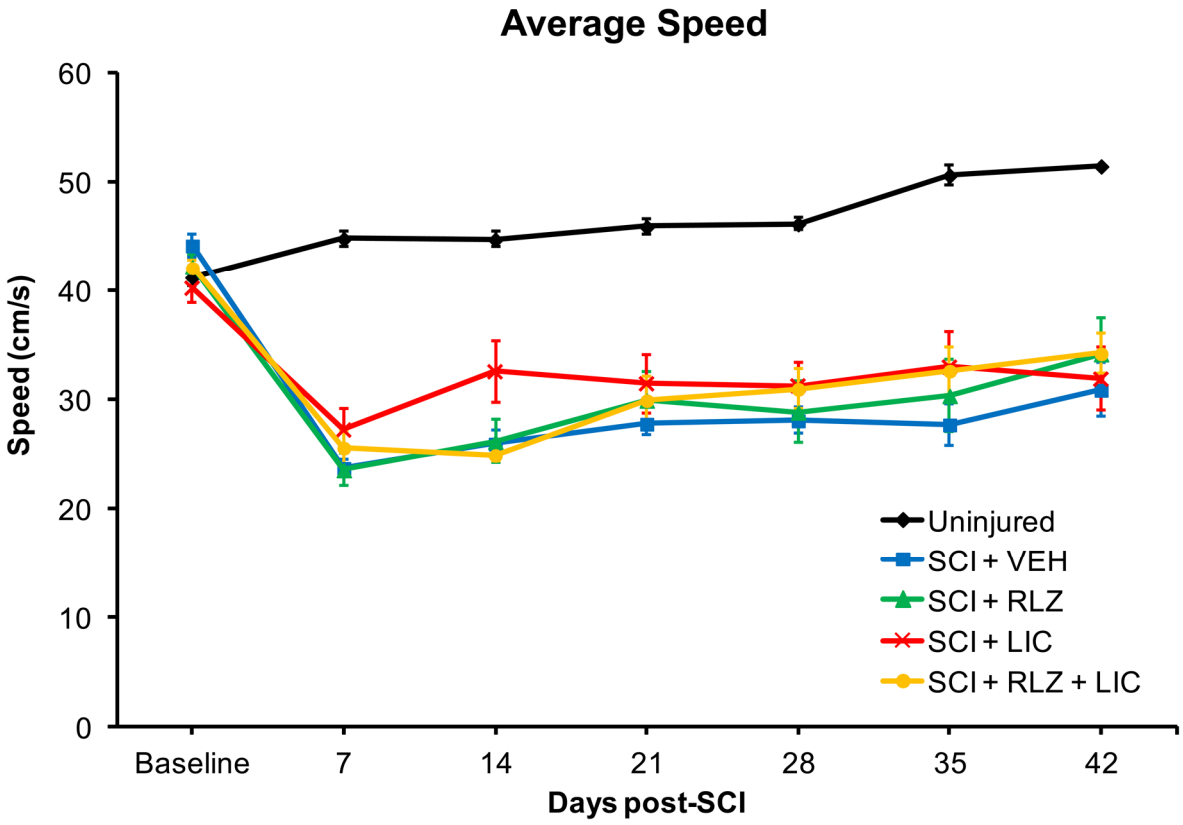

Figure 5.3. Average speed of movement. Average speed (cm/s) of rats' movement during the 20-minute testing period. All data are mean ± s.e.m.

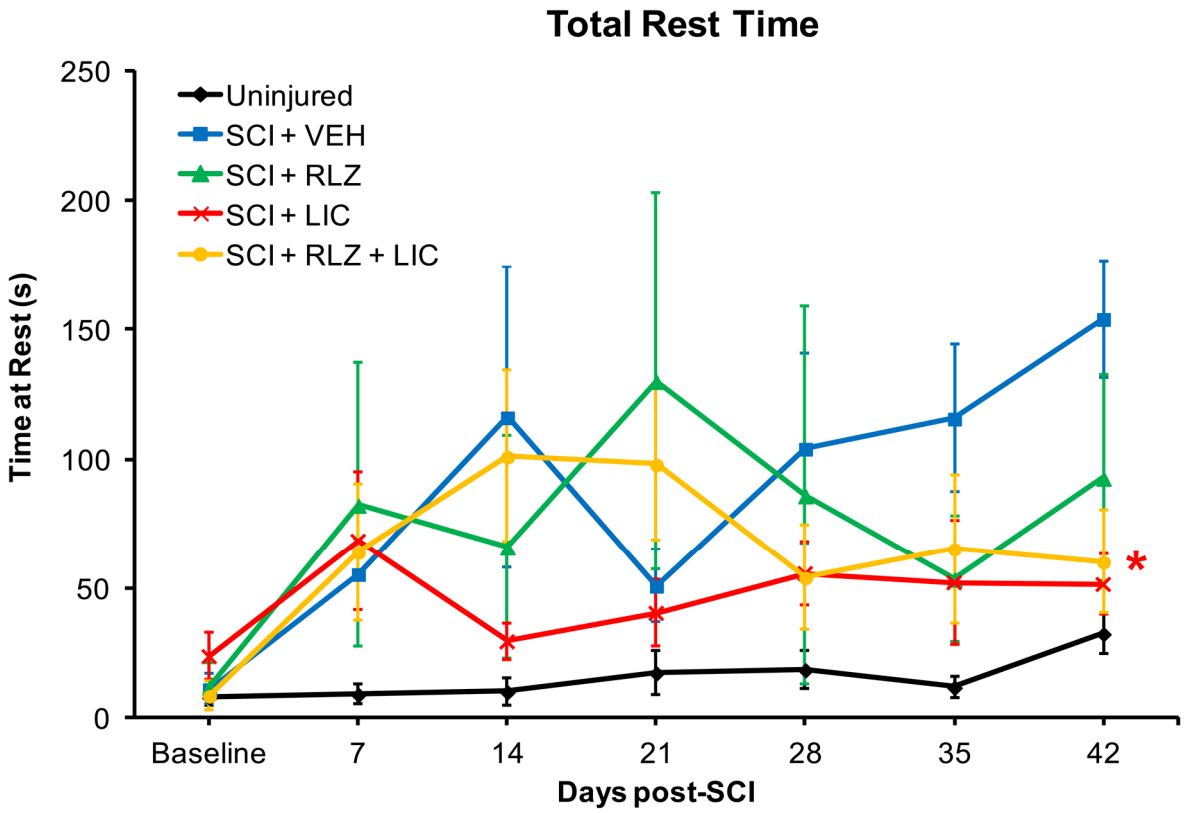

Figure 5.4. Total time spent at rest. Average resting time (s) by rats during the 20-minute testing period. All data are mean ± s.e.m. *, $p < 0.05$ versus SCI + VEH.

Fine and Ambulatory Movement: Animals' total fine movement over the 20-minute testing period is displayed in **Figure 5.5a**. The amount of fine movement observed in SCI groups was higher than that of uninjured controls at every assessed time point after injury, though statistical significance was only achieved for the following comparisons: SCI + VEH at DPI 21, -28, -35, and -42; SCI + RLZ at DPI 14 and -35; SCI + LIC at DPI 7, -21, -35, and -42; SCI + RLZ + LIC at DPI 7, -21, -35, and -42. There were no significant differences between injured groups at any time point. For ambulatory movement (**Fig. 5.5b**), all SCI groups exhibited significantly reductions versus uninjured controls at all time points post-injury. There were no treatment-dependent effects on ambulatory movement between SCI groups.

Rearing: The total number of rearing events exhibited by each group is displayed in **Figure 5.6a**. At each time point from DPI 7 through DPI 35, total rearing events exhibited by each injured group are significantly lower than that of uninjured controls; however, at DPI 42 only the SCI + VEH group is significantly lower than controls. At DPI 42, number of rearing events of the SCI + LIC + RLZ group was significantly higher than in the SCI + VEH group. Total time spent rearing is displayed in **Figure 5.6b**. Total rearing time is significantly reduced at DPI 7, -14, -21, and -28 for all SCI groups versus uninjured controls. At DPI 35, only SCI + RLZ + LIC exhibited significantly reduced rearing time versus controls, and there were no significant differences detected between groups at DPI 42.

Despite the wealth of activity data assessed here, we conclude that the only robust and significant result of this study was the improvement in BBB scores exhibited by both licofelone-treated groups from DPI 14 to -42. Though there were two significant effects of licofelone treatment on activity parameters at DPI 42 (**Figs. 5.4** & **5.6a**), it is doubtful that these slight improvements are functionally meaningful. In contrast, the more than three-point improvement in BBB scores that we have observed in licofelone-treated rats has a large degree of functional significance (See *Chapter 6*).

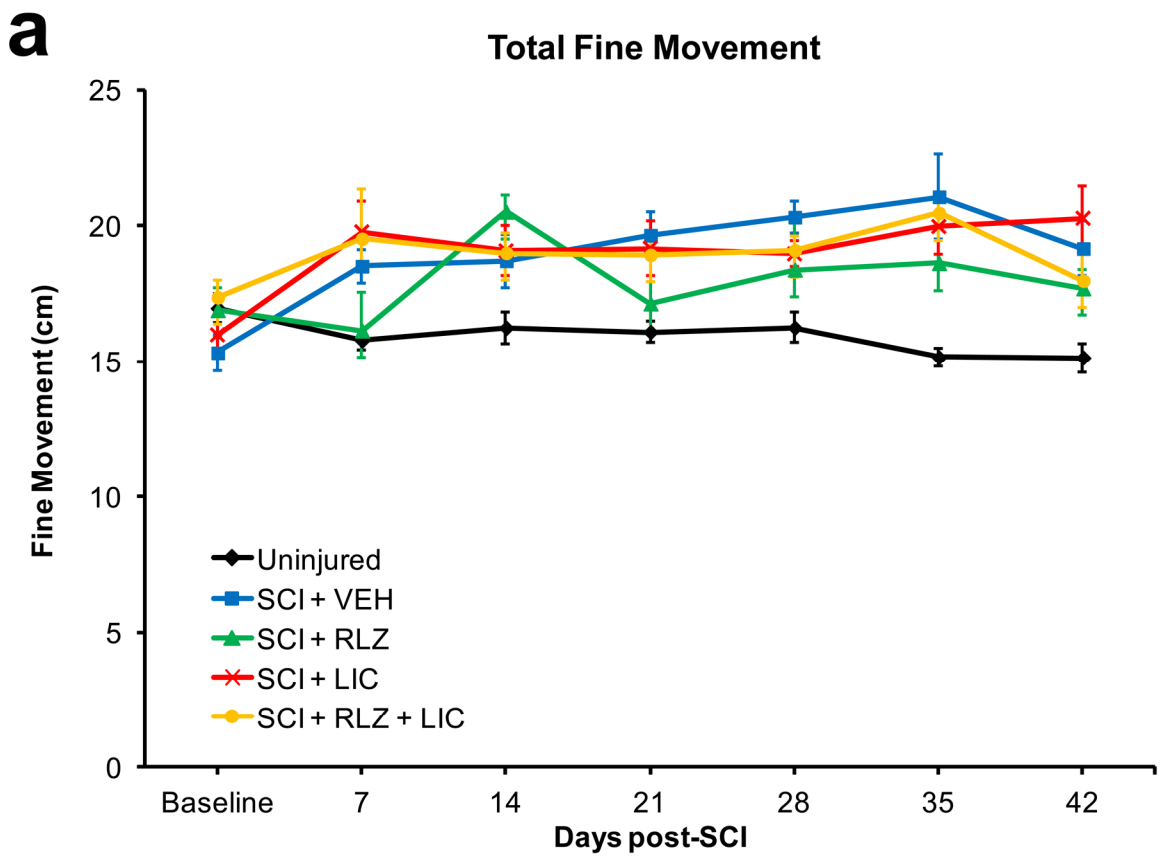
a
Total Fine Movement
Fine Movement (cm)
25
20
15
10
5
0
Uninjured
SCI + VEH
SCI + RLZ
SCI + LIC
SCI + RLZ + LIC
Baseline
7
14
21
28
35
42
Days post-SCI

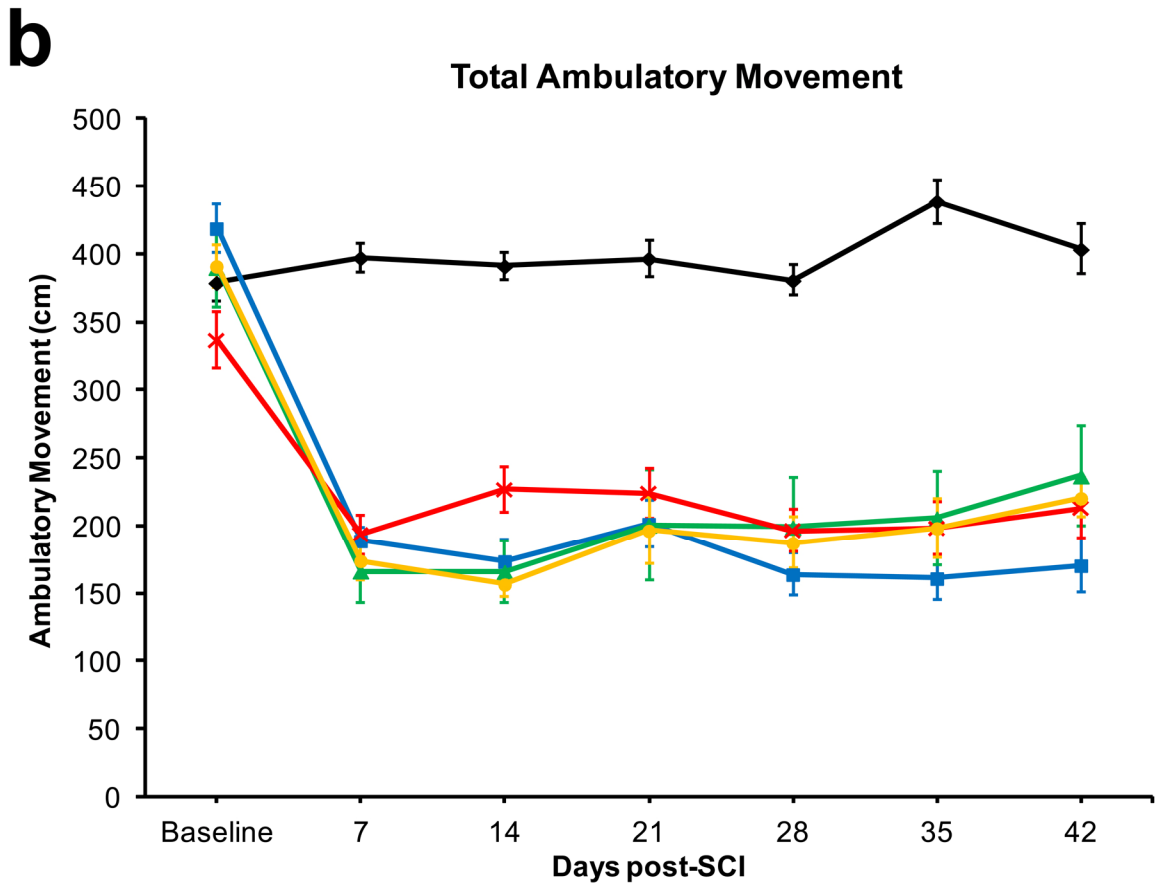
b
Total Ambulatory Movement
Ambulatory Movement (cm)
500
450
400
350
300
250
200
150
100
50
0
Baseline
7
14
21
28
35
42
Days post-SCI

(On previous page)

Figure 5.5. Total fine and ambulatory movement. Total fine movement (**a**) and ambulatory movement (**b**) during the 20-minute testing period. All data are mean ± s.e.m.

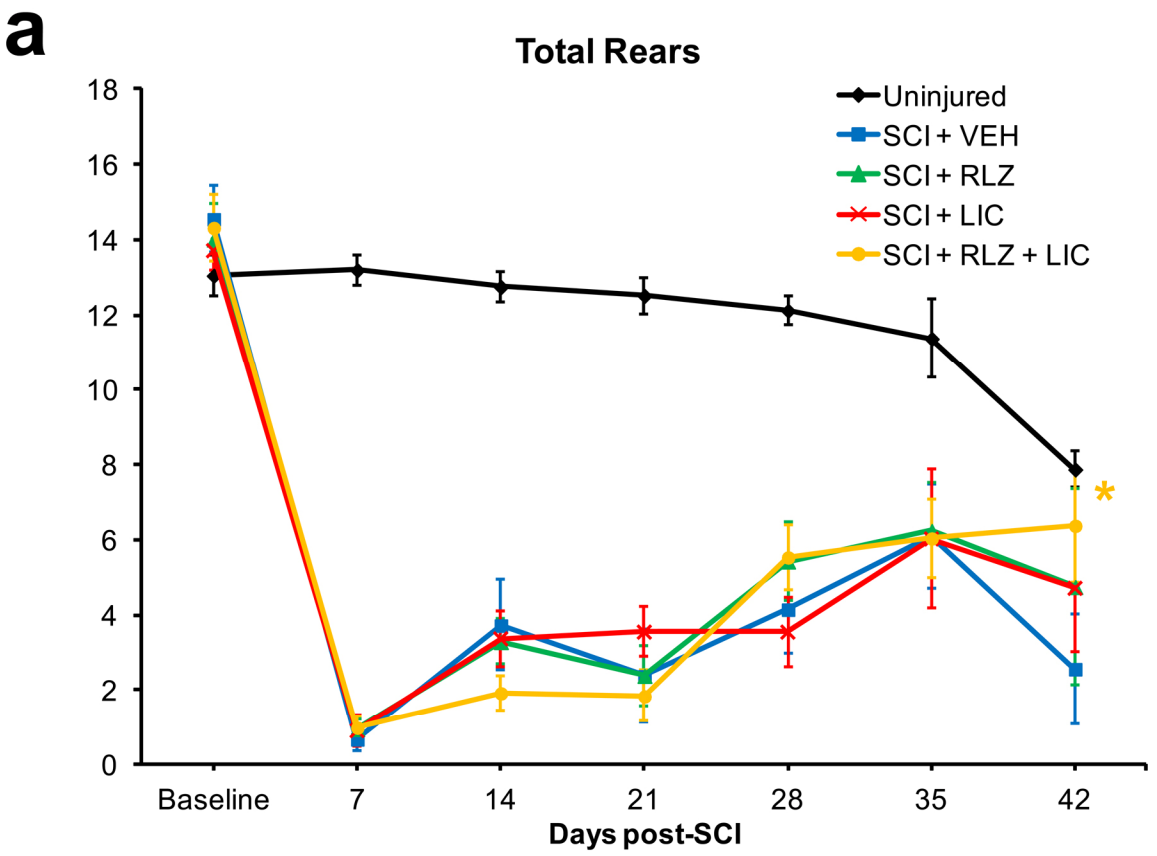
a
Total Rears
Uninjured
SCI + VEH
SCI + RLZ
SCI + LIC
SCI + RLZ + LIC
18
16
14
12
10
8
6
4
2
0
*
Baseline
7
14
21
28
35
42
Days post-SCI

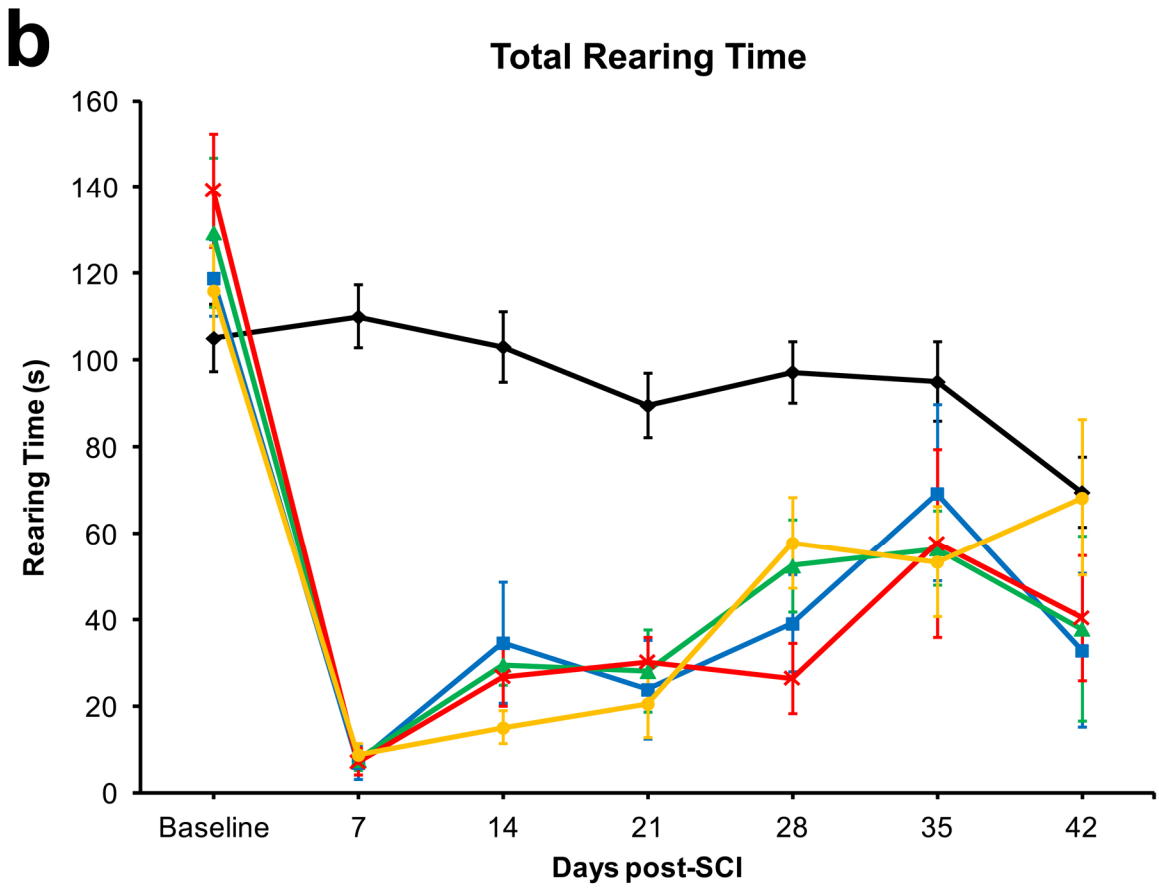
b
Total Rearing Time
Rearing Time (s)
160
140
120
100
80
60
40
20
0
Baseline
7
14
21
28
35
42
Days post-SCI

(On previous page)

Figure 5.6. Total rearing events and time spent rearing. Total number of rearing events (**a**) and total time (s) spent in the rearing posture (**b**) during the 20-minute testing period. All data are mean ± s.e.m. *, $p < 0.05$ versus SCI + VEH.

CHAPTER 6

Conclusions, Translational Significance, and Future Directions

Potential Roles for Other ABC Transporters in the Injured Spinal Cord

In the current study, we have shown that P-glycoprotein is only one among several ABC transporters that undergo differential expression following SCI. Our microarray results (**TABLE 3.1**) indicate that several genes belonging to the ABC transporter family are also significantly increased or decreased within the spinal cord lesion site at 7 days after injury. Aside from *abcb1*, among the genes that we have found to be up-regulated by injury were *abcb4* (+6.07-fold, $p < 0.001$), *abcb7* (+2.06-fold, $p = 0.006$), *abcc3* (+2.14-fold, $p < 0.001$), and *abcg1* (+3.36-fold, $p < 0.001$). Of these, *abcc3*, the gene encoding Multidrug resistance-associated protein 3 (Mrp3), is the only member which has been described in the literature as exhibiting drug transport activity; thus, it is not implausible that increased expression of Mrp3 may also contribute to spinal cord drug resistance following traumatic SCI.

ABC transporter genes that were down-regulated following injury included *abca5* (-2.59-fold, $p = 0.002$), *abcb6* (-1.71-fold, $p < 0.001$), *abcb9* (-3.91-fold, $p < 0.001$), *abcc2* (-13.92-fold, $p < 0.001$), *abcc6* (-3.44-fold, $p = 0.008$), *abcc8* (-3.00-fold, $p < 0.001$), *abcd2* (-5.54-fold, $p < 0.001$), *abcd3* (-1.55-fold, $p < 0.001$), and *abcg2* (-1.62-fold, $p = 0.010$). Of these, *abcc2* (*mrp2*) is of particular interest in terms of drug transport. The Mrp2 gene product is functionally similar to Pgp; it is expressed on the luminal membrane of brain capillary endothelial cells, where it transports a wide variety of compounds, including drugs susceptible to multidrug resistance as well as endogenous organic anions (9). Pgp and Mrp2 have some overlapping activity; for example, up-regulated Pgp functions in a compensatory role for anti-epileptic drug transport in rats deficient in Mrp2 (323). To date, there have been no reports describing an affinity of Mrp2 for riluzole, so whether reduced activity of this transporter may influence riluzole disposition, *e.g.*, in the current study, remains to be determined.

In contrast, the gene product of *abcg2*, Breast cancer resistance protein (Bcrp), was recently shown by Milane *et al*. to transport riluzole at the blood-brain barrier in mice (324). Though much less is known about the regulation of Bcrp expression compared to that of Pgp, this group also demonstrated that repeated riluzole treatment led to increased Bcrp efflux activity and decreased brain riluzole levels in *mdr1a*$^{-/-}$ mice (324), implying that Bcrp can be up-regulated at the blood-brain barrier by drug treatment. Here, we have shown that repeated riluzole treatment does not alter Pgp expression in the injured spinal cord, but we did not assess Bcrp levels. Therefore, we cannot rule out the possibility that enhanced Bcrp expression in the

spinal cord lesion site, following repeated riluzole treatment, may contribute to reduction of spinal cord riluzole levels. Interestingly, Milane and colleagues did not observe any differences in Bcrp expression or function in mice expressing the mutant human G86R SOD1 isoform (224), despite their observations of increased Pgp expression and activity in this model. This disparity suggests that the pathological mechanisms driving Pgp overexpression in neurological disease do not necessarily also regulate Bcrp expression in the same way. We have observed a 1.62-fold decrease in *abcg2* expression one week following injury within the spinal cord lesion site, compared to a 10-fold increase in *abcb1* expression. Based on this data, it is obvious that the pathological processes within the injured spinal cord do not modulate expression of these two transporters in equal ways. It has recently been shown that Bcrp and Pgp act in concert to diminish drug delivery in brain cancer (325); thus, it is not inconceivable that a similar mechanism might be observed in SCI. Whether Bcrp and other drug transporters negatively influence spinal cord drug delivery following SCI remains an important question for future study. Active drug transport at the blood-brain/-spinal cord barriers is not entirely understood, as it is an extraordinarily complex system comprised of multiple, tightly regulated family members that often exhibit functional redundancy (182). Thus, the pathological consequences of SCI may very well include altered expression and activity of multiple drug transporters, with potential to alter the CNS disposition of a multitude of bioactive drugs. Future studies are needed to examine the roles of other drug transporter proteins in the injured spinal cord and the extent to which they might also contribute to multidrug resistance.

Given the broad functional diversity of the ABC transporter family members, it is conceivable that some of these proteins, which carry out biological functions other than drug transport, may function in roles that otherwise influence SCI pathology. The most dramatically up-regulated of the ABC transporter genes that we observed at 7 days post-SCI (apart from *abcb1*) was *abcb4*, which encodes Mdr2, a phosphatidylcholine transporter that plays a crucial role in the liver, transporting hepatic phospholipids into the bile. It is known that Mdr2 is expressed in the brain at low levels, but its function in the CNS is unknown (326). Additionally, *abcg1*, encoding the White1 transporter, is important for cholesterol homeostasis, suggesting possible implications for the regulation of myelination following SCI. The *abcd2* gene, which encodes the adrenoleukodystrophy-related protein (Aldrp), is expressed in peroxisomal membranes. Aldrp plays a vital function in the transport of very long-chain fatty acids (VLCFA) during normal fatty acid oxidation (326). In the metabolic disease

adrenoleukodystrophy (ALD), dysfunction of *abcd1* and *abcd2* results in accumulation of VLCFA, causing lipotoxicity-induced, demyelinating inflammation of the brain (299). Interestingly, it has recently been shown that this lipotoxic effect of VLCFA accumulation is mediated through 5-LOX activity and enhanced production of the pro-inflammatory CysLTs and LTB_4 (327). Perhaps the substantial down-regulation of *abcd2* observed here at 7 days post-SCI may impart a similar VLCFA-mediated lipotoxic effect via increased production of leukotrienes. These are only speculations, and there is a limit to the information that can be gleaned from a study of differential gene expression within such a complex pathophysiological system. Regardless, our array data may provide important clues into the multifaceted pathological response of ABC transporter family members to SCI, and serve as a useful starting point toward the design of further investigations of the potentially injurious (or neuroprotective) influences of these proteins within the injured spinal cord.

P-glycoprotein Expression Patterns in the Injured Spinal Cord

We have shown that Pgp immunoreactivity in the uninjured spinal cord is restricted to blood capillary endothelial cells (**Figs. 3.2, 3.3**). This finding is consistent with the vast majority of previously published accounts (203). Only one group has repeatedly reported Pgp expression on the cell membranes of astrocyte end-foot processes (301-304). However, whether Pgp has a functional role in astrocytes or other cells in the brain parenchyma, under normal or disease conditions, is not known. We have not extensively examined cellular distribution of Pgp immunoreactivity following SCI in this study, but we did observe that Pgp expression remained localized to spinal cord vasculature at one week post-SCI (**Fig. 3.4**). Thus, it is reasonable to assume that our immunoblot quantification of Pgp levels is an accurate representation of Pgp expression in capillary EC membranes at the BSCB.

Here, we have reported increased Pgp expression within the spinal lesion site from as early as 72 hours post-injury, up to 10 months after injury (**Fig. 3.8**). Due to the practical limitations of these experimental studies, we have only assessed protein expression levels at four acute and chronic time points: 72 hours, 7 days, 4 months, and 10 months post-SCI. We have not examined earlier time points, so it is possible that Pgp up-regulation may occur even earlier than 72 hours within the injured spinal cord. Similarly, we have not examined Pgp expression at time points between one week and four months. During this substantial time window, the

BSCB is generally thought to regain most of its functional integrity; however, some reports have demonstrated prolonged BSCB permeability for months following injury (177, 189). In the context of the sparse and incomplete information that has been gained about BSCB function during the sub-acute and chronic phases of SCI, it will be interesting to see whether future investigations reveal a relationship between the temporal dynamics of BSCB leakiness and the expression patterns of selective transport systems such as Pgp. Characterizing the relationship between "passive" barrier dysfunction (*e.g.*, loss of tight junctional integrity) and differential regulation of "active" barrier function (*i.e.*, Pgp up-regulation) will increase our understanding of how changes in BSCB properties contribute to outcome following traumatic injury to the spinal cord. Certainly, further studies are warranted in order to gain a more complete understanding of the temporal regulation of expression of Pgp (and possibly other drug transporters) within the spinal cord lesion site.

Similarly, another question of high interest is whether the delayed increases in cervical and lumbar Pgp expression that we report here (**Figs. 3.9, 3.10**) mirror a progressive spatial spread of passive BSCB deficits. Previous studies in our laboratory have identified increased BSCB permeability to large molecules such as albumin and IgG that is detectable 1 cm rostral to the lesion site 1 month after contusion injury at T10, as far rostral as the brainstem by 8 months post-SCI, and as far caudal as the lumbar cord by 9 months post-SCI (unpublished data; experiments performed by Dr. Raymond Grill). Our laboratory has also shown that this progressive barrier dysfunction correlates with reduced vascular expression of the adherens junction protein, vascular endothelial (VE)-cadherin (unpublished data). Together, these observations provide compelling evidence for a temporal and spatial spread of passive BSCB dysfunction. In this study, we have detected increased Pgp expression in cervical (C6-C7) spinal cord tissue as early as one week after injury; this alteration appears to be sustained for as long as 10 months (**Fig. 3.9**). We have also made similar observations in lumbar spinal cord tissue at 4 and 10 months post-SCI (**Fig. 3.10**). We have not evaluated Pgp expression in other areas of the spinal cord or brainstem in this project, but we plan to investigate this possibility in future studies. If SCI is followed by a progressive spread of increased vascular Pgp expression, similar to the spread in passive BSCB dysfunction that we have previously observed, there may be important implications for drug delivery in the chronic phase of SCI. Further study is also needed to investigate whether the active and passive components of BSCB pathology are distinct, or whether they might be driven by common molecular mechanisms. If the latter is

true, simultaneously targeting both of these aspects of BSCB dysfunction by antagonizing a common signaling network may be a desirable therapeutic goal.

Functional Significance of P-glycoprotein Up-regulation

P-glycoprotein is an incredibly promiscuous drug transporter with an affinity not only for endogenous substrates, but also for xenobiotic compounds. How—and why—Pgp has evolved to recognize such a large variety of substrates is an intriguing philosophical question. Some insight might be gained by examining the biochemical basis for the transporter's ability to recognize such a large variety of structurally disparate compounds. Aller and colleagues (199) recently elucidated the crystal structure of Pgp in the presence and absence of bound substrate. They found that the transporter possesses a large substrate binding domain, which contains multiple hydrophobic, aromatic, and polar residues (**Fig. 6.1**). Unique subsets of these residues' side chains make contact with different drug compounds within the binding pocket, thereby forming the basis for the protein's substrate poly-specificity (199).

Most Pgp substrates are small and hydrophobic, and consequently exhibit an increased tendency to partition into the cell membrane (328). It is therefore easy to appreciate the evolutionary advantage gained by stationing such a highly promiscuous and efficient efflux system at a biological barrier that is susceptible to transcellular diffusion of potentially toxic molecules. These properties endow Pgp with an unparalleled ability to protect the various sensitive tissues at which it is expressed (*e.g.*, the CNS (329), the testes (204), and even the developing fetus (205)) from exposure to harmful compounds in the blood. ABC transporters are ancient, and these proteins are expressed in organisms as distant from humans as bacteria. Each member of this very diverse family has some type of specialized active transport activity, but only the MDR (ABCB), MRP (ABCC), and BCRP (ABCG) family members confer multidrug resistance in humans. One perplexing philosophical question, therefore, is why Pgp evolved the ability to recognize such a large variety of synthetic drugs that do not occur in nature. It is difficult to speculate as to why Pgp evolved substrate poly-specificity before the advent of modern medicine. It is likely that Pgp originated from related ABC transporters that functioned in the transport of endogenous substrates (a function that Pgp also retains), and that

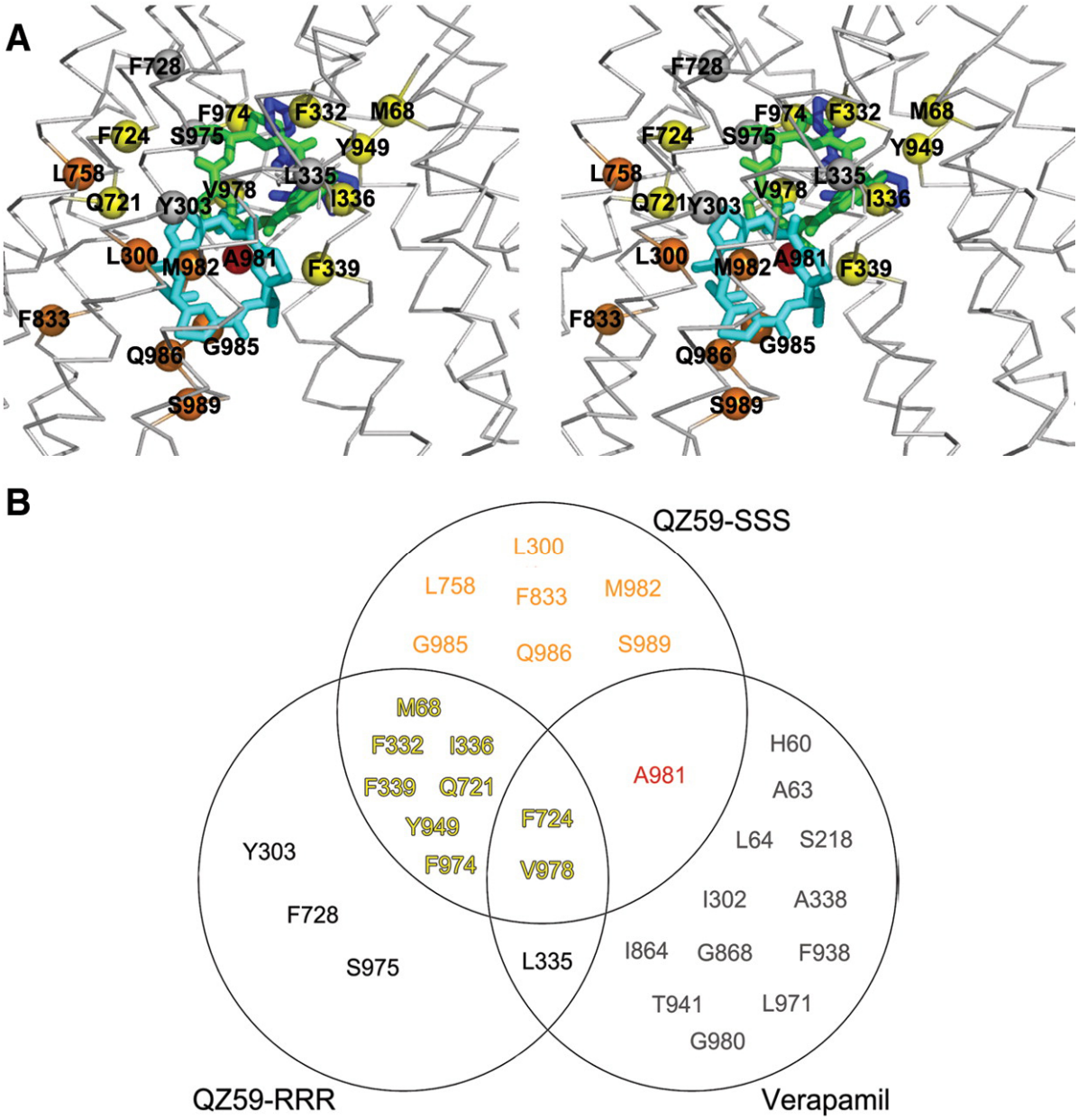

Figure 6.1. Drug-binding residues of P-glycoprotein. QZ59-RRR and QZ59-SSS are two stereoisomers of cyclic hexapeptide inhibitors. (**A**) Crystal structures of drug-bound Pgp substrate binding pockets. Binding of each of these drugs, as well as the Pgp substrate drug verapamil, within the Pgp substrate binding domain involve associations with unique subsets of amino acid side chains (**B**) within the binding pocket. Figure from: **Structure of P-Glycoprotein Reveals a Molecular Basis for Poly-Specific Drug Binding.** Stephen G. Aller, Jodie Yu, Andrew Ward, Yue Weng, Srinivas Chittaboina, Rupeng Zhuo, Patina M. Harrell, Yenphuong T. Trinh, Qinghai Zhang, Ina L. Urbatsch, and Geoffrey Chang. *Science* 27 March 2009: **323** (5922), 1718-1722. Reprinted with permission (199).

at some point during evolutionary history, Pgp gained an increased substrate promiscuity that conferred the organism(s) expressing it with a biological advantage. This advantage lies in its ability to "adapt" its binding site to accommodate a diverse variety of substrates, thus providing barrier defense against new and previously unencountered substances. In this way, Pgp activity is analogous to that of the cytochrome P450 (CYP) class of enzymes, which perform oxidative breakdown of substances in a diverse range of organisms from bacteria to humans. There is an incredible range of CYP family members and isoforms, and like Pgp, they act on diverse substrates including a large number of synthetic xenobiotics. It is easy to understand the evolutionary advantage of enzymes with such labile binding sites in the context of detoxification of exogenous, potentially harmful substances.

It is these same qualities of Pgp, however, that often prevent therapeutic levels of blood-borne drugs from reaching the CNS, unless such high doses are used that peripheral side effects may be experienced (182). Similarly, the up-regulation of Pgp expression following repeated drug treatment is probably a protective response that evolved in order to more efficiently protect the organism against a repetitive barrage of toxic insults. Others have shown that up-regulation of Pgp can be driven by inflammation and oxidative stress—molecular processes that are principally associated with disease and injury. Pgp up-regulation might therefore serve as an endogenous protective response. In neurological disease and trauma, it is plausible that blood-brain/-spinal cord barrier up-regulation of Pgp could be spurred in part by passive deficits in blood-CNS barrier integrity. The resulting increase in extravasation of circulating substances through the barrier would lead to accumulation of toxic blood-borne compounds and endogenous metabolites; thus, an increase in efflux transport activity at the blood-CNS interface would function to protect the CNS tissue by contributing to clearance of toxic metabolites.

Dual Modulation of the Blood-Spinal Cord Barrier by Anti-Inflammatory Therapy

It seems logical to assume that increased paracellular flow of substances from the circulating blood into the CNS would effectively increase delivery of systemic drugs to the CNS. Paradoxically, however, increased passive permeability of the blood-CNS barriers may not necessarily assure drug permeability, and in some cases may actually reduce brain drug

concentrations. Marchi and colleagues showed that osmotic blood-brain barrier disruption caused increased serum protein extravasation and reduced levels of free phenytoin (an anti-epileptic drug) in the brain (330), an effect likely attributed to increased drug-protein binding. A similar effect may occur in SCI, where vasogenic edema resulting from BSCB opening may increase sequestration of drug molecules by extravasated albumin in the injured spinal cord tissue. If this is the case, it is possible that passive BSCB dysfunction, in addition to alterations in active transport, also contribute to reduced efficacy of systemically-delivered therapeutic drugs.

It is interesting to consider the possible contributions of inflammation to both passive and active aspects of BSCB function following traumatic injury to the spinal cord. Extensive work by Potschka and colleagues has implicated the COX-2/PGE_2/EP1 signaling axis as key in driving Pgp overexpression at the blood-brain barrier following seizure activity (235, 236, 244). In light of our observations that licofelone is effective in attenuating BSCB Pgp levels during acute SCI (**Fig. 4.13**), it is highly likely that similar regulatory mechanisms of Pgp expression are at work in both pathologies. This is not altogether surprising, as it is well known that neuroinflammation drives multiple pathophysiological mechanisms that contribute to the progression of CNS disease. It is well established that inflammation modulates opening of the blood-brain barrier (331); likewise, following SCI and peripheral nerve injury, inflammatory mediators promote BSCB permeability (72, 178, 332, 333). Thus, treatment with anti-inflammatory drugs such as licofelone may serve a double purpose in improving BSCB function after SCI, by both preventing inflammation-driven up-regulation of drug efflux transport via Pgp, and attenuating inflammatory-mediated opening of the BSCB. Previous work by other groups has demonstrated that treatment with the COX inhibitors ibuprofen and indomethacin reduces edema and BSCB permeability following SCI (124, 127). Though we have not yet addressed whether licofelone treatment can also improve aspects of passive BSCB function, we intend to evaluate this possibility in future studies in our laboratory.

Previous reports have shown that the COX and 5-LOX signaling pathways are critical factors shaping the pathological molecular processes and influencing functional outcome during acute SCI (121, 142, 144, 246). It is these observations that have fueled our laboratory's interest in simultaneous COX/5-LOX inhibition as a means not only to target Pgp up-regulation, but also to combat other aspects of SCI pathophysiology and potentially improve

functional outcome. We have shown that licofelone completely abolishes the sharp increase in PGE_2 production observed 24 hours after injury (**Fig. 4.11**). However, our failure to detect quantifiable levels of LTB_4 is a caveat that undermines the argument for a therapeutic role for 5-LOX inhibition in these studies. One possible explanation is that LTB_4 production may only occur very early after injury, and fall to baseline (uninjured) levels by 24 hours after SCI. This possibility is supported by the work of Moreland and colleagues (141), in which peak LTB_4 production was observed within the first 4 hours post-SCI in rabbits and returned to control levels by 24 hours. An alternative approach would be to evaluate the effects of licofelone on CysLT production, given that we have previously observed a marked elevation in CysLT levels 24 hours post-SCI (**Fig. 4.1**).

We have shown that acute licofelone treatment is efficacious in partially abrogating the up-regulation of Pgp by SCI (**Fig. 4.13**), providing strong support for the inflammatory modulation of Pgp expression within the injured spinal cord. Potschka's group have revealed COX-mediated PGE_2 signaling to be a major factor promoting Pgp expression in the epileptic brain (187), and more recently other groups have reported similar findings in cancer cells (238, 241, 309). We have hypothesized the likelihood of a comparable regulatory mechanism in SCI, given the common pathological cascades (*e.g.*, inflammation, oxidative stress, excitotoxicity) that are exhibited in these diseases. In the absence of a systematic study comparing Pgp levels following COX inhibition versus combined COX/5-LOX inhibition in spinal cord-injured rats, it is difficult to speculate whether licofelone treatment would be more efficacious than a COX inhibitor such as ibuprofen. It is also known that oxidative stress drives Pgp up-regulation in brain capillary ECs (334). We have shown that expression of all three enzymes—COX-1, COX-2, and 5-LOX—is increased 72 hours after injury (**Fig. 4.2**), so it is feasible that licofelone's effect on Pgp expression at this time point is partially due to blocking the oxidative stress produced by COX- and 5-LOX- metabolism of AA. Certainly, more mechanistic studies are needed to investigate this possibility.

Novel Evidence of Inflammation and Oxidative Stress in Chronic Spinal Cord Injury

Inflammation plays a major role in shaping the pathophysiology of acute SCI. During the hours-to-days following the initial impact to the spinal cord, the inflammatory response contributes to disruption of vascular integrity (72), formation of the glial scar (100),

cytotoxicity (98), and sensitization of neural pathways (30). In contrast, relatively few studies have undertaken the task of characterizing the molecular milieu of the spinal cord beyond one to two months post-injury. Recently, studies have reported the presence of infiltrating peripheral immune cells and activated microglia within the spinal cord up to 1 year post-SCI (69, 70). These findings raise the possibility that neuroinflammation might not simply be a transient phenomenon, but may rather continue into the chronic phase of injury, fueling ongoing pathological processes that plague SCI patients with long-standing injuries, such as neuropathic pain.

In the current study, we have provided novel evidence of both pro-inflammatory AA metabolism and oxidative stress within the chronically-injured spinal cord. The presence of LTB_4 and PGE_2 in the spinal cord lesion site 9 months after injury (**Fig. 4.6**) is compelling evidence that the inflammatory response is not simply a phenomenon confined to the earlier, acute phase of injury. Rather, our results have demonstrated that pro-inflammatory signaling through COX and 5-LOX pathways is also present in the chronically-injured spinal cord. Furthermore, using a high-throughput metabolomic screen (**Figs. 4.7-4.9** & **TABLE 4.1**), we have shown that the chronically-injured spinal cord contains elevated levels of oxidative stress markers and a depletion of endogenous anti-oxidative and anti-inflammatory compounds. This included elevated levels of the major indicators of cellular ROS damage, oxidized glutathione (335), cysteine-glutathione disulfide (336), and dehydroascorbate (337). Chronic SCI tissue also possessed increased levels of 13-HODE and 9-HODE, markers of oxidative stress and lipid peroxidation (338). Additionally, chronically-injured spinal cords contained decreased levels of the antioxidant alpha-tocopherol, which plays an especially important role in protecting the highly sensitive CNS from pathological lipid peroxidation (339). These are significant findings, due to the existing deficiency in knowledge of the molecular environment within the chronically-injured spinal cord. Our observations of neuroinflammation and oxidative stress in the far chronic period will contribute to understanding of the pathological mechanisms that shape the myriad adverse conditions, including neuropathic pain, that are the hallmark of the chronic phase of SCI.

Ours is the first study featuring a metabolomic profile of chronically-injured spinal cord tissue. In this report, we have placed an emphasis on the metabolic alterations indicative of oxidative stress and inflammation in the cord, because of their previously identified role in

promoting up-regulation of P-glycoprotein (214). However, our metabolomic screen has illuminated a large number of additional metabolic alterations in various other biochemical pathways (**Figs. 4.7, 4.8** & **TABLE 4.1**). Our metabolomic results reveal chronic alterations in nucleotide metabolism, reductions in levels of several metabolites associated with neurotransmission, decreased phospholipid levels, and alterations in cholesterol metabolism, among many other changes. We have also detected increases in glycolytic intermediates in the chronically injured spinal cord, such as glucose (+2.73 fold), glucose-6-phosphate (+2.53 fold), and fructose-6-phosphate (+2.29 fold). In view of our results of chronically increased Pgp expression, we anticipate that enhanced glycolysis in the chronically injured spinal cord may reflect an increased need for energy to fuel active transport systems, as has been previously described in multidrug-resistant tumors (340). Lending support to this idea, a recent metabolic profiling study has shown increased glycolysis and phospholipid turnover in drug resistant tumor cells (341). As a side note, the possible relationship between increased glycolytic flux and heightened active transporter activity may also be worth considering in another form of neurotrauma, traumatic brain injury (TBI), which is often accompanied by brain hyperglycolysis (342). Though Pgp-mediated drug resistance has not yet been characterized in TBI, injury-associated resistance to pharmacotherapy has previously been observed (343).

Our observations of chronic inflammation in the injured spinal cord also led us to investigate the effects of dual COX/5-LOX inhibition in the chronic phase of SCI. We observed that months-delayed licofelone treatment resulted in statistically significant increases in a number of compounds that exhibit anti-inflammatory and anti-oxidative properties (**Fig. 4.10 & TABLE 4.2**). However, the precise mechanism by which licofelone mediates this effect is unclear, as AA metabolism is a complex cascade with a plethora of molecular targets. Based on the wide range of metabolic pathways enhanced by licofelone, it is possible that licofelone may activate a "master regulator" of the antioxidant response such as nuclear factor erythroid-2-related factor-2 (Nrf2), which induces transcription of multiple protective anti-oxidant genes (344). Due to experimental constraints, we did not evaluate the effect of licofelone treatment on prostaglandin and leukotriene production in the chronically-injured spinal cord. However, we intend to investigate this in future studies, as the eicosanoids have been shown to play a significant role in the development and maintenance of neuropathic pain (345, 346), a condition that afflicts a substantial percentage of individuals with chronic SCI (276).

One might anticipate that a lack of Pgp efflux activity at the BSCB would result in enhanced spinal cord drug delivery under normal (non-disease state) conditions. An interesting finding of this study is that uninjured *mdr1a*$^{-/-}$ rats did not exhibit greater spinal cord riluzole penetration compared to uninjured wild-type rats (**Fig. 3.12**). This is in contrast to Milane's observation that *mdr1a*$^{-/-}$ mice showed 1.4-fold higher brain uptake of riluzole than *mdr1a*$^{+/+}$ mice (225). The most logical explanation for this discrepancy is that the rat may possess some degree of compensatory riluzole efflux due to activity of other drug transporters, such as Bcrp. Further analysis will be needed to substantiate this possibility. Regardless, our observation that loss of Pgp is sufficient to abolish an injury-induced decrease in spinal cord riluzole uptake, is a very strong piece of evidence showing that Pgp is responsible for the reduction in blood-to-spinal cord riluzole delivery that we have observed following SCI.

Also interesting is our finding that *mdr1a*$^{-/-}$ rats with SCI have significantly lower plasma levels of riluzole than their injured, wild-type counterparts (**Fig. 3.13**). Following *i.p.* drug delivery, clearance of drug from the plasma is regulated to a large extent by active transport-mediated excretion of drug by the liver and kidneys into the bile and urine, respectively. Importantly, Pgp activity is involved in both of these aspects of drug clearance (347, 348). In the liver, Pgp transports drugs from the hepatocytes into the bile, and in renal epithelial cells the transporter acts in a similar role of drug transport to the urine. One might therefore expect healthy *mdr1a*$^{-/-}$ rats to exhibit reduced drug clearance from the plasma due to loss of hepatic and renal Pgp function. Our results show that this is not the case, and suggest that compensatory drug transport activity might also serve to explain the lack of significant difference in plasma drug levels between uninjured wild-type and knockout rats. However, the sizeable SCI-induced reduction in riluzole plasma levels of *mdr1a*$^{-/-}$ rats, but not wild-type rats, is somewhat puzzling. In their characterization of the *mdr1a*$^{-/-}$ rat, Chu *et al*. showed that these animals retain strong expression of what is presumably the Mdr1b gene product in the liver, but only faint expression in the kidney (**Fig. 3.14**) (307). Perhaps, then, this closely related isoform becomes up-regulated following SCI in the absence of Mdr1a function. Though the current study has not addressed Mdr1a/1b expression in the liver, kidneys, or intestines, Chu *et al.* also reported a five-fold increase in *mdr1b* expression in the liver, and a two-fold decrease of *mdr1b*

expression in the kidney of male *mdr1a* knockout rats, compared to wild-type animals[9]. Taken together with experimental evidence that Mdr1b efflux activity can increase in response to inflammation (245), it seems quite plausible that increased liver Mdr1b function may explain the augmented drug plasma clearance in *mdr1a*$^{-/-}$ rats with systemic inflammation resulting from SCI (31).

We chose riluzole for these studies because of the obvious clinical relevance of examining post-SCI drug resistance using a drug that is currently in clinical trials. However, studies in the *mdr1a*$^{-/-}$ rat are very likely complicated by our use of riluzole to measure Pgp activity, since this drug is also a substrate for the Bcrp efflux transporter. Hence, it is possible that compensatory Bcrp activity at the BSCB, intestines, liver, and kidneys of the *mdr1a*$^{-/-}$ rat may obfuscate the interpretation of these results to some degree. Chu *et al.* did not detect any change in *abcg2* expression in the liver, kidneys, intestine, or brain of the male *mdr1a*$^{-/-}$ rat, though the reported expression patterns are those of healthy, uninjured rats (307). Areas of ongoing investigation in our laboratory will include the characterization of Mdr1b and Bcrp expression in the liver, kidney, intestine, and spinal cord of wild-type and *mdr1a*$^{-/-}$ rats in response to SCI. However, to determine the exact contribution of Pgp-mediated transport to the development of spinal cord drug resistance after SCI, future studies would necessitate the use of drugs that are "pure" Pgp substrates, such as the opioid-receptor antagonist loperamide.

Curiously, we have also observed a significant reduction in plasma riluzole levels 72 hours post-SCI in (wild-type) rats treated with licofelone in combination with riluzole, but not in rats treated with riluzole alone (**Fig. 4.15**). Despite this considerable drop in plasma drug levels, raw spinal cord concentrations of riluzole are not decreased. The net effect of these factors is a significantly higher normalized spinal cord riluzole bioavailability compared to riluzole-treated injured rats as well as uninjured controls (**Fig. 4.14**). This implies two actions of licofelone. First, licofelone enhances the plasma-to-spinal cord penetration of riluzole, presumably by partial attenuation of Pgp up-regulation (**Fig. 4.13**). Second, licofelone also enhances the plasma clearance of riluzole. How the latter might occur is a subject of speculation that might be better addressed by assessing expression patterns of efflux transporters (Pgp, Bcrp) in the

[9] The *mdr1a* knockout rats characterized by Chu *et al.* were Wistar Hannover rats and the *mdr1a* knockout rats utilized in the present study were Sprague Dawley. Thus, differences in genetic background could conceivably contribute to different pharmacokinetics between the strains used in our study and those used previously.

liver and kidneys of rats following SCI, with and without licofelone treatment. However, as there is no difference from control drug plasma levels in the injured, riluzole-alone group, it seems unlikely that the effect observed in the licofelone group would be due to licofelone's modulatory effect on transporter-mediated excretion of riluzole. Perhaps instead, licofelone enhances drug metabolism in the liver, possibly through a CYP-mediated mechanism. Alternatively, it is possible that the high dose of licofelone (100 mg/kg) used in this study induces an up-regulation in liver enzymes underlying this observation. Whatever the mechanism, a reduction in plasma drug levels is an unexpected result of licofelone therapy that is counterproductive to the goal of this study—to enhance therapeutic delivery of drugs such as riluzole while achieving efficacy with lower doses. Hence, this is a very important question that will be addressed in future investigations in our laboratory.

Licofelone as a Neuroprotective Agent

We have shown that treatment with licofelone, beginning at 3 hours post-injury and continued for two weeks, is sufficient to improve functional outcome following SCI. This conclusion is based on the improvement in BBB scores that we observed in rats treated with either licofelone alone, or both licofelone and riluzole, versus rats treated with vehicle alone (**Fig. 5.1** & **TABLE 5.1**). We are confident that the improvement in BBB scores we have observed with licofelone treatment (3.0-point improvement in both licofelone-treated groups versus vehicle-treated group) is robust and meaningful, because of the conservative statistical analytic methods used to interpret the effects of treatment, as well as the functional significance corresponding to the observed behavioral improvements.

Dr. Stephen W. Scheff, a researcher at the University of Kentucky, has presented an argument for the use of appropriate statistics in analysis of BBB data, suggesting that parametric statistical analysis may often be appropriate (349). However, rather than promoting one specific analytical method over another, Scheff emphasizes that a cautious interpretation of BBB data, using a statistical comparison best suited to the distribution of data, as well as judicious choice of post hoc analysis, is crucial. After all, most studies utilizing an outcome of BBB locomotor scores are chiefly interested in assessing the efficacy of potential SCI treatments, and because of the researcher's vested interest in identifying effective therapies, it is best to take a more cautious approach to data analysis. Scheff concludes his argument by

emphasizing that "investigators [should] choose to be more conservative in their choice of post hoc statistics in order that only those difference that are strongly revealed can be identified as appropriate avenues for further investigation in SCI experiments."

We have therefore taken a conservative approach to statistical analysis of BBB data in this study and utilized the Kruskal-Wallis test for single time point comparisons of nonparametric data, followed by a Dunn's post test to determine significant effects of treatment at each individual time point. We feel that a nonparametric analysis is generally more appropriate for cautious interpretation of BBB data. This is chiefly because the BBB locomotor rating scale is comprised of ordered (ranked) data, with no numerical values between individual scores, and with the improvement between points on the scale not being numerically equal (*e.g.*, the functional difference between a 0 and a 2 is unequal to the functional difference between a 17 and a 19). Importantly, our BBB data was not normally distributed in this study, making the choice of a nonparametric statistical test appropriate in this case.

It is important to remark on the significance of the extent of hindlimb functional improvement we have observed in licofelone-treated animals. At the end of this study, vehicle-treated SCI rats exhibited an average BBB score of 9.1 ± 0.5 (mean ± s.e.m.). The distribution of individual animals' scores on DPI 42 is displayed in **Figure 6.2**. Vehicle-treated rats were scored between 7 (n = 2) and 11 (n = 1), with the most frequent score being 10 (n = 3) on DPI 42. A BBB score of 10 is characterized by occasional (≤50% of the time) weight supported plantar stepping, with no forelimb (FL)-hindlimb (HL) coordination (See **APPENDIX B**). These scores are consistent with those of previous studies. Other groups have reported similar time courses of locomotor recovery in vehicle-treated rats following the same moderate spinal contusion injury paradigm (parameters = 150 kdynes, 1 s dwell) (See **Fig. 5.1**) (350, 351). Of the vehicle-treated group, 4 of 8 exhibited any plantar stepping, and only one exhibited frequent (50-94% of the time) stepping[10]. Additionally, only one rat from this group showed any FL-HL coordination.

[10] There were originally nine rats in the SCI + vehicle group, but one of the rats died between DPI 35 and -42, thus only eight animals were assessed on DPI 42. Similarly, one of the riluzole-treated rats died between DPI 35 and -42, thus DPI 42 scores reflect six animals in the riluzole group.

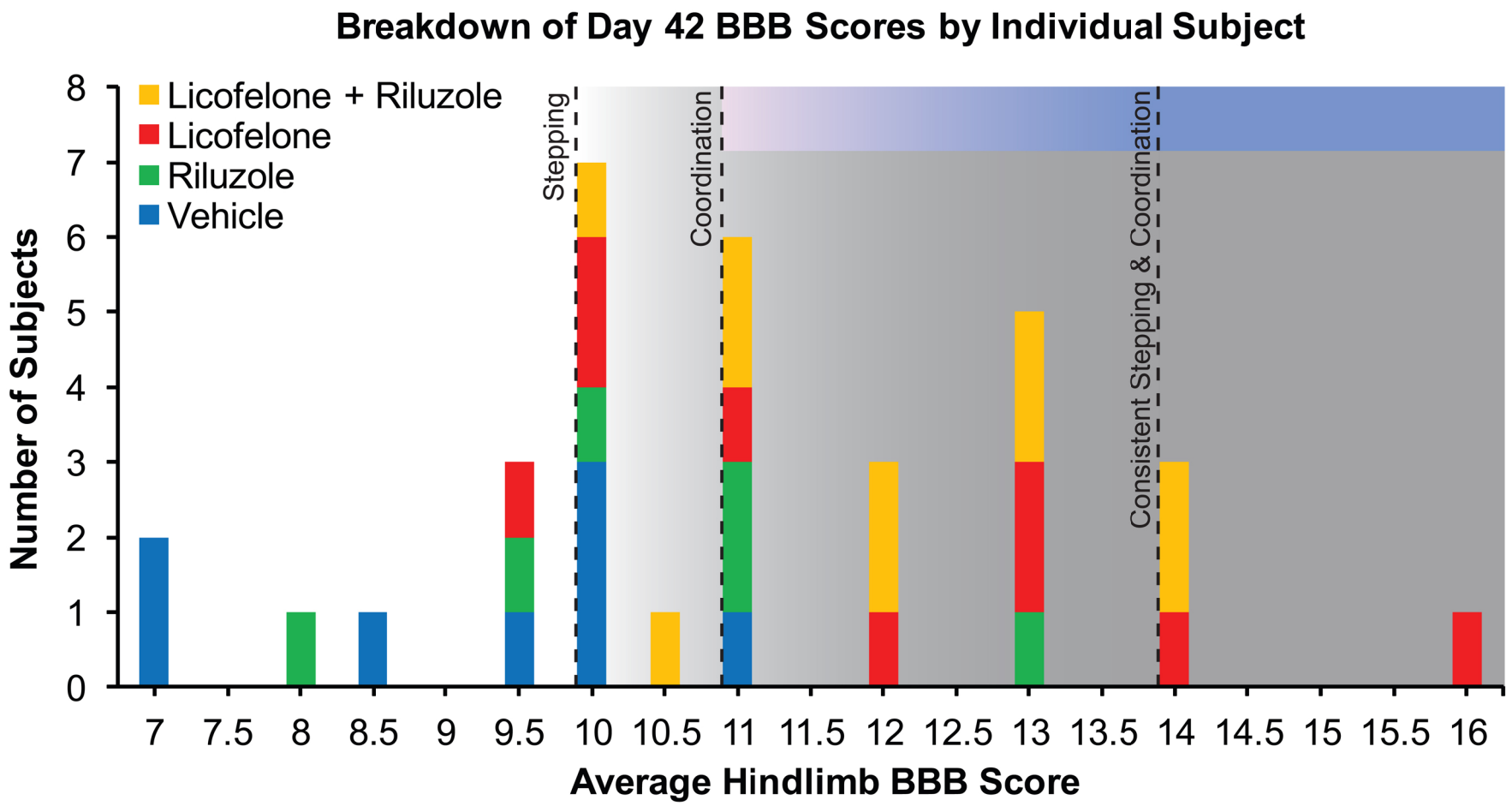
Breakdown of Day 42 BBB Scores by Individual Subject
Licofelone + Riluzole
Licofelone
Riluzole
Vehicle
Stepping
Coordination
Consistent Stepping & Coordination
Number of Subjects
0
1
2
3
4
5
6
7
8
7
7.5
8
8.5
9
9.5
10
10.5
11
11.5
12
12.5
13
13.5
14
14.5
15
15.5
16
Average Hindlimb BBB Score

(On previous page)

Figure 6.2. Distribution of individual BBB scores on post-injury day 42. Data is presented as the number of animals in each treatment group receiving each score on day 42 post-injury. BBB scores represent an average rating for both hindlimbs of one subject. BBB scores associated with plantar stepping are contained within the gray shaded area; gradient shading indicates stepping frequency, with consistent plantar stepping beginning at 14. Blue shaded area illustrates the range of BBB scores associated with forelimb-hindlimb coordination; gradient shading indicates frequency of coordination, with consistent coordination beginning at 14.

Average BBB scores of riluzole-treated animals were slightly higher, and ranged between 8 (n = 1) and 13 (n = 1). The most frequently observed DPI 42 score for this group was 11 (n = 2), which corresponds to frequent (50-94%) to consistent (95-100% of the time) weight supported plantar stepping without coordination. Only one out of seven riluzole-treated rats achieved frequent coordination. The time course of locomotor recovery observed in our riluzole group is remarkably similar to that reported by Mu *et al.* (81), who treated with riluzole at 2 and 4 hours after injury, then once daily for one week; at 42 DPI, the authors reported an average BBB score of about 12 for their riluzole-treated animals.

In contrast, rats treated with both licofelone and riluzole had noticeably higher DPI 42 BBB scores, ranging from 10 (n = 1) to 14 (n = 2); rats treated with licofelone alone exhibited a greater range of locomotor function, ranging from 9.5 (n = 1) to 16 (n = 1). Importantly, 89% (8 of 9) of the licofelone group, and 100% (10 of 10) of the licofelone + riluzole group exhibited plantar stepping. This is a clear functional advantage compared to 50% of the vehicle group, and 67% of the riluzole group, that displayed plantar stepping. Also notable is the proportion of animals per group that exhibited coordination (12.5% of vehicle, 50% of riluzole, 67% of licofelone, 80% of licofelone + riluzole). The only animals to exhibit both consistent stepping and consistent coordination in this study were animals that received licofelone. Furthermore, both licofelone-treated groups exhibited significantly improved BBB scores beginning at DPI 14 (**Fig. 5.1** & **TABLE 5.1**), and sustained throughout the end of the study. Because of these observations, we assert that licofelone treatment, both alone and in conjunction with riluzole, confers significant neuroprotection that is sustained well after discontinuation of treatment.

The vast majority of the animals at the end of this study fell within one of two categories: 1) the period which Basso *et al.* termed the "intermediate recovery phase" (BBB score between 8 and 12), defined as the period of functional recovery following SCI in which rats have established plantar placement of the hindpaws and display various levels of coordinated FL-HL movement; or 2) the "late recovery phase" (BBB score between 13 and 21), in which finer aspects of locomotor function, such as toe clearance, limited paw rotation during swing, and improved balance, are regained (280) (**TABLE 6.1**). Only two rats, both of which were in the vehicle-treated group, remained in the "early recovery phase", scoring below 8 on DPI 42.

Treatment Group	Early Recovery Phase (*n*)	Intermediate Recovery Phase (*n*)	Late Recovery Phase (*n*)
Vehicle	25% (*2*)	75% (*6*)	-
Riluzole	-	83% (*5*)	17% (*1*)
Licofelone	-	56% (*5*)	44% (*4*)
Licofelone + Riluzole	-	60% (*6*)	40% (*4*)

TABLE 6.1. Percentage of animals in each phase of recovery on DPI 42, by treatment group. Phases of recovery following SCI are defined in: A Sensitive and Reliable Locomotor Rating Scale for Open Field Testing in Rats, D. Michele Basso, Michael S. Beattie, Jacqueline C. Bresnahan, Journal of Neurotrauma. February 1995: 1-21. (280)

Stepping and coordination are very important aspects of locomotor functional recovery in rat models of SCI. The region of the BBB scale pertaining to differences in stepping and coordination frequency is associated with functionally important milestones in the overall recovery of locomotor ability. For example, the three-point separation between a BBB score of 9 (plantar placement with weight support in stance only or dorsal stepping, with no plantar stepping) and 12 (frequent to consistent plantar stepping and occasional FL-HL coordination) corresponds to a much more functionally significant improvement than, say, the difference between a score of 1 (slight movement of one or two joints) and 4 (slight movement of all three joints) (**APPENDIX B**). An animal with a BBB score of 9 can support its body weight, and, at best, may exhibit bouts of disjointed, uncoordinated dorsal stepping. In contrast, an animal with a BBB score of 12 possesses a higher degree of motor control, and shows substantially improved regulation of muscles and joints involved in the normal biomechanics of coordinated stepping. Thus, the improvements in BBB scores conferred by licofelone treatment at the end of this study are not only statistically significant, but moreover, are associated with physiologically important functional gains that dramatically enhance overall locomotor ability. Moreover, though we have limited our assessment to a 6-week period following injury, recovery of function in licofelone-treated animals did not appear to plateau by 6 weeks post-

SCI. Thus, it is possible that the improvement in locomotor recovery conferred by licofelone treatment could continue beyond this time point, leading to an even better functional outcome.

In the current study, we have also utilized the photobeam activity system to evaluate additional measures of locomotor function and overall activity at multiple time points after injury. Among the parameters assessed by the PAS were distance and speed of locomotion, time spent resting, fine and ambulatory movement, and rearing. Rearing is thought to be a particularly useful indicator of clinically relevant physiological functions, like postural control, that are important for upright walking in human patients (322). Other readouts of the PAS (*e.g.*, extent of ambulatory movement, total distance, speed, and rest time) reflect the ease with which an animal can freely move about. For example, increased distance and speed of movement during the testing period might be observed in an animal with better control of stepping and coordination compared to an animal with a lower level of locomotor control; the latter animal might expend more energy dragging its hindlimbs or compensating for uncoordinated, inefficient stepping, and spend more time resting to recover. However, factors such as increased time spent resting without any movement may also be attributed to various factors such as pain state (321), so activity data must be interpreted judiciously.

Though we analyzed multiple different aspects of overall activity in this study, we only detected two statistically significant effects of treatment on activity parameters. First, we observed that the licofelone-treated group spent significantly less time at rest than the vehicle-treated group on DPI 42 (SCI + vehicle = 154 ± 22.6 s; SCI + licofelone = 51 ± 11.9 s, $p < 0.05$) during the 20-minute testing period (**Fig. 5.4**). Though this effect was only significant on DPI 42, the total resting time of the licofelone group was consistently lowest and closest to that of uninjured controls compared to all other treatment groups from DPI 14 to -42. This observation may indicate that licofelone treatment enhances the ability to locomote, or the ease of locomotion, in rats recovering from SCI. Secondly, we observed that rats treated with both licofelone and riluzole exhibited significantly more rearing during the testing period than did injured, vehicle-treated rats (SCI + vehicle = 2.6 ± 1.5; SCI + licofelone = 6.4 ± 1.5, $p < 0.05$) (**Fig. 5.6a**). This may be indicative of improved muscle control in the trunk in rats treated with licofelone and riluzole, contributing to an enhanced ability to rear up on hindlimbs, a functional measure that may correlate to postural control in human SCI patients. Other than these two results, our PAS data did not reveal any statistically significant effects of treatment.

Notably, we have failed to detect any significant improvements in locomotor function in riluzole-treated animals during this study. These results are consistent with previous findings, which did not detect any improvement in behavior in animals treated with riluzole beginning at 2 hours post-SCI and continued for one week (81). In fact, the only studies reporting positive effects of riluzole treatment on functional outcome have utilized a treatment window of 15-30 minutes post-SCI (77, 78, 82). Taken together, these results suggest that riluzole may exert therapeutic efficacy for SCI only if administered very early after injury. If this is the case, the lack of therapeutic efficacy at later treatment windows may be due to enhanced efflux transport, as we have reported in this study (See *Chapters 3 & 4*). However, it is also plausible that the dose of riluzole used in this study is simply inefficient to confer enough neuroprotection to translate into significant functional improvement. Despite the ability of licofelone to enhance blood-to-spinal cord delivery of riluzole (**Fig. 4.14**), we have detected no significant difference between locomotor scores of licofelone-treated and licofelone-and-riluzole-treated groups in this study. Thus, more systematic studies are needed to optimize factors such as dose and treatment schedule, in order to more thoroughly assess the therapeutic potential of combined treatment with licofelone and riluzole for acute SCI.

Several studies have reported neuroprotective efficacy of NSAIDs, when administered prior to experimental SCI (119, 123-128), at the time of injury (129-132, 135), or after a short delay period (*e.g.*, 15 min post-SCI) (121). Unfortunately, there are very few published reports of improved behavioral outcome following a clinically relevant treatment window with COX inhibitors. Two recent studies have reported beneficial effects of delayed, sustained ibuprofen treatment for improving functional recovery in rats after SCI. Fu *et al.* (136) reported a ~2.0-point increase in BBB scores, along with improved performance in other locomotor assessments, in rats treated with 60 mg/kg/d ibuprofen (osmotic pump) beginning at 7 days after spinal contusion injury and continuing for one month (SCI + vehicle ≈ 13.5, SCI + ibuprofen ≈ 15.5). Similarly, Wang and colleagues (352) reported increased BBB scores (SCI + vehicle ≈ 7.7, SCI + ibuprofen ≈ 9.4) in rats treated with 70 mg/kg/d ibuprofen (osmotic pump) beginning at 3 days post-SCI and continuing for one month. That both of these studies have reported statistically significant gains in locomotor function following a days-long delay in treatment with ibuprofen, is exciting. These findings suggest that a delayed window of efficacy may exist when targeting the pro-inflammatory COX arm of the secondary injury cascade following SCI. However, neither of these studies evaluated gastric mucosal erosion following

the extended course of ibuprofen treatment, despite the known deleterious GI side effects of long-term NSAID use. Because of the improved GI tolerance of licofelone (320), as well as the evidence showing that antagonism of 5-LOX signaling supports functional improvement in preclinical SCI studies (142, 144, 145), it would therefore be interesting to evaluate whether simultaneous COX/5-LOX inhibition would exhibit neuroprotective efficacy following delayed treatment similar to that used in the aforementioned ibuprofen studies.

Ultimately, it is difficult to compare our results to these two reports, as there are considerable differences in experimental design, type and severity of injury, and time course of treatment. However, the three-point improvement in BBB scores that we have observed with licofelone is a robust and significant finding that has never before been shown in experimental studies of anti-inflammatory therapies. We have used a clinically relevant SCI model, a spinal contusion/compression injury that approximates the type of human SCI most often observed in the clinic (4). Furthermore, we have demonstrated significant and sustained functional recovery following a clinically relevant delay in treatment (3 hours post-SCI) via the clinically relevant oral route with licofelone, a drug that has successfully passed Phase III clinical trials and is safe in humans. For these reasons, we conclude that licofelone exhibits high translational potential as a treatment to improve functional recovery following SCI.

The central question of how licofelone works within the spinal cord to supply this neuroprotective efficacy will be among the most important future areas of investigation. We have not yet examined histological outcome measures—such as lesion size, neuronal and glial cell counts, white matter tract sparing, extent of myelination, or BSCB structural alterations—in the rats utilized for the current study. All of these parameters are important contributors to neurological outcome following SCI, and assessing them will be critical for developing a mechanistic model of how licofelone might confer enhanced functional outcome. Though licofelone has not been studied in published reports of neurological trauma, some insight as to the molecular basis for its neuroprotective properties might be gained from studies of rodent models of Huntington's disease (162, 163). In these preclinical studies, licofelone treatment enhanced oxidative defenses and reduced levels of anti-inflammatory compounds in the brain, a finding similar to what we have observed in chronic SCI (**Fig. 4.10** & **TABLE 4.2**). The authors also observed reduction in the size of chemically-induced striatal lesions with licofelone treatment, which corresponded to enhanced functional outcome. It is possible that the anti-

inflammatory and anti-oxidative properties of this drug may exhibit a similar effect on the spinal cord lesion site in our model. Further studies are needed to evaluate this possibility and better characterize the biochemical and cellular changes within the injured spinal cord that result from licofelone treatment.

§

Overall Translational Significance of this Study

I. P-glycoprotein overexpression causes spinal cord drug resistance following SCI

There is currently no proven effective treatment for SCI, so the vast majority of SCI patients face a lifetime of paralysis, intractable pain, and other complications (263). We have identified an important pathophysiological mechanism arising early after SCI that imparts the spinal cord with resistance to a wide variety of drugs, thus establishing a major, previously unknown barrier to effective therapeutic intervention for SCI. This finding holds important implications not only for the acute delivery of neuroprotective drugs immediately after SCI, but also for the long-term clinical management of pain and muscle spasticity in chronic SCI patients. We propose that overcoming Pgp-mediated drug resistance, thereby enhancing spinal cord bioavailability of systemically-administered neuroprotective drugs after SCI, will provide a significant therapeutic advantage to patients who otherwise have very little hope for functional recovery.

The neuroprotective drug riluzole is currently being evaluated in a Phase I clinical trial as an intervention for SCI, with daily delivery for 14 days subsequent to injury (87). Our observations of increased Pgp expression and diminished spinal cord riluzole bioavailability during the acute phase of SCI strongly support the existence of Pgp-mediated drug resistance in the injured spinal cord. Importantly, we have shown that licofelone treatment can enhance blood-to-spinal cord delivery of riluzole during acute SCI. We anticipate that this finding has potential to develop into a new combinatorial treatment strategy to attenuate the expression of

post-SCI drug resistance and improve therapeutic efficacy for riluzole, as well as a variety of other neuroprotective drugs.

Based on the data obtained in this study, we propose a working model (**Fig. 6.3**) in which Pgp expression at the BSCB is up-regulated following traumatic SCI, resulting in a reduction in spinal cord bioavailability of systemically-delivered drugs that are Pgp substrates. Because of previously established mechanisms of Pgp up-regulation in other neurological disease models, we hypothesize that this process is driven by pro-inflammatory COX signaling. We have shown that acute treatment with the dual COX/5-LOX inhibitor licofelone is sufficient to both attenuate Pgp overexpression and enhance blood-to-spinal cord delivery of riluzole during the acute phase of SCI.

Importantly, this work has defined a new combinatorial mechanism with applications to human disease beyond SCI research. Pgp overexpression is a recognized obstacle to effective treatment of neurological diseases such as ALS (224) and epilepsy (222), as well as multiple types of cancer (353). The ability to target the molecular signaling pathways driving Pgp up-regulation with licofelone is therefore a highly useful strategy with potential to impact any pathological condition in which Pgp activity reduces efficacy of drug treatment.

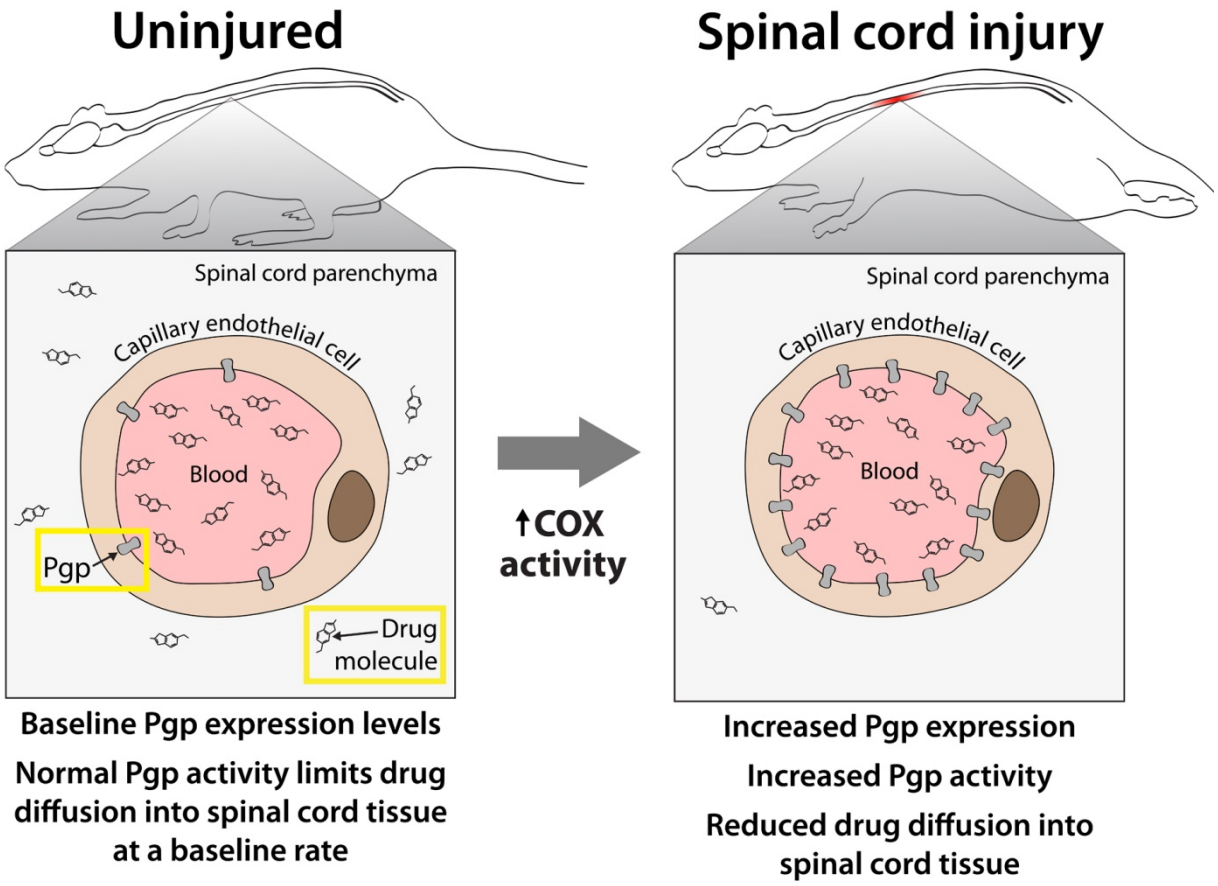

Figure 6.3. Working model of P-glycoprotein-mediated drug resistance in the injured spinal cord. (**a**) Under normal conditions, Pgp is expressed on the luminal surface of endothelial cells lining blood vessels at the BSCB. Blood-borne drug molecules must diffuse through the endothelial cell in order to enter spinal cord tissue. However, the drug efflux transport activity of Pgp pumps drugs back into the bloodstream at a discrete rate, thus limiting spinal cord drug concentrations. (**b**) Following SCI, pro-inflammatory COX signaling within the damaged spinal cord tissue drives Pgp overexpression at the BSCB. This increased Pgp expression and drug transport activity results in diminished drug delivery to the spinal cord. Treating rats with the dual COX/5-LOX inhibitor licofelone after SCI attenuates spinal cord Pgp overexpression, thus enhancing spinal cord drug delivery and efficacy of treatment.

II. Licofelone treatment promotes significant neurological recovery following SCI

Inflammation is a major factor involved in shaping outcome during the early, acute phase of traumatic SCI, and there is much evidence that pro-inflammatory COX and 5-LOX activity are key among the adverse pathological processes negatively affecting functional outcome following SCI. Antagonizing the COX-2 (119) or 5-LOX (142, 144) pathways independently has led to modest reductions in the pathological and behavioral deficits following SCI. However, the therapeutic potential of combined COX and 5-LOX inhibition to improve functional outcome following SCI has not previously been assessed.

We have shown that, in a clinically relevant model of spinal contusion/compression injury, oral licofelone treatment significantly and robustly improves hindlimb locomotor function in rats, starting from two weeks after injury. Furthermore, we have demonstrated that this functional improvement is sustained following cessation of treatment, for up to four weeks. We have utilized a clinically relevant delayed treatment window (beginning at 3 hours after injury), thus our findings display high translational potential for movement to clinical trials.

Furthermore, our findings indicate that licofelone is more effective as a neuroprotective intervention for acute SCI than riluzole, a drug which is currently undergoing clinical trials as a promising SCI intervention. Thus, licofelone holds great promise as a stand-alone therapeutic intervention to improve functional recovery following SCI.

APPENDIX A

ASIA Impairment Scale

&

Autonomic Assessment Form

Patient Name _____

Examiner Name _____ Date/Time of Exam_____

INTERNATIONAL STANDARDS FOR NEUROLOGICAL CLASSIFICATION OF SPINAL CORD INJURY

ISCOS

AMERICAN SPINAL INJURY ASSOCIATION

MOTOR

KEY MUSCLES (scoring on reverse side)

	R	L	
C5	☐	☐	Elbow flexors
C6	☐	☐	Wrist extensors
C7	☐	☐	Elbow extensors
C8	☐	☐	Finger flexors (distal phalanx of middle finger)
T1	☐	☐	Finger abductors (little finger)

UPPER LIMB TOTAL (MAXIMUM) ☐ + ☐ = ☐ (25) (25) (50)

Comments:

L2	☐	☐	Hip flexors
L3	☐	☐	Knee extensors
L4	☐	☐	Ankle dorsiflexors
L5	☐	☐	Long toe extensors
S1	☐	☐	Ankle plantar flexors

(VAC) Voluntary anal contraction (Yes/No) ☐

LOWER LIMB TOTAL (MAXIMUM) ☐ + ☐ = ☐ (25) (25) (50)

	LIGHT TOUCH R	LIGHT TOUCH L	PIN PRICK R	PIN PRICK L
C2				
C3				
C4				
C5				
C6				
C7				
C8				
T1				
T2				
T3				
T4				
T5				
T6				
T7				
T8				
T9				
T10				
T11				
T12				
L1				
L2				
L3				
L4				
L5				
S1				
S2				
S3				
S4-5				
TOTALS (MAXIMUM)	☐ (56)	☐ (56)	☐ + ☐ = ☐ (56)	(56)

SENSORY

KEY SENSORY POINTS

0 = absent
1 = altered
2 = normal
NT = not testable

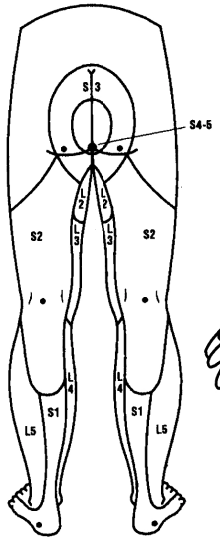

(DAP) Deep anal pressure (yes/No) ☐

PIN PRICK SCORE (max: 112) ☐ + ☐ = ☐

LIGHT TOUCH SCORE (max: 112) ☐ = ☐

• Key Sensory Points

NEUROLOGICAL LEVEL *The most caudal segment with normal function*	*SENSORY* / *MOTOR*	R ☐ ☐ / L ☐ ☐	**SINGLE NEUROLOGICAL LEVEL** ☐	**COMPLETE OR INCOMPLETE?** ☐ *Incomplete = Any sensory or motor function in S4-S5*	**ASIA IMPAIRMENT SCALE (AIS)** ☐	*(In complete injuries only)* **ZONE OF PARTIAL PRESERVATION** *Most caudal level with any innervation*	*SENSORY* / *MOTOR* R ☐ ☐ L ☐ ☐

REV 04/11

Muscle Function Grading

0 = total paralysis

1 = palpable or visible contraction

2 = active movement, full range of motion (ROM) with gravity eliminated

3 = active movement, full ROM against gravity

4 = active movement, full ROM against gravity and moderate resistance in a muscle specific position.

5 = (normal) active movement, full ROM against gravity and full resistance in a muscle specific position expected from an otherwise unimpaired peson.

5* = (normal) active movement, full ROM against gravity and sufficient resistance to be considered normal if identified inhibiting factors (i.e. pain, disuse) were not present.

NT = not testable (i.e. due to immobilization, severe pain such that the patient cannot be graded, amputation of limb, or contracture of >50% of the range of motion).

ASIA Impairment (AIS) Scale

☐ **A = Complete.** No sensory or motor function is preserved in the sacral segments S4-S5.

☐ **B = Sensory Incomplete.** Sensory but not motor function is preserved below the neurological level and includes the sacral segments S4-S5 (light touch, pin prick at S4-S5: or deep anal pressure (DAP)), AND no motor function is preserved more than three levels below the motor level on either side of the body.

☐ **C = Motor Incomplete.** Motor function is preserved below the neurological level**, and more than half of key muscle functions below the single neurological level of injury (NLI) have a muscle grade less than 3 (Grades 0-2).

☐ **D = Motor Incomplete.** Motor function is preserved below the neurological level**, and at least half (half or more) of key muscle functions below the NLI have a muscle grade ≥ 3.

☐ **E = Normal.** If sensation and motor function as tested with the ISNCSCI are graded as normal in all segments, and the patient had prior deficits, then the AIS grade is E. Someone without an initial SCI does not receive an AIS grade.

**For an individual to receive a grade of C or D, i.e. motor incomplete status, they must have either (1) voluntary anal sphincter contraction or (2) sacral sensory sparing with sparing of motor function more than three levels below the motor level for that side of the body. The Standards at this time allows even non-key muscle function more than 3 levels below the motor level to be used in determining motor incomplete status (AIS B versus C).

NOTE: When assessing the extent of motor sparing below the level for distinguishing between AIS B and C, the ***motor level*** on each side is used; whereas to differentiate between AIS C and D (based on proportion of key muscle functions with strength grade 3 or greater) the ***single neurological level*** is used.

Steps in Classification

The following order is recommended in determining the classification of individuals with SCI.

1. Determine sensory levels for right and left sides.
2. Determine motor levels for right and left sides.
   Note: in regions where there is no myotome to test, the motor level is presumed to be the same as the sensory level, if testable motor function above that level is also normal.
3. Determine the single neurological level.
   This is the lowest segment where motor and sensory function is normal on both sides, and is the most cephalad of the sensory and motor levels determined in steps 1 and 2.
4. Determine whether the injury is Complete or Incomplete. (i.e. absence or presence of sacral sparing)
   If voluntary anal contraction = **No** *AND all S4-5 sensory scores =* **0** *AND deep anal pressure =* **No,** *then injury is COMPLETE. Otherwise, injury is incomplete.*
5. Determine ASIA Impairment Scale (AIS) Grade:

Is injury Complete? If **YES,** AIS=A and can record ZPP (lowest dermatome or myotome on each side with some preservation)

NO ↓

Is injury motor Incomplete? If **NO**, AIS=B (Yes=voluntary anal contraction OR motor function more than three levels below the motor level on a given side, if the patient has sensory incomplete classification)

YES ↓

Are at least half of the key muscles below the single neurological level graded 3 or better?

NO ↓ AIS=C

YES ↓ AIS=D

If sensation and motor function is normal in all segments, AIS=E

Note: AIS E is used in follow-up testing when an individual with a documented SCI has recovered normal function. If at initial testing no deficits are found, the individual is neurologically intact; the ASIA Impairment Scale does not apply.

AUTONOMIC STANDARDS ASSESSMENT FORM

Patient Name: _____

Anatomic Diagnosis: (Supraconal □, Conal □, Cauda Equina □)

General Autonomic Function

System/Organ	*Findings*	*Abnormal conditions*	*Check mark*
Autonomic control of the heart	Normal		
	Abnormal	Bradycardia	
		Tachycardia	
		Other dysrhythmias	
	Unknown		
	Unable to assess		
Autonomic control of blood pressure	Normal		
	Abnormal	Resting systolic blood pressure below 90 mmHg	
		Orthostatic hypotension	
		Autonomic dysreflexia	
	Unknown		
	Unable to assess		
Autonomic control of sweating	Normal		
	Abnormal	Hyperhydrosis above lesion	
		Hyperhydrosis below lesion	
		Hypohydrosis below lesion	
	Unknown		
	Unable to assess		
Temperature regulation	Normal		
	Abnormal	Hyperthermia	
		Hypothermia	
	Unknown		
	Unable to assess		
Autonomic and Somatic Control of Broncho-pulmonary System	Normal		
	Abnormal	Unable to voluntarily breathe requiring full ventilatory support	
		Impaired voluntary breathing requiring partial vent support	
		Voluntary respiration impaired does not require vent support	
	Unknown		

Lower Urinary Tract, Bowel and Sexual Function

System/Organ		*Score*
Lower Urinary Tract		
Awareness of the need to empty the bladder		
Ability to prevent leakage (continence)		
Bladder emptying method _____ (specify)		
Bowel		
Sensation of need for a bowel movement		
Ability to Prevent Stool Leakage (Continence)		
Voluntary sphincter contraction		
Sexual Function		
Genital arousal (erection or lubrication)	Psychogenic	
	Reflex	
Orgasm		
Ejaculation (male only)		
Sensation of Menses (female only)		

2 = Normal function, 1=Reduced or Altered Neurological Function
0=Complete loss of control NT=Unable to assess due to preexisting or concomitant problems

Urodynamic Evaluation

System/Organ	*Findings*	*Check mark*
Sensation during filling	Normal	
	Increased	
	Reduced	
	Absent	
	Non-specific	
Detrusor Activity	Normal	
	Overactive	
	Underactive	
	Acontractile	
Sphincter	Normal urethral closure mechanism	
	Normal urethral function during voiding	
	Incompetent	
	Detrusor sphincter dyssynergia	
	Non-relaxing sphincter	

Date of Injury_____ Date of Assessment_____ Examiner_____

This assessment should use the terminology found in the International SCI Data Set
(ASIA and ISCoS - http://www.asia-spinalinjury.org/bulletinBoard/dataset.php)

APPENDIX B

Basso, Beattie, and Bresnahan Open Field Locomotor Scale

&

Definition of Terms Used in the BBB Scale

0 No observable hind limb (HL) movement

1 Slight movement of one or two joints, usually the hip and/or knee

2 Extensive movement of one joint or extensive movement of one joint and slight movement of one other joint

3 Extensive movement of two joints

4 Slight movement of all three joints of the HL

5 Slight movement of two joints and extensive movement of the third

6 Extensive movement of two joints and slight movement of the third

7 Extensive movement of all three joints of the HL

8 Sweeping with no weight support or plantar placement of the paw with no weight support

9 Plantar placement of the paw with weight support in stance only (*i.e.*, when stationary) or occasional, frequent, or consistent weight supported dorsal stepping and no plantar stepping

10 Occasional weight supported plantar steps, no forelimb (FL)-HL coordination

11 Frequent to consistent weight supported plantar steps and no FL-HL coordination

12 Frequent to consistent weight supported plantar steps and occasional FL-HL coordination

13 Frequent to consistent weight supported plantar steps and frequent FL-HL coordination

14 Consistent weight supported plantar steps, consistent FL-HL coordination; and predominant paw position during locomotion is rotated (internally or externally) when it makes initial contact with the surface as well as just before it is lifted off at the end of stance or frequent plantar stepping, consistent FL-HL coordination, and occasional dorsal stepping

15 Consistent plantar stepping and consistent FL-HL coordination; and no toe clearance or occasional toe clearance during forward limb advancement; predominant paw position is parallel to the body at initial contact

16 Consistent plantar stepping and consistent FL-HL coordination during gait; and toe clearance occurs frequently during forward limb advancement; predominant paw position is parallel at initial contact and rotated at lift off

17 Consistent plantar stepping and consistent FL-HL coordination during gait; and toe clearance occurs frequently during forward limb advancement; predominant paw position is parallel at initial contact and lift off

18 Consistent plantar stepping and consistent FL-HL coordination during gait; and toe clearance occurs consistently during forward limb advancement; predominant paw position is parallel at initial contact and rotated at lift off

19 Consistent plantar stepping and consistent FL-HL coordination during gait; and toe clearance occurs consistently during forward limb advancement; predominant paw position is parallel at initial contact and lift off; and tail is down part or all of the time

20 Consistent plantar stepping and consistent coordinated gait; consistent toe clearance; predominant paw position is parallel at initial contact and lift off; tail consistently up; and trunk instability

21 Consistent plantar stepping and coordinated gait, consistent toe clearance, predominant paw position is parallel throughout stance, consistent trunk stability, tail consistently up

DEFINITIONS OF TERMS USED IN THE BBB LOCOMOTOR RATING SCALE

Slight: Partial joint movement through less than half the range of joint motion

Extensive: Movement through more than half of the range of motion

Sweeping: Rhythmic movement of HL in which all three joints are extended, then fully flex and extend again; animal is usually sidelying, the plantar surface of paw may or may not contact the ground; no weight support across the HL is evident

No Weight Support: No contraction of the extensor muscles of the HL during plantar placement of the paw; or no elevation of the hindquarter

Weight Support: Contraction of the extensor muscles of the HL during plantar placement of the paw, or elevation of the hindquarter

Plantar Stepping: The paw is in *plantar* contact with weight support then the HL is advanced forward and *plantar* contact with weight support is reestablished

Dorsal Stepping: Weight is supported through the dorsal surface of the paw at some point in the step cycle

FL-HL Coordination: For every FL step an HL step is taken and the HLs alternate

Occasional: Less than or equal to half; ≤50%

Frequent: More than half but not always; 51-94%

Consistent: Nearly always or always; 95-100%

Trunk Instability: Lateral weight shifts that cause waddling from side to side or a partial collapse of the trunk

Bibliography

1. Christopher & Dana Reeve Foundation Paralysis Resource Center. One Degree of Separation: Paralysis and Spinal Cord Injury in the United States. Short Hills, NJ. 2009. Available from: http://www.christopherreeve.org/atf/cf/%7B3d83418f-b967-4c18-8ada-adc2e5355071%7D/8112REPTFINAL.PDF.
2. National Spinal Cord Injury Statistical Center. 2010 Annual Statistical Report. Birmingham, AL: University of Alabama. 2011. Available from: https://www.nscisc.uab.edu/PublicDocuments/reports/pdf/2010%20NSCISC%20Annual%20Statistical%20Report%20-%20Complete%20Public%20Version.pdf.
3. Sekhon, L. H., and M. G. Fehlings. 2001. Epidemiology, demographics, and pathophysiology of acute spinal cord injury. Spine (Phila Pa 1976) 26:S2-12.
4. Norenberg, M. D., J. Smith, and A. Marcillo. 2004. The pathology of human spinal cord injury: defining the problems. J Neurotrauma 21:429-440.
5. Bunge, R. P., W. R. Puckett, J. L. Becerra, A. Marcillo, and R. M. Quencer. 1993. Observations on the pathology of human spinal cord injury. A review and classification of 22 new cases with details from a case of chronic cord compression with extensive focal demyelination. Adv Neurol 59:75-89.
6. Hodgetts, S. I., G. W. Plant, and A. R. Harvey. 2008. Spinal Cord Injury: experimental animal models and relation to human therapy. In The spinal cord: a Christopher and Dana Reeve Foundation text and atlas. C. Watson, G. Paxinos, and G. Kayalioglu, editors. Elsevier/Academic Press. 209-237.
7. Kirshblum, S. C., S. P. Burns, F. Biering-Sorensen, W. Donovan, D. E. Graves, A. Jha, M. Johansen, L. Jones, A. Krassioukov, M. Mulcahey, M. Schmidt-Read, and W. Waring. 2012. International standards for neurological classification of spinal cord injury (Revised 2011). J Spinal Cord Med 34:535-546.
8. Coleman, W. P., and F. H. Geisler. 2004. Injury severity as primary predictor of outcome in acute spinal cord injury: retrospective results from a large multicenter clinical trial. Spine J 4:373-378.

9. Geisler, F. H., W. P. Coleman, G. Grieco, and D. Poonian. 2001. Measurements and recovery patterns in a multicenter study of acute spinal cord injury. Spine (Phila Pa 1976) 26:S68-86.
10. Ditunno, J. F., Jr., P. L. Ditunno, V. Graziani, G. Scivoletto, M. Bernardi, V. Castellano, M. Marchetti, H. Barbeau, H. L. Frankel, J. M. D'Andrea Greve, H. Y. Ko, R. Marshall, and P. Nance. 2000. Walking index for spinal cord injury (WISCI): an international multicenter validity and reliability study. Spinal Cord 38:234-243.
11. Field-Fote, E. C., G. G. Fluet, S. D. Schafer, E. M. Schneider, R. Smith, P. A. Downey, and C. D. Ruhl. 2001. The Spinal Cord Injury Functional Ambulation Inventory (SCI-FAI). J Rehabil Med 33:177-181.
12. Itzkovich, M., M. Tripolski, G. Zeilig, H. Ring, N. Rosentul, J. Ronen, R. Spasser, R. Gepstein, and A. Catz. 2002. Rasch analysis of the Catz-Itzkovich spinal cord independence measure. Spinal Cord 40:396-407.
13. Mahoney, F. I., and D. W. Barthel. 1965. Functional Evaluation: The Barthel Index. Md State Med J 14:61-65.
14. Kandel, E. R., J. H. Schwartz, and T. M. Jessell. 2000. Principles of neural science. McGraw-Hill, Health Professions Division, New York.
15. Young, W. Spinal Cord Injury Levels & Classification. 2010. Available from: http://www.sci-info-pages.com/levels.html.
16. Ditunno, J. F., J. W. Little, A. Tessler, and A. S. Burns. 2004. Spinal shock revisited: a four-phase model. Spinal Cord 42:383-395.
17. Tator, C. H. 1983. Spine-spinal cord relationships in spinal cord trauma. Clin Neurosurg 30:479-494.
18. Anderson, K. D. 2004. Targeting recovery: priorities of the spinal cord-injured population. J Neurotrauma 21:1371-1383.
19. Bracken, M. B., M. J. Shepard, W. F. Collins, Jr., T. R. Holford, D. S. Baskin, H. M. Eisenberg, E. Flamm, L. Leo-Summers, J. C. Maroon, L. F. Marshall, and et al. 1992. Methylprednisolone or naloxone treatment after acute spinal cord injury: 1-year follow-up data. Results of the second National Acute Spinal Cord Injury Study. J Neurosurg 76:23-31.

20. Weidner, N., A. Ner, N. Salimi, and M. H. Tuszynski. 2001. Spontaneous corticospinal axonal plasticity and functional recovery after adult central nervous system injury. Proc Natl Acad Sci U S A 98:3513-3518.
21. Steward, O., B. Zheng, M. Tessier-Lavigne, M. Hofstadter, K. Sharp, and K. M. Yee. 2008. Regenerative growth of corticospinal tract axons via the ventral column after spinal cord injury in mice. J Neurosci 28:6836-6847.
22. Kwon, B. K., L. H. Sekhon, and M. G. Fehlings. 2010. Emerging repair, regeneration, and translational research advances for spinal cord injury. Spine (Phila Pa 1976) 35:S263-270.
23. Benevento, B. T., and M. L. Sipski. 2002. Neurogenic bladder, neurogenic bowel, and sexual dysfunction in people with spinal cord injury. Phys Ther 82:601-612.
24. Dunn, M. 1977. Social discomfort in the patient with spinal cord injury. Arch Phys Med Rehabil 58:257-260.
25. Berkowitz, M., C. Harvey, C. G. Greene, and S. E. Wilson. 1993. Economic Consequences of Traumatic Spinal Cord Injury. Demos Medical Publishing, LLC, New York.
26. Monga, M., J. Bernie, and M. Rajasekaran. 1999. Male infertility and erectile dysfunction in spinal cord injury: a review. Arch Phys Med Rehabil 80:1331-1339.
27. Sipski, M. L., and A. Arenas. 2006. Female sexual function after spinal cord injury. Prog Brain Res 152:441-447.
28. Polosa, C. 2005. Autonomic dysfunction after spinal cord injury. Elsevier, Boston.
29. Rabchevsky, A. G., and P. H. Kitzman. 2011. Latest approaches for the treatment of spasticity and autonomic dysreflexia in chronic spinal cord injury. Neurotherapeutics 8:274-282.
30. Hulsebosch, C. E., B. C. Hains, E. D. Crown, and S. M. Carlton. 2009. Mechanisms of chronic central neuropathic pain after spinal cord injury. Brain Res Rev 60:202-213.
31. Gris, D., E. F. Hamilton, and L. C. Weaver. 2008. The systemic inflammatory response after spinal cord injury damages lungs and kidneys. Exp Neurol 211:259-270.
32. Hundt, H., J. C. Fleming, J. T. Phillips, A. Lawendy, K. R. Gurr, S. I. Bailey, D. Sanders, R. Bihari, D. Gray, N. Parry, C. S. Bailey, and A. Badhwar. 2011. Assessment of hepatic inflammation after spinal cord injury using intravital microscopy. Injury 42:691-696.

33. Herrera, J. J., R. J. Haywood-Watson, 2nd, and R. J. Grill. 2010. Acute and chronic deficits in the urinary bladder after spinal contusion injury in the adult rat. J Neurotrauma 27:423-431.
34. Dulin, J. N., M. L. Moore, K. W. Gates, J. H. Queen, and R. J. Grill. 2011. Spinal cord injury causes sustained disruption of the blood-testis barrier in the rat. PLoS One 6:e16456.
35. Stein, D. M., J. Menaker, K. McQuillan, C. Handley, B. Aarabi, and T. M. Scalea. 2010. Risk factors for organ dysfunction and failure in patients with acute traumatic cervical spinal cord injury. Neurocrit Care 13:29-39.
36. Delamarter, R. B., J. Sherman, and J. B. Carr. 1995. Pathophysiology of spinal cord injury. Recovery after immediate and delayed decompression. J Bone Joint Surg Am 77:1042-1049.
37. Furlan, J. C., V. Noonan, D. W. Cadotte, and M. G. Fehlings. 2009. Timing of decompressive surgery of spinal cord after traumatic spinal cord injury: an evidence-based examination of pre-clinical and clinical studies. J Neurotrauma 28:1371-1399.
38. Fehlings, M. G., and R. G. Perrin. 2006. The timing of surgical intervention in the treatment of spinal cord injury: a systematic review of recent clinical evidence. Spine (Phila Pa 1976) 31:S28-35; discussion S36.
39. Dillman, D., and A. Brambrink. 2008. Intraoperative Management of Spinal Cord Injury. In Acute Brain and Spinal Cord Injury: Evolving Paradigms and Management. A. Bhardwaj, D. B. Ellegala, and J. R. Kirsch, editors. Informa Healthcare USA, Inc., New York. 357-372.
40. Hurlbert, R. J., and M. G. Hamilton. 2008. Methylprednisolone for acute spinal cord injury: 5-year practice reversal. Can J Neurol Sci 35:41-45.
41. Sayer, F. T., E. Kronvall, and O. G. Nilsson. 2006. Methylprednisolone treatment in acute spinal cord injury: the myth challenged through a structured analysis of published literature. Spine J 6:335-343.
42. Eck, J. C., D. Nachtigall, S. C. Humphreys, and S. D. Hodges. 2006. Questionnaire survey of spine surgeons on the use of methylprednisolone for acute spinal cord injury. Spine (Phila Pa 1976) 31:E250-253.
43. Baptiste, D. C., and M. G. Fehlings. 2007. Update on the treatment of spinal cord injury. Prog Brain Res 161:217-233.

44. Young, W. 2002. Spinal cord contusion models. Prog Brain Res 137:231-255.
45. Gruner, J. A. 1992. A monitored contusion model of spinal cord injury in the rat. J Neurotrauma 9:123-126; discussion 126-128.
46. Constantini, S., and W. Young. 1994. The effects of methylprednisolone and the ganglioside GM1 on acute spinal cord injury in rats. J Neurosurg 80:97-111.
47. Chen, J. 2009. Animal models of acute neurological injuries. Humana Press, Totowa, NJ.
48. Scheff, S. W., A. G. Rabchevsky, I. Fugaccia, J. A. Main, and J. E. Lumpp, Jr. 2003. Experimental modeling of spinal cord injury: characterization of a force-defined injury device. J Neurotrauma 20:179-193.
49. Grill, R. J. 2005. User-defined variables that affect outcome in spinal cord contusion/compression models. Exp Neurol 196:1-5.
50. Nakae, A., K. Nakai, K. Yano, K. Hosokawa, M. Shibata, and T. Mashimo. 2011. The animal model of spinal cord injury as an experimental pain model. J Biomed Biotechnol:939023.
51. Anderson, P. N., J. Fabes, and D. Hunt. 2007. The Role of Inhibitory Molecules in Limiting Axonal Regeneration in the Mammalian Spinal Cord. In Model Organisms in Spinal Cord Regeneration. C. G. Becker, and T. Becker, editors. WILEY-VCH Verlag GmbH & Co. KGaA, Weinheim.
52. Thuret, S., L. D. Moon, and F. H. Gage. 2006. Therapeutic interventions after spinal cord injury. Nat Rev Neurosci 7:628-643.
53. Tetzlaff, W., E. B. Okon, S. Karimi-Abdolrezaee, C. E. Hill, J. S. Sparling, J. R. Plemel, W. T. Plunet, E. C. Tsai, D. Baptiste, L. J. Smithson, M. D. Kawaja, M. G. Fehlings, and B. K. Kwon. 2010. A systematic review of cellular transplantation therapies for spinal cord injury. J Neurotrauma 28:1611-1682.
54. Min, S. H., S. H. Lee, H. Shim, J. S. Park, Y. I. Lee, H. W. Kim, and J. K. Hyun. 2011. Development of complete thoracic spinal cord transection model in rats for delayed transplantation of stem cells. Spine (Phila Pa 1976) 36:E155-163.
55. Gale, K., H. Kerasidis, and J. R. Wrathall. 1985. Spinal cord contusion in the rat: behavioral analysis of functional neurologic impairment. Exp Neurol 88:123-134.
56. Yezierski, R. P. 1996. Pain following spinal cord injury: the clinical problem and experimental studies. Pain 68:185-194.

57. Courtine, G., M. B. Bunge, J. W. Fawcett, R. G. Grossman, J. H. Kaas, R. Lemon, I. Maier, J. Martin, R. J. Nudo, A. Ramon-Cueto, E. M. Rouiller, L. Schnell, T. Wannier, M. E. Schwab, and V. R. Edgerton. 2007. Can experiments in nonhuman primates expedite the translation of treatments for spinal cord injury in humans? Nat Med 13:561-566.

58. Fujiki, M., Z. Zhang, L. Guth, and O. Steward. 1996. Genetic influences on cellular reactions to spinal cord injury: activation of macrophages/microglia and astrocytes is delayed in mice carrying a mutation (WldS) that causes delayed Wallerian degeneration. J Comp Neurol 371:469-484.

59. Guth, L., Z. Zhang, and O. Steward. 1999. The unique histopathological responses of the injured spinal cord. Implications for neuroprotective therapy. Ann N Y Acad Sci 890:366-384.

60. Byrnes, K. R., S. T. Fricke, and A. I. Faden. 2010. Neuropathological differences between rats and mice after spinal cord injury. J Magn Reson Imaging 32:836-846.

61. Tuszynski, M. H., R. Grill, L. L. Jones, H. M. McKay, and A. Blesch. 2002. Spontaneous and augmented growth of axons in the primate spinal cord: effects of local injury and nerve growth factor-secreting cell grafts. J Comp Neurol 449:88-101.

62. Levine, J. M., G. J. Levine, B. F. Porter, K. Topp, and L. J. Noble-Haeusslein. 2011. Naturally occurring disk herniation in dogs: an opportunity for pre-clinical spinal cord injury research. J Neurotrauma 28:675-688.

63. Kuluz, J., A. Samdani, D. Benglis, M. Gonzalez-Brito, J. P. Solano, M. A. Ramirez, A. Luqman, R. De los Santos, D. Hutchinson, M. Nares, K. Padgett, D. He, T. Huang, A. Levi, R. Betz, and D. Dietrich. 2010. Pediatric spinal cord injury in infant piglets: description of a new large animal model and review of the literature. J Spinal Cord Med 33:43-57.

64. Rossignol, S., C. Chau, N. Giroux, E. Brustein, L. Bouyer, J. Marcoux, C. Langlet, D. Barthelemy, J. Provencher, H. Leblond, H. Barbeau, and T. A. Reader. 2002. The cat model of spinal injury. Prog Brain Res 137:151-168.

65. Dumont, R. J., D. O. Okonkwo, S. Verma, R. J. Hurlbert, P. T. Boulos, D. B. Ellegala, and A. S. Dumont. 2001. Acute spinal cord injury, part I: pathophysiologic mechanisms. Clin Neuropharmacol 24:254-264.

66. David, S., and A. Kroner. 2011. Repertoire of microglial and macrophage responses after spinal cord injury. Nat Rev Neurosci 12:388-399.
67. Hagg, T., and M. Oudega. 2006. Degenerative and spontaneous regenerative processes after spinal cord injury. J Neurotrauma 23:264-280.
68. Blight, A. R. 1985. Delayed demyelination and macrophage invasion: a candidate for secondary cell damage in spinal cord injury. Cent Nerv Syst Trauma 2:299-315.
69. Beck, K. D., H. X. Nguyen, M. D. Galvan, D. L. Salazar, T. M. Woodruff, and A. J. Anderson. 2010. Quantitative analysis of cellular inflammation after traumatic spinal cord injury: evidence for a multiphasic inflammatory response in the acute to chronic environment. Brain 133:433-447.
70. Fleming, J. C., M. D. Norenberg, D. A. Ramsay, G. A. Dekaban, A. E. Marcillo, A. D. Saenz, M. Pasquale-Styles, W. D. Dietrich, and L. C. Weaver. 2006. The cellular inflammatory response in human spinal cords after injury. Brain 129:3249-3269.
71. Bramlett, H. M., and W. D. Dietrich. 2007. Progressive damage after brain and spinal cord injury: pathomechanisms and treatment strategies. Prog Brain Res 161:125-141.
72. Sinescu, C., F. Popa, V. T. Grigorean, G. Onose, A. M. Sandu, M. Popescu, G. Burnei, V. Strambu, and C. Popa. 2010. Molecular basis of vascular events following spinal cord injury. J Med Life 3:254-261.
73. Totoiu, M. O., and H. S. Keirstead. 2005. Spinal cord injury is accompanied by chronic progressive demyelination. J Comp Neurol 486:373-383.
74. Guest, J. D., E. D. Hiester, and R. P. Bunge. 2005. Demyelination and Schwann cell responses adjacent to injury epicenter cavities following chronic human spinal cord injury. Exp Neurol 192:384-393.
75. Hill, C. E., M. S. Beattie, and J. C. Bresnahan. 2001. Degeneration and sprouting of identified descending supraspinal axons after contusive spinal cord injury in the rat. Exp Neurol 171:153-169.
76. Patel, C. B., D. M. Cohen, P. Ahobila-Vajjula, L. M. Sundberg, T. Chacko, and P. A. Narayana. 2009. Effect of VEGF treatment on the blood-spinal cord barrier permeability in experimental spinal cord injury: dynamic contrast-enhanced magnetic resonance imaging. J Neurotrauma 26:1005-1016.

77. Kwon, B. K., E. Okon, J. Hillyer, C. Mann, D. Baptiste, L. C. Weaver, M. G. Fehlings, and W. Tetzlaff. 2010. A systematic review of non-invasive pharmacologic neuroprotective treatments for acute spinal cord injury. J Neurotrauma 28:1545-1588.
78. Stutzmann, J. M., J. Pratt, T. Boraud, and C. Gross. 1996. The effect of riluzole on post-traumatic spinal cord injury in the rat. Neuroreport 7:387-392.
79. Springer, J. E., R. D. Azbill, S. E. Kennedy, J. George, and J. W. Geddes. 1997. Rapid calpain I activation and cytoskeletal protein degradation following traumatic spinal cord injury: attenuation with riluzole pretreatment. J Neurochem 69:1592-1600.
80. Mu, X., R. D. Azbill, and J. E. Springer. 2000. Riluzole improves measures of oxidative stress following traumatic spinal cord injury. Brain Res 870:66-72.
81. Mu, X., R. D. Azbill, and J. E. Springer. 2000. Riluzole and methylprednisolone combined treatment improves functional recovery in traumatic spinal cord injury. J Neurotrauma 17:773-780.
82. Schwartz, G., and M. G. Fehlings. 2001. Evaluation of the neuroprotective effects of sodium channel blockers after spinal cord injury: improved behavioral and neuroanatomical recovery with riluzole. J Neurosurg 94:245-256.
83. McAdoo, D. J., M. G. Hughes, L. Nie, B. Shah, C. Clifton, S. Fullwood, and C. E. Hulsebosch. 2005. The effect of glutamate receptor blockers on glutamate release following spinal cord injury. Lack of evidence for an ongoing feedback cascade of damage --> glutamate release --> damage --> glutamate release --> etc. Brain Res 1038:92-99.
84. Ates, O., S. R. Cayli, I. Gurses, Y. Turkoz, O. Tarim, C. O. Cakir, and A. Kocak. 2007. Comparative neuroprotective effect of sodium channel blockers after experimental spinal cord injury. J Clin Neurosci 14:658-665.
85. Kitzman, P. H. 2009. Effectiveness of riluzole in suppressing spasticity in the spinal cord injured rat. Neurosci Lett 455:150-153.
86. Simard, J. M., O. Tsymbalyuk, K. Keledjian, A. Ivanov, S. Ivanova, and V. Gerzanich. 2011. Comparative effects of glibenclamide and riluzole in a rat model of severe cervical spinal cord injury. Exp Neurol 233:566-574.
87. The Methodist Hospital System. Safety of Riluzole in Patients With Acute Spinal Cord Injury. In: ClinicalTrials.gov [Internet]. Bethesda (MD): National Library of Medicine

(US). 2009- [cited 2012 Feb 29]. Available from: http://www.clinicaltrials.gov/ct2/show/NCT00876889 NLM Identifier: NCT00876889.

88. Doble, A. 1996. The pharmacology and mechanism of action of riluzole. Neurology 47:S233-241.

89. Cadotte, D. W., and M. G. Fehlings. 2010. Spinal Cord Injury: A Systematic Review of Current Treatment Options. Clin Orthop Relat Res.

90. Bracken, M. B. 2012. Steroids for acute spinal cord injury. Cochrane Database Syst Rev 1:CD001046.

91. Chinnock, P., and I. Roberts. 2005. Gangliosides for acute spinal cord injury. Cochrane Database Syst Rev:CD004444.

92. Hugenholtz, H. 2003. Methylprednisolone for acute spinal cord injury: not a standard of care. CMAJ 168:1145-1146.

93. Bracken, M. B., M. J. Shepard, K. G. Hellenbrand, W. F. Collins, L. S. Leo, D. F. Freeman, F. C. Wagner, E. S. Flamm, H. M. Eisenberg, J. H. Goodman, and et al. 1985. Methylprednisolone and neurological function 1 year after spinal cord injury. Results of the National Acute Spinal Cord Injury Study. J Neurosurg 63:704-713.

94. Bracken, M. B., M. J. Shepard, W. F. Collins, T. R. Holford, W. Young, D. S. Baskin, H. M. Eisenberg, E. Flamm, L. Leo-Summers, J. Maroon, and et al. 1990. A randomized, controlled trial of methylprednisolone or naloxone in the treatment of acute spinal-cord injury. Results of the Second National Acute Spinal Cord Injury Study. N Engl J Med 322:1405-1411.

95. Hurlbert, R. J. 2000. Methylprednisolone for acute spinal cord injury: an inappropriate standard of care. J Neurosurg 93:1-7.

96. Steeves, J. D., J. W. Fawcett, M. H. Tuszynski, D. Lammertse, A. E. P. Curt, J. F. Ditunno, P. H. Ellaway, M. G. Fehlings, J. D. Guest, N. Kleitman, P. F. Bartlett, A. R. Blight, V. Dietz, B. H. Dobkin, L. A. Havton, R. Grossman, D. J. Short, M. Nakamura, H. Katoh, W. P. Coleman, M. Gaviria, A. Privat, M. W. Kalichman, and C. Rask. Experimental Treatments for Spinal Cord Injury: What you should know if you are considering participation in a clinical trial.: International Campaign for Cures of spinal cord injury Paralysis,. 2007. Available from: http://www.christopherreeve.org/atf/cf/%7B219882e9-dfff-4cc0-95ee-3a62423c40ec%7D/ICCP_CLINICAL_TRIALS.PDF.

97. Steinhoff, M., R. W. Groves, P. E. LeBoit, and T. A. Luger. 2010. Inflammation. Wiley-Blackwell.
98. Alexander, J. K., and P. G. Popovich. 2009. Neuroinflammation in spinal cord injury: therapeutic targets for neuroprotection and regeneration. Prog Brain Res 175:125-137.
99. Fitch, M. T., and J. Silver. 2008. CNS injury, glial scars, and inflammation: Inhibitory extracellular matrices and regeneration failure. Exp Neurol 209:294-301.
100. Fitch, M. T., C. Doller, C. K. Combs, G. E. Landreth, and J. Silver. 1999. Cellular and molecular mechanisms of glial scarring and progressive cavitation: in vivo and in vitro analysis of inflammation-induced secondary injury after CNS trauma. J Neurosci 19:8182-8198.
101. Bethea, J. R. 2000. Spinal cord injury-induced inflammation: a dual-edged sword. Prog Brain Res 128:33-42.
102. Trivedi, A., A. D. Olivas, and L. J. Noble-Haeusslein. 2006. Inflammation and Spinal Cord Injury: Infiltrating Leukocytes as Determinants of Injury and Repair Processes. Clin Neurosci Res 6:283-292.
103. Schwartz, M., O. Butovsky, W. Bruck, and U. K. Hanisch. 2006. Microglial phenotype: is the commitment reversible? Trends Neurosci 29:68-74.
104. McTigue, D. M., P. G. Popovich, L. B. Jakeman, and B. T. Stokes. 2000. Strategies for spinal cord injury repair. Prog Brain Res 128:3-8.
105. Murakami, M., Y. Nakatani, G. Atsumi, K. Inoue, and I. Kudo. 1997. Regulatory functions of phospholipase A2. Crit Rev Immunol 17:225-283.
106. López-Vales, R., N. Ghasemlou, A. Redensek, B. J. Kerr, E. Barbayianni, G. Antonopoulou, C. Baskakis, K. I. Rathore, V. Constantinou-Kokotou, D. Stephens, T. Shimizu, E. A. Dennis, G. Kokotos, and S. David. 2011. Phospholipase A2 superfamily members play divergent roles after spinal cord injury. FASEB J 25:4240-4252.
107. Liu, N. K., and X. M. Xu. 2010. Phospholipase A2 and its molecular mechanism after spinal cord injury. Mol Neurobiol 41:197-205.
108. Farooqui, A. A., L. A. Horrocks, and T. Farooqui. 2007. Modulation of inflammation in brain: a matter of fat. J Neurochem 101:577-599.
109. Murakami, M., and I. Kudo. 2006. Prostaglandin E synthase: a novel drug target for inflammation and cancer. Curr Pharm Des 12:943-954.

110. Huang, W., A. Bhavsar, R. E. Ward, J. C. Hall, J. V. Priestley, and A. T. Michael-Titus. 2009. Arachidonyl trifluoromethyl ketone is neuroprotective after spinal cord injury. J Neurotrauma 26:1429-1434.
111. Farooqui, A. A., M. L. Litsky, T. Farooqui, and L. A. Horrocks. 1999. Inhibitors of intracellular phospholipase A2 activity: their neurochemical effects and therapeutical importance for neurological disorders. Brain Res Bull 49:139-153.
112. Smith, W. L., D. L. DeWitt, and R. M. Garavito. 2000. Cyclooxygenases: structural, cellular, and molecular biology. Annu Rev Biochem 69:145-182.
113. McQuay, H. J., and R. A. Moore. 2005. NSAIDs and Coxibs: Clinical use. In Wall and Melzack's Textbook of Pain. S. B. McMahon, and M. Koltzenburg, editors. Churchill Livingstone. 1-10.
114. Smith, W. L., and R. Langenbach. 2001. Why there are two cyclooxygenase isozymes. J Clin Invest 107:1491-1495.
115. Smith, W. L. 1992. Prostanoid biosynthesis and mechanisms of action. Am J Physiol 263:F181-191.
116. Milatovic, D., T. J. Montine, and M. Aschner. 2011. Prostanoid signaling: dual role for prostaglandin E2 in neurotoxicity. Neurotoxicology 32:312-319.
117. Andreasson, K. 2009. Emerging roles of PGE2 receptors in models of neurological disease. Prostaglandins Other Lipid Mediat 91:104-112.
118. Vanegas, H., and H. G. Schaible. 2001. Prostaglandins and cyclooxygenases [correction of cycloxygenases] in the spinal cord. Prog Neurobiol 64:327-363.
119. Hains, B. C., J. A. Yucra, and C. E. Hulsebosch. 2001. Reduction of pathological and behavioral deficits following spinal cord contusion injury with the selective cyclooxygenase-2 inhibitor NS-398. J Neurotrauma 18:409-423.
120. Zhao, P., S. G. Waxman, and B. C. Hains. 2007. Extracellular signal-regulated kinase-regulated microglia-neuron signaling by prostaglandin E2 contributes to pain after spinal cord injury. J Neurosci 27:2357-2368.
121. Resnick, D. K., S. H. Graham, C. E. Dixon, and D. W. Marion. 1998. Role of cyclooxygenase 2 in acute spinal cord injury. J Neurotrauma 15:1005-1013.
122. Resnick, D. K., P. Nguyen, and C. F. Cechvala. 2001. Regional and temporal changes in prostaglandin E2 and thromboxane B2 concentrations after spinal cord injury. Spine J 1:432-436.

123. Fujita, Y., T. Shingu, M. Kurihara, H. Miyake, T. Kono, M. Tsujimura, and K. Mori. 1985. Evaluation of a low dose administration of aspirin, dipyridamol and steroid. Therapeutic effects on motor function and protective effects on Na+-K+-activated ATPase activity against lipid peroxidation in an experimental model of spinal cord injury. Paraplegia 23:56-57.

124. Sharma, H. S., Y. Olsson, F. Nyberg, and P. K. Dey. 1993. Prostaglandins modulate alterations of microvascular permeability, blood flow, edema and serotonin levels following spinal cord injury: an experimental study in the rat. Neuroscience 57:443-449.

125. Winkler, T., H. S. Sharma, E. Stalberg, and Y. Olsson. 1993. Indomethacin, an inhibitor of prostaglandin synthesis attenuates alteration in spinal cord evoked potentials and edema formation after trauma to the spinal cord: an experimental study in the rat. Neuroscience 52:1057-1067.

126. Sharma, H. S., Y. Olsson, and J. Cervos-Navarro. 1993. Early perifocal cell changes and edema in traumatic injury of the spinal cord are reduced by indomethacin, an inhibitor of prostaglandin synthesis. Experimental study in the rat. Acta Neuropathol 85:145-153.

127. Sharma, H. S., and T. Winkler. 2002. Assessment of spinal cord pathology following trauma using early changes in the spinal cord evoked potentials: a pharmacological and morphological study in the rat. Muscle Nerve Suppl 11:S83-91.

128. Harada, N., Y. Taoka, and K. Okajima. 2006. Role of prostacyclin in the development of compression trauma-induced spinal cord injury in rats. J Neurotrauma 23:1739-1749.

129. Simpson, R. K., Jr., D. S. Baskin, A. W. Dudley, L. Bogue, and F. Rothenberg. 1991. The influence of long-term nifedipine or indomethacin therapy on neurologic recovery from experimental spinal cord injury. J Spinal Disord 4:420-427.

130. Guth, L., Z. Zhang, N. A. DiProspero, K. Joubin, and M. T. Fitch. 1994. Spinal cord injury in the rat: treatment with bacterial lipopolysaccharide and indomethacin enhances cellular repair and locomotor function. Exp Neurol 126:76-87.

131. Guth, L., Z. Zhang, and E. Roberts. 1994. Key role for pregnenolone in combination therapy that promotes recovery after spinal cord injury. Proc Natl Acad Sci U S A 91:12308-12312.

132. Guven, M. B., B. Cirak, N. Yuceer, and F. Ozveren. 1999. Is indomethacin harmful in spinal cord injury treatment? An experimental study. Pediatr Neurosurg 31:189-193.
133. Resnick, D. K., P. Nguyen, and C. F. Cechvala. 2001. Selective cyclooxygenase 2 inhibition lowers spinal cord prostaglandin concentrations after injury. Spine J 1:437-441.
134. Schwab, J. M., S. Conrad, T. Elbert, K. Trautmann, R. Meyermann, and H. J. Schluesener. 2004. Lesional RhoA+ cell numbers are suppressed by anti-inflammatory, cyclooxygenase-inhibiting treatment following subacute spinal cord injury. Glia 47:377-386.
135. Pantovic, R., P. Draganic, V. Erakovic, B. Blagovic, C. Milin, and A. Simonic. 2005. Effect of indomethacin on motor activity and spinal cord free fatty acid content after experimental spinal cord injury in rabbits. Spinal Cord 43:519-526.
136. Fu, Q., J. Hue, and S. Li. 2007. Nonsteroidal anti-inflammatory drugs promote axon regeneration via RhoA inhibition. J Neurosci 27:4154-4164.
137. Xing, B., H. Li, H. Wang, D. Mukhopadhyay, D. Fisher, C. J. Gilpin, and S. Li. 2011. RhoA-inhibiting NSAIDs promote axonal myelination after spinal cord injury. Exp Neurol 231:247-260.
138. Serhan, C. N. 2005. Lipoxins and aspirin-triggered 15-epi-lipoxins are the first lipid mediators of endogenous anti-inflammation and resolution. Prostaglandins Leukot Essent Fatty Acids 73:141-162.
139. Svensson, C. I., M. Zattoni, and C. N. Serhan. 2007. Lipoxins and aspirin-triggered lipoxin inhibit inflammatory pain processing. J Exp Med 204:245-252.
140. Kanaoka, Y., and J. A. Boyce. 2004. Cysteinyl leukotrienes and their receptors: cellular distribution and function in immune and inflammatory responses. J Immunol 173:1503-1510.
141. Moreland, D. B., D. S. Soloniuk, and M. J. Feldman. 1989. Leukotrienes in experimental spinal cord injury. Surg Neurol 31:277-280.
142. Genovese, T., A. Rossi, E. Mazzon, R. Di Paola, C. Muia, R. Caminiti, P. Bramanti, L. Sautebin, and S. Cuzzocrea. 2008. Effects of zileuton and montelukast in mouse experimental spinal cord injury. Br J Pharmacol 153:568-582.
143. Piazza, G. J. 1996. Lipoxygenase and lipoxygenase pathway enzymes. AOCS Press, Champaign, Ill.

144. Genovese, T., E. Mazzon, A. Rossi, R. Di Paola, G. Cannavo, C. Muia, C. Crisafulli, P. Bramanti, L. Sautebin, and S. Cuzzocrea. 2005. Involvement of 5-lipoxygenase in spinal cord injury. J Neuroimmunol 166:55-64.

145. Saiwai, H., Y. Ohkawa, H. Yamada, H. Kumamaru, A. Harada, H. Okano, T. Yokomizo, Y. Iwamoto, and S. Okada. 2010. The LTB4-BLT1 axis mediates neutrophil infiltration and secondary injury in experimental spinal cord injury. Am J Pathol 176:2352-2366.

146. Green, G. A. 2001. Understanding NSAIDs: from aspirin to COX-2. Clin Cornerstone 3:50-60.

147. Moore, R. A., S. Derry, C. J. Phillips, and H. J. McQuay. 2006. Nonsteroidal anti-inflammatory drugs (NSAIDs), cyxlooxygenase-2 selective inhibitors (coxibs) and gastrointestinal harm: review of clinical trials and clinical practice. BMC Musculoskelet Disord 7:79.

148. Bombardier, C., L. Laine, A. Reicin, D. Shapiro, R. Burgos-Vargas, B. Davis, R. Day, M. B. Ferraz, C. J. Hawkey, M. C. Hochberg, T. K. Kvien, and T. J. Schnitzer. 2000. Comparison of upper gastrointestinal toxicity of rofecoxib and naproxen in patients with rheumatoid arthritis. VIGOR Study Group. N Engl J Med 343:1520-1528, 1522 p following 1528.

149. Rainsford, K. D. 2007. Anti-inflammatory drugs in the 21st century. Subcell Biochem 42:3-27.

150. Szczeklik, A. 1997. Mechanism of aspirin-induced asthma. Allergy 52:613-619.

151. Okunishi, K., and M. Peters-Golden. 2011. Leukotrienes and airway inflammation. Biochim Biophys Acta 1810:1096-1102.

152. Hirsch, F. R., and S. M. Lippman. 2005. Advances in the biology of lung cancer chemoprevention. J Clin Oncol 23:3186-3197.

153. Ye, Y. N., W. K. Wu, V. Y. Shin, I. C. Bruce, B. C. Wong, and C. H. Cho. 2005. Dual inhibition of 5-LOX and COX-2 suppresses colon cancer formation promoted by cigarette smoke. Carcinogenesis 26:827-834.

154. Mao, J. T., M. D. Roth, K. J. Serio, F. Baratelli, L. Zhu, E. C. Holmes, R. M. Strieter, and S. M. Dubinett. 2003. Celecoxib modulates the capacity for prostaglandin E2 and interleukin-10 production in alveolar macrophages from active smokers. Clin Cancer Res 9:5835-5841.

155. Mao, J. T., I. H. Tsu, S. M. Dubinett, B. Adams, T. Sarafian, F. Baratelli, M. D. Roth, and K. J. Serio. 2004. Modulation of pulmonary leukotriene B4 production by cyclooxygenase-2 inhibitors and lipopolysaccharide. Clin Cancer Res 10:6872-6878.
156. Fiorucci, S., R. Meli, M. Bucci, and G. Cirino. 2001. Dual inhibitors of cyclooxygenase and 5-lipoxygenase. A new avenue in anti-inflammatory therapy? Biochem Pharmacol 62:1433-1438.
157. Leval, X., F. Julemont, J. Delarge, B. Pirotte, and J. M. Dogne. 2002. New trends in dual 5-LOX/COX inhibition. Curr Med Chem 9:941-962.
158. Cicero, A. F., and L. Laghi. 2007. Activity and potential role of licofelone in the management of osteoarthritis. Clin Interv Aging 2:73-79.
159. Alvaro-Gracia, J. M. 2004. Licofelone--clinical update on a novel LOX/COX inhibitor for the treatment of osteoarthritis. Rheumatology (Oxford) 43 Suppl 1:i21-25.
160. Martel-Pelletier, J., D. Lajeunesse, P. Reboul, and J. P. Pelletier. 2003. Therapeutic role of dual inhibitors of 5-LOX and COX, selective and non-selective non-steroidal anti-inflammatory drugs. Ann Rheum Dis 62:501-509.
161. Aggarwal, N. T., S. L. Pfister, K. M. Gauthier, Y. Chawengsub, J. E. Baker, and W. B. Campbell. 2009. Chronic hypoxia enhances 15-lipoxygenase-mediated vasorelaxation in rabbit arteries. Am J Physiol Heart Circ Physiol 296:H678-688.
162. Kalonia, H., P. Kumar, and A. Kumar. 2011. Licofelone attenuates quinolinic acid induced Huntington like symptoms: Possible behavioral, biochemical and cellular alterations. Prog Neuropsychopharmacol Biol Psychiatry 35:607-615.
163. Kumar, P., H. Kalonia, and A. Kumar. 2011. Role of LOX/COX pathways in 3-nitropropionic acid-induced HD like symptoms in rats: Protective role of Licofelone. Br J Pharmacol.
164. Gupta, A., A. Kumar, and S. K. Kulkarni. 2010. Licofelone attenuates MPTP-induced neuronal toxicity: behavioral, biochemical and cellular evidence. Inflammopharmacology 18:223-232.
165. Sharma, H. S. 2005. Pathophysiology of blood-spinal cord barrier in traumatic injury and repair. Curr Pharm Des 11:1353-1389.
166. Bartanusz, V., D. Jezova, B. Alajajian, and M. Digicaylioglu. 2011. The blood-spinal cord barrier: Morphology and Clinical Implications. Ann Neurol.

167. Ge, S., and J. S. Pachter. 2006. Isolation and culture of microvascular endothelial cells from murine spinal cord. J Neuroimmunol 177:209-214.
168. Beggs, J. L., and J. D. Waggener. 1976. Transendothelial vesicular transport of protein following compression injury to the spinal cord. Lab Invest 34:428-439.
169. Noble, L. J., and D. S. Maxwell. 1983. Blood-spinal cord barrier response to transection. Exp Neurol 79:188-199.
170. Patterson, C. E., R. A. Rhoades, and J. G. Garcia. 1992. Evans blue dye as a marker of albumin clearance in cultured endothelial monolayer and isolated lung. J Appl Physiol 72:865-873.
171. Bilgen, M., R. Abbe, and P. A. Narayana. 2001. Dynamic contrast-enhanced MRI of experimental spinal cord injury: in vivo serial studies. Magn Reson Med 45:614-622.
172. Bilgen, M., B. Dogan, and P. A. Narayana. 2002. In vivo assessment of blood-spinal cord barrier permeability: serial dynamic contrast enhanced MRI of spinal cord injury. Magn Reson Imaging 20:337-341.
173. Noble, L. J., and J. R. Wrathall. 1989. Distribution and time course of protein extravasation in the rat spinal cord after contusive injury. Brain Res 482:57-66.
174. Pan, W., and A. J. Kastin. 2001. Increase in TNFalpha transport after SCI is specific for time, region, and type of lesion. Exp Neurol 170:357-363.
175. Pan, W., A. J. Kastin, L. Gera, and J. M. Stewart. 2001. Bradykinin antagonist decreases early disruption of the blood-spinal cord barrier after spinal cord injury in mice. Neurosci Lett 307:25-28.
176. Pan, W., B. Csernus, and A. J. Kastin. 2003. Upregulation of p55 and p75 receptors mediating TNF-alpha transport across the injured blood-spinal cord barrier. J Mol Neurosci 21:173-184.
177. Cohen, D. M., C. B. Patel, P. Ahobila-Vajjula, L. M. Sundberg, T. Chacko, S. J. Liu, and P. A. Narayana. 2009. Blood-spinal cord barrier permeability in experimental spinal cord injury: dynamic contrast-enhanced MRI. NMR Biomed 22:332-341.
178. Mautes, A. E., M. R. Weinzierl, F. Donovan, and L. J. Noble. 2000. Vascular events after spinal cord injury: contribution to secondary pathogenesis. Phys Ther 80:673-687.
179. Bernacki, J., A. Dobrowolska, K. Nierwinska, and A. Malecki. 2008. Physiology and pharmacological role of the blood-brain barrier. Pharmacol Rep 60:600-622.

180. Takigawa, T., T. Yonezawa, T. Yoshitaka, J. Minaguchi, M. Kurosaki, M. Tanaka, Y. Sado, A. Ohtsuka, T. Ozaki, and Y. Ninomiya. 2009. Separation of the perivascular basement membrane provides a conduit for inflammatory cells in a mouse spinal cord injury model. J Neurotrauma 27:739-751.
181. Sharma, H. S., P. Alm, and J. Westman. 1998. Nitric oxide and carbon monoxide in the brain pathology of heat stress. Prog Brain Res 115:297-333.
182. Begley, D. J. 2004. ABC transporters and the blood-brain barrier. Curr Pharm Des 10:1295-1312.
183. Loscher, W., and H. Potschka. 2005. Drug resistance in brain diseases and the role of drug efflux transporters. Nat Rev Neurosci 6:591-602.
184. Varatharajan, L., and S. A. Thomas. 2009. The transport of anti-HIV drugs across blood-CNS interfaces: summary of current knowledge and recommendations for further research. Antiviral Res 82:A99-109.
185. Pahnke, J., L. C. Walker, K. Scheffler, and M. Krohn. 2009. Alzheimer's disease and blood-brain barrier function-Why have anti-beta-amyloid therapies failed to prevent dementia progression? Neurosci Biobehav Rev 33:1099-1108.
186. Brockmann, K. 2009. The expanding phenotype of GLUT1-deficiency syndrome. Brain Dev 31:545-552.
187. Potschka, H. 2010. Modulating P-glycoprotein regulation: future perspectives for pharmacoresistant epilepsies? Epilepsia 51:1333-1347.
188. Chamberlain, M. C. 2010. Anticancer therapies and CNS relapse: overcoming blood-brain and blood-cerebrospinal fluid barrier impermeability. Expert Rev Neurother 10:547-561.
189. Whetstone, W. D., J. Y. Hsu, M. Eisenberg, Z. Werb, and L. J. Noble-Haeusslein. 2003. Blood-spinal cord barrier after spinal cord injury: relation to revascularization and wound healing. J Neurosci Res 74:227-239.
190. Kim, Y., Y. K. Park, H. Y. Cho, J. Kim, and Y. W. Yoon. 2011. Long-term changes in expressions of spinal glutamate transporters after spinal cord injury. Brain Res 1389:194-199.
191. Lepore, A. C., J. O'Donnell, A. S. Kim, E. J. Yang, A. Tuteja, A. Haidet-Phillips, C. P. O'Banion, and N. J. Maragakis. 2011. Reduction in expression of the astrocyte

glutamate transporter, GLT1, worsens functional and histological outcomes following traumatic spinal cord injury. Glia.

192. Lepore, A. C., J. O'Donnell, J. F. Bonner, C. Paul, M. E. Miller, B. Rauck, R. A. Kushner, J. D. Rothstein, I. Fischer, and N. J. Maragakis. 2011. Spatial and temporal changes in promoter activity of the astrocyte glutamate transporter GLT1 following traumatic spinal cord injury. J Neurosci Res 89:1001-1017.

193. Nesic, O., J. Lee, Z. Ye, G. C. Unabia, D. Rafati, C. E. Hulsebosch, and J. R. Perez-Polo. 2006. Acute and chronic changes in aquaporin 4 expression after spinal cord injury. Neuroscience 143:779-792.

194. Nesic, O., J. D. Guest, D. Zivadinovic, P. A. Narayana, J. J. Herrera, R. J. Grill, V. U. Mokkapati, B. B. Gelman, and J. Lee. 2010. Aquaporins in spinal cord injury: the janus face of aquaporin 4. Neuroscience 168:1019-1035.

195. Jones, P. M., and A. M. George. 2004. The ABC transporter structure and mechanism: perspectives on recent research. Cell Mol Life Sci 61:682-699.

196. Linton, K. J., and C. F. Higgins. 2007. Structure and function of ABC transporters: the ATP switch provides flexible control. Pflugers Arch 453:555-567.

197. Fromm, M. F. 2004. Importance of P-glycoprotein at blood-tissue barriers. Trends Pharmacol Sci 25:423-429.

198. Hartz, A. M., and B. Bauer. 2010. ABC transporters in the CNS - an inventory. Curr Pharm Biotechnol 12:656-673.

199. Aller, S. G., J. Yu, A. Ward, Y. Weng, S. Chittaboina, R. Zhuo, P. M. Harrell, Y. T. Trinh, Q. Zhang, I. L. Urbatsch, and G. Chang. 2009. Structure of P-glycoprotein reveals a molecular basis for poly-specific drug binding. Science 323:1718-1722.

200. Hunter, J., B. H. Hirst, and N. L. Simmons. 1993. Drug absorption limited by P-glycoprotein-mediated secretory drug transport in human intestinal epithelial Caco-2 cell layers. Pharm Res 10:743-749.

201. Muller, M., and P. L. Jansen. 1997. Molecular aspects of hepatobiliary transport. Am J Physiol 272:G1285-1303.

202. Okamura, N., M. Hirai, Y. Tanigawara, K. Tanaka, M. Yasuhara, K. Ueda, T. Komano, and R. Hori. 1993. Digoxin-cyclosporin A interaction: modulation of the multidrug transporter P-glycoprotein in the kidney. J Pharmacol Exp Ther 266:1614-1619.

203. Begley, D. J. 2005. P-glycoprotein: The prototypical BBB efflux transporter. In Efflux Transporters and the Blood-brain barrier. E. M. Taylor, editor. Nova Science Publishers, Inc., New York. 107-135.
204. Su, L., C. Y. Cheng, and D. D. Mruk. 2009. Drug transporter, P-glycoprotein (MDR1), is an integrated component of the mammalian blood-testis barrier. Int J Biochem Cell Biol 41:2578-2587.
205. Vahakangas, K., and P. Myllynen. 2009. Drug transporters in the human blood-placental barrier. Br J Pharmacol 158:665-678.
206. Kennedy, B. G., and N. J. Mangini. 2002. P-glycoprotein expression in human retinal pigment epithelium. Mol Vis 8:422-430.
207. Oude Elferink, R. P., and J. Zadina. 2001. MDR1 P-glycoprotein transports endogenous opioid peptides. Peptides 22:2015-2020.
208. Masuda, M., E. Nakai, and T. Mizutani. 2008. Study of oxidized lipids as endogenous substrates of P-gp (ABCB1). Drug Metab Lett 2:238-244.
209. Uchiyama-Kokubu, N., M. Naito, M. Nakajima, and T. Tsuruo. 2004. Transport of somatostatin and substance P by human P-glycoprotein. FEBS Lett 574:55-61.
210. Uhr, M., F. Holsboer, and M. B. Muller. 2002. Penetration of endogenous steroid hormones corticosterone, cortisol, aldosterone and progesterone into the brain is enhanced in mice deficient for both mdr1a and mdr1b P-glycoproteins. J Neuroendocrinol 14:753-759.
211. Lam, F. C., R. Liu, P. Lu, A. B. Shapiro, J. M. Renoir, F. J. Sharom, and P. B. Reiner. 2001. beta-Amyloid efflux mediated by p-glycoprotein. J Neurochem 76:1121-1128.
212. Ernest, S., and E. Bello-Reuss. 1999. Secretion of platelet-activating factor is mediated by MDR1 P-glycoprotein in cultured human mesangial cells. J Am Soc Nephrol 10:2306-2313.
213. Schinkel, A. H. 1999. P-Glycoprotein, a gatekeeper in the blood-brain barrier. Adv Drug Deliv Rev 36:179-194.
214. Miller, D. S., B. Bauer, and A. M. Hartz. 2008. Modulation of P-glycoprotein at the blood-brain barrier: opportunities to improve central nervous system pharmacotherapy. Pharmacol Rev 60:196-209.

215. Fojo, A. T., K. Ueda, D. J. Slamon, D. G. Poplack, M. M. Gottesman, and I. Pastan. 1987. Expression of a multidrug-resistance gene in human tumors and tissues. Proc Natl Acad Sci U S A 84:265-269.
216. Juliano, R. L., and V. Ling. 1976. A surface glycoprotein modulating drug permeability in Chinese hamster ovary cell mutants. Biochim Biophys Acta 455:152-162.
217. Bates, S. F., C. Chen, R. Robey, M. Kang, W. D. Figg, and T. Fojo. 2002. Reversal of multidrug resistance: lessons from clinical oncology. Novartis Found Symp 243:83-96; discussion 96-102, 180-105.
218. 2000. Cancer multidrug resistance. Nat Biotechnol 18 Suppl:IT18-20.
219. Thomas, H., and H. M. Coley. 2003. Overcoming multidrug resistance in cancer: an update on the clinical strategy of inhibiting p-glycoprotein. Cancer Control 10:159-165.
220. Coley, H. M. 2009. Overcoming multidrug resistance in cancer: clinical studies of p-glycoprotein inhibitors. Methods Mol Biol 596:341-358.
221. Volk, H. A., and W. Loscher. 2005. Multidrug resistance in epilepsy: rats with drug-resistant seizures exhibit enhanced brain expression of P-glycoprotein compared with rats with drug-responsive seizures. Brain 128:1358-1368.
222. Bauer, B., A. M. Hartz, A. Pekcec, K. Toellner, D. S. Miller, and H. Potschka. 2008. Seizure-induced up-regulation of P-glycoprotein at the blood-brain barrier through glutamate and cyclooxygenase-2 signaling. Mol Pharmacol 73:1444-1453.
223. Spudich, A., E. Kilic, H. Xing, U. Kilic, K. M. Rentsch, H. Wunderli-Allenspach, C. L. Bassetti, and D. M. Hermann. 2006. Inhibition of multidrug resistance transporter-1 facilitates neuroprotective therapies after focal cerebral ischemia. Nat Neurosci 9:487-488.
224. Milane, A., C. Fernandez, L. Dupuis, M. Buyse, J. P. Loeffler, R. Farinotti, V. Meininger, and G. Bensimon. 2010. P-glycoprotein expression and function are increased in an animal model of amyotrophic lateral sclerosis. Neurosci Lett 472:166-170.
225. Milane, A., C. Fernandez, S. Vautier, G. Bensimon, V. Meininger, and R. Farinotti. 2007. Minocycline and riluzole brain disposition: interactions with p-glycoprotein at the blood-brain barrier. J Neurochem 103:164-173.

226. Hartz, A. M., D. S. Miller, and B. Bauer. 2010. Restoring blood-brain barrier P-glycoprotein reduces brain amyloid-beta in a mouse model of Alzheimer's disease. Mol Pharmacol 77:715-723.

227. Furuno, T., M. T. Landi, M. Ceroni, N. Caporaso, I. Bernucci, G. Nappi, E. Martignoni, E. Schaeffeler, M. Eichelbaum, M. Schwab, and U. M. Zanger. 2002. Expression polymorphism of the blood-brain barrier component P-glycoprotein (MDR1) in relation to Parkinson's disease. Pharmacogenetics 12:529-534.

228. Kortekaas, R., K. L. Leenders, J. C. van Oostrom, W. Vaalburg, J. Bart, A. T. Willemsen, and N. H. Hendrikse. 2005. Blood-brain barrier dysfunction in parkinsonian midbrain in vivo. Ann Neurol 57:176-179.

229. Bartels, A. L., A. T. Willemsen, R. Kortekaas, B. M. de Jong, R. de Vries, O. de Klerk, J. C. van Oostrom, A. Portman, and K. L. Leenders. 2008. Decreased blood-brain barrier P-glycoprotein function in the progression of Parkinson's disease, PSP and MSA. J Neural Transm 115:1001-1009.

230. Vogelgesang, S., I. Cascorbi, E. Schroeder, J. Pahnke, H. K. Kroemer, W. Siegmund, C. Kunert-Keil, L. C. Walker, and R. W. Warzok. 2002. Deposition of Alzheimer's beta-amyloid is inversely correlated with P-glycoprotein expression in the brains of elderly non-demented humans. Pharmacogenetics 12:535-541.

231. Kwan, P., H. M. Li, E. Al-Jufairi, R. Abdulla, M. Gonzales, A. H. Kaye, C. Szoeke, H. K. Ng, K. S. Wong, and T. J. O'Brien. 2010. Association between temporal lobe P-glycoprotein expression and seizure recurrence after surgery for pharmacoresistant temporal lobe epilepsy. Neurobiol Dis 39:192-197.

232. de Klerk, O. L., A. T. Willemsen, F. J. Bosker, A. L. Bartels, N. H. Hendrikse, J. A. den Boer, and R. A. Dierckx. 2010. Regional increase in P-glycoprotein function in the blood-brain barrier of patients with chronic schizophrenia: a PET study with [(11)C]verapamil as a probe for P-glycoprotein function. Psychiatry Res 183:151-156.

233. Langford, D., A. Grigorian, R. Hurford, A. Adame, R. J. Ellis, L. Hansen, and E. Masliah. 2004. Altered P-glycoprotein expression in AIDS patients with HIV encephalitis. J Neuropathol Exp Neurol 63:1038-1047.

234. Potschka, H. 2010. Targeting regulation of ABC efflux transporters in brain diseases: A novel therapeutic approach. Pharmacology & Therapeutics 125:118-127.

235. Pekcec, A., B. Unkruer, J. Schlichtiger, J. Soerensen, A. M. Hartz, B. Bauer, E. A. van Vliet, J. A. Gorter, and H. Potschka. 2009. Targeting prostaglandin E2 EP1 receptors prevents seizure-associated P-glycoprotein up-regulation. J Pharmacol Exp Ther 330:939-947.

236. van Vliet, E. A., G. Zibell, A. Pekcec, J. Schlichtiger, P. M. Edelbroek, L. Holtman, E. Aronica, J. A. Gorter, and H. Potschka. 2009. COX-2 inhibition controls P-glycoprotein expression and promotes brain delivery of phenytoin in chronic epileptic rats. Neuropharmacology.

237. Rowland, L. P., and N. A. Shneider. 2001. Amyotrophic lateral sclerosis. N Engl J Med 344:1688-1700.

238. Ye, C. G., W. K. Wu, J. H. Yeung, H. T. Li, Z. J. Li, C. C. Wong, S. X. Ren, L. Zhang, K. P. Fung, and C. H. Cho. 2011. Indomethacin and SC236 enhance the cytotoxicity of doxorubicin in human hepatocellular carcinoma cells via inhibiting P-glycoprotein and MRP1 expression. Cancer Lett 304:90-96.

239. Zrieki, A., R. Farinotti, and M. Buyse. 2008. Cyclooxygenase inhibitors down regulate P-glycoprotein in human colorectal Caco-2 cell line. Pharm Res 25:1991-2001.

240. Liu, B., L. Qu, and H. Tao. 2009. Cyclo-oxygenase 2 up-regulates the effect of multidrug resistance. Cell Biol Int 34:21-25.

241. Xia, W., T. Zhao, J. Lv, S. Xu, J. Shi, S. Wang, X. Han, and Y. Sun. 2009. Celecoxib enhanced the sensitivity of cancer cells to anticancer drugs by inhibition of the expression of P-glycoprotein through a COX-2-independent manner. J Cell Biochem 108:181-194.

242. Koszdin, K. L., D. D. Shen, and C. M. Bernards. 2000. Spinal cord bioavailability of methylprednisolone after intravenous and intrathecal administration: the role of P-glycoprotein. Anesthesiology 92:156-163.

243. Bernards, C. M. 2006. Cyclosporine-A-mediated inhibition of p-glycoprotein increases methylprednisolone entry into the central nervous system. Spinal Cord 44:414-420.

244. Zibell, G., B. Unkruer, A. Pekcec, A. M. Hartz, B. Bauer, D. S. Miller, and H. Potschka. 2009. Prevention of seizure-induced up-regulation of endothelial P-glycoprotein by COX-2 inhibition. Neuropharmacology 56:849-855.

245. Yu, C., G. Argyropoulos, Y. Zhang, A. J. Kastin, H. Hsuchou, and W. Pan. 2008. Neuroinflammation activates Mdr1b efflux transport through NFkappaB: promoter analysis in BBB endothelia. Cell Physiol Biochem 22:745-756.

246. Rafati, D. S., K. Geissler, K. Johnson, G. Unabia, C. Hulsebosch, O. Nesic-Taylor, and J. R. Perez-Polo. 2008. Nuclear factor-kappaB decoy amelioration of spinal cord injury-induced inflammation and behavior outcomes. J Neurosci Res 86:566-580.

247. Braughler, J. M., and E. D. Hall. 1982. Correlation of methylprednisolone levels in cat spinal cord with its effects on (Na+ + K+)-ATPase, lipid peroxidation, and alpha motor neuron function. J Neurosurg 56:838-844.

248. Braughler, J. M., and E. D. Hall. 1984. Effects of multi-dose methylprednisolone sodium succinate administration on injured cat spinal cord neurofilament degradation and energy metabolism. J Neurosurg 61:290-295.

249. Braughler, J. M., and E. D. Hall. 1983. Uptake and elimination of methylprednisolone from contused cat spinal cord following intravenous injection of the sodium succinate ester. J Neurosurg 58:538-542.

250. Braughler, J. M., and E. D. Hall. 1982. Pharmacokinetics of methylprednisolone in cat plasma and spinal cord following a single intravenous dose of the sodium succinate ester. Drug Metab Dispos 10:551-552.

251. Fehlings, M. G., C. H. Tator, and R. D. Linden. 1989. The effect of nimodipine and dextran on axonal function and blood flow following experimental spinal cord injury. J Neurosurg 71:403-416.

252. Fehlings, M. G., and S. Agrawal. 1995. Role of sodium in the pathophysiology of secondary spinal cord injury. Spine (Phila Pa 1976) 20:2187-2191.

253. Tator, C. H. 1996. Experimental and clinical studies of the pathophysiology and management of acute spinal cord injury. J Spinal Cord Med 19:206-214.

254. Tator, C. H. 1998. Biology of neurological recovery and functional restoration after spinal cord injury. Neurosurgery 42:696-707; discussion 707-698.

255. Amar, A. P., and M. L. Levy. 1999. Pathogenesis and pharmacological strategies for mitigating secondary damage in acute spinal cord injury. Neurosurgery 44:1027-1039; discussion 1039-1040.

256. Pointillart, V., M. E. Petitjean, L. Wiart, J. M. Vital, P. Lassie, M. Thicoipe, and P. Dabadie. 2000. Pharmacological therapy of spinal cord injury during the acute phase. Spinal Cord 38:71-76.

257. University of Calgary. Minocycline and Perfusion Pressure Augmentation in Acute Spinal Cord Injury. In: ClinicalTrials.gov [Internet]. Besthesda (MD): National Library of Medicine (US). 2007- [cited 2012 Mar 13]. Available from: http://www.clinicaltrials.gov/ct2/show/NCT00559494 NLM Identifier: NCT00559494.

258. Marchand, F., C. Tsantoulas, D. Singh, J. Grist, A. K. Clark, E. J. Bradbury, and S. B. McMahon. 2009. Effects of Etanercept and Minocycline in a rat model of spinal cord injury. Eur J Pain 13:673-681.

259. Young, W., and M. B. Bracken. 1992. The Second National Acute Spinal Cord Injury Study. J Neurotrauma 9 Suppl 1:S397-405.

260. Zeidman, S. M., G. S. Ling, T. B. Ducker, and R. G. Ellenbogen. 1996. Clinical applications of pharmacologic therapies for spinal cord injury. J Spinal Disord 9:367-380.

261. Tator, C. H. 2006. Review of treatment trials in human spinal cord injury: issues, difficulties, and recommendations. Neurosurgery 59:957-982; discussion 982-957.

262. Bracken, M. B., M. J. Shepard, T. R. Holford, L. Leo-Summers, E. F. Aldrich, M. Fazl, M. G. Fehlings, D. L. Herr, P. W. Hitchon, L. F. Marshall, R. P. Nockels, V. Pascale, P. L. Perot, Jr., J. Piepmeier, V. K. Sonntag, F. Wagner, J. E. Wilberger, H. R. Winn, and W. Young. 1998. Methylprednisolone or tirilazad mesylate administration after acute spinal cord injury: 1-year follow up. Results of the third National Acute Spinal Cord Injury randomized controlled trial. J Neurosurg 89:699-706.

263. Hawryluk, G. W., J. Rowland, B. K. Kwon, and M. G. Fehlings. 2008. Protection and repair of the injured spinal cord: a review of completed, ongoing, and planned clinical trials for acute spinal cord injury. Neurosurg Focus 25:E14.

264. Saitoh, H., M. Hatakeyama, O. Eguchi, M. Oda, and M. Takada. 1998. Involvement of intestinal P-glycoprotein in the restricted absorption of methylprednisolone from rat small intestine. J Pharm Sci 87:73-75.

265. Wells, J. E., R. J. Hurlbert, M. G. Fehlings, and V. W. Yong. 2003. Neuroprotection by minocycline facilitates significant recovery from spinal cord injury in mice. Brain 126:1628-1637.

266. Stirling, D. P., K. Khodarahmi, J. Liu, L. T. McPhail, C. B. McBride, J. D. Steeves, M. S. Ramer, and W. Tetzlaff. 2004. Minocycline treatment reduces delayed oligodendrocyte death, attenuates axonal dieback, and improves functional outcome after spinal cord injury. J Neurosci 24:2182-2190.

267. Yune, T. Y., J. Y. Lee, G. Y. Jung, S. J. Kim, M. H. Jiang, Y. C. Kim, Y. J. Oh, G. J. Markelonis, and T. H. Oh. 2007. Minocycline alleviates death of oligodendrocytes by inhibiting pro-nerve growth factor production in microglia after spinal cord injury. J Neurosci 27:7751-7761.

268. Festoff, B. W., S. Ameenuddin, P. M. Arnold, A. Wong, K. S. Santacruz, and B. A. Citron. 2006. Minocycline neuroprotects, reduces microgliosis, and inhibits caspase protease expression early after spinal cord injury. J Neurochem 97:1314-1326.

269. Lee, S. M., T. Y. Yune, S. J. Kim, D. W. Park, Y. K. Lee, Y. C. Kim, Y. J. Oh, G. J. Markelonis, and T. H. Oh. 2003. Minocycline reduces cell death and improves functional recovery after traumatic spinal cord injury in the rat. J Neurotrauma 20:1017-1027.

270. Uhr, M., T. Steckler, A. Yassouridis, and F. Holsboer. 2000. Penetration of amitriptyline, but not of fluoxetine, into brain is enhanced in mice with blood-brain barrier deficiency due to mdr1a P-glycoprotein gene disruption. Neuropsychopharmacology 22:380-387.

271. Schwartz, G., and M. G. Fehlings. 2002. Secondary injury mechanisms of spinal cord trauma: a novel therapeutic approach for the management of secondary pathophysiology with the sodium channel blocker riluzole. Prog Brain Res 137:177-190.

272. Wang, S. J., K. Y. Wang, and W. C. Wang. 2004. Mechanisms underlying the riluzole inhibition of glutamate release from rat cerebral cortex nerve terminals (synaptosomes). Neuroscience 125:191-201.

273. Hama, A., and J. Sagen. 2010. Antinociceptive Effect of Riluzole in Rats with Neuropathic Spinal Cord Injury Pain. J Neurotrauma.

274. Petitjean, M. E., V. Pointillart, F. Dixmerias, L. Wiart, F. Sztark, P. Lassie, M. Thicoipe, and P. Dabadie. 1998. [Medical treatment of spinal cord injury in the acute stage]. Ann Fr Anesth Reanim 17:114-122.

275. Zhang, L., X. D. Liu, L. Xie, and G. J. Wang. 2003. P-glycoprotein restricted transport of nimodipine across blood-brain barrier. Acta Pharmacol Sin 24:903-906.

276. Baastrup, C., and N. B. Finnerup. 2008. Pharmacological management of neuropathic pain following spinal cord injury. CNS Drugs 22:455-475.
277. Potschka, H., M. Fedrowitz, and W. Loscher. 2002. P-Glycoprotein-mediated efflux of phenobarbital, lamotrigine, and felbamate at the blood-brain barrier: evidence from microdialysis experiments in rats. Neurosci Lett 327:173-176.
278. Luna-Tortos, C., M. Fedrowitz, and W. Loscher. 2008. Several major antiepileptic drugs are substrates for human P-glycoprotein. Neuropharmacology 55:1364-1375.
279. Wiffen, P. J., S. Derry, and R. A. Moore. 2011. Lamotrigine for acute and chronic pain. Cochrane Database Syst Rev 2:CD006044.
280. Basso, D. M., M. S. Beattie, and J. C. Bresnahan. 1995. A sensitive and reliable locomotor rating scale for open field testing in rats. J Neurotrauma 12:1-21.
281. Colorado, R. A., J. Shumake, N. M. Conejo, H. Gonzalez-Pardo, and F. Gonzalez-Lima. 2006. Effects of maternal separation, early handling, and standard facility rearing on orienting and impulsive behavior of adolescent rats. Behav Processes 71:51-58.
282. Reitman, Z. J., G. Jin, E. D. Karoly, I. Spasojevic, J. Yang, K. W. Kinzler, Y. He, D. D. Bigner, B. Vogelstein, and H. Yan. 2011. Profiling the effects of isocitrate dehydrogenase 1 and 2 mutations on the cellular metabolome. Proc Natl Acad Sci U S A 108:3270-3275.
283. Saeed, A. I., N. K. Bhagabati, J. C. Braisted, W. Liang, V. Sharov, E. A. Howe, J. Li, M. Thiagarajan, J. A. White, and J. Quackenbush. 2006. TM4 microarray software suite. Methods Enzymol 411:134-193.
284. Maltese, A., F. Maugeri, F. Drago, and C. Bucolo. 2005. Simple determination of riluzole in rat brain by high-performance liquid chromatography and spectrophotometric detection. J Chromatogr B Analyt Technol Biomed Life Sci 817:331-334.
285. Colovic, M., E. Zennaro, and S. Caccia. 2004. Liquid chromatographic assay for riluzole in mouse plasma and central nervous system tissues. J Chromatogr B Analyt Technol Biomed Life Sci 803:305-309.
286. Marie, J. P., R. Zittoun, and B. I. Sikic. 1991. Multidrug resistance (mdr1) gene expression in adult acute leukemias: correlations with treatment outcome and in vitro drug sensitivity. Blood 78:586-592.

287. Baldini, N., K. Scotlandi, G. Barbanti-Brodano, M. C. Manara, D. Maurici, G. Bacci, F. Bertoni, P. Picci, S. Sottili, M. Campanacci, and et al. 1995. Expression of P-glycoprotein in high-grade osteosarcomas in relation to clinical outcome. N Engl J Med 333:1380-1385.

288. Tan, B., D. Piwnica-Worms, and L. Ratner. 2000. Multidrug resistance transporters and modulation. Curr Opin Oncol 12:450-458.

289. Merino, V., N. V. Jimenez-Torres, and M. Merino-Sanjuan. 2004. Relevance of multidrug resistance proteins on the clinical efficacy of cancer therapy. Curr Drug Deliv 1:203-212.

290. Perez-Tomas, R. 2006. Multidrug resistance: retrospect and prospects in anti-cancer drug treatment. Curr Med Chem 13:1859-1876.

291. Noble, L. J., A. E. Mautes, and J. J. Hall. 1996. Characterization of the microvascular glycocalyx in normal and injured spinal cord in the rat. J Comp Neurol 376:542-556.

292. Ng, W. F., F. Sarangi, R. L. Zastawny, L. Veinot-Drebot, and V. Ling. 1989. Identification of members of the P-glycoprotein multigene family. Mol Cell Biol 9:1224-1232.

293. Devault, A., and P. Gros. 1990. Two members of the mouse mdr gene family confer multidrug resistance with overlapping but distinct drug specificities. Mol Cell Biol 10:1652-1663.

294. Regina, A., A. Koman, M. Piciotti, B. El Hafny, M. S. Center, R. Bergmann, P. O. Couraud, and F. Roux. 1998. Mrp1 multidrug resistance-associated protein and P-glycoprotein expression in rat brain microvessel endothelial cells. J Neurochem 71:705-715.

295. Schinkel, A. H., U. Mayer, E. Wagenaar, C. A. Mol, L. van Deemter, J. J. Smit, M. A. van der Valk, A. C. Voordouw, H. Spits, O. van Tellingen, J. M. Zijlmans, W. E. Fibbe, and P. Borst. 1997. Normal viability and altered pharmacokinetics in mice lacking mdr1-type (drug-transporting) P-glycoproteins. Proc Natl Acad Sci U S A 94:4028-4033.

296. Schinkel, A. H., J. J. Smit, O. van Tellingen, J. H. Beijnen, E. Wagenaar, L. van Deemter, C. A. Mol, M. A. van der Valk, E. C. Robanus-Maandag, H. P. te Riele, and et al. 1994. Disruption of the mouse mdr1a P-glycoprotein gene leads to a deficiency in the blood-brain barrier and to increased sensitivity to drugs. Cell 77:491-502.

297. Pan, W., C. Yu, H. Hsuchou, and A. J. Kastin. 2010. The role of cerebral vascular NFkappaB in LPS-induced inflammation: differential regulation of efflux transporter and transporting cytokine receptors. Cell Physiol Biochem 25:623-630.

298. Wijnholds, J. 2005. Multidrug resistance-associated proteins and efflux of organic anions at the blood-brain and blood cerebrospinal fluid barriers. In Efflux transporters and the blood-brain barrier. E. M. Taylor, editor. Nova Biomedical Books, New York. 137-156.

299. Pujol, A., I. Ferrer, C. Camps, E. Metzger, C. Hindelang, N. Callizot, M. Ruiz, T. Pampols, M. Giros, and J. L. Mandel. 2004. Functional overlap between ABCD1 (ALD) and ABCD2 (ALDR) transporters: a therapeutic target for X-adrenoleukodystrophy. Hum Mol Genet 13:2997-3006.

300. Coley, H. M. 2010. Overcoming multidrug resistance in cancer: clinical studies of p-glycoprotein inhibitors. Methods Mol Biol 596:341-358.

301. Pardridge, W. M., P. L. Golden, Y. S. Kang, and U. Bickel. 1997. Brain microvascular and astrocyte localization of P-glycoprotein. J Neurochem 68:1278-1285.

302. Golden, P. L., and W. M. Pardridge. 1999. P-Glycoprotein on astrocyte foot processes of unfixed isolated human brain capillaries. Brain Res 819:143-146.

303. Golden, P. L., and W. M. Pardridge. 2000. Brain microvascular P-glycoprotein and a revised model of multidrug resistance in brain. Cell Mol Neurobiol 20:165-181.

304. Schlachetzki, F., and W. M. Pardridge. 2003. P-glycoprotein and caveolin-1alpha in endothelium and astrocytes of primate brain. Neuroreport 14:2041-2046.

305. Cordon-Cardo, C., J. P. O'Brien, D. Casals, L. Rittman-Grauer, J. L. Biedler, M. R. Melamed, and J. R. Bertino. 1989. Multidrug-resistance gene (P-glycoprotein) is expressed by endothelial cells at blood-brain barrier sites. Proc Natl Acad Sci U S A 86:695-698.

306. Milane, A., L. Tortolano, C. Fernandez, G. Bensimon, V. Meininger, and R. Farinotti. 2009. Brain and plasma riluzole pharmacokinetics: effect of minocycline combination. J Pharm Pharm Sci 12:209-217.

307. Chu, X., Z. Zhang, J. Yabut, S. Horwitz, J. Levorse, X. Q. Li, L. Zhu, H. Lederman, R. Ortiga, J. Strauss, X. Li, K. A. Owens, J. Dragovic, T. Vogt, R. Evers, and M. K. Shin. 2012. Characterization of multidrug resistance 1a/P-glycoprotein knockout rats generated by zinc finger nucleases. Mol Pharmacol 81:220-227.

308. Bauer, B., A. M. Hartz, and D. S. Miller. 2007. Tumor necrosis factor alpha and endothelin-1 increase P-glycoprotein expression and transport activity at the blood-brain barrier. Mol Pharmacol 71:667-675.

309. Szczuraszek, K., V. Materna, A. Halon, G. Mazur, T. Wrobel, K. Kuliczkowski, A. Maciejczyk, M. Zabel, M. Drag, M. Dietel, H. Lage, and P. Surowiak. 2009. Positive correlation between cyclooxygenase-2 and ABC-transporter expression in non-Hodgkin's lymphomas. Oncol Rep 22:1315-1323.

310. Yu, N., Q. Di, H. Liu, Y. Hu, Y. Jiang, Y. K. Yan, Y. F. Zhang, and Y. D. Zhang. 2011. Nuclear factor-kappa B activity regulates brain expression of P-glycoprotein in the kainic acid-induced seizure rats. Mediators Inflamm 2011:670613.

311. Aoki, Y., D. Qiu, G. H. Zhao, and P. N. Kao. 1998. Leukotriene B4 mediates histamine induction of NF-kappaB and IL-8 in human bronchial epithelial cells. Am J Physiol 274:L1030-1039.

312. Kawano, T., H. Matsuse, Y. Kondo, I. Machida, S. Saeki, S. Tomari, K. Mitsuta, Y. Obase, C. Fukushima, T. Shimoda, and S. Kohno. 2003. Cysteinyl leukotrienes induce nuclear factor kappa b activation and RANTES production in a murine model of asthma. J Allergy Clin Immunol 112:369-374.

313. Sanchez-Galan, E., A. Gomez-Hernandez, C. Vidal, J. L. Martin-Ventura, L. M. Blanco-Colio, B. Munoz-Garcia, L. Ortega, J. Egido, and J. Tunon. 2009. Leukotriene B4 enhances the activity of nuclear factor-kappaB pathway through BLT1 and BLT2 receptors in atherosclerosis. Cardiovasc Res 81:216-225.

314. Jatana, M., S. Giri, M. A. Ansari, C. Elango, A. K. Singh, I. Singh, and M. Khan. 2006. Inhibition of NF-kappaB activation by 5-lipoxygenase inhibitors protects brain against injury in a rat model of focal cerebral ischemia. J Neuroinflammation 3:12.

315. Chen, S. H., H. Fahmi, Q. Shi, and M. Benderdour. 2010. Regulation of microsomal prostaglandin E2 synthase-1 and 5-lipoxygenase-activating protein/5-lipoxygenase by 4-hydroxynonenal in human osteoarthritic chondrocytes. Arthritis Res Ther 12:R21.

316. Rakonczay, Z., Jr., P. Hegyi, T. Takacs, J. McCarroll, and A. K. Saluja. 2008. The role of NF-kappaB activation in the pathogenesis of acute pancreatitis. Gut 57:259-267.

317. Bauer, B., A. M. Hartz, G. Fricker, and D. S. Miller. 2004. Pregnane X receptor up-regulation of P-glycoprotein expression and transport function at the blood-brain barrier. Mol Pharmacol 66:413-419.

318. Kwon, B. K., W. Tetzlaff, J. N. Grauer, J. Beiner, and A. R. Vaccaro. 2004. Pathophysiology and pharmacologic treatment of acute spinal cord injury. Spine J 4:451-464.

319. Maxis, K., A. Delalandre, J. Martel-Pelletier, J. P. Pelletier, N. Duval, and D. Lajeunesse. 2006. The shunt from the cyclooxygenase to lipoxygenase pathway in human osteoarthritic subchondral osteoblasts is linked with a variable expression of the 5-lipoxygenase-activating protein. Arthritis Res Ther 8:R181.

320. Bias, P., A. Buchner, B. Klesser, and S. Laufer. 2004. The gastrointestinal tolerability of the LOX/COX inhibitor, licofelone, is similar to placebo and superior to naproxen therapy in healthy volunteers: results from a randomized, controlled trial. Am J Gastroenterol 99:611-618.

321. Mills, C. D., J. J. Grady, and C. E. Hulsebosch. 2001. Changes in exploratory behavior as a measure of chronic central pain following spinal cord injury. J Neurotrauma 18:1091-1105.

322. Xu, G. Y., M. G. Hughes, L. Zhang, L. Cain, and D. J. McAdoo. 2005. Administration of glutamate into the spinal cord at extracellular concentrations reached post-injury causes functional impairments. Neurosci Lett 384:271-276.

323. Hoffmann, K., and W. Loscher. 2007. Upregulation of brain expression of P-glycoprotein in MRP2-deficient TR(-) rats resembles seizure-induced up-regulation of this drug efflux transporter in normal rats. Epilepsia 48:631-645.

324. Milane, A., S. Vautier, H. Chacun, V. Meininger, G. Bensimon, R. Farinotti, and C. Fernandez. 2009. Interactions between riluzole and ABCG2/BCRP transporter. Neurosci Lett 452:12-16.

325. Agarwal, S., A. M. Hartz, W. F. Elmquist, and B. Bauer. 2011. Breast cancer resistance protein and P-glycoprotein in brain cancer: two gatekeepers team up. Curr Pharm Des 17:2793-2802.

326. Kim, W. S., C. S. Weickert, and B. Garner. 2008. Role of ATP-binding cassette transporters in brain lipid transport and neurological disease. J Neurochem 104:1145-1166.

327. Khan, M., J. Singh, A. G. Gilg, T. Uto, and I. Singh. 2010. Very long-chain fatty acid accumulation causes lipotoxic response via 5-lipoxygenase in cerebral adrenoleukodystrophy. J Lipid Res 51:1685-1695.

328. Gottesman, M. M., and I. Pastan. 1993. Biochemistry of multidrug resistance mediated by the multidrug transporter. Annu Rev Biochem 62:385-427.
329. Demeule, M., A. Regina, J. Jodoin, A. Laplante, C. Dagenais, F. Berthelet, A. Moghrabi, and R. Beliveau. 2002. Drug transport to the brain: key roles for the efflux pump P-glycoprotein in the blood-brain barrier. Vascul Pharmacol 38:339-348.
330. Marchi, N., G. Betto, V. Fazio, Q. Fan, C. Ghosh, A. Machado, and D. Janigro. 2009. Blood-brain barrier damage and brain penetration of antiepileptic drugs: role of serum proteins and brain edema. Epilepsia 50:664-677.
331. de Vries, H. E., J. Kuiper, A. G. de Boer, T. J. Van Berkel, and D. D. Breimer. 1997. The blood-brain barrier in neuroinflammatory diseases. Pharmacol Rev 49:143-155.
332. Schnell, L., S. Fearn, M. E. Schwab, V. H. Perry, and D. C. Anthony. 1999. Cytokine-induced acute inflammation in the brain and spinal cord. J Neuropathol Exp Neurol 58:245-254.
333. Echeverry, S., X. Q. Shi, S. Rivest, and J. Zhang. 2011. Peripheral nerve injury alters blood-spinal cord barrier functional and molecular integrity through a selective inflammatory pathway. J Neurosci 31:10819-10828.
334. Hong, H., Y. Lu, Z. N. Ji, and G. Q. Liu. 2006. Up-regulation of P-glycoprotein expression by glutathione depletion-induced oxidative stress in rat brain microvessel endothelial cells. J Neurochem 98:1465-1473.
335. Schafer, F. Q., and G. R. Buettner. 2001. Redox environment of the cell as viewed through the redox state of the glutathione disulfide/glutathione couple. Free Radic Biol Med 30:1191-1212.
336. Eriksson, B., and S. A. Eriksson. 1967. Synthesis and characterization of the L-cysteine-glutathione mixed disulfide. Acta Chem Scand 21:1304-1312.
337. Foyer, C. H., and G. Noctor. 2011. Ascorbate and glutathione: the heart of the redox hub. Plant Physiol 155:2-18.
338. Yoshida, Y., M. Hayakawa, and E. Niki. 2005. Total hydroxyoctadecadienoic acid as a marker for lipid peroxidation in vivo. Biofactors 24:7-15.
339. Adibhatla, R. M., and J. F. Hatcher. 2010. Lipid oxidation and peroxidation in CNS health and disease: from molecular mechanisms to therapeutic opportunities. Antioxid Redox Signal 12:125-169.

340. Broxterman, H. J., H. M. Pinedo, C. M. Kuiper, G. J. Schuurhuis, and J. Lankelma. 1989. Glycolysis in P-glycoprotein-overexpressing human tumor cell lines. Effects of resistance-modifying agents. FEBS Lett 247:405-410.

341. Klawitter, J., D. J. Kominsky, J. L. Brown, U. Christians, D. Leibfritz, J. V. Melo, S. G. Eckhardt, and N. J. Serkova. 2009. Metabolic characteristics of imatinib resistance in chronic myeloid leukaemia cells. Br J Pharmacol 158:588-600.

342. Bergsneider, M., D. A. Hovda, E. Shalmon, D. F. Kelly, P. M. Vespa, N. A. Martin, M. E. Phelps, D. L. McArthur, M. J. Caron, J. F. Kraus, and D. P. Becker. 1997. Cerebral hyperglycolysis following severe traumatic brain injury in humans: a positron emission tomography study. J Neurosurg 86:241-251.

343. Dinan, T. G., and M. Mobayed. 1992. Treatment resistance of depression after head injury: a preliminary study of amitriptyline response. Acta Psychiatr Scand 85:292-294.

344. Nguyen, T., P. Nioi, and C. B. Pickett. 2009. The Nrf2-antioxidant response element signaling pathway and its activation by oxidative stress. J Biol Chem 284:13291-13295.

345. Ma, W., J. G. Chabot, F. Vercauteren, and R. Quirion. 2010. Injured nerve-derived COX2/PGE2 contributes to the maintenance of neuropathic pain in aged rats. Neurobiol Aging 31:1227-1237.

346. Noguchi, K., and M. Okubo. 2011. Leukotrienes in nociceptive pathway and neuropathic/inflammatory pain. Biol Pharm Bull 34:1163-1169.

347. Lin, J. H., and M. Yamazaki. 2003. Role of P-glycoprotein in pharmacokinetics: clinical implications. Clin Pharmacokinet 42:59-98.

348. Glavinas, H., P. Krajcsi, J. Cserepes, and B. Sarkadi. 2004. The role of ABC transporters in drug resistance, metabolism and toxicity. Curr Drug Deliv 1:27-42.

349. Scheff, S. W., D. A. Saucier, and M. E. Cain. 2002. A statistical method for analyzing rating scale data: the BBB locomotor score. J Neurotrauma 19:1251-1260.

350. Carlton, S. M., J. Du, H. Y. Tan, O. Nesic, G. L. Hargett, A. C. Bopp, A. Yamani, Q. Lin, W. D. Willis, and C. E. Hulsebosch. 2009. Peripheral and central sensitization in remote spinal cord regions contribute to central neuropathic pain after spinal cord injury. Pain 147:265-276.

351. Durham-Lee, J. C., V. U. Mokkapati, K. M. Johnson, and O. Nesic. 2011. Amiloride improves locomotor recovery after spinal cord injury. J Neurotrauma 28:1319-1326.

352. Wang, X., S. Budel, K. Baughman, G. Gould, K. H. Song, and S. M. Strittmatter. 2009. Ibuprofen enhances recovery from spinal cord injury by limiting tissue loss and stimulating axonal growth. J Neurotrauma 26:81-95.
353. Coley, H. M. Overcoming multidrug resistance in cancer: clinical studies of p-glycoprotein inhibitors. Methods Mol Biol 596:341-358.

Vita

Jennifer Natalie Dulin was born in Independence, Missouri on October 2, 1983 to Cynthia Kay Dulin and Donald Bedford Dulin, Jr. After graduating from William P. Clements High School in Sugar Land, Texas in 2001, she matriculated at Texas A&M University in College Station, Texas. She received the degree of Bachelor of Science in Biochemistry and graduated *cum laude* from Texas A&M in May of 2005. From 2005 to 2007 she worked in research labs at UT Southwestern Medical Center in Dallas, Texas, and MD Anderson Cancer Center in Houston, Texas. In January of 2008 she entered The University of Texas Graduate School of Biomedical Sciences at Houston. She performed her dissertation work in the lab of Raymond J. Grill, Ph.D. in the Department of Integrative Biology and Pharmacology at The University of Texas Medical School. Jennifer will graduate with her Doctorate of Philosophy in Neurosciences in May of 2012.